

May 2020

# Compositional Analysis of Pottery from Middle Woodland Waukesha Phase Sites in Southeastern Wisconsin and Havana Hopewell Related Sites in Northeastern and Northwestern Illinois

Megan Elizabeth Thornton  
*University of Wisconsin-Milwaukee*

Follow this and additional works at: <https://dc.uwm.edu/etd>



Part of the [Archaeological Anthropology Commons](#)

---

## Recommended Citation

Thornton, Megan Elizabeth, "Compositional Analysis of Pottery from Middle Woodland Waukesha Phase Sites in Southeastern Wisconsin and Havana Hopewell Related Sites in Northeastern and Northwestern Illinois" (2020). *Theses and Dissertations*. 2428.  
<https://dc.uwm.edu/etd/2428>

This Thesis is brought to you for free and open access by UWM Digital Commons. It has been accepted for inclusion in Theses and Dissertations by an authorized administrator of UWM Digital Commons. For more information, please contact [open-access@uwm.edu](mailto:open-access@uwm.edu).

COMPOSITIONAL ANALYSIS OF POTTERY FROM MIDDLE WOODLAND WAUKESHA  
PHASE SITES IN SOUTHEASTERN WISCONSIN AND HAVANA HOPEWELL RELATED SITES  
IN NORTHEASTERN AND NORTHWESTERN ILLINOIS

by

Megan Elizabeth Thornton

A Thesis Submitted in  
Partial Fulfillment of the  
Requirements for the Degree of

Master of Science

in Anthropology

at

The University of Wisconsin-Milwaukee

May 2020

## ABSTRACT

### COMPOSITIONAL ANALYSIS OF POTTERY FROM MIDDLE WOODLAND WAUKESHA PHASE SITES IN SOUTHEASTERN WISCONSIN AND HAVANA HOPEWELL RELATED SITES IN NORTHEASTERN AND NORTHWESTERN ILLINOIS

by

Megan Elizabeth Thornton

The University of Wisconsin-Milwaukee, 2020  
Under the Supervision of Professor John D. Richards, Ph.D.

This thesis provides a compositional analysis of a selected sample of Middle Woodland ceramic sherds from sites in southeastern Wisconsin and northern Illinois. The analysis compares the ceramic pastes from Middle Woodland pottery from nine different archaeological sites. These sites include the Peterson, Finch, Alberts, and Crab Apple Point sites in Wisconsin, the Sloan, Albany Village, Blythe, DeWitte/Liphardt Habitation sites in northwestern Illinois, and the Kautz site in northeastern Illinois.

The analysis includes a review of available documentation, as well as descriptions and characterizations of sherds utilizing an attribute-based analysis of metric, morphological, and petrographic data. In southeastern Wisconsin, the Middle Woodland occupation is poorly understood, and sites with Middle Woodland components have been suggested to be part of the Waukesha phase. Haas's (2019b) recent work at the Finch site has been the first detailed examination of the Waukesha phase since Salzer's (n.d.) seminal study (Goldstein 1992). Although the phase is considered to represent some degree of interaction with Illinois Havana-Hopewell (Jeske 2006; Mason 2001; Salzer 1986), direct evidence of such interaction is lacking. This analysis provides a comparative dataset to be used in future comparisons of Waukesha Phase ceramics. The results of the petrographic analysis suggest an overall homogeneity of paste

composition between the samples selected for this thesis. Statistical analysis of the data was unable to identify specific samples or recipes by region. The results of this project suggest that paste recipes may have been widely shared between people in southern Wisconsin and northern Illinois and may indicate existing relationships within groups in the study region.

© Copyright by Megan Thornton, 2020  
All Rights Reserved

# TABLE OF CONTENTS

List of Figures .....	vii
List of Tables .....	xv
Acknowledgements .....	xvi
Chapter 1: Introduction .....	1
Chapter 2: Background .....	7
Introduction.....	7
Southeast Wisconsin Sites Selected for Petrographic Analysis .....	10
Northwestern Illinois/Mississippi River Trench Sites Selected for Petrographic Analysis.....	24
Northeastern Illinois.....	36
Ceramic Petrography.....	39
Chapter 3: Methods .....	41
Introduction.....	41
Sample Selection .....	42
Attribute Data Collection .....	43
Petrographic Analysis .....	45
Ternary Diagram.....	48
Statistical Analysis .....	52
Chapter 4: Analysis and Results .....	53
Introduction.....	53
Morphological and Metric Data .....	55
Petrographic Analysis: Mineralogy.....	82
Petrographic Analysis: Body Composition .....	139
Regional Comparisons.....	196
Chapter 5: Summary and Conclusion .....	209
Summary .....	209
Conclusions.....	211
Future Research .....	214
References Cited .....	216

Appendix A: Ceramic Attribute Analysis Database .....	225
Appendix B: Ceramic Mineralogy Database .....	236
Appendix C: Point Counting Raw data .....	239
Appendix D: Composition Statistical Analysis Data .....	242
Appendix E: Ternary Diagrams .....	255

## LIST OF FIGURES

Figure 1.1 Archaeological site locations in Illinois and Wisconsin.....	2
Figure 2.1 Location of the Peterson site in Waukesha Co., Wisconsin.....	12
Figure 2.2 Location of the Finch site in Jefferson Co., Wisconsin.....	16
Figure 2.3 Location of the Alberts site in Jefferson Co., Wisconsin.....	21
Figure 2.4 Location of the Crab Apple Point site in Jefferson Co., Wisconsin. ....	23
Figure 2.5 Location of the Sloan site in Mercer Co., Illinois.....	26
Figure 2.6 Location of the Albany site in Whiteside Co., Illinois.....	29
Figure 2.7 Location of the Blythe site in Hancock Co., Illinois. ....	33
Figure 2.8 Location of the DeWitte/Liphardt Habitation site in Rock Island Co., Illinois. ....	35
Figure 2.9 Location of the Kautz site in DuPage Co., Illinois. ....	37
Figure 3.1 Example ternary diagram of ceramic paste composition data (after Schneider 2015, Figure 6.10). ....	50
Figure 3.2 Example ternary diagram of ceramic body composition data (after Schneider 2015, Figure 6.6). ....	51
Figure 4.1 Sample 1, Hopewell Incised bowl; left, rim profile shown with interior to right; center, sherd exterior; right, sherd interior. ....	55
Figure 4.2 Sample 2, Steuben Punctated jar; left, rim profile shown with interior to right; center, sherd exterior; right, sherd interior. ....	57
Figure 4.3 Sample 3, Steuben Punctated jar; left, rim profile shown with interior to right; center, sherd exterior; right, sherd interior. ....	58
Figure 4.4 Sample 4, Steuben Punctated jar; left, rim profile shown with interior to right; center, sherd exterior; right, sherd interior. ....	59



Figure 4.5 Sample 5, Shorewood Cord Roughened jar; left, rim profile shown with interior to right; center, sherd exterior; right, sherd interior.....	60
Figure 4.6 Sample 6, Kegonsa Stamped jar; left, rim profile shown with interior to right; center, sherd exterior; right, sherd interior.....	61
Figure 4.7 Sample 7, Steuben Punctated jar; left, rim profile shown with interior to right; center, sherd exterior; right, sherd interior.....	62
Figure 4.8 Sample 8, Havana Zoned body sherd; left, sherd exterior; right, sherd interior.....	63
Figure 4.9 Sample 9, Naples Stamped body sherd; left, sherd exterior; right, sherd interior.....	64
Figure 4.10 Sample 10, Kegonsa Stamped jar; left, rim profile shown with interior to right; center, sherd exterior; right, sherd interior (profile after Haas 2019b, Appendix D).....	65
Figure 4.11 Sample 11, Naples Stamped body sherd; left, sherd exterior; right, sherd interior.....	66
Figure 4.12 Sample 12, Shorewood Cord Roughened jar; left, rim profile shown with interior to right; center, sherd exterior; right, sherd interior (profile after Haas 2019b, Appendix D).....	67
Figure 4.13 Sample 13, Hopewell-related jar; left, rim profile shown with interior to right; center, sherd exterior; right, sherd interior (profile after Haas 2019b, Appendix D).....	68
Figure 4.14 Sample 14, Havana Plain jar rim; left, rim profile shown with interior to right; center, sherd exterior; right, sherd interior.....	69
Figure 4.15 Thin section image of black interior slip on Havana Plain sample 14 (Cross-Polarized Light, 4X).....	69
Figure 4.16 Sample 15, Naples Stamped jar rim; left, rim profile shown with interior to right; center, sherd exterior; right, sherd interior.....	70
Figure 4.17 Sample 16, Havana Plain jar rim; left, rim profile shown with interior to right; center, sherd exterior; right, sherd interior.....	71
Figure 4.18 Sample 17, Hopewell Ware jar rim; left, rim profile shown with interior to right; center, sherd exterior; right, sherd interior.....	72
Figure 4.19 Sample 18, Hopewell Zoned Stamped body sherd; left, sherd exterior; right, sherd interior.....	73
Figure 4.20 Sample 19, Unclassified Havana Ware jar rim; left, rim profile shown with interior to right; center, sherd exterior; right, sherd interior.....	74

Figure 4.21 Sample 20, Naples Stamped jar rim; left, rim profile shown with interior to right; center, sherd exterior; right, sherd interior. ....	75
Figure 4.22 Sample 21, Hopewell Zoned Stamped body sherd; left, sherd exterior; right, sherd interior. ....	76
Figure 4.23 Sample 22, Naples Stamped jar rim; left, rim profile shown with interior to right; center, sherd exterior; right, sherd interior. ....	77
Figure 4.24 Sample 23, Havana Zoned jar rim; left, rim profile shown with interior to right; center, sherd exterior; right, sherd interior. ....	78
Figure 4.25 Sample 24, Havana Cordmarked jar rim; left, rim profile shown with interior to right; center, sherd exterior; right, sherd interior. ....	79
Figure 4.26 Sample 25, Shorewood Cord Roughened jar rim; left, rim profile shown with interior to right; center, sherd exterior; right, sherd interior. ....	80
Figure 4.27 Sample 26, Havana Cordmarked jar rim; left, rim profile shown with interior to right; center, sherd exterior; right, sherd interior. ....	81
Figure 4.28 Sample 27, Hummel Stamped jar rim; left, rim profile shown with interior to right; center, sherd exterior; right, sherd interior. ....	82
Figure 4.29 Thin section image of Sample 1 (Plane Polarized Light, 4X). ....	87
Figure 4.30 Thin section image of Sample 1 (Cross Polarized Light, 4X). ....	87
Figure 4.31 Thin section image of Sample 2 (Plane Polarized Light, 4X). ....	88
Figure 4.32 Thin section image of Sample 2 (Cross Polarized Light, 4X). ....	89
Figure 4.33 Thin section image of Sample 3 (Plane Polarized Light, 4X). ....	90
Figure 4.34 Thin section image of Sample 3 (Cross Polarized Light, 4X). ....	91
Figure 4.35 Thin section image of Sample 4 (Plane Polarized Light, 4X). ....	92
Figure 4.36 Thin section image of Sample 4 (Cross Polarized Light, 4X). ....	93
Figure 4.37 Thin section image of Sample 5 (Plane Polarized Light, 4X). ....	94
Figure 4.38 Thin section image of Sample 5 (Cross Polarized Light, 4X). ....	95

Figure 4.39 Thin section image of Sample 6 (Plane Polarized Light, 4X). .....	96
Figure 4.40 Thin section image of Sample 6 (Cross Polarized Light, 4X). .....	97
Figure 4.41 Thin section image of Sample 7 (Plane Polarized Light, 4X). .....	98
Figure 4.42 Thin section image of Sample 7 (Cross Polarized Light, 4X). .....	99
Figure 4.43 Thin section image of Sample 8 (Plane Polarized Light, 4X). .....	100
Figure 4.44 Thin section image of Sample 8 (Cross Polarized Light, 4X). .....	101
Figure 4.45 Thin section image of Sample 9 (Plane Polarized Light, 4X). .....	102
Figure 4.46 Thin section image of Sample 9 (Cross Polarized Light, 4X). .....	103
Figure 4.47 Thin section image of Sample 10 (Plane Polarized Light, 4X). .....	104
Figure 4.48 Thin section image of Sample 10 (Plane Polarized Light, 4X). .....	105
Figure 4.49 Thin section image of Sample 11 (Plane Polarized Light, 4X). .....	106
Figure 4.50 Thin section image of Sample 11 (Cross Polarized Light, 4X). .....	107
Figure 4.51 Thin section image of Sample 12 (Plane Polarized Light, 4X). .....	108
Figure 4.52 Thin section image of Sample 12 (Cross Polarized Light, 4X). .....	109
Figure 4.53 Thin section image of Sample 13 (Plane Polarized Light, 4X). .....	110
Figure 4.54 Thin section image of Sample 13 (Cross Polarized Light, 4X). .....	111
Figure 4.55 Thin section image of Sample 14 (Plane Polarized Light, 4X). .....	112
Figure 4.56 Thin section image of Sample 14 (Cross Polarized Light, 4X). .....	113
Figure 4.57 Thin section image of Sample 15 (Plane Polarized Light, 4X). .....	114
Figure 4.58 Thin section image of Sample 15 (Cross Polarized Light, 4X). .....	115
Figure 4.59 Thin section image of Sample 16 (Plane Polarized Light, 4X). .....	116

Figure 4.60 Thin section image of Sample 16 (Cross Polarized Light, 4X). .....	117
Figure 4.61 Thin section image of Sample 17 (Plane Polarized Light, 4X). .....	118
Figure 4.62 Thin section image of Sample 17 (Cross Polarized Light, 4X). .....	119
Figure 4.63 Thin section image of Sample 18 (Plane Polarized Light, 4X). .....	120
Figure 4.64 Thin section image of Sample 18 (Cross Polarized Light, 4X). .....	121
Figure 4.65 Thin section image of Sample 19 (Plane Polarized Light, 4X). .....	122
Figure 4.66 Thin section image of Sample 19 (Cross Polarized Light, 4X). .....	123
Figure 4.67 Thin section image of Sample 20 (Plane Polarized Light, 4X). .....	124
Figure 4.68 Thin section image of Sample 20 (Cross Polarized Light, 4X). .....	125
Figure 4.69 Thin section image of Sample 21 (Plane Polarized Light, 4X). .....	126
Figure 4.70 Thin section image of Sample 21 (Cross Polarized Light, 4X). .....	127
Figure 4.71 Thin section image of Sample 22 (Plane Polarized Light, 4X). .....	128
Figure 4.72 Thin section image of Sample 22 (Cross Polarized Light, 4X). .....	129
Figure 4.73 Thin section image of Sample 23 (Plane Polarized Light, 4X). .....	130
Figure 4.74 Thin section image of Sample 23 (Cross Polarized Light, 4X). .....	131
Figure 4.75 Thin section image of Sample 24 (Plane Polarized Light, 4X). .....	132
Figure 4.76 Thin section image of Sample 24 (Cross Polarized Light, 4X). .....	133
Figure 4.77 Thin section image of Sample 25 (Plane Polarized Light, 4X). .....	134
Figure 4.78 Thin section image of Sample 25 (Cross Polarized Light, 4X). .....	135
Figure 4.79 Thin section image of Sample 26 (Plane Polarized Light, 4X). .....	136
Figure 4.80 Thin section image of Sample 26 (Cross Polarized Light, 4X). .....	137

Figure 4.81 Thin section image of Sample 27 (Plane Polarized Light, 4X). .....	138
Figure 4.82 Thin section image of Sample 27 (Cross Polarized Light, 4X). .....	139
Figure 4.83 Ternary diagram of Sample 1 paste composition. ....	143
Figure 4.84 Ternary diagram of Sample 1 body composition. ....	144
Figure 4.85 Ternary diagram of Sample 2 paste composition. ....	145
Figure 4.86 Ternary diagram of Sample 2 body composition. ....	146
Figure 4.87 Ternary diagrams of Sample 3 paste composition. ....	147
Figure 4.88 Ternary diagrams of Sample 3 body composition. ....	148
Figure 4.89 Ternary diagram of Sample 4 paste composition. ....	149
Figure 4.90 Ternary diagram of Sample 4 body composition. ....	150
Figure 4.91 Ternary diagram of Sample 5 paste composition. ....	151
Figure 4.92 Ternary diagram of Sample 5 body composition. ....	152
Figure 4.93 Ternary diagram of Sample 6 paste composition .....	153
Figure 4.94 Ternary diagram of Sample 6 body composition. ....	154
Figure 4.95 Ternary diagram of Sample 7 paste composition. ....	155
Figure 4.96 Ternary diagram of Sample 7 body composition. ....	156
Figure 4.97 Ternary diagram of Sample 8 paste composition. ....	157
Figure 4.98 Ternary diagram of Sample 8 body composition. ....	158
Figure 4.99 Ternary diagram of Sample 9 paste composition. ....	159
Figure 4.100 Ternary diagram of Sample 9 body composition. ....	160
Figure 4.101 Ternary diagram of Sample 10 paste composition. ....	161

Figure 4.102 Ternary diagram of Sample 10 body composition.....	162
Figure 4.103 Ternary diagram of Sample 11 paste composition.....	163
Figure 4.104 Ternary diagram of Sample 11 body composition.....	164
Figure 4.105 Ternary diagram of Sample 12 paste composition.....	165
Figure 4.106 Ternary diagram of Sample 12 body composition.....	166
Figure 4.107 Ternary diagram of Sample 13 paste composition.....	167
Figure 4.108 Ternary diagram of Sample 13 body composition.....	168
Figure 4.109 Ternary diagram of Sample 14 paste composition.....	169
Figure 4.110 Ternary diagram of Sample 14 body composition.....	170
Figure 4.111 Ternary diagram of Sample 15 paste composition.....	171
Figure 4.112 Ternary diagram of Sample 15 body composition.....	172
Figure 4.113 Ternary diagram of Sample 16 paste composition.....	173
Figure 4.114 Ternary diagram of Sample 16 body composition.....	174
Figure 4.115 Ternary diagram of Sample 17 paste composition.....	175
Figure 4.116 Ternary diagram of Sample 17 body composition.....	176
Figure 4.117 Ternary diagram of Sample 18 paste composition.....	177
Figure 4.118 Ternary diagram of Sample 18 body composition.....	178
Figure 4.119 Ternary diagram of Sample 19 paste composition.....	179
Figure 4.120 Ternary diagram of Sample 19 body composition.....	180
Figure 4.121 Ternary diagram of Sample 20 paste composition.....	181
Figure 4.122 Ternary diagram of Sample 20 body composition.....	182

Figure 4.123 Ternary diagram of Sample 21 paste composition. ....	183
Figure 4.124 Ternary diagram of Sample 21 body composition. ....	184
Figure 4.125 Ternary diagram of Sample 22 paste composition. ....	185
Figure 4.126 Ternary diagram of Sample 22 body composition. ....	186
Figure 4.127 Ternary diagram of Sample 23 paste composition. ....	187
Figure 4.128 Ternary diagram of Sample 23 body composition. ....	188
Figure 4.129 Ternary diagram of Sample 24 paste composition. ....	189
Figure 4.130 Ternary diagram of Sample 24 body composition. ....	190
Figure 4.131 Ternary diagram of Sample 25 paste composition. ....	191
Figure 4.132 Ternary diagram of Sample 25 body composition. ....	192
Figure 4.133 Ternary diagram of Sample 26 paste composition. ....	193
Figure 4.134 Ternary diagram of Sample 26 body composition. ....	194
Figure 4.135 Ternary diagram of Sample 27 paste composition. ....	195
Figure 4.136 Ternary diagram of Sample 27 body composition. ....	196
Figure 4.137 Ternary diagram of paste composition based on pottery type. The orange points represent samples from southeast Wisconsin sites, blue points represent samples from Illinois sites. ....	204
Figure 4.138 Ternary diagram plotting the estimation of variance of the full vector of the linear regression model of paste composition. The 90% and 99% confidence intervals are represented by ellipses around each site. ....	205
Figure 4.139 Ternary diagram of body composition based on pottery type. The orange points represent sherds from southeast Wisconsin sites, blue points represent sherds from northern Illinois sites. ....	207
Figure 4.140 Ternary diagram plotting the estimation of variance of the full vector of the linear regression model of body composition. The 90% and 99% confidence intervals are represented by ellipses around each site. ....	208

## LIST OF TABLES

Table 4.1 Sample Morphological and Metric Data .....	54
Table 4.2 Percentage of Minerals Identified in Each Sample .....	85
Table 4.3 Body and Paste Counts, Percentages, and Size Indices .....	141
Table 5.1 Summary of Paste Data by Site .....	212
Table 5.2 Summary of Body Data by Site.....	213



## ACKNOWLEDGEMENTS

First and foremost, I would like to thank my committee members Dr. Jason Sherman and Dr. Robert Jeske. I appreciate the advice you have given me regarding this thesis. I would like to thank my advisor, Dr. John Richards, for your constant support and mentorship. Thank you for presenting me with numerous academic and professional opportunities while I have been a student.

To the people who assisted with my research, especially the people who shared their data with me, including Dr. Jennifer Haas, Pete Geraci, and Andrew Saleh. To Dr. Seth Schneider, thank you for mentoring and assisting me with both the petrographic analysis and statistical testing of the results. Additionally, I would like to thank the Wisconsin Archeological Society for presenting me with the Research Award to conduct this analysis.

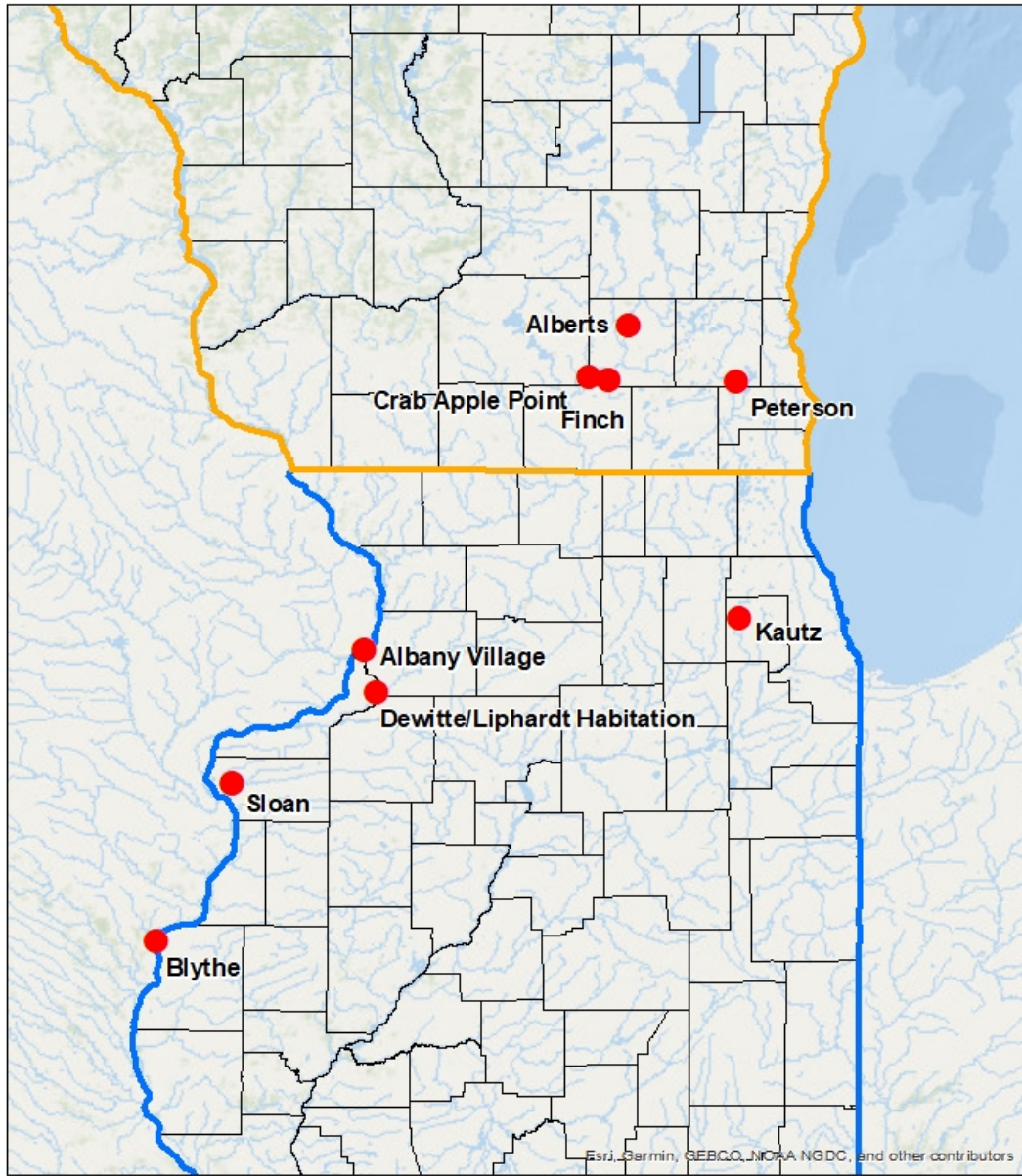
To the many people at UWM-CRM, I am grateful for the chance to learn and work alongside each of you. To all the students I was fortunate enough to supervise in the UWM-ARL Collections Internship program and the 2019 Aztalan Field School, thank you for your hours of hard work. Thank you to the students from my academic cohort, including those of you in the Museum Studies program, for being friends throughout this process.

To my family, especially my parents and grandparents, thank you for always supporting me and listening when I needed to talk. You encouraged me to follow whatever path I chose and understood my desire to learn. Finally, I want to thank Andrew Saleh. I am so grateful to go through this experience this with you. You kept me motivated, made maps, and pushed me when I needed it. I will cherish the many times we took a camping trip on a moment's notice so we could explore a new adventure together.

## CHAPTER 1: INTRODUCTION

This thesis examines ceramic paste compositional variability between sites from the Middle Woodland Waukesha Phase in southeastern Wisconsin and Middle Woodland sites in northwestern and northeastern Illinois. The analysis focuses on Havana-Hopewell related pottery from the Wisconsin and Illinois sites. Using thin sections of the sherds, petrographic analysis was conducted to identify minerals present in the samples and examine compositional variation in the paste and body of the ceramics.

The project examined twenty-seven ceramic sherds from nine sites with Middle Woodland components located in southeast Wisconsin and northern Illinois (Figure 1.1). The number of samples from each site varies. From the Wisconsin sites, seven samples were selected from the Peterson site (47WK199), six samples from Finch (47JE902), and a single sample was chosen from both the Alberts (47JE887) and Crab Apple Point (47JE93) sites. From the northwestern Illinois sites, eight samples were selected from the Sloan site (11MC86), and a single sample was drawn from the Albany Village (11WT1), Blythe (11HA40), and DeWitte/Liphardt Habitation (11RI57) sites. A single sherd was sampled from the Kautz site (11DU46/1) in northeastern Illinois in order to provide an eastern Illinois example of Havana Zoned pottery to compare to the western Illinois sample.



**Archaeological Site Locations in Illinois and Wisconsin**

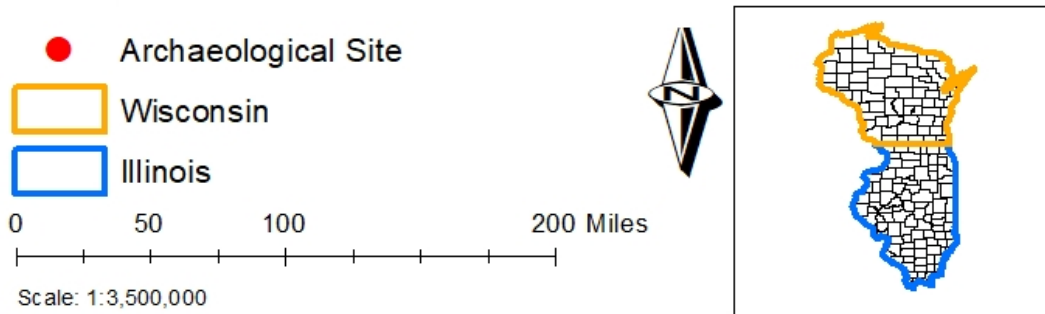


Figure 1.1 Archaeological site locations in Illinois and Wisconsin.

The analysis detailed below was designed to determine if Havana-Hopewell stylistic influences were adapted to locally-produced pottery, or if Havana vessels recovered from southeast Wisconsin sites represent imports from locations further south. To do this, two main goals were established. The first was to determine the extent to which all samples are similar or different. The second was to determine if inter-regional or inter-site analysis could be used to identify statistically significant patterns to examine if the paste and recipe composition of the samples can be used to separate or identify samples by region.

An attempt was made to select sherds broadly representative of region-wide Middle Woodland ceramic traditions. Sherds chosen represent three primary wares including Rock Ware, diagnostic of Waukesha Phase Middle Woodland in southeast Wisconsin, Havana Ware, and Hopewell Ware, both more reflective of a northern Illinois River distribution. To a great degree, sample selection was predicated on availability of samples suitable for destructive analysis and for which permission to conduct the work could be obtained. Thus, it cannot be argued that the analyzed sample set is truly representative of ceramic paste variability within the study area. Nonetheless, results of this study demonstrate the utility of this kind of analysis and represent a necessary first step in designing a more extensive project based on a larger, more inclusive sample set. All sherds and associated ceramic thin sections used in this thesis are curated by the University of Wisconsin Milwaukee (UWM) Archaeological Research Laboratory (ARL).

The Middle Woodland period is dated between AD 100 to 400 (Stevenson et al. 1997) in southeast Wisconsin and northern Illinois. In southeast Wisconsin, the Middle Woodland component of an archaeological site is often one of several multi-component habitations at the site (Goldstein 1992:158; Jeske 2006:299). Recent research at the Finch site in Jefferson County

by Haas (2019b) suggests that the dates acquired from Middle Woodland vessels overlap those of preceding Early Woodland vessels. Additionally, lithic analysis indicates inter-regional trade between Wisconsin and groups to the south for raw material types (Haas 2019b). This suggests that the introduction of Middle Woodland style vessels at sites in southeast Wisconsin may follow existing inter-regional contact between people in the Wisconsin region and groups to the south (Haas 2019b). Archaeological investigations at the Finch, Peterson, and Alberts sites have included specific research into the Middle Woodland components of each site (Brazeau et al. 1980; Haas 2019a, 2019b; Haas et al. 2015; Jeske and Kaufmann 2000; Jeske 2006; Salzer n.d.; Watson et al. 2003; WHPD; Wood 1936), while research at the Crab Apple Point site has primarily focused on the Late Woodland, Oneota, and historic components at the site (Auten et al. 2017; Jeske 2003; Pozza 2016; Schneider et al. 2017; Spector 1975).

In Illinois, the lower Illinois River Valley is considered a core area of the Hopewell Interaction Sphere (Fie 2008). Much of the research into Middle Woodland sites has been conducted in this part of Illinois or at mortuary and habitation sites exhibiting highly stylized Hopewell artifacts (Charles 2012). Illinois sites from which sherd samples were drawn include sites that have been subjected to long-term archaeological investigations such as the Sloan, Albany Village, and Kautz sites (Benchley et al. 1979; Benchley and Dudzik 1976; Benchley and Gregg 1975; Geraci 2016; Herold 1971; Schenian 1983; Wenner 1960). In addition, sherds were also obtained from sites known only from data produced by the Illinois Predictive Model Surveys conducted by UWM; these include the Blythe and DeWitte/Liphardt Habitation sites (Benchley and Billeck 1977; Fowler and Dudzik 1973; IIAPS).

My thesis research included both attribute-based analysis and petrographic analysis. The initial attribute-based ceramic analysis of the selected sherds identified temper and paste

characterization, grain size and texture, and the paste core cross-sections. I also recorded metric and morphological data, including rim, lip, neck, and shoulder form, rim profile, orifice shape, surface finish, and decorative treatments. The data from this analysis were inventoried using a digital database for future access.

To conduct the petrographic analysis, thin sections of sherds from the selected sites in southeastern Wisconsin and northern Illinois were processed and analyzed for paste composition and identification of minerals. The thin sections were prepared by National Petrographic Services, Inc. James Stoltman's (1989) point counting technique was used to collect qualitative and quantitative data on grain sizes and minerals in the pastes analyzed. All other equipment and supplies necessary to complete the project were provided by the UWM ARL. Upon completion of this thesis, ceramic thin sections will be accessioned into the ARL's permanent collections. Data sets and thin sections will be made available for additional analyses by other researchers.

Petrographic analysis is used to "obtain an unbiased estimate of the constituents of a sample" (Stoltman 1989). Point counting and mineral identification have been used by other scholars to identify the possible interaction of people between sites (Chivis 2016; Schneider 2015). In his analysis of Middle Woodland ceramics from western Michigan and northwestern Indiana, Chivis (2016:12) acknowledges the need to include a visual attribute-based analysis in addition to the petrographic analysis as the "visual styles have extensive distributions because highly visible decorative traits are easily copied and shared among far-flung peoples." While the samples selected for this analysis were all chosen based on the visual attributes of Middle Woodland decoration, the petrographic analysis can help to identify similarities in the recipes used to make the clay paste eventually used to construct the vessels. The quantitative data set was collected by counting the number of points across the sample in thin section and classifying

each point as matrix, silt, sand, or temper. The qualitative data was collected based on the classification of each point and the additional classification of sand and temper inclusions based on size grade and the temper type. Finally, the points that represented identifiable minerals in the paste were also counted and classified by mineral type. The quantitative and qualitative components of petrographic analysis, both identifying and inventorying the temper and minerals within a sample, can be used to compare the vessels “with their presumed source areas, assess the cultural affinities of newly recognized or uncertain ceramic types, or analyze the paste variation that may exist between different functional categories within or between archaeological assemblages” (Stoltman 1989:158). To do this, a ternary diagram application was used to visualize and present the compositional data.

This thesis is organized as follows. Chapter 2 provides background information on Middle Woodland occupations in southeast Wisconsin and northern Illinois, the specific Middle Woodland sites from Wisconsin and Illinois used in this analysis, and the use of petrographic analysis in archaeological research. Chapter 3 presents the methods used in this analysis to select samples from each site and to conduct morphological, metric, mineralogical, compositional, and statistical analyses. Chapter 4 presents the results of the analysis by individual samples and summarizes the regional comparisons between the Wisconsin and Illinois sites. Chapter 5 reviews the results from the analysis, evaluates the homogeneity between samples across the sites and regions, and suggests additional research opportunities to expand upon this analysis.

## CHAPTER 2: BACKGROUND

### Introduction

Across the North American mid-continent, the Middle Woodland period is dated between 200 BC and AD 500. Three important traits are used to define this spatial and temporal period: “the construction of conical burial mounds; evidence of plant cultivation; and pottery decorated by pressing tools such as notched bone or cord-wrapped sticks into the wet, unfired clay” (Stevenson et al. 1997:157). The Middle Woodland period throughout the midcontinent is often identified with and compared to the Hopewell culture in Illinois and Ohio. The term Hopewell has been used to describe a phase of the Middle Woodland period characterized by riverine-based regional integration visible through the earthworks and exotic artifacts deposited in funerary contexts (Abrams 2009). There are two primary centers of the Hopewell phase: Ohio Hopewell in southeastern Ohio and Havana-Hopewell in the lower Illinois River valley. Connections between Middle Woodland groups and influence from Hopewell centers to other Middle Woodland sites have been contextualized through the Hopewell Interaction Sphere (Caldwell 1964; Struever 1964). Trade of exotic materials originating from Appalachia, the Upper Mississippi Valley, the Great Lakes, Yellowstone, and the Gulf and Atlantic coasts (Seaman 1977; Struever 1964, 1965) have been used as evidence for the Interaction Sphere. Because of early interpretations, the Hopewell phenomenon was defined as a singular interregional term by archaeologists rather than local cultural contexts (Chivis 2016).

Boundaries have been used to contextualize regional traditions within the Middle Woodland period. The Havana tradition is the regional boundary which encompasses the sites in this study. The Havana tradition is “largely co-extensive with the Prairie Peninsula” (Brown 1964:120), ranging from “northeastern Oklahoma and western Missouri eastward to include the



Illinois River system... as far south as the mouth of the Kaskaskia River, as far north as the Red Cedar River in Wisconsin” Struever (1964:91). Brown (1964) extends the boundary of the Havana tradition east to include parts of northwestern Indiana and southwestern Michigan, with some evidence of the Havana tradition extending into the Saginaw Bay area.

Pottery, other artifact types, and mortuary practices characteristic of the Hopewell phase are identified in major river valleys across several regional traditions during the Middle Woodland period. In the Illinois Valley. Struever (1964) categorizes the Hopewell phase of the Havana tradition based on the fully developed Hopewell pottery series. Brown (1964) further argues that pottery diagnostic of the Hopewell phase is often a minority type in Illinois sites compared to other Havana style, utilitarian, vessels. However, pottery exhibiting Hopewell decorative styles have a wider regional distribution expanding across the various regional Middle Woodland traditions. Struever (1965:211) suggests that the Hopewell phase does not represent “local expressions of a homogenous culture.” Instead, the stylistic variability and the differences in distribution may represent differing cultural systems rather than a pan-regional “Hopewellian mortuary complex” (Struever 1964:88).

In Illinois, most Middle Woodland sites are identified based on research conducted at mortuary mound groups and large village sites (Yingst 1990). Along the Illinois River, Middle Woodland sites can be sorted into separate types including regional centers, base camps, small seasonal camps, and mortuary sites (Benchley et al. 1979). Many of these mortuary sites include elaborate burial mounds. Both mortuary and habitation sites contain exotic and stylized Hopewell artifacts (Brose and Greber 1979; Charles 2012; Charles and Buikstra 2006). Research into demographic and biological variability in the lower Illinois Valley has been conducted by Asch (1976), Buikstra (1976), and Charles (1992). This research indicates the transitional nature

of the Middle Woodland period, where populations increased, and the localization of subsistence intensified between the Early Woodland and early Late Woodland periods (Charles 1992). The lower Illinois River Valley has historically been a focus of Middle Woodland research because it is considered one of the core areas of the Hopewell Interaction Sphere (Fie 2008).

Most Middle Woodland sites in Wisconsin are multi-component and are not solely associated with that period (Goldstein 1992:158; Jeske 2006:299). In southern Wisconsin, the Middle Woodland period is divided between southwest and southeast Wisconsin. In the southwest, the Trempealeau (circa AD 100-200) and Millville (circa AD 200-500) phases are used to categorize Middle Woodland components. Sites in southeastern Wisconsin contain less elaborate grave goods and mound construction, which has caused archaeologists to separate the southeastern part of the state from the Trempealeau and Millville phases and call the Middle Woodland components in this part of the state the Waukesha phase (Goldstein 1984; Haas 2019b; Jeske 2006; Salzer n.d.).

The Waukesha Focus was originally attributed to sites in Waukesha County with burial mounds and artifacts similar to Hopewellian sites in the northern Illinois River valley (Bennett 1952; McKern 1942; Salzer n.d.). In Salzer's (n.d.:4) unpublished manuscript "The Waukesha Focus: Hopewell in Southeastern Wisconsin", he suggests the extension of the Waukesha Focus taxonomy to "include all Middle Woodland manifestations in the southeastern Wisconsin-northeastern Illinois area" (Salzer n.d.) He makes this suggestion to account for "the technological patterns of southeastern Wisconsin during the Middle Woodland period when a series of strong stylistic concepts from the central and northern Illinois valley become apparent" (Salzer n.d.:279). Salzer did not attempt to map the limits of his expanded Focus so the location of the southern boundary of the proposed taxon is unclear. An additional problem with Salzer's

designation of the Waukesha Focus is the suggested variability in settlements. Salzer notes common pottery types, identified at the Highsmith Site, including Kegonsa Stamped, Shorewood Cord Roughened, Dane Cord Marked, Highsmith Plain, and Cooper's Shores Collared. Additional exotic ceramics styles (Salzer n.d.:283) are also present at sites with Waukesha Focus components including Havana Zoned, Havana Plain, Havana Cordmarked, Naples Stamped, Steuben Punctated, Sisters Creek Punctate, and Classic Hopewell.

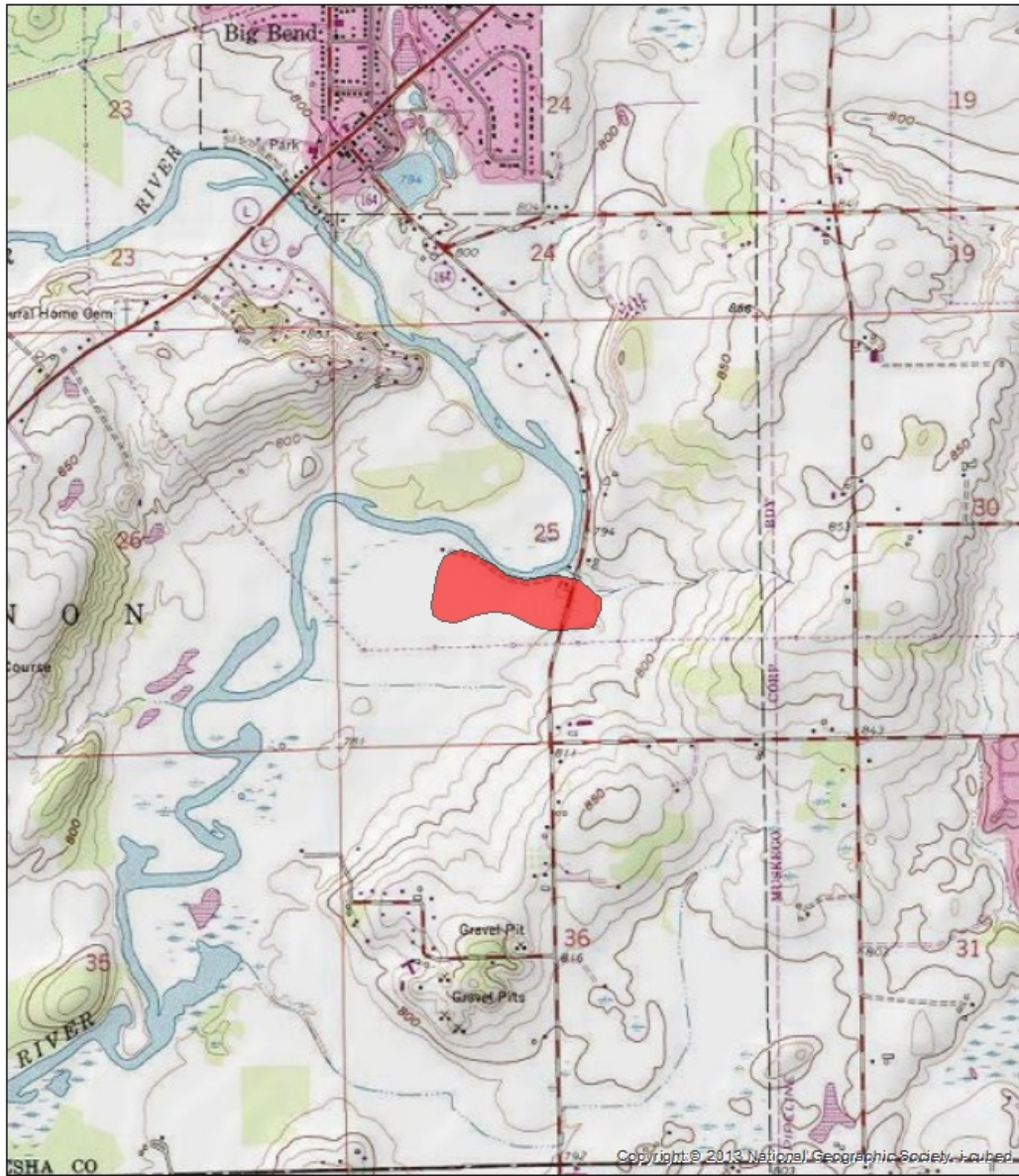
All sites in this analysis were selected because of the presence of Middle Woodland pottery types. Additionally, all are within the geographic extent of Havana-Hopewell related Middle Woodland occupations. The Wisconsin sites are all situated within southeast Wisconsin within the conventional limits of the Waukesha Focus. However, the Illinois site sample is distributed more widely. The Sloan and Blythe sites are located farthest south and are situated along the Mississippi River in central Illinois. The Albany Village and DeWitte/Liphardt Habitation sites are also situated near the Mississippi River but are located in northwest Illinois. The Kautz site is the only site in the sample that can be said to be located in northeast Illinois and thus situated within Salzer's proposed expanded southern boundary of the Waukesha Focus.

### **Southeast Wisconsin Sites Selected for Petrographic Analysis**

#### *Peterson (47WK199)*

The Peterson site (47WK199) is located in Waukesha County, Wisconsin (Figure 2.1). The site was initially identified by Increase Lapham in 1855, and a map of the site location along the Fox River is included in his book, *Antiquities of Wisconsin*. At that time, Lapham called the Fox River the Pishtaka River to "distinguish it from the numerous other rivers of the same name" (Lapham 1855:23). In 1902, the Wisconsin Archeological Society measured the mounds at the

site and Lafayette Ellarson excavated the largest conical mound at the site. Ellarson discovered a burial chamber in the mound, which included human remains, two stone pipes, and “fragments of rouletted pottery” (Wood 1936:219). At this time, the land was owned by Henry E. Nicolai. In 1923, Charles E. Brown documented the site as “Nicolai Mounds” and synthesized the Wisconsin Archeological Society measurements and Ellarson’s excavations in an issue of *The Wisconsin Archeologist*.



**Location of the Peterson Site in Waukesha Co., Wisconsin**

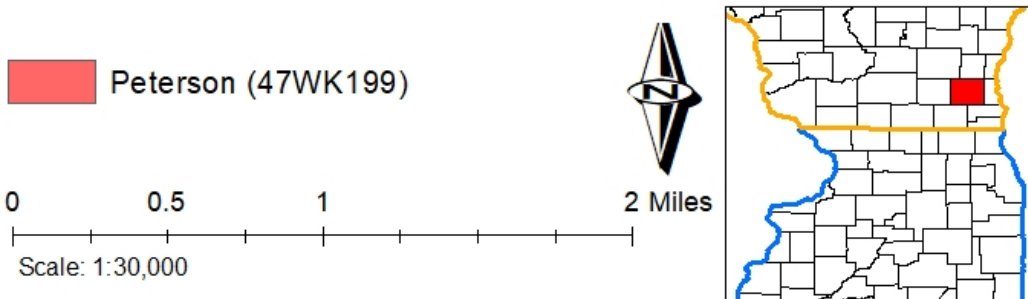


Figure 2.1 Location of the Peterson site in Waukesha Co., Wisconsin

Further excavation of the site occurred after Mr. Henry J. Peterson partially unearthed a burial while grading a portion of his land. Mr. Peterson notified the Milwaukee Public Museum (MPM) and invited staff to investigate the site (Wood 1936:215). E.F. Wood and W.C. McKern arrived after much of the mound had been removed. The archaeologists relied on observers' information to document the stratigraphy of the mound. A rectilinear burial pit was at the base of the mound with a charcoal and ash layer above it. Another intrusive burial was in the mound, "placed after the mound was built" (Wood 1936:216). According to Wood, the burial at the base of the mound contained a minimum of seventeen individuals, including "seven adult males, three adult females, two sub-adults and four infants or children of indeterminate sex" (Wood 1936:217). The only artifacts documented in the burial were fifteen shell beads, "placed about the neck of one individual" (Wood 1936:219). Wood suggests that this site may be a component of a new "Wisconsin focus of the Central Basin phase" (Wood 1936:219). He also notes that there are several specimens from Waukesha County in the MPM collections that seem to represent this cultural phase, including the pipes and fragments of rouletted pottery from the mound excavated by Ellarson in 1902 (Wood 1936). According to the Archaeological Site Inventory (ASI), the artifacts are housed at the MPM.

Between 1977 and 1980, the Peterson village site was surveyed, and test excavations were conducted by the Great Lakes Archaeological Research Center (GLARC). Surface collection recovered cultural material indicative of Middle Woodland and Late Woodland occupations (Brazeau et al. 1980:83). The presence of both Middle and Late Woodland diagnostic artifacts recovered from test excavations indicate that the site was occupied during these periods. The site was listed in the National Register of Historic Places (NHRP) in 1982. In 2001, a compliance project along the south bank of the Fox River required archaeological

investigations by GLARC (Wisconsin Historic Preservation Database [WHPD]). Mechanical stripping of a gravel field road using a backhoe resulted in the identification of 150 subsurface features. Forty-four of the features were identified as prehistoric features including pits, post-molds, a hearth, and a possible house basin. Lithic, ground stone, copper, and ceramic artifacts were recovered from the features. According to a summary of the Peterson site investigations, the Middle Woodland ceramic types at the site include Steuben Punctated, Havana Plain, and unclassified Middle Woodland. Late Woodland ceramic types include Madison Cord Impressed, Madison Plain, Weaver Plain, and Point Sauble Collared (Haas 2017). In 2012, the site was monitored during the installation of utilities. The ASI form indicates no prehistoric cultural material was recovered and cultural features were disturbed at the time of this monitoring (WHPD). No formal report has been published on the compliance work conducted at the Peterson site.

The samples used in the present analysis come from both the 1980 and 2001 excavation projects. Two samples, a Hopewell-like incised sherd (2019001) and a Steuben Punctated sherd (2019007), come from the 1980 excavations. There is little detail about the context of these artifacts. More information is available for the samples recovered during the 2001 excavation. Two Steuben Punctated samples (2019002 and 2019003) were recovered from the same pit feature, Feature 53. Another Steuben Punctated sample (2019004) came from a pottery concentration within Feature 77, identified as a possible post mold. A Shorewood Cord Roughened sample (2019005) was recovered from Feature 107, a basin-shaped pit. The last sample from the site, part of a Kegonsa Stamped vessel (2019006), was excavated and brought to the lab in bulk as part of a soil matrix sample from Feature 97, a diffuse oval shaped pit.

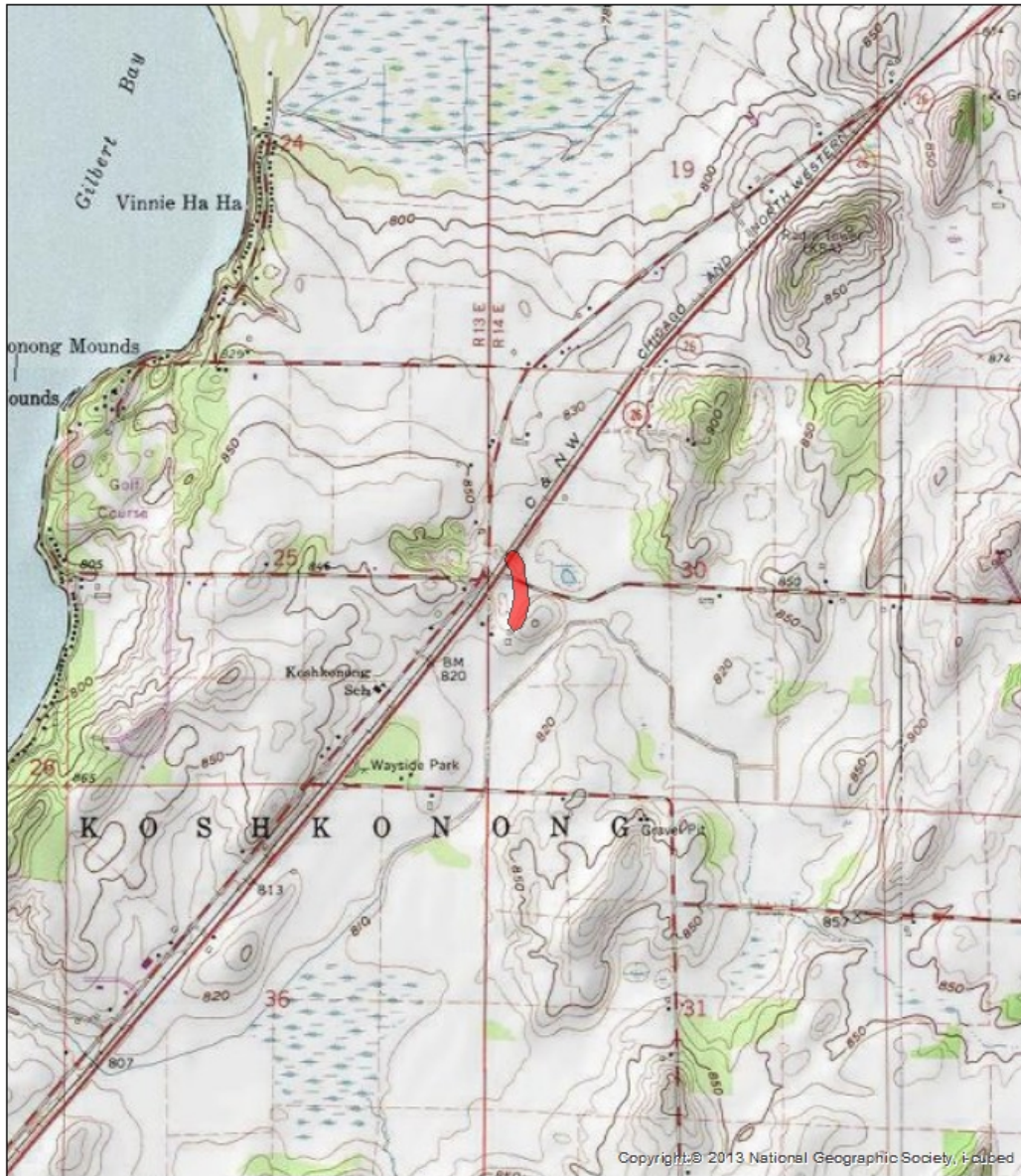
### *Finch (47JE902)*

The Finch site (47JE902) is in Jefferson County in southeastern Wisconsin (Figure 2.2). The site occupies “a locally prominent hill and a small terrace adjacent to a spring fed pond east of Lake Koshkonong and the Rock River drainage” (Haas 2019b:69). Initially the site was reported as a historic cemetery location; however, only a small portion of the historic cemetery was located and excavations recovered dense prehistoric artifact concentrations (Haas 2019a, 2019b; Haas et al. 2015).

Between 1999 and 2002, GLARC conducted an archaeological survey project along the proposed alternate routes of the STH 26 reconstruction. This large-scale project investigated possible sites in Dodge, Jefferson, and Rock counties. The Finch site was one of the Jefferson County sites within the boundaries of the project. Based on the recovery of chipped stone and pottery fragments during the Phase I survey, Phase II evaluation was conducted to determine if the site was eligible for listing on the NRHP. The Phase II evaluation identified an intensive Middle Woodland occupation, as well as Early and Late Woodland components. Based on these results, the site was recommended to be listed on the NRHP, and if the STH 26 reconstruction could not avoid the site, a data mitigation plan was suggested (Watson et al. 2003).

The highway reconstruction project was unable to avoid impacting the site and data recovery was necessary. The Phase III mitigation was begun in 2009 and continued through 2012. Approximately 1,200 square meters were excavated at the site, over 100,000 artifacts were recovered, and 153 cultural features were identified (Haas 2019b:72). The diagnostic material culture from the site indicates multi-component settlement including Early and Late Paleoindian, Early, Middle, and Late Archaic, and Early, Middle, and Late Woodland components.





**Location of the Finch Site in Jefferson Co., Wisconsin**

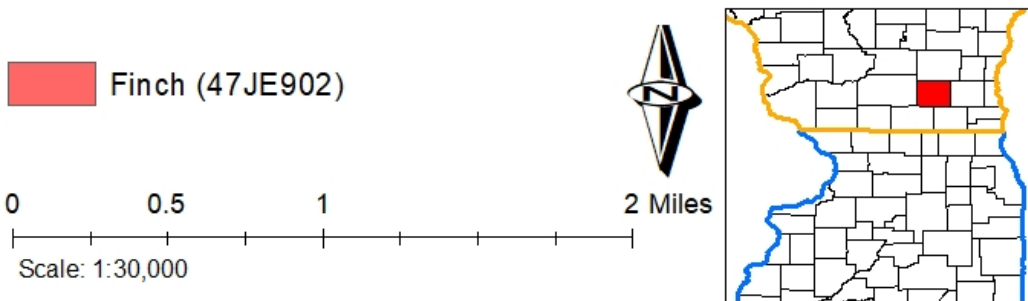


Figure 2.2 Location of the Finch site in Jefferson Co., Wisconsin.

The Middle Woodland component of the site was recognized by the presence of Snyders and Steuben hafted bifaces, ceramic vessels including Havana ware, Naples Stamped, Sister Creeks Punctated, Kegonsa Stamped, Shorewood Cord Roughened, and Hopewell-related pottery. Additionally, some transitional wares including Deer Creek Incised and Douglass Net Marked are included in the assemblage. Middle Woodland activity areas included a domestic living space that included feature types such as a temporary housing structure, cooking pits, multi-functional pits, and a hearth. Another Middle Woodland activity area is suggested to represent animal resource processing due to the presence of cooking pits or hearths, and multi-functional pits and a high density of lithic tools (Haas 2019b).

In a recent analysis of the Finch site in southeast Wisconsin (Haas 2019b; Haas and Picard 2019), the Middle Woodland vessels were classified according to Salzer's typological categories including Rock Ware, Havana Ware, Seed Jar, and Hopewell-Related. The Rock Ware types include the Kegonsa Stamped and Shorewood Cord Roughened styles, a category diagnostic of the Waukesha phase (Haas 2019b; Salzer n.d.). The Havana Ware types include Havana Plain, Havana Zoned, Naples Stamped, and Sister Creeks Punctated. Only one example of both the Seed Jar and Hopewell Related categories were recovered from the Finch site. Radiocarbon dates from Kegonsa Stamped and Shorewood Cord Roughened vessels at the Finch site were the first direct dates acquired for the Rock Ware category (Haas 2019b). These dates fall within the range of the Havana culture and other Illinois and Wisconsin Middle Woodland phases including North Bay, Nokomis, and Steuben. Additionally, the Middle Woodland dates from the Finch site also overlap accepted dates of 500 BC to AD 100 (Stevenson et al. 1997:155) for Early Woodland occupations in southern Wisconsin.

Lithic analysis suggests that both Early Woodland and Middle Woodland inhabitants of the Finch site used locally available Galena chert as well as non-local material sourced from southern and southwestern locations including west-central Illinois and southeastern Iowa. Investigations into grave goods and foodways also suggest that groups in southeastern Wisconsin did not adapt Havana-Hopewell cultural influences as fully as southwestern Wisconsin and other areas (Benchley et al. 1997; Haas 2019b; Salzer nd; Stevenson et al. 1997). Haas (2019b:356) uses this information to suggest that the Middle Woodland occupations in southeastern Wisconsin may not have been “embedded within a broader Havana-Hopewellian regional or symbolic community,” and populations of Havana-Hopewell people may not have physically migrated into the area. Instead, it is suggested that the existing Early Woodland populations likely already had persistent inter-regional contact with southern groups. This challenges previous interpretations that Middle Woodland populations in southeastern Wisconsin were indicative of southern Havana-Hopewell populations migrating into southeastern Wisconsin (Haas 2019b).

As the Finch site was most recently documented in both a UWM-CRM ROI (Haas 2019a) and Haas’s dissertation (2019b), the ceramics from this site were already well organized and sherds were refit, identified and assigned specific vessel numbers. The excavation area for the Finch site was very large. To facilitate descriptions and analysis, the site area was arbitrarily divided into five regions. The samples selected for this analysis were recovered from three of these regions: Region B, Region C, and Region D. Region B is situated in the central-north portion of the site, Region C is in the central portion of the site, and Region D is directly south of Region C in the central portion of the site. The individual sherds used for this analysis were

recovered from unit contexts, while other sherds from the same vessels may have been recovered from other contexts throughout the site.

Vessel 2002 is Havana Zoned. The sherd (2019008) used in this analysis from that vessel was recovered from level 3 of Unit 301 in Region D. However, other sherds from this vessel were recovered from Feature 114, a cooking pit, in Unit 325 of Region D. Vessel 2004 is Naples Stamped. The sherd (2019009) used in this analysis from that vessel was recovered from level 4 of Unit 231 in Region C. Vessel 2008 is Kegonsa Stamped. The sherd (2019010) used in this analysis from that vessel was recovered in level 4 of Unit 356 in Region B. Vessel 2020 is Naples Stamped. The sherd (2019011) used in this analysis from that vessel was recovered from level 8 of Unit 172 in Region D. Vessel 2038 is Shorewood Cord Roughened. The sherd (2019012) used in this analysis from that vessel was recovered from level 6 of Unit 61 in Region D. Vessel 3034 is Hopewell-related. The sherd (2019013) used in this analysis from that vessel was recovered from level 6 of Unit 266 in Region D.

### *Alberts (47JE887)*

The Alberts site is part of a complex of sites along the east bank of the Rock River, north of the confluence with Johnson Creek, in Jefferson County, Wisconsin (Jeske 2006; Jeske and Kaufmann 2000) (Figure 2.3). The complex consists of both a habitation site (47JE903) and a mound site (47JE887), which had both a conical and linear mound, and artifacts representing Late Archaic, Early, Middle and Late Woodland, and Upper Mississippian components with some stratigraphic integrity (Jeske and Kaufmann 2000). The habitation site is primarily a Late Woodland occupation located immediately adjacent to the river and marshlands. The mound site

is located on a terrace directly north of the habitation site. The two components are separated by a small spring-fed stream (Jeske and Kaufmann 2000).

Richard Slattery conducted excavations at the site complex between 1964 and 1969, including a test of the conical mound in 1969 (Jeske and Kaufmann 2000). The habitation component is situated on sandy soils that were not heavily cultivated in the twentieth-century. Slattery's excavation in the habitation area recovered features from Early, Middle, and Late Woodland periods, as well as a possible Mississippian component (Jeske and Kaufmann 2000).

When testing the mound component, Slattery excavated 5-x-5-foot squares across the conical mound, excavating six squares total. The approximate diameter of the mound was 6 meters and at the time of excavation, the mound was only 25 cm high. The excavations of the mound did not show evidence that it was used for burial as no bones, grave features, or signs of mortuary rituals were recovered (Jeske and Kaufmann 2000:92). Artifacts recovered from feature contexts during Slattery's excavations include grit-tempered pottery, a Late Archaic/Early Woodland Durst point, Late Woodland Madison ware, Starved Rock Collared and possible Langford series rim sherds, a Middle Woodland point, and a Middle Woodland Havana Cordmarked vessel. In one of the 5-x-5-foot test units, near the center of the mound, a large boulder was placed directly on top of a crushed and burned Havana-style vessel. Jeske (2006) suggests that the mound and related features may be associated with a long-established fire and water dichotomy, and that the location of the Havana-style vessel, beneath the large rock, and near the Early Woodland fire pit was significant. The sample selected for this analysis (2019024) was a sherd from the Havana vessel that was underneath the large rock in the mound site component.



**Location of the Alberts Site in Jefferson Co., Wisconsin**

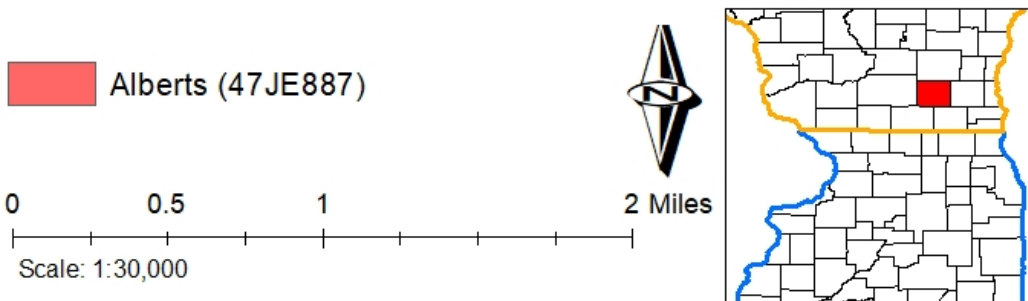
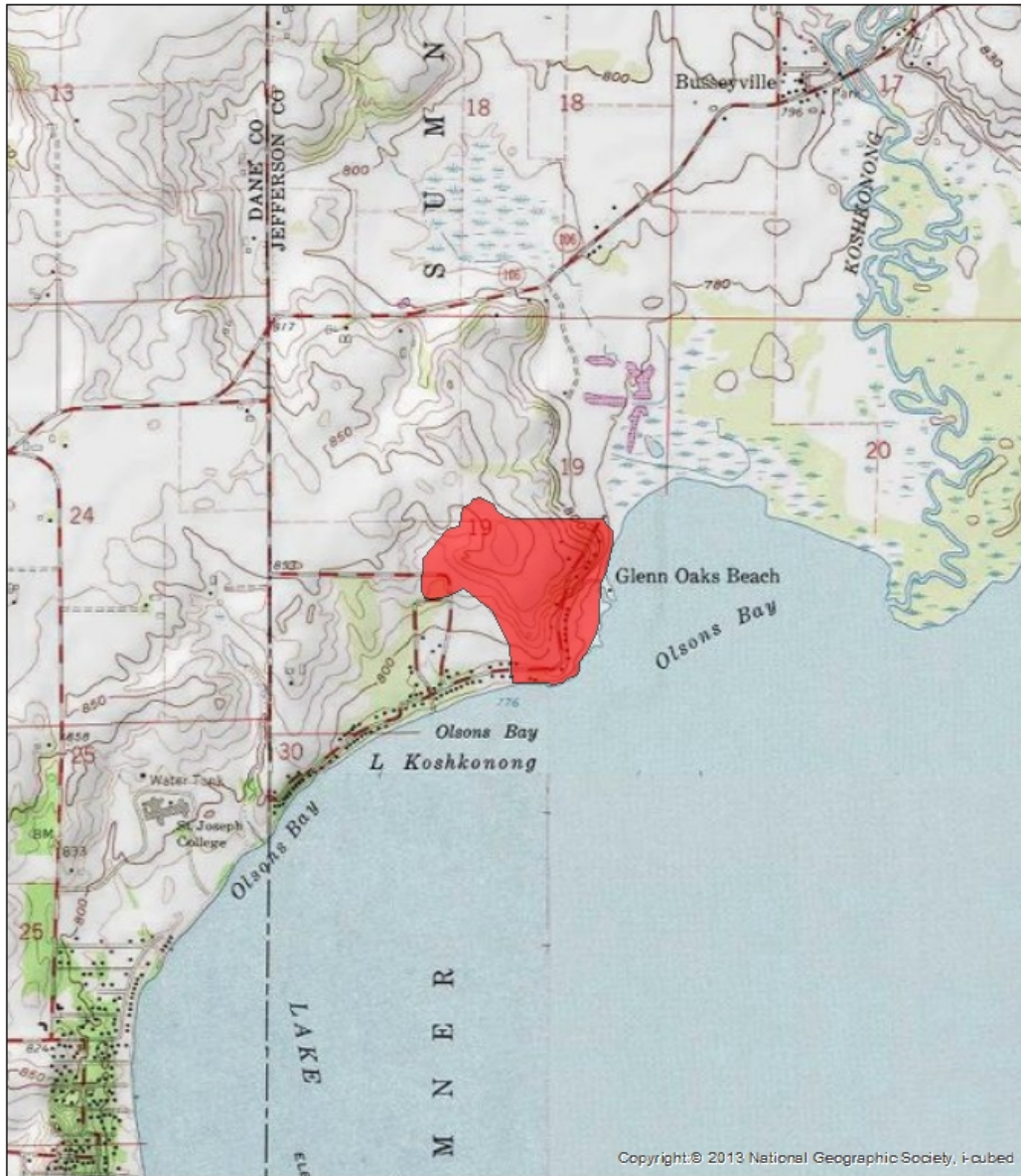


Figure 2.3 Location of the Alberts site in Jefferson Co., Wisconsin.

### *Crab Apple Point (47JE93)*

The Crab Apple Point (CAP) site is in the Lake Koshkonong area approximately 500 feet north of the Lake Koshkonong shoreline. Lake Koshkonong is located in Jefferson County, WI, and the lake “itself is actually a broad expansion of the Rock River” (Spector 1975:272-274) (Figure 2.4). Many archaeological sites have been documented around Lake Koshkonong. In 1908, Stout and Skavlem noted over 30 sites surrounding the lake during their initial survey (Stout and Skavlem 1908). More recent research in the Lake Koshkonong locality has been conducted by Hall (1962), Southeast Wisconsin Archaeology Project researchers (Goldstein 1984) and the Program in Midwest Archaeology (PIMA) at UWM directed by Dr. Robert Jeske (2003).

Archaeological documentation at the CAP site began in 1890 when Stephen Peet identified numerous mounds and a cabin used by Le Sellier, a French trader from the early nineteenth-century (Schneider et al. 2017:15). Later, Stout and Skavlem (1906) surveyed the site and surrounding archaeological sites in the Lake Koshkonong area. Janet Spector (1975) also conducted research at the CAP site focusing on the eighteenth-century Ho-Chunk occupations. Mr. Jim Bussey, a collector and partial landowner of the site allowed Robert Birmingham to study artifacts that had been collected on the plowed surface of the site. The collection contained both historic and abundant Oneota material; the Oneota component was “located on top of a bluff above the adjacent historic component” (Pozza 2016:21). Jacqueline Pozza (2016) completed her Master’s thesis research comparing copper artifacts from four sites in the Lake Koshkonong locality, including the Crab Apple Point site.



**Location of the Crab Apple Point Site in Jefferson Co., Wisconsin**

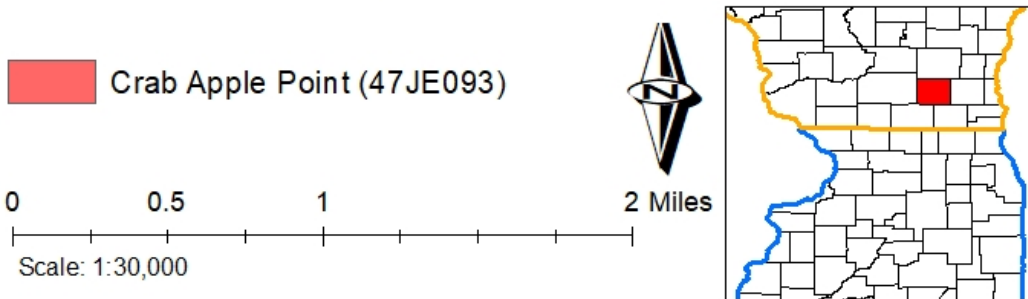


Figure 2.4 Location of the Crab Apple Point site in Jefferson Co., Wisconsin.



In 2017, a collection of ceramics from the Crab Apple Point Site (47JE93) was donated to the UWM-Anthropology Department by Mr. Bussey. These ceramics were collected from the plowed surface of his farm field and therefore only have site-wide provenience information, as the stratified provenience has been lost. In Fall 2017, the UWM Anthropology 535 class completed an analysis of 657 sherds from the collection. These sherds included fifty-three decorated body sherds, seven neck sherds, and 538 rims. Of the sherds in this collection, 91.5% were shell tempered, suggesting that most of the pottery was produced during the Oneota cultural tradition (Auten et al. 2017). The 37 grit-tempered sherds from this collection include both Middle Woodland and Late Woodland types. A sherd from a Shorewood Cord Roughened vessel was selected for this petrographic analysis (2019025).

## **Northwestern Illinois/Mississippi River Trench Sites Selected for Petrographic Analysis**

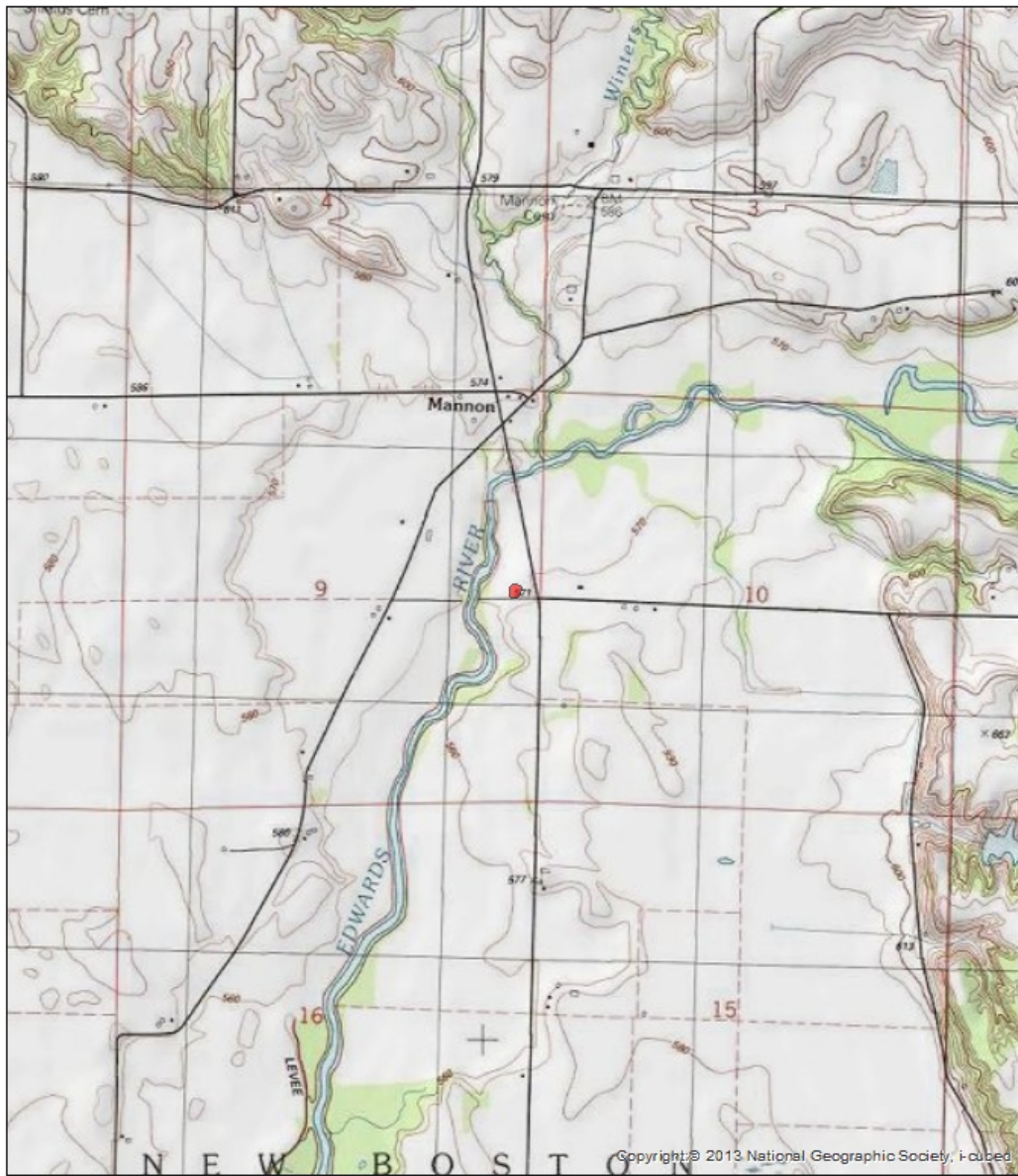
### *Sloan (11MC86)*

The Sloan site is a multi-component site in Mercer County, Illinois (Figure 2.5). The location of the site is “approximately five miles northeast of New Boston, Illinois and ten miles south of Muscatine, Iowa.... The site is situated along the upper and lower portions of a Pleistocene terrace in the Mississippi River bottomlands... approximately 200 meters east of the Edwards River which enters the Mississippi bottomland just north of the site area” (Benchley et al. 1979:3). Three other known Middle Woodland sites are located within ¼ mile of the site along the same geological terrace formation (Benchley et al. 1979).

The Illinois Archaeological Survey (IAS) first recorded the site in 1974 after collecting lithic debitage, grit tempered pottery sherds, and a hoe chip during surface survey. In spring

1978, IAS conducted the first phase of archaeological survey within the right-of-way of Highway Project 1210 for the Illinois Department of Transportation. They identified archaeological material within the highway right-of-way. The UWM ARL began working at the site between late summer 1978 and spring 1979. This second phase of investigations was used to evaluate the site and recover data to determine if the site would be eligible to be included on the NRHP. This work was completed in two phases to sample the site within the highway right-of-way, and to recover data necessary to better understand the site structure. During this investigation, the site was divided into four separate areas: upper terrace, terrace slope, lower terrace, and bottomland. Additionally, a large midden was present in the northern portion of the lower terrace slope. Once excavated, ten features were identified below the midden (Benchley et al. 1979).

The material culture present at the site includes Middle Woodland, Late Woodland, and Historic European artifacts. The material remains on the upper terrace suggests that it was used less in prehistoric times than the lower terrace. Features identified in the upper terrace include two storage/refuse pits and one hearth, but there was no evidence of structures in this portion of the site. The lower terrace suggests much more prominent use during prehistoric times. Features include over 30 storage/refuse pits, the large midden, and scattered post molds that suggest some type of structure. The lower terrace also contained a greater number and variety of artifacts (Benchley et al. 1979:143). The prehistoric pottery recovered from the site can be assigned to Havana and Weaver ware types. The Middle Woodland component of the Sloan Site is primarily dated to the later part of the Middle Woodland based on the ceramics recovered from the midden (Benchley et al. 1979:108).



**Location of the Sloan Site in Mercer Co., Illinois**

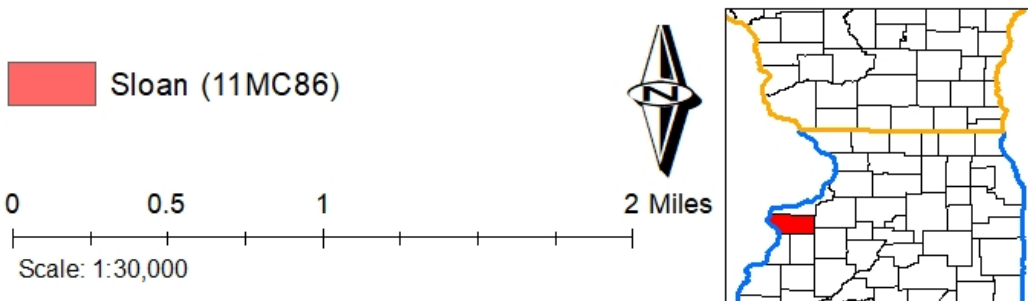


Figure 2.5 Location of the Sloan site in Mercer Co., Illinois.

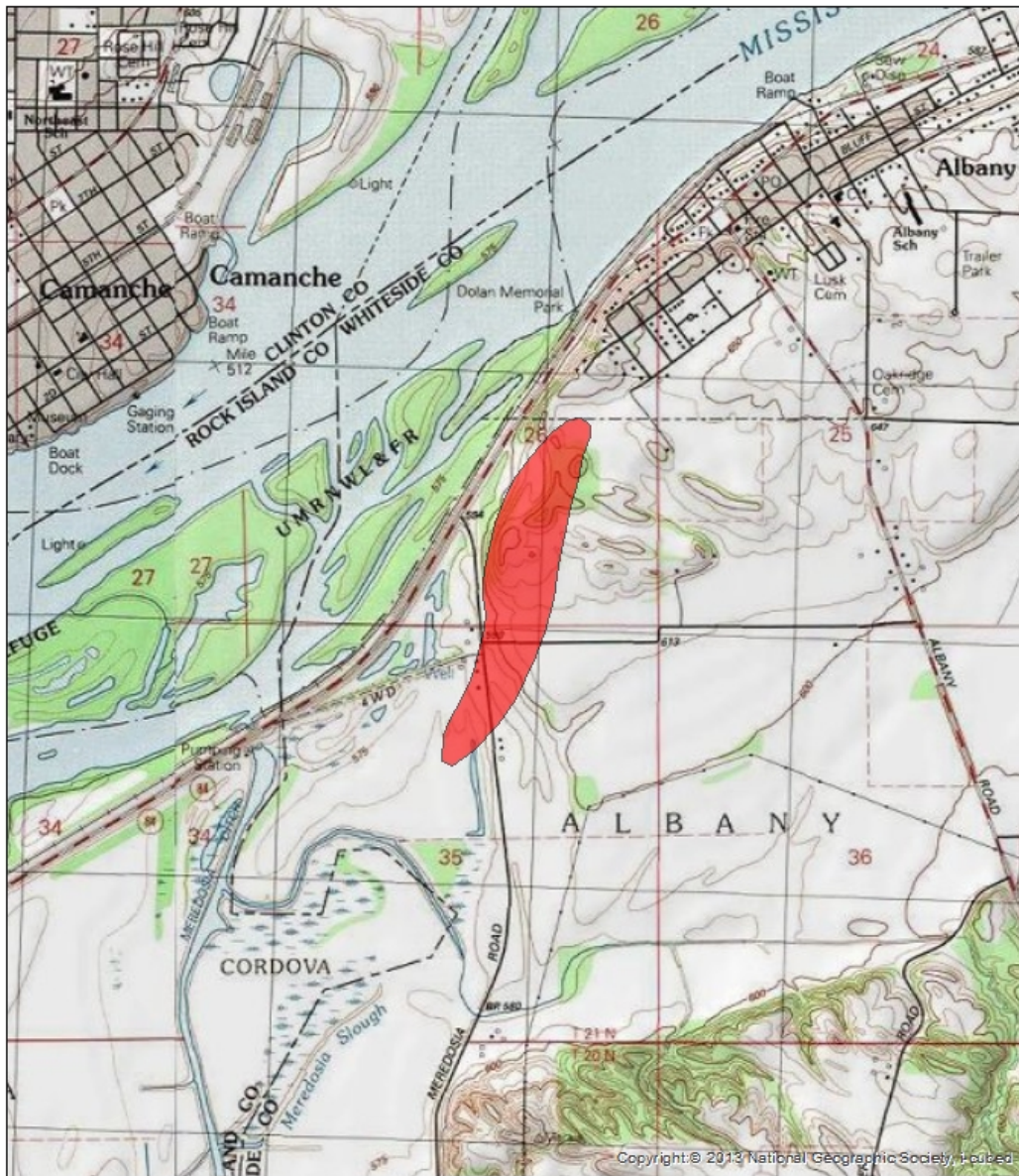
The eight ceramic samples from the Sloan site that were used in this thesis are from the UWM ARL investigations from 1978-1979. The ceramics were recovered in various contexts throughout the investigations. A Naples Stamped Cord-Wrapped Stick variety sherd (2019020) was recovered on the surface. Two Havana Plain samples (2019014 and 2019016) were recovered from Test Pit 31. A Havana Zoned Dentate sherd (2019021) was recovered from Test Pit 39. Three samples were recovered from the midden: Hopewell Rocker Stamped (2019018) in level 4, Naples Stamped Cord-Wrapped Stick (2019015) in level 5, and an unclassified Havana (2019019) in level 6. An additional Hopewell-type sample (2019017) was recovered in Feature 40, a basin that was located beneath the midden.

#### *Albany Village/Albany Mound Group (11WT1)*

The Albany site is located in Whiteside County, Illinois (Figure 2.6). Earliest investigations at the Albany site began in 1873 when the site was first mapped, and two mounds were excavated by W.H. Pratt (Benchley and Gregg 1975). At that time, 81 mounds were identified, and early mound investigations were conducted by the Davenport Academy of Natural Science in Davenport, Iowa. Several mounds were excavated around the turn of the twentieth century. These early excavations did not include detailed descriptions of the cultural material, human remains, and mound construction. However, some topographic maps of the mounds were created, and a checklist of cultural material was generated (Benchley and Gregg 1975).

In 1971, Elaine Bluhm Herold compiled the earlier excavations into a book about the site. In this research she created a list of material culture from the site, including common Middle Woodland artifacts such as marine shell, sheet mica, and Havana related ceramics (Herold 1971;

Benchley and Gregg 1975). Private collections of artifacts from the village area of the Albany Site were examined also. These collections contained additional Havana and Hopewell materials such as copper awls, lithic tools made from obsidian, Flint Ridge chert and Hixton Silicified Sandstone, a ceramic figurine fragment, a Hopewell red-filmed bowl, cut mica, and several types of Havana and Canton ware (Benchley and Gregg 1975). Unfortunately, the provenience of these materials was not well documented and much of the village site was destroyed by the construction of Route 80 in 1930 and the reconstruction of Meredosia Road in 1959 (Benchley and Gregg 1975).



**Location of the Albany Village/Albany Mound Group Site in Whiteside Co., Illinois**

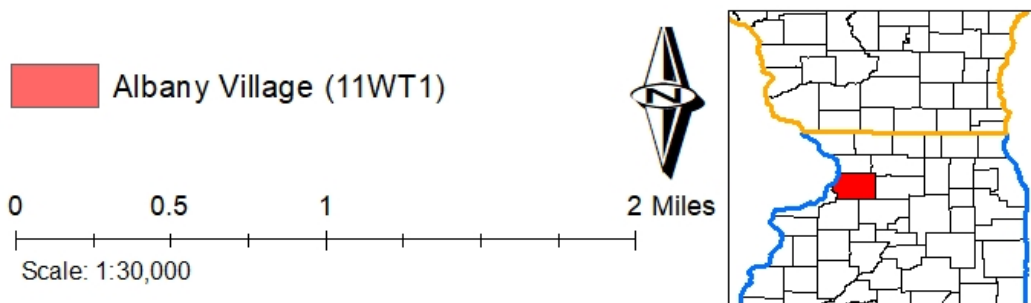


Figure 2.6 Location of the Albany site in Whiteside Co., Illinois.

The checklist of material and Herold's research was used by archaeologists from UWM to make some interpretations of the cultural history of the site. Based on the presence of Black Sand Incised and Morton Incised pottery, it is expected that the site contained a later Early Woodland period occupation. Early and Middle Havana occupation is represented by ceramic types, lithic types, and exotic raw materials. In addition, the Canton ware assemblage represents Late Woodland occupation (Benchley and Gregg 1975). Of the 81 mounds originally identified at the site, only 36 were located by UWM archaeologists (Benchley and Dudzik 1976).

In 1975 the UWM ARL was contracted by the Illinois Department of Conservation to complete survey of the site area as well as the broader Meredosia Levee and Drainage District near Albany, Illinois. This project was established to define the Albany site boundaries as well as locate any other archaeological sites within the construction right-of-way (Benchley and Gregg 1975). During this survey, cultural material from Early, Middle, and Late Woodland periods were recovered from the site. Test units were also excavated to further understand the subsurface context at the site. The material culture excavated from Test Unit 3 showed evidence of a deep midden context, with artifacts accumulated from Early Havana through Weaver periods (300 BC – AD 750). While not all parts of the site harbor material evidence throughout this timeframe, it can be suggested that there was some continuous occupation within the site area during these periods (Benchley and Gregg 1975). The sample selected for this analysis is a Naples Stamped rim sherd (2019022) from Level 7 of Test Unit 3, within the midden context. Other ceramics from this level include Weaver ware, Havana ware with rocker stamped and punctate decorations, and a Steuben Punctated sherd.

## *Illinois Predictive Model Surveys*

During the 1970s, UWM was contracted to develop predictive models for archaeological site locations along rivers in Illinois. As part of the project, both the Upper Mississippi River Valley and the Rock River Drainage were subjected to pedestrian survey to identify previously unrecorded archaeological sites. Because these large-scale surveys identified over 100 sites during each project, little detail was provided for the individual sites, including Blythe (11HA40) and DeWitte/Liphardt Habitation (11RI57), that are included in the present analysis. For both surveys, archaeologists collaborated with local collectors who could provide information about parts of the survey area that contained greater concentrations of artifacts. Therefore, more specific details about the context of each site was not available and sample sherds have only site-level provenience.

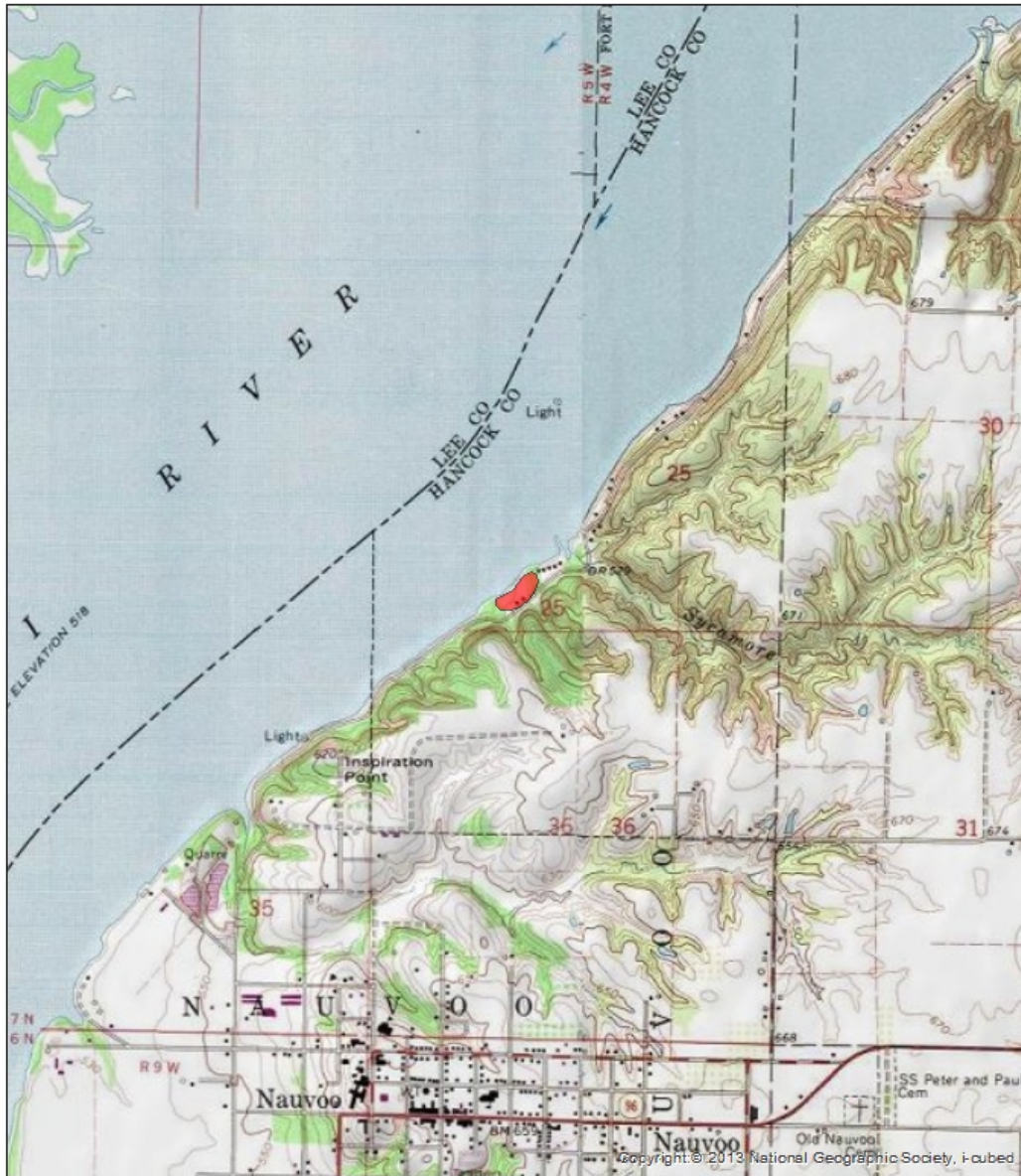
### *Blythe (11HA40) – Upper Mississippi River*

In 1973, a twelve-week reconnaissance project was established within a region of “approximately forty river-miles” (Fowler and Dudzik 1973:76) within the Mississippi River floodplains and the valley slopes of the tributaries in Henderson and Hancock counties, Illinois (Fowler and Dudzik 1973). One of the sites identified in Hancock County was the Blythe site (11HA40) (Figure 2.7).

According to the IAS site catalog, the site was first identified during the UWM survey after the archaeologists were directed by local collector Charles Harrison. At that time, the westernmost portion of the site was eroding out of a bank along the Mississippi river. Cultural material recovered from the site include lithic flakes and an expanding stem point, bone fragments, fire-cracked rock, and cordmarked, plain, and cord-impressed pottery. A Havana



Cordmarked sherd (sample 2019026) from the Blythe site (11HA40) was selected for this analysis. Cultural features were also identified and were located along the eroding bank; both features were interpreted as garbage pits (IIAPS).



**Location of the Blythe Site in Hancock Co., Illinois**

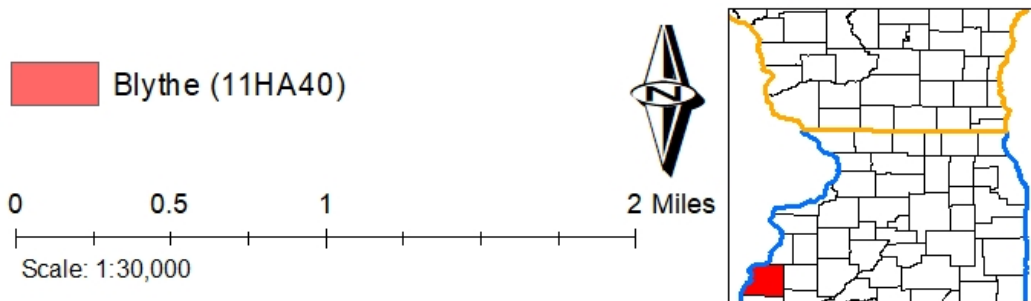
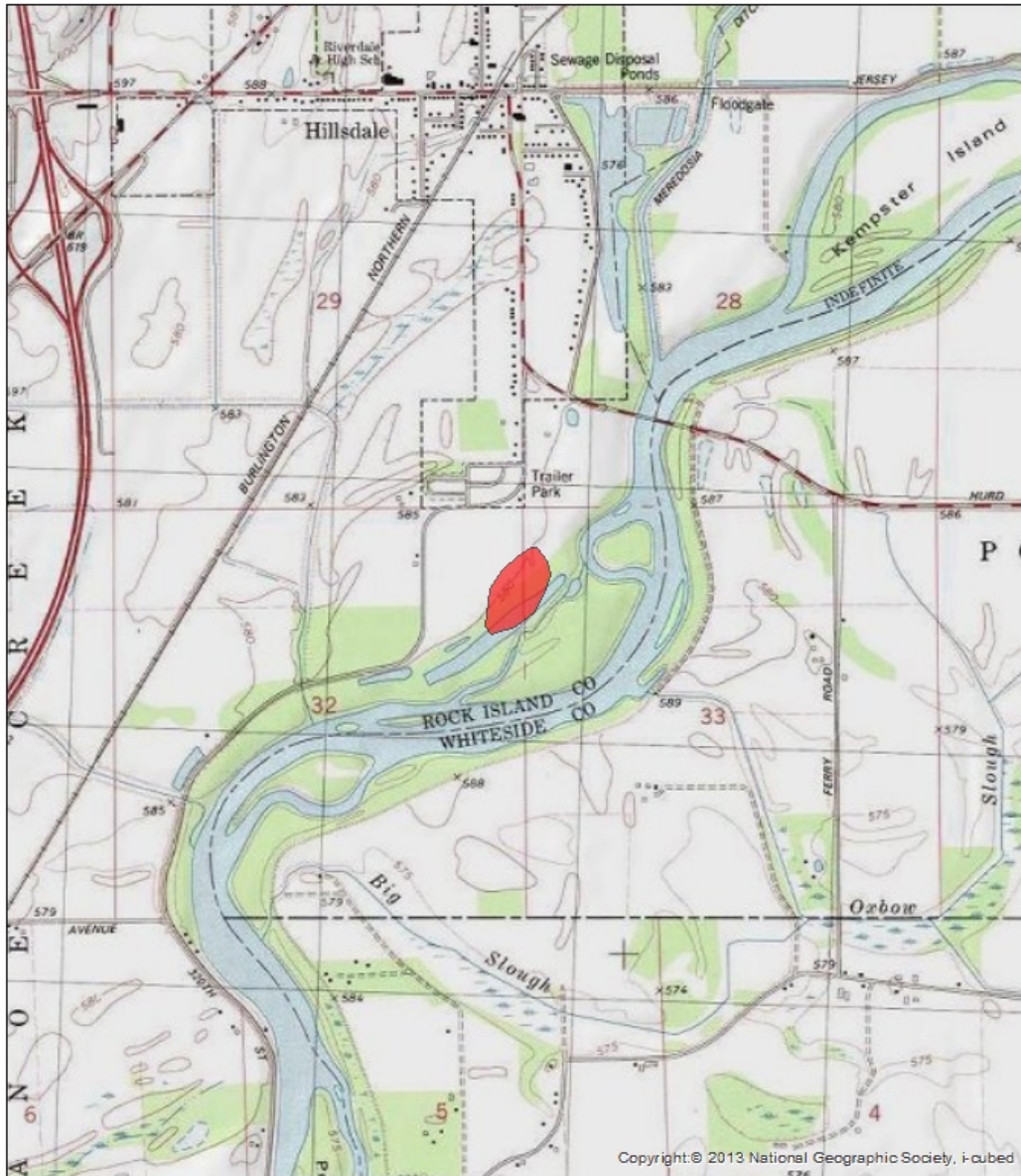


Figure 2.7 Location of the Blythe site in Hancock Co., Illinois.

### *DeWitte/Liphardt Habitation (11RI57) – Rock River*

In 1977, the UWM ARL was contracted by the Illinois Department of Conservation to conduct pedestrian survey in the Rock River drainage (Benchley and Billeck 1977). The survey area was constrained to the “mouth of the Green River to the south and Hillsdale, Illinois to the north” (Benchley and Billeck 1977:1). The DeWitte/Liphardt Habitation site (11RI57) was one of the sites surveyed for this project in Rock Island county (Figure 2.8).

According to the IAS site catalog, the site was initially identified and mapped by Newman and Elliott in 1933. It is located on a long sand ridge approximately 200 feet west of the Rock River, abutting a slough on the north end. Previously documented artifacts recovered from the site include lithic flakes and projectile points, and cordmarked, punctate decorated and incised pottery sherds. The earlier catalog sheet notes that “large quantities of mussel shell, animal bone, and fire-cracked rock are plowed up” annually. The site is attributed to Early, Middle, and Late Woodland occupations (IIAPS). During the 1977 survey, a local collector, Mr. Webb, allowed UWM archaeologists to inspect his collection from the site, and it was noted that he gave several sherds to UWM. A Hummel Stamped sherd (sample 2019027) from the DeWitte/Liphardt Habitation site (11RI57) was selected for this analysis.



**Location of the DeWitte/Liphardt Habitation Site in Rock Island Co., Illinois**

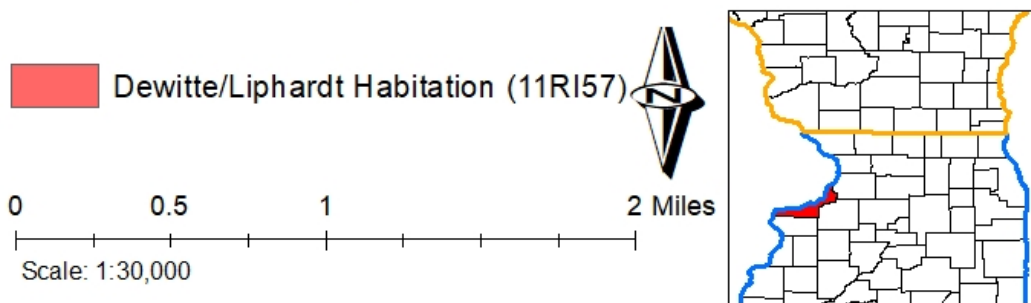
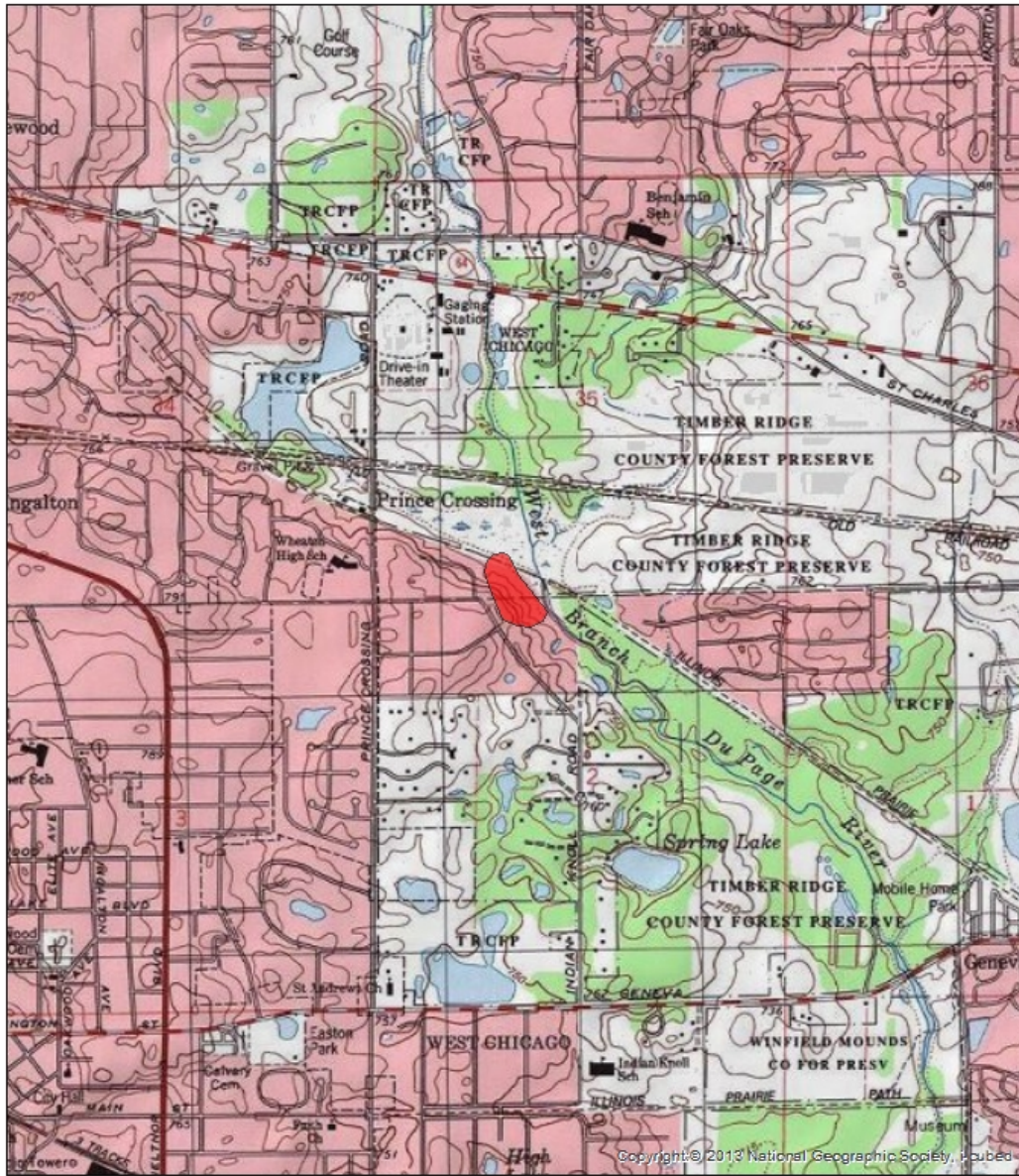


Figure 2.8 Location of the DeWitte/Liphardt Habitation site in Rock Island Co., Illinois.

## **Northeastern Illinois**

### *Kautz (11DU46/1)*

The Kautz site is located in DuPage County in northeastern Illinois (Figure 2.9). The site is located on a knoll above the floodplain, approximately 200 yards west of the West Branch of the DuPage River (Geraci 2016). It was originally identified by Joseph T. Kautz, the landowner who had collected artifacts from his farm (Geraci 2016:41). In the 1950s, archaeologists were made aware of the site, possibly while conducting a survey of sites along the DuPage River. Sanford Gates, David Wenner and Hank Rodemaker contacted the Kautz family to document the site (Gates 1983; Geraci 2016). It is suspected that during this time the pig pen area of the site, where “the Kautz’s had collected points” was assigned the 11DU5 site number (Geraci 2016; Wenner 1960:1-2). David Wenner and a group of volunteers including students from the University of Chicago and family members of Gates and Rodemaker returned to the site in 1958 after the landowner dug two small areas about a foot deep and found additional archaeological material in a separate, uncultivated area of the Kautz’s farm (Geraci 2016; Wenner 1960). These artifacts included “several dozen large Hopewell sherds and rims” (Wenner 1960:2). The archaeologists investigated the two small areas and recovered bone, Late Woodland pottery, and a Middle Woodland sherd. Wenner (1960:2) also described the pottery recovered by the landowner as being large for the area and having “dentate, zone dentate, beveled rims, notched lips (interior)” decorations.



**Location of the Kautz Site in DuPage Co., Illinois**

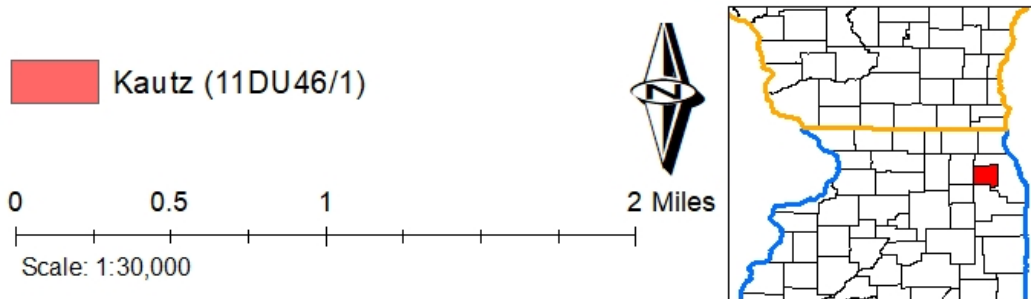


Figure 2.9 Location of the Kautz site in DuPage Co., Illinois.

Due to the presence of Hopewellian artifacts at the site, Wenner conducted excavations in November of 1958. Wenner assigned the site number 11DU46 to track the site and the material excavated there. At this time, no formal database of Illinois archaeological sites existed, so the site was not formally recorded until after the excavations. When the IAS was established, the site was cataloged as part of a statewide database, and the site was assigned number 11DU1 (Geraci 2016). Excavations were led by Wenner and a crew of volunteers and continued until at least July 1960, when the excavation notes stop. During this time, the excavations were organized into two separate units. Fifty 5-x-5-foot squares and five 1-x-5-foot squares were excavated in Unit 1 and six 5-x-5-foot squares were excavated from Unit 2. The excavated squares were removed in two stratigraphic levels. The upper level (Level I) was a dark black humus (buried A-horizon) that extended approximately six to eight inches below the sod layer (7-10 inches below the surface). Below this was a transitional dark grey clay horizon with gravel-sized rocks (Level II) above the original brownish-yellow clay and gravel (Bt Horizon) (Geraci 2016:43; Schenian 1983; Wenner 1960).

Artifacts recovered from the site include chipped stone tools, debitage, ceramic sherds, rough rock, faunal material, as well as some historic material (Geraci 2016; Schenian 1983; Wenner 1960). A single sherd of Havana Zoned (sample 2019023) from the Kautz site was selected for the thin section analysis. The sherd likely was recovered from excavation square 0E 15N but original documentation for this square could not be located with the other paperwork that is currently housed in the UWM ARL Archives facility (Accession# 1960.2, Object ID# 1960.2.7). Nonetheless, it is likely that the sampled sherd came from the 0E 15N square in Unit 1 based on the artifact label (I:0E 15N/I). Maps detailing the distribution of artifacts within each

square suggest that artifacts recovered from Square 0E 15N included 18 prehistoric ceramics, 27 lithics, 6 bones, as well as 8 pieces of historic glass.

## **Ceramic Petrography**

Petrography is a specialized technique initially developed by the geological sciences to estimate the mineral composition of a rock. To identify this composition, rock samples are sliced into thin sections that are affixed to glass microscope slides. Slides are then viewed using a variety of microscopy techniques that allow identification of the mineral constituents of a sample. These thin cross-sections of the samples provide an “unbiased sample of the composition of the rectangular prism from which it is cut” (Chayes 1956). By counting the minerals that make up the sample and calculating the percentage of each mineral against the volume of the rock or the percentage of individual grains, an analyst can determine the overall composition of the rock from which the thin section is taken (Chayes 1956; Stoltman 1989). The percentages from the thin section can then be extrapolated to determine these percentages across the whole rock.

Archaeologists have adapted the method used by geologists to analyze the composition of archaeological ceramics. Riederer (2004) identifies three types of information that can be gained from conducting thin section analysis. First, the process provides precise and detailed information on the mineralogical composition of the temper and natural inclusions in the paste; second, it allows the calculation of accurate percentages of temper and inclusions in the paste, as well as size distribution; and third, it can be used to estimate baking temperature if the minerals have been transformed at high temperatures.

In Middle Woodland contexts, the trade of exotic materials of the Hopewell Interaction Sphere are often studied due to the specific locations of raw material origin. For cultural



materials like pottery, the same level of research has not been emphasized. James Stoltman's work is an exception (Stoltman 2015; Stoltman and Mainfort 2002). However, this type of research can be useful to understand exchange within a particular region (Fie 2008).

Archaeologists can use petrographic analysis to look at the more localized cultural contexts and identify variations between the recipes of ceramic production that may be characteristic of certain groups in a particular region. Through the identification of minerals, petrographic analysis can be used to identify the physical movement of pottery between sites or regions. If transportation occurs, it is expected that the pottery at one site would contain the same minerals as another site (Chivis 2016; Bishop et al. 1982; Schneider 2015).

The local geology in a region is often important to interpret petrographic analyses. In southeast Wisconsin and northeast Illinois, the bedrock geology is primarily made up of sedimentary rocks from the Silurian and Ordovician periods of the Paleozoic Era. These may include dolomites, shales, some limestone and some sandstone (Wisconsin Department of Natural Resources 2011). In the northwest region of Illinois, the Pennsylvanian, Mississippian, Silurian, and Ordovician periods of the Paleozoic Era are predominately represented by dolomites and limestone, with some Lower Ordovician sandstone also present (Illinois State Geological Survey 2005). The bedrock geology of a region may indicate what types of rocks were available as tempering agents.

## CHAPTER 3: METHODS

### Introduction

This thesis examines the variability in ceramic pastes from Middle Woodland sites in Wisconsin and Illinois to identify possible patterns in ceramic production. This chapter discusses the methods used to select the samples used in the analysis and collect the initial attribute-based information of the samples; conduct petrographic analysis using thin sections to identify temper and paste characterization, grain size and texture, and minerals in the samples; use ternary diagrams to analyze the data collected for this thesis; and conduct statistical analysis based on the compositional data.

While this study uses a limited sample, the methods described here can be used for further analysis of Middle Woodland vessels to build a comparative database of Waukesha phase and Havana Hopewell ceramic pastes. The attribute-based ceramic analysis of the selected sherds identifies temper and paste characterization, grain size and texture, and paste core cross-sections. The analysis also reports a variety of metric and morphological data as detailed below. All data from this analysis has been compiled in a digital database for ease of future access. The maps throughout this thesis were created using ArcGIS software by Esri (Esri 2020).

Thin sections of sherds from selected sites were prepared by National Petrographic Service, Inc. at a cost of \$23.50 per sample. This cost includes slide preparation, impregnation of samples with epoxy, and a slide cover. The samples were analyzed for paste composition and identification of minerals by the author. Collections from all the included sites are housed at the UWM ARL and permission to conduct the destructive analysis was granted by the ARL. Upon completion of this thesis project, ceramic thin sections will be accessioned into the ARL's

permanent collections. Data sets and thin sections will be made available for additional analyses by other researchers.

## **Sample Selection**

The initial selection strategy was aimed at collecting a robust sample of Waukesha Phase pottery types from multiple sites in southeast Wisconsin. The sample was later expanded to include examples of Havana Hopewell pottery from multiple sites in northwest Illinois. A single sample from northeast Illinois was also included in the analysis. Sample selection was constrained by the need to select sherds that were available in the UWM ARL collections and for which permission to conduct destructive analysis was granted.

Upon selection of the samples, an inventory was created in a Microsoft Access database to track details for each of the samples. Ceramic attribute and archaeological provenience data were collected for each sample and added to the inventory. Each sample was assigned a unique sample number which included the year that the sample was selected and a sequential number, the sample numbers ranged from 2019001 to 2019027. Identification information included site name, site number, lot number, artifact number, unit number, vessel number and Research Growth Initiative (RGI) sample number. Not all samples had the same provenience-based information, but the inventory was completed to the extent that it could be for each sample (for example, not all samples had lot numbers and only those sherds formerly analyzed as part of an RGI grant awarded to John Richards and Robert Jeske were identified by those numbers). The attribute-based information included documenting the sherd type (rim, body, etc.), vessel form, rim stance, rim form, rim width, lip form, surface treatment, temper, paste core, decoration style, decoration location, and pottery type. Metric data recorded included orifice diameter, wall

thickness, rim width, and weight. Each sherd in this study represents an individual vessel, diagnostic of the Middle Woodland period in northern Illinois and southeast Wisconsin.

Attribute data were collected before submitting sherds to be processed into thin sections as this is a destructive process that can destroy part or all of the sherd. The morphological analysis compares the attribute data from the samples among the selected sites. Primarily, the samples are rim sherds of diagnostic Middle Woodland vessels. In some cases, like three of the Finch site samples, body sherds definitely associated with an identified vessel were used to reduce destructive processes on rim sherds. Additionally, two body sherds were selected as samples from the Sloan site due to the diagnostic decorative style on the exterior of the samples.

### **Attribute Data Collection**

Vessel morphology was difficult to determine for some samples because the only extant sherd was the piece used for this analysis, and at times the sherds were relatively small. Rim sherds in the sample are almost all jar forms but one sample (2019001) from the Peterson site comes from a Hopewell-like incised bowl.

Rim profiles were drawn for each sample and orifice diameters were estimated using a graduated circle chart. The diameter is estimated by comparing the rim curvature to the concentric circles on the chart. The rim sherds can provide the most information regarding vessel shape and size.

Rim stance is the orientation of the rim to the horizontal plane of the orifice. Direct, slightly everted, slightly inverted, everted, and indeterminate rim stances were identified in this analysis. Direct rims have a wall thickness that is similar to the thickness of the vessel wall

below the neck and follow the contour of the vessel side (Shepard 1956:246). Following Haas (2019b), everted and slightly everted rims have an orientation exceeding 90 degrees, and slightly inverted stances have an orientation less than 90 degrees. Rims that were too small to determine the rim stance were labeled as indeterminate.

The rim shape classifies changes in wall thickness from the neck to lip of a vessel. Rim shapes identified in this analysis include folded, pinched, and unmodified. Folded rims have a visible crease on the exterior rim margin where the clay was folded over. Pinched rims become less thick towards the lip. Unmodified rims are the same thickness from the neck to the lip (Haas 2019b). The lip of the vessels also varied between flattened, beveled, and rounded. Flattened lips “create a planar surface along the outer rim margin on a direct rim” and “separates the outer and inner rim margins” (Haas 2019b; Richards 1992). Rounded lips have a gentle convex separation between the exterior and interior surface. Beveled lips create a sloped flattening of the rim towards the exterior or interior of the vessel (Haas 2019b).

The firing and cooling atmospheres of production can be determined by the coloring of vessel paste cores (Rice 1987; Rye 1981; Sinopoli 1991). Generally, dark-colored cores represent a reduced atmosphere where airflow around the vessel is restricted, and light-colored cores represent an oxidized atmosphere where the airflow is unrestricted. Vessels showed some variability, including oxidized interior surface and reduced exterior surface, reduced interior surface and oxidized exterior surface, and oxidized exterior surface and reduced core. Some vessels had uneven core coloring and could not be classified as one of the standard patterns.

Temper is the aplastic material added to natural clay that modifies the properties of the clay paste during production (Rice 1987:406). The samples in this analysis all contain grit, or

crushed rock, tempering. Two samples contain a mixture of both grit and grog temper (2019018 and 2019020). Granite, limestone, and chert were identified in the ceramics. The minerals in both the clay matrix and the grit temper were identified during the petrographic analysis.

The surface finish of both interior and exterior vessel walls was recorded. Smoothed, cordmarked, and smoothed-over cordmarked surface treatments were identified in this collection of ceramics.

Decorative elements were recorded and measured using digital calipers to determine width and length, or diameter of circular decorative elements, when possible. Types of decoration include punctates, bosses, incised lines, cord-wrapped stick impressions, cord impressions, and stamping (linear, rocker, dentate, cord-wrapped stick) varieties.

Additional metric data were also collected for each sample. Because of the destructive process of thin sectioning, the metric data were collected before the samples were sent to be processed. The weight in grams of samples was recorded for each sample using a digital scale. The thickness of the samples was recorded at both the rim and the wall of the samples. These measurements were collected using a digital calipers and averages were calculated taking the mean of two measurements on either side of the sherd sample. Rim thickness was measured at opposite sides at the top of the rims. Wall thickness was generally measured at the furthest points from the rim, where the sample was unexfoliated, on both sides of sample.

### **Petrographic Analysis**

Ceramic thin section petrography was used to collect data on ceramic paste composition. The technique allowed identification of the mineral constituents of the paste as well as estimates

of the percentage of sand, silt, and clay present. The methods used in this research are based on the work of Stoltman (1989, 1991, 2001, 2015) as well as Schneider (2015). The sherds from each site were processed into ceramic thin sections, in which a small piece was cut from the original sherd, attached to a microscope slide, and ground to a thickness of 33 microns (National Petrographic Service, Inc. 2018) The process of point counting and mineral identification was conducted under the direct supervision of Dr. Seth Schneider who has utilized the technique on a variety of Illinois and Wisconsin pottery types.

Prior to sending samples to National Petrographic, each sherd was given an arbitrary identification number (2019001 through 2019027) and sherds were then placed in individual bags with the corresponding numbers. These numbers were used by National Petrographic to track samples. Once a sample was adhered to a microscope slide, the corresponding sample number was engraved into the glass.

After the samples were processed into thin sections and placed on microscopic slides, a polarized OMAX Trinocular Infinity Polarizing Microscope M838PL Series with a measuring eyepiece was used to observe the paste and mineral inclusions for each sample. To conduct the analysis, a 1 mm interval grid was used to collect at least 100 points from each sample. At every 1 mm point, the grain directly below the eyepiece crosshair was identified for that location. These points were recorded under several categories, including matrix, silt, sand, grit temper, grog temper, or voids. Any clay minerals (<0.002 mm) that were too small to be identified or measured were classified as matrix. Silt particles (0.002-0.0625 mm) were visible but too small to be classified as sand or temper. The sand, grit and grog tempers were further divided into size grades based on grain size scales. These sizes included fine (0.0625-0.24 mm), medium (0.25-0.49 mm), coarse (0.5-0.99 mm), very coarse (1.0-1.99 mm), and gravel ( $\geq 2.0$  mm). In general,

sand grains were identified as natural inclusions and differentiated from temper because of the relatively round shape and single mineral make-up, while grit temper grains were generally more angular in shape and contained multiple minerals (Chivis 2016; Druc 2015; Stoltman 1989, 1991, 2001, 2011; Schneider 2015). Fowler (1955) identifies crushed rock as the tempering agent in Havana ware and crushed limestone and other crushed rock in Hopewell ware. Minerals can be identified based on their distinct colors, relief, extinction of light in cross-polarized light, and interference signals produced by their crystalline structure (Perkins 1998; Schneider 2015:265-267).

Each sample was counted individually, beginning at one edge of the sample and traversing back and forth across the x-axis stopping at one-millimeter intervals to observe which part of the paste was located below the crosshair on the microscope reticle. For all samples, the points were collected with the microscope at the 10x power. To identify specific minerals, or to calculate the size of natural or human added inclusions the objective was switched to the different magnifications (4x, 20x, etc.) depending on specific cases. It was necessary to keep track of which objective was being used to calculate the size of the inclusions, as the calculation varied depending on the power. In total, a minimum of 100 points were counted for each sample, not including voids. If a sample did not yield at least 100 counts in the first round, the thin section was rotated 180 degrees and counted a second time. Based on the size of the samples, more than 100 points were often counted, as the points were tracked until the entire plane of the cross-section was sampled. The use of this systematic sampling method was employed to guarantee that an unbiased and representative sample of ceramic paste was calculated for each sherd (Chayes 1954; Stoltman 1989, 1991; Schneider 2015).



A chart was used to keep track of each point counted during this process. Anything that was too small to be measured was marked as matrix. If an inclusion was silt sized (0.002-0.0625 mm), it was marked as such. Due to the small size of silt-grain particles, the minerals at this size were not always identifiable. If the minerals could be identified on any silt size particles, they were tracked on a mineral identification chart. If an inclusion was larger than silt size, its coarseness was tracked based on the size, and whether it was naturally occurring or added as grit or grog. Naturally occurring inclusions were marked as sand particles and were identified as single-mineral inclusions with rounded edges. Added grit inclusions often showed characteristics of multiple minerals and more angular edges. This is an indication that that the grit inclusions were derived from crushed pieces of stone or conglomerate. Additionally, two samples (2019018 and 2019020) contained grog inclusions. In both of these samples the grog was in the fine size category and marked as added temper.

### **Ternary Diagram**

Using the point data, proportions of each sample composition were calculated based on the presence of clay, silt, sand and temper. Using these proportions, the body, “the bulk composition of a ceramic vessel, including clays, larger natural mineral inclusions in the silt, sand, and gravel size ranges, and temper”, (Stoltman 1991:109) and paste, “the aggregate of natural minerals, i.e., clays and larger mineral inclusions, to which temper was later added to produce the body from which a vessel was made” (Stoltman 1991:109-110), were distinguished for each vessel. The point counting data for both the body and paste were documented in tabular form. To more easily interpret the data, the proportions were entered into an Excel table and incorporated into a ternary diagram using Todd Thompson Software’s TriPlot (v 4.1.2) (obtained from <http://mypage.iu.edu/~tthomps/programs/html/tnttriplot.htm>).

The ternary diagram visually displays the amount of variation between samples. The poles of the body diagram are labeled: matrix (both clay and silt), temper, and sand (all natural mineral inclusions larger than silt). This diagram is used to visually represent the “relative volumetric proportions of all mineral inclusions in each vessel, with particular emphasis on temper” (Stoltman 1991:111). The paste diagram poles are labeled as: clay, silt, and sand. The paste diagram is used to “provide a visual representation of the relative volumetric proportions of the silt, sand, and clay in the untampered raw materials from which each vessel was manufactured” (Stoltman 1991:111). For both body and paste diagrams, the voids that were counted during the analysis were not included (Stoltman 1991; Schneider 2015). Examples of ternary diagrams displaying paste and body composition data are provided in Figures 3.1 and 3.2.

The ternary diagrams can be used to visualize any clustering in the samples based on various factors. The diagrams can display the ratios of both paste and body across all sites in the analysis, based on location, either separating Illinois from Wisconsin sites, or further separating the sites along the Mississippi River from the more eastern Illinois sites. The diagrams can display the comparisons between samples of specific decorative and diagnostic styles, including Waukesha types, Havana wares, Hopewell-related wares, and unclassified Havana/Middle Woodland.

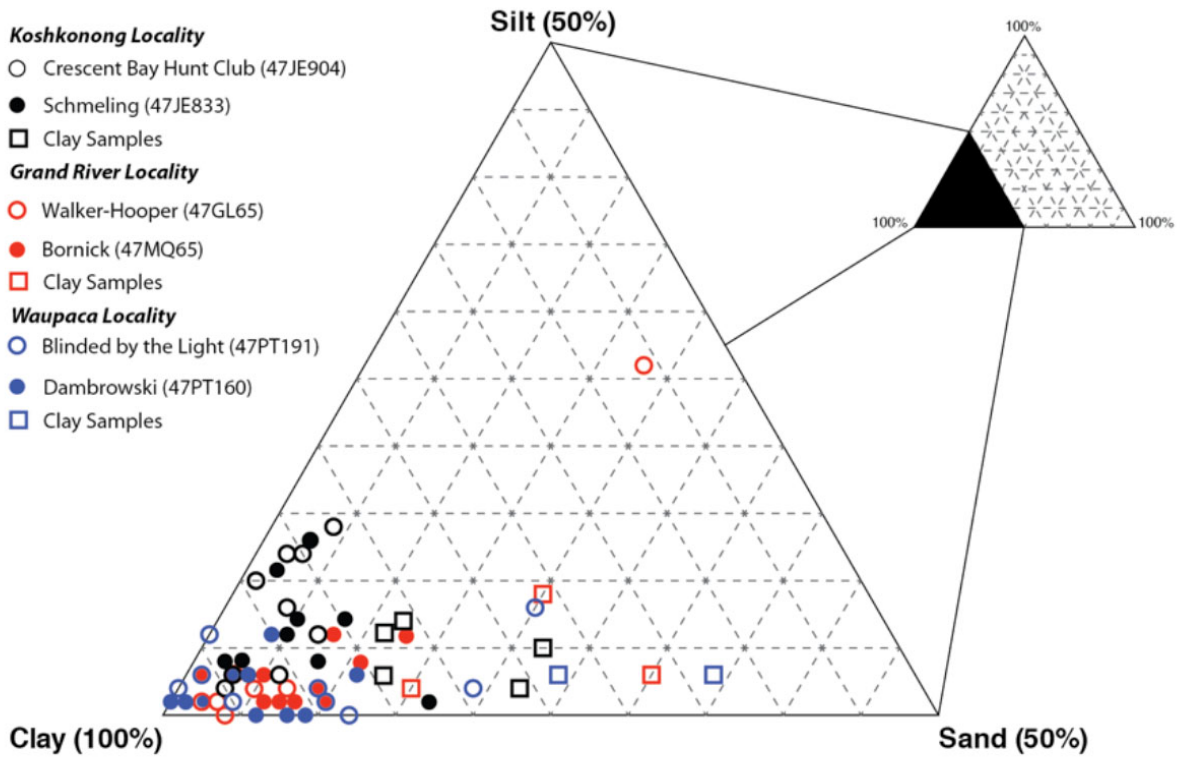


Figure 3.1 Example ternary diagram of ceramic paste composition data (after Schneider 2015, Figure 6.10).

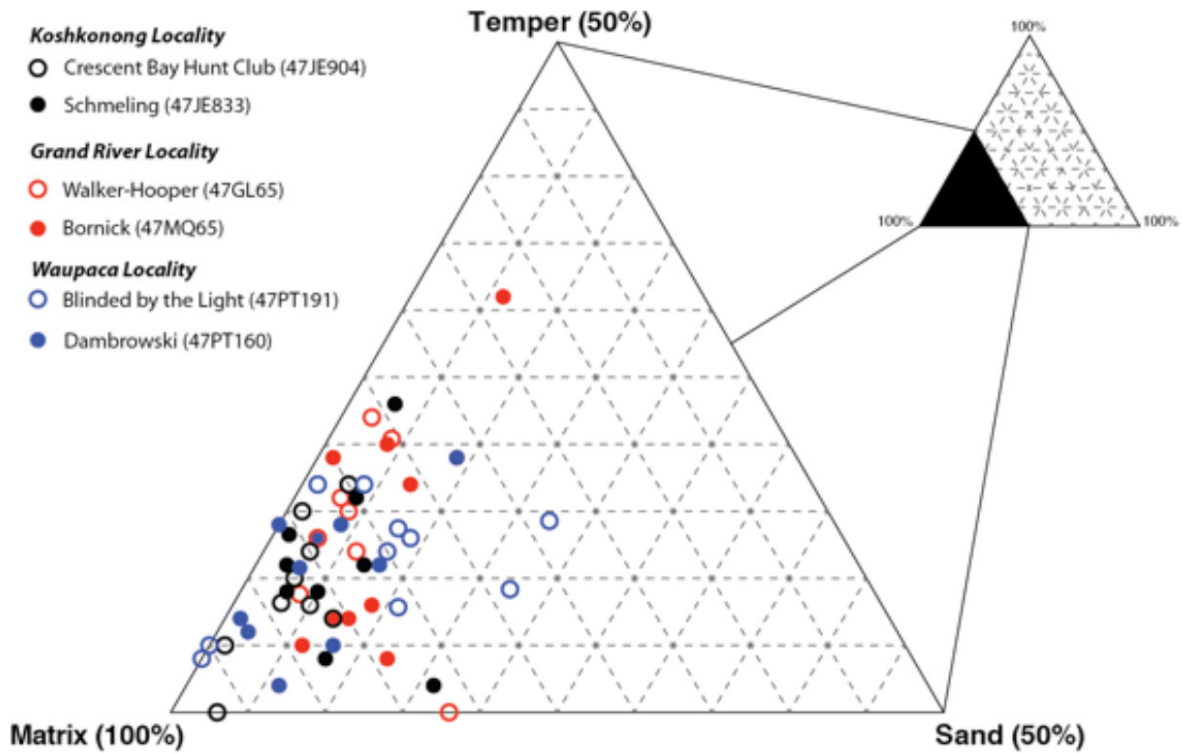


Figure 3.2 Example ternary diagram of ceramic body composition data (after Schneider 2015, Figure 6.6).

In addition to tracking if inclusions are natural or human-added and the size grade of each inclusion, mineral and rock types were also identified and inventoried. This inventory was used to “identify those minerals whose presence, absence, or relative abundance would seem to warrant special consideration” (Stoltman 1989:149) such as possibly diagnostic inclusions in certain ceramic pastes. The qualitative identification of minerals in ceramics is used in conjunction with the quantitative proportions of body and paste to more accurately compare items between archaeological assemblages, and to identify the type of temper, rather than just the size grade and presence of temper (Stoltman 1989, 1991).

## Statistical Analysis

Using the R (v 3.6.3) statistical software program (The R Foundation for Statistical Computing 2020), the point counting data were subjected to simple statistical regression analysis. For the paste compositional analysis, the proportions of clay, silt, and sand were subjected to Analysis of Variance (ANOVA) statistical tests to determine the amount of variation in the natural pastes between sites. For the body compositional analysis, the proportions of clay, sand, and temper were subjected to ANOVA statistical tests to determine the amount of variation in the recipes between sites. An isometric log-ratio transformation was used to open the closed composition data and move it into Euclidean space, and the regression analysis was used to see if the compositions can be predicted by sites. The plotout function creates isoproportion lines and 90% and 99% confidence intervals for each site. The confidence intervals are represented by ellipses around each site point. The ellipses cross the isoproportion line that identifies the relationship between each compositional variable in the ternary diagram. Ellipses that cross the isoproportion lines indicate no significant difference in the composition between the sites. Ellipses that do not cross the isoproportion lines and plot apart indicate significant difference in composition between sites. (Seth Schneider 2020, personal communication). This form of analysis was chosen as a supplement to the ternary diagrams compiled using the TriPlot software. The analysis was applied to refine the compositional differences observed in the petrographic data tables and ternary diagrams from the point counting.

## CHAPTER 4: ANALYSIS AND RESULTS

### Introduction

Table 4.1 lists basic morphological and metric data for the sample assemblage.

Additional attribute data may be found in Appendix A.

TABLE 4.1 SAMPLE MORPHOLOGICAL AND METRIC DATA

Sample	Site Name (Number)	Type	Exterior	Interior	Temper	Core (Int/Ext)	Wall Thickness Avg. (mm)	Rim Shape	Rim Width Avg. (mm)	Lip Shape	Orifice Diameter (cm)	Orifice %	Vessel Form	Ware Type	Pottery Type	Weight (g)
2019001	Peterson (47WK199)	Rim	smooth	smooth	grit	reduced	5.795	folded	7.045	flattened	20	5	bowl	Hopewell-Related	Hopewell-Like Incised	6.22
2019002	Peterson (47WK199)	Rim	smoothed-over cordmarked	smooth	grit	ro	6.275	folded	7.71	beveled	18	5	jar	Havana Ware	Steuben Punctated	12.68
2019003	Peterson (47WK199)	Rim	smooth	smooth	grit	uneven	7.4	folded	9.46	beveled	20	2.5	jar	Havana Ware	Steuben Punctated	25.17
2019004	Peterson (47WK199)	Rim	smoothed-over cordmarked	smooth	grit	or	7.39	unmodified	7.43	rounded	30	2.5	jar	Havana Ware	Steuben Punctated	13.04
2019005	Peterson (47WK199)	Rim	cordmarked	smooth	grit	uneven	7.63	folded	7.24	flattened	20	5	jar	Rock Ware	Shorewood Cord Roughened	26.57
2019006	Peterson (47WK199)	Rim	cordmarked	smooth	grit	uneven	9.655	folded	9.995	rounded	40	7	jar	Rock Ware	Regona Stamped	39.9
2019007	Peterson (47WK199)	Rim	smoothed-over cordmarked	smooth	grit	reduced	5.665	pinched	5.775	beveled	27	3	jar	Havana Ware	Steuben Punctated	38.5
2019008	Finch (47E902)	Body	smoothed-over cordmarked	smooth	grit	uneven	9.855	unmodified	0	flattened	30	4	conoidal jar	Havana Ware	Havana Zoned	32.7
2019009	Finch (47E902)	Body	cordmarked	smooth	grit	oxidized	9.21	unmodified	0	flattened	30	2.5	conoidal jar	Havana Ware	Naples Stamped	27.7
2019010	Finch (47E902)	Rim	cordmarked	smooth	grit	uneven	8.595	unmodified	8.04	rounded	20	10	globular jar	Rock Ware	Regona Stamped	40.58
2019011	Finch (47E902)	Body	cordmarked	smooth	grit	oxidized	9.615	folded	0	flattened	30	10	conoidal jar	Havana Ware	Naples Stamped	21.29
2019012	Finch (47E902)	Rim	cordmarked	smooth	grit	reduced	9.31	folded	9.73	flattened	22	5	conoidal jar	Rock Ware	Shorewood Cord Roughened	19.78
2019013	Finch (47E902)	Rim	smoothed-over cordmarked	smooth	grit	oxidized	6.9	folded	5.955	rounded	16	20	subconoidal jar	Hopewell-Related	Hopewell-Related	9.11
2019014	Sloan (11MC36)	Rim	smooth	smooth	grit	reduced	6.71	unmodified	6.615	rounded	11	1	jar	Havana Ware	Havana Plain	5.7
2019015	Sloan (11MC36)	Rim	smooth	smooth	grit	oro	12.54	unmodified	10.065	beveled	30	5	jar	Havana Ware	Naples Stamped	37.1
2019016	Sloan (11MC36)	Rim	smooth	smooth	grit	reduced	6.665	folded	7.435	beveled	17	3.5	jar	Havana Ware	Havana Plain	5.21
2019017	Sloan (11MC36)	Rim	smoothed-over cordmarked	smooth	grit	reduced	5.275	unmodified	5.535	flattened	25	3.5	jar	Hopewell-Related	Hopewell - crosshatched rim	10.9
2019018	Sloan (11MC36)	Body	smooth	smooth	grit	reduced	5.96	N/A	0	N/A	0	0	unidentified	Hopewell-Related	Hopewell - rocker stamped	18.91
2019019	Sloan (11MC36)	Rim	smoothed-over cordmarked	smooth	grit	uneven	8.13	unmodified	7.42	beveled	35	6	unidentified	Havana Ware	Unclassified Havana	40.43
2019020	Sloan (11MC36)	Rim	cordmarked	smooth	grit/grog	oro	9.31	unmodified	9.985	beveled	20	3	jar	Havana Ware	Naples Stamped	12.34
2019021	Sloan (11MC36)	Body	smooth	smooth	grit	uneven/reduced	8.72	N/A	0	N/A	0	0	unidentified	Havana Ware	Havana Zoned	17.9
2019022	Albany Village (11WT1)	Rim	smooth	smooth	grit	reduced	7.235	unmodified	7.635	beveled	12	4	jar	Havana Ware	Naples Stamped	10.69
2019023	Kautz (11DU46)	Rim	smooth	smooth	grit	reduced	9.925	unmodified	10.1	flattened	21	7	jar	Havana Ware	Havana Zoned	42.8
2019024	Alberts (47E887)	Rim	cordmarked	exfoliated	grit	oxidized	7.84	unmodified	8.575	beveled	17	9	jar	Havana Ware	Havana Cordmarked	35.23
2019025	CAV (47E93)	Rim	cordmarked	smooth	grit	uneven	8.825	unmodified	8.985	rounded	18	3	jar	Rock Ware	Shorewood Cord Roughened	11.3
2019026	Blythe (11H440)	Rim	cordmarked	smooth	grit	uneven	8.13	pinched	5.355	rounded	25	8	jar	Havana Ware	Havana Cordmarked	54.86
2019027	DeWitte/Lipharat Habitation (11R157)	Rim	smooth	smooth	grit	reduced	6.895	unmodified	6.96	flattened	20	8	unidentified	Havana Ware	Hummel Stamped	21.7

## Morphological and Metric Data

### *Sample 1*

Sample 1 was recovered from the Peterson site (47WK199). The sample is a rim sherd from a vessel that compares favorably to the Lower Illinois Valley type, Hopewell Incised. The type was defined by Griffin (1952) and references the similar Ohio Valley types. Bowls do occur in Havana Hopewell assemblages but are relatively rare. The sherd represents about 5% of the orifice of a small bowl with a 20 cm orifice diameter and an average wall thickness of 5.8 mm. The vessel has a folded rim with a slightly inverted stance and flattened lip (Figure 4.1). Exterior and interior surfaces are smoothed. The body is grit-tempered with a uniformly dark paste core. Decoration is restricted to the exterior rim margin and consists of parallel, horizontal lines placed inferior to the vessel orifice.



Figure 4.1 Sample 1, Hopewell Incised bowl; left, rim profile shown with interior to right; center, sherd exterior; right, sherd interior.



## *Sample 2*

Sample 2 was recovered from the Peterson site (47WK199). The sample is a rim sherd from a Steuben Punctated vessel. Griffin's (1952) original description of Steuben Punctated vessels suggested that they are most common in the central and northern Illinois Valley. However, Wolforth (1995) more recently has shown that Steuben Punctated ceramics are found in very low frequency in the Central Illinois River Valley. He argues that a "Steuben Microstyle zone" exists in the upper Illinois and Des Plaines drainages within northern Illinois and southern Wisconsin. Wolforth suggests this distribution reflects a late Middle Woodland, Havana-related occupation he terms the Steuben phase. The Sample 2 sherd represents about 5% of the orifice of a jar with an 18 cm orifice diameter and an average wall thickness of 6.3 mm. The vessel has a folded rim with a slightly everted stance and beveled lip (Figure 4.2). The exterior surface is smoothed-over cordmarked and interior surface is smoothed. The paste is grit tempered with an oxidized exterior margin and reduced interior margin paste core. Decoration is restricted to the exterior rim margin and consists of two rows of punctates placed inferior to the vessel orifice.

### Sample 2019002



Figure 4.2 Sample 2, Steuben Punctated jar; left, rim profile shown with interior to right; center, sherd exterior; right, sherd interior.

### Sample 3

Sample 3 was recovered from the Peterson site (47WK199). The sample is a rim sherd from a Steuben Punctated vessel. The sherd represents about 2.5% of the orifice of a jar with a 20 cm orifice diameter and an average wall thickness of 7.4 mm. The vessel has a folded rim with a direct stance and beveled lip (Figure 4.3). The exterior and interior surfaces are smoothed. The paste is grit tempered with an uneven paste core. Decoration is restricted to the exterior rim margin and consists of two rows of punctates placed inferior to the vessel orifice.



Figure 4.3 Sample 3, Steuben Punctated jar; left, rim profile shown with interior to right; center, sherd exterior; right, sherd interior.

#### *Sample 4*

Sample 4 was recovered from the Peterson site (47WK199). The sample is a rim sherd from a Steuben Punctated vessel. The sherd represents about 2.5% of the orifice of a jar with a 30 cm orifice diameter and average wall thickness of 7.4 mm. The vessel has an unmodified rim with a slightly everted rim stance and rounded lip (Figure 4.4). The exterior surface is smoothed-over cordmarked and the interior surface is smoothed. The paste is grit tempered with a reduced exterior and oxidized interior paste core. Decoration is restricted to the exterior rim margin and consists of two rows of punctates placed inferior to the vessel orifice.

### Sample 2019004



Figure 4.4 Sample 4, Steuben Punctated jar; left, rim profile shown with interior to right; center, sherd exterior; right, sherd interior.

### *Sample 5*

Sample 5 was recovered from the Peterson site (47WK199). The sample is a rim sherd from a Shorewood Cord Roughened vessel (Baerreis 1952). Shorewood Cord Roughened is one of the pottery types classified by Salzer (n.d.) as Rock Ware. These types are considered diagnostic of the Waukesha Phase (Haas 2019b). The sherd represents about 5% of the orifice of a jar with a 20 cm orifice diameter and an average wall thickness of 7.6 mm. The vessel has a folded rim with a direct rim stance and flattened lip (Figure 4.5). The exterior surface is cordmarked and the interior surface is smoothed. The paste is grit tempered with an uneven paste core. The sample is perforated by a hole that goes through the vessel wall below the rim.



Figure 4.5 Sample 5, Shorewood Cord Roughened jar; left, rim profile shown with interior to right; center, sherd exterior; right, sherd interior.

### *Sample 6*

Sample 6 was recovered from the Peterson site (47WK199). The sample is a rim sherd from a Kegonsa Stamped vessel (Baerreis 1952). Kegonsa Stamped is another diagnostic Waukesha Phase pottery type from the Rock Ware category (Salzer n.d.; Haas 2019b). The sherd represents about 7% of the orifice of a jar with a 40 cm orifice diameter and average wall thickness of 9.7 mm (Figure 4.6). The vessel has a folded rim with a slightly everted stance and rounded lip. The exterior surface is cordmarked and the interior surface is smoothed. The paste is grit tempered with an uneven paste core. The vessel lip is slightly notched transverse to the vessel orifice due to the application of a rounded dowel.



Figure 4.6 Sample 6, Kegonsa Stamped jar; left, rim profile shown with interior to right; center, sherd exterior; right, sherd interior.

### *Sample 7*

Sample 7 was recovered from the Peterson site (47WK199). The sample is a rim sherd from a Steuben Punctated vessel. The sherd represents about 3% of the orifice of a jar with a 27 cm orifice diameter and an average wall thickness of 5.7 mm. The vessel has a pinched rim with a direct stance and beveled lip (Figure 4.7). The exterior surface is poorly smoothed-over cordmarked and the interior surface is smoothed. The paste is grit tempered with a uniformly dark paste core. Decoration is restricted to the exterior rim margin and consists of a row of punctates placed inferior to the vessel orifice.



Figure 4.7 Sample 7, Steuben Punctated jar; left, rim profile shown with interior to right; center, sherd exterior; right, sherd interior.

### *Sample 8*

Sample 8 is a body sherd from a Havana Zoned (Griffin 1952) vessel. The sherd exhibits incised lines that separate plain areas from decorated zones. According to Haas and Picard (2019) and Haas (2019b) this sample is part of a conoidal jar (not shown) recovered from the Finch site (47JE902). The body sherd was selected for analysis in order to preserve the associated rim sherd. The rim sherd represents about 4% of the 30 cm diameter orifice and has an average wall thickness of 9.9 mm. The vessel has an unmodified rim with a direct stance and flattened lip. The exterior surface is smoothed-over cordmarked and the interior surface is smoothed (Haas 2019b; Haas and Picard 2019). The paste is grit-tempered with an uneven paste core. The decoration on the exterior of the Sample 8 includes an incised line separating a zone of dentate stamps from an undecorated, smooth area (Figure 4.8).

### Sample 2019008



Figure 4.8 Sample 8, Havana Zoned body sherd; left, sherd exterior; right, sherd interior.

### *Sample 9*

Sample 9 was recovered from the Finch site (47JE902). The sample is a body sherd from a Naples Stamped vessel. The type is part of the Havana complex, decorated with cord-wrapped stick, dentate or ovoid stamps over a plain or cordmarked surface (Griffin 1952). The body sherd was selected for analysis in order to preserve the associated rim sherd. The Sample 9 sherd is part of a conoidal jar (not shown) with an orifice diameter of 30 cm (about 2.5% of the vessel orifice is present) and an average wall thickness of 9.2 mm. The vessel has an unmodified rim with a slightly everted stance and flattened lip (Haas 2019b; Haas and Picard 2019). The paste is grit tempered and with an evenly oxidized paste core. The decoration on the exterior of the Sample 9 sherd includes cord-wrapped stick stamps over partially smoothed-over cordmarking, the interior surface is smooth (Figure 4.9).





Figure 4.9 Sample 9, Naples Stamped body sherd; left, sherd exterior; right, sherd interior.

### *Sample 10*

Sample 10 was recovered from the Finch site (47JE902). The sample is a rim sherd from a Kegonsa Stamped vessel (Baerreis 1952). The sample represents about 10% of the orifice of a globular jar with a 20 cm orifice diameter and an average wall thickness of 8.6 mm. The vessel has an unmodified rim with a direct stance and rounded lip (Figure 4.10). The exterior surface is cordmarked and the interior surface is smooth. The paste is grit tempered with an uneven paste core. Decorations include exterior bosses on the rim, which appear as punctates on the interior, as well as tooled notches along the interior lip margin.



Figure 4.10 Sample 10, Kegonsa Stamped jar; left, rim profile shown with interior to right; center, sherd exterior; right, sherd interior (profile after Haas 2019b, Appendix D).

### *Sample 11*

Sample 11 is a body sherd from a Naples Stamped vessel (Griffin 1952) recovered from the Finch site (47JE902). The body sherd (Figure 4.11) was selected for analysis in order to preserve the associated rim sherd. The sherd is part of a conoidal jar (not shown). About 10% of the 30 cm diameter orifice is present. Average wall thickness is 9.6 mm. The vessel has a folded rim with a direct stance and flattened lip (Haas 2019b; Haas and Picard 2019). The exterior surface of Sample 11 is cordmarked and the interior surface is smoothed. The sherd is grit tempered with a uniformly oxidized paste core. Decoration includes linear stamps on the exterior surface.

## Sample 2019011



Figure 4.11 Sample 11, Naples Stamped body sherd; left, sherd exterior; right, sherd interior.

### *Sample 12*

Sample 12 is a rim sherd from a Shorewood Cord Roughened vessel recovered from the Finch site (47JE902). The sample represents <5% of the orifice of a conoidal jar with a 22 cm orifice diameter with an average wall thickness of 9.3 mm. The vessel has a folded rim with a direct stance and flattened lip (Figure 4.12). The exterior surface is cordmarked and the interior surface is smoothed. The paste is grit tempered with a uniformly dark paste core. The sample is undecorated.



Figure 4.12 Sample 12, Shorewood Cord Roughened jar; left, rim profile shown with interior to right; center, sherd exterior; right, sherd interior (profile after Haas 2019b, Appendix D).

### *Sample 13*

Sample 13 is a rim sherd from a Hopewell-Related subconoidal jar recovered from the Finch site (47JE902). The Sample 13 sherd represents <5% of a 16 cm diameter vessel, but additional sherds from the same vessel represent approximately 20% of the orifice. The vessel has an average wall thickness of 6.9 mm (Haas 2019b; Haas and Picard 2019). The vessel has a folded rim with an everted stance and rounded lip. Exterior and interior surfaces are smoothed. The paste is grit-tempered with a uniformly oxidized paste core. Decoration on the vessel (not shown) includes trailed lines, where “the upper rim area features a triangle formed in four

parallel line” as well as “plain tool notching on the interior lip margin that extends across the lip surface to the front of the vessel” (Haas and Picard 2019:280) (Figure 4.13).



Figure 4.13 Sample 13, Hopewell-related jar; left, rim profile shown with interior to right; center, sherd exterior; right, sherd interior (profile after Haas 2019b, Appendix D).

#### *Sample 14*

Sample 14 is a rim sherd from a vessel identified as Havana Plain (Griffin 1952). The sample was recovered from the Sloan site (11MC86). Havana Plain vessels have a smoothed surface that may be decorated with rim bosses. The Sample 14 sherd represents about 1% of the orifice of a jar with an approximate orifice diameter of 11 cm and average wall thickness of 6.7 mm. The vessel has an unmodified rim with an indeterminate stance and rounded lip (Figure 4.14). Exterior and interior surfaces are smoothed. The interior surface is slipped black as is evident in the thin section image shown in Figure 4.15. The paste is grit tempered with a uniformly dark paste core. Decoration includes a boss on the exterior rim margin.



Figure 4.14 Sample 14, Havana Plain jar rim; left, rim profile shown with interior to right; center, sherd exterior; right, sherd interior.

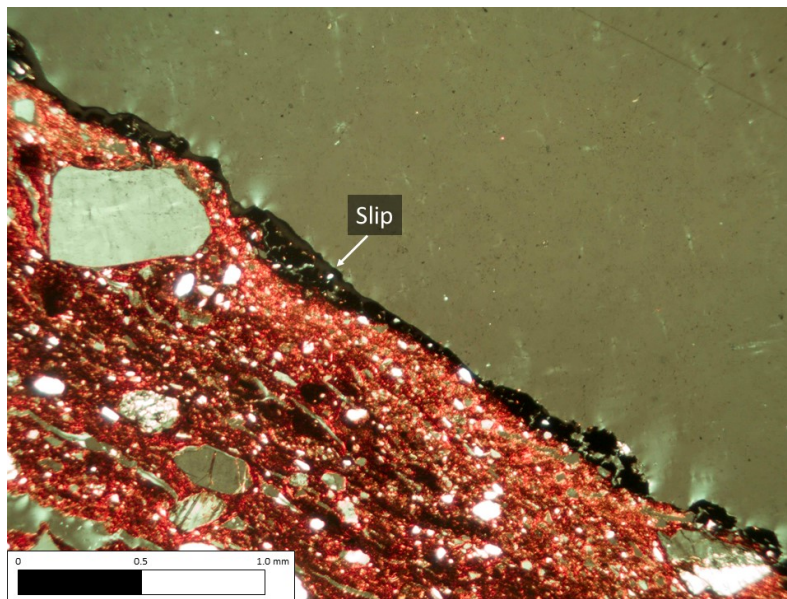


Figure 4.15 Thin section image of black interior slip on Havana Plain sample 14 (Cross-Polarized Light, 4X).

### *Sample 15*

Sample 15 is a sherd that compares favorably to the Havana Ware type, Naples Stamped (Griffin 1952). The sample was recovered from the Sloan site (11MC86). The sherd represents

about 5% of the orifice of a jar with a 30 cm orifice diameter and an average wall thickness of 12.5 mm. The vessel has an unmodified rim with a direct stance and beveled interior rim margin (Figure 4.16). Exterior and interior surfaces are smoothed. The paste is tempered with a combination of limestone, grit, and grog with an oxidized exterior surface and a reduced core. Decoration includes cord-wrapped stick stamping on the exterior rim margin directly below the lip, and hemispherical bosses that appear to encircle the vessel orifice, located approximately 3 cm below the vessel lip. The bosses were produced by impressing a tool from the interior of the vessel, thus leaving a deep circular punctate on the interior rim margin. A single cord-impressed line is present also, extending from the vessel lip on the exterior rim margin to intersect with the horizontal row of bosses.



Figure 4.16 Sample 15, Naples Stamped jar rim; left, rim profile shown with interior to right; center, sherd exterior; right, sherd interior.

### Sample 16

Sample 16 is a rim sherd from a Havana Plain vessel (Griffin 1952). The sample was recovered from the Sloan site (11MC86). The sherd represents about 3.5% of the orifice of a jar with a 17 cm orifice diameter and an average wall thickness of 6.7 mm. The vessel has a folded rim with an indeterminate stance and beveled lip (Figure 4.17). Exterior and interior surfaces are smoothed. The paste is grit-tempered with a uniformly dark paste core. Decoration includes a boss on the exterior rim margin.

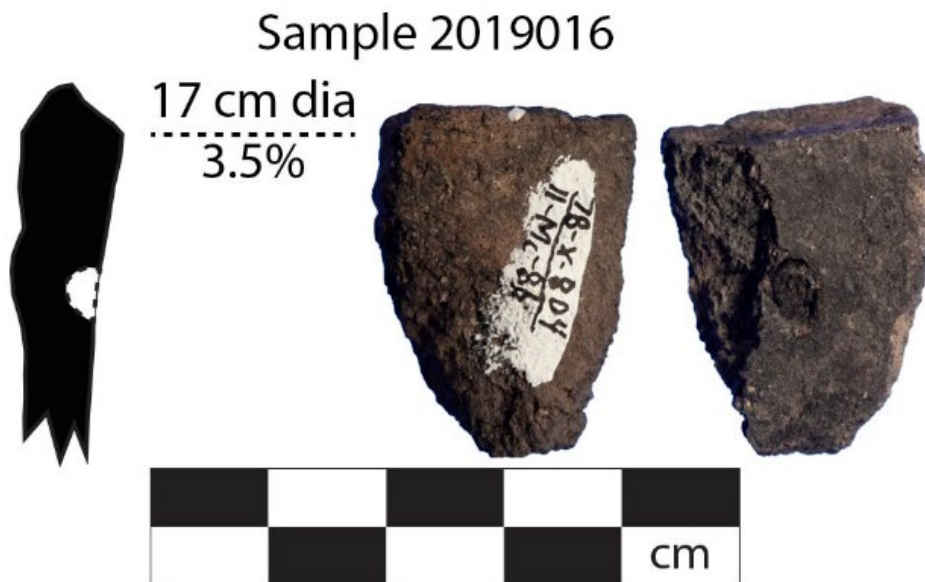


Figure 4.17 Sample 16, Havana Plain jar rim; left, rim profile shown with interior to right; center, sherd exterior; right, sherd interior.

### Sample 17

Sample 17 is a rim sherd from a vessel favorable to a Hopewell Ware vessel (Griffin 1952). The sample was recovered from the Sloan site (11MC86). Crosshatching on the exterior rim margin directly below the lip is typically distinctive of the Hopewell style defined by Griffin



(1952). The sherd represents about 3.5% of the orifice of a jar with a 25 cm orifice diameter and an average wall thickness of 5.3 mm. The vessel has an unmodified rim with a slightly inverted stance and flattened lip (Figure 4.18). The exterior surface is smoothed-over cordmarked and the interior surface is smoothed. The paste is grit tempered with a uniformly dark paste core. Decoration is restricted to the exterior rim margin and consists of finely cross-hatched incised lines placed inferior to the vessel orifice. Unlike other Hopewell rims, the Sample 17 sherd does not bear punctates directly below the cross-hatched decoration.



Figure 4.18 Sample 17, Hopewell Ware jar rim; left, rim profile shown with interior to right; center, sherd exterior; right, sherd interior.

### *Sample 18*

Sample 18 is body sherd from a Hopewell Zoned Stamped vessel (Griffin 1952). The sample was recovered from the Sloan site (11MC86). The type is defined by curvilinear lines that separate areas of stamp impressions from smoothed areas (Griffin 1952). The Sample 18

sherd has an average wall thickness of 6 mm. The vessel form and rim details could not be determined because the body sherd was the only known piece of the vessel recovered. Exterior and interior surfaces are smoothed. The paste is grit, limestone, and grog-tempered with a uniformly dark paste core. Decoration includes an incised horizontal line separating a horizontal band of rocker-stamping from a smoothed surface area below (Figure 4.19).

### Sample 2019018



Figure 4.19 Sample 18, Hopewell Zoned Stamped body sherd; left, sherd exterior; right, sherd interior.

### *Sample 19*

Sample 19 is a rim sherd from an unclassified Havana Hopewell vessel (Griffin 1952). The sample was recovered from the Sloan site (11MC86). The sample was identified as reminiscent of Hopewell pottery due to the row of punctates separating the diagonally incised upper rim band (Benchley et al. 1979). The sherd represents about 6% of the orifice of a jar with

a 35 cm orifice diameter and an average wall thickness of 8.1 mm. The vessel has an unmodified rim with a slightly everted stance and beveled lip (Figure 4.20). The exterior surface is smoothed-over cordmarked and the interior is smoothed. The paste is grit-tempered with an uneven paste core. Decoration includes a band of diagonally oriented incised lines on the exterior rim margin directly below the vessel lip. Four vertical, partially smoothed over cord-impressions extend from the band of incising to about 4 cm below the vessel lip. A horizontal band of punctates encircle the vessel directly below the band of incising and a zone of dentate stamping is present below the punctates. A circular perforation, drilled from the vessel exterior, is present within the zone of dentate stamping. The vessel interior is undecorated.



Figure 4.20 Sample 19, Unclassified Havana Ware jar rim; left, rim profile shown with interior to right; center, sherd exterior; right, sherd interior.

### *Sample 20*

Sample 20 is a rim sherd from a Naples Stamped vessel (Griffin 1952). The sample was recovered from the Sloan site (11MC86). The sherd represents about 3% of the orifice of a jar with a 20 cm orifice diameter and an average wall thickness of 9.3 mm. The vessel has an

unmodified rim with a slightly inverted stance and beveled lip (Figure 4.21). The exterior surface is cordmarked and the interior surface is smoothed. The paste is grit and grog-tempered with oxidized exterior margins and a reduced paste core. Decoration includes diagonal cord-wrapped stick stamping on the exterior rim margin placed inferior to the vessel orifice.



Figure 4.21 Sample 20, Naples Stamped jar rim; left, rim profile shown with interior to right; center, sherd exterior; right, sherd interior.

### *Sample 21*

Sample 21 is a body sherd from a Havana Zoned vessel (Griffin 1952). The sample was recovered from the Sloan site (11MC86). The average wall thickness is 8.7 mm. The vessel form and rim details could not be determined because the body sherd was the only piece of the vessel recovered. The interior and exterior surfaces are smoothed. The sherd exhibits exterior

decorations including an incised groove separating a zone of dentate stamping from a smoothed zone (Figure 4.22).



Figure 4.22 Sample 21, Hopewell Zoned Stamped body sherd; left, sherd exterior; right, sherd interior.

### *Sample 22*

Sample 22 is a rim sherd from a Naples Stamped vessel (Griffin 1952). The sample was recovered from the Albany Village site (11WT1). The sherd represents about 4% of a jar with a 12 cm orifice diameter and an average wall thickness of 7.3 mm. The vessel has an unmodified rim with a slightly inverted stance and beveled lip (Figure 4.23). Exterior and interior surfaces are smoothed. The paste is grit-tempered with a uniformly dark paste core. Decorations include dentate stamping on the exterior rim margin, a row of bosses below the dentate stamping, and a single row of dentate stamps below the bosses.



Figure 4.23 Sample 22, Naples Stamped jar rim; left, rim profile shown with interior to right; center, sherd exterior; right, sherd interior.

### *Sample 23*

Sample 23 is a rim sherd from a Havana Zoned vessel (Griffin 1952). The sample was recovered from the Kautz site (11DU46). The sherd represents about 7% of the orifice of a jar with a 21 cm orifice diameter and an average wall thickness of 9.9 mm. The vessel has an unmodified rim with a direct stance and flattened lip (Figure 4.24). Exterior and interior surfaces are smoothed. The paste is grit tempered with a uniformly dark paste core. Decoration includes a horizontal band of parallel, diagonally-oriented lines of dentate stamping, extending about 4 cm from just below the vessel lip on the exterior rim margin. Below the band of dentates is a smoothed zone bordered by a horizontal incised line. Additional dentate stamping is present below this line. The vessel interior is undecorated except for cord-wrapped stick stamping on the interior rim margin.



Figure 4.24 Sample 23, Havana Zoned jar rim; left, rim profile shown with interior to right; center, sherd exterior; right, sherd interior.

### *Sample 24*

Sample 24 is a rim sherd from a vessel that compares favorably to the Havana Ware type, Havana Cordmarked (Baerreis 1952; Griffin 1952:104; Jeske and Kaufmann 2000:85). The sample was recovered from the Alberts site (47JE887). The sherd represents about 9% of the orifice of a jar with a 17 cm orifice diameter and an average wall thickness of 7.8 mm. The vessel has an unmodified rim with a slightly everted stance and beveled lip (Figure 4.25). The exterior is cordmarked and the interior is partially exfoliated. The paste is grit-tempered with a uniformly oxidized paste core. Decoration includes a boss on the exterior rim margin as well as cord-wrapped stick stamping on the interior lip margin.

Sample 2019024



Figure 4.25 Sample 24, Havana Cordmarked jar rim; left, rim profile shown with interior to right; center, sherd exterior; right, sherd interior.

*Sample 25*

Sample 25 is a rim sherd from a Shorewood Cord Roughened vessel (Baerreis 1952). The sample was recovered from the Crab Apple Point site (47JE93). The sherd represents about 3% of the orifice of a jar with an 18 cm orifice diameter and an average wall thickness of 8.8 mm. The vessel has an unmodified rim with a direct stance and rounded lip (Figure 4.26). The exterior surface is cordmarked and the interior surface is smoothed. The paste is grit-tempered with an uneven paste core. A boss below the rim is the only decorative element on the sherd.



## Sample 2019025



Figure 4.26 Sample 25, Shorewood Cord Roughened jar rim; left, rim profile shown with interior to right; center, sherd exterior; right, sherd interior.

### *Sample 26*

Sample 26 is a rim sherd from a Havana Cordmarked vessel (Griffin 1952). The sample was recovered from the Blythe site (11HA40). The Havana Cordmarked style is more commonly recovered from sites in the Lower Illinois Valley and Mississippi Valley, while Havana Plain styles are more common in the central Illinois Valley (Griffin 1952). The sherd represents about 8% of the orifice of a jar with a 25 cm orifice diameter and average wall thickness of 8.1 mm. The vessel has a pinched rim with an everted stance and rounded lip (Figure 4.27). The exterior

surface is cordmarked and the interior surface is smoothed. The paste is grit-tempered with an uneven paste core. Decoration includes a row of bosses on the exterior lower rim margin.



Figure 4.27 Sample 26, Havana Cordmarked jar rim; left, rim profile shown with interior to right; center, sherd exterior; right, sherd interior.

### *Sample 27*

Sample 27 is a rim sherd of Hummel Stamped (Griffin 1952). The sample was recovered from the DeWitte/Liphardt Habitation site (11RI57). The style is a variation of Naples Stamped, where the vertical rows of stamping pendant to the lip are curved rather than straight (Griffin

1952). The sherd represents about 8% of the orifice of a jar with a 20 cm orifice diameter and an average wall thickness of 6.9 mm. The vessel has an unmodified rim with a slightly inverted stance and flattened lip (Figure 4.28). Exterior and interior surfaces are smoothed. The paste is grit-tempered with a uniformly dark paste core. Decoration is restricted to the exterior rim margin and consists of curved dentate stamps perpendicular to the rim.



Figure 4.28 Sample 27, Hummel Stamped jar rim; left, rim profile shown with interior to right; center, sherd exterior; right, sherd interior.

### Petrographic Analysis: Mineralogy

Both quantitative and qualitative data were collected on the mineralogical constituents of the pastes. Each identifiable mineral was counted on each sample where it was present. Additionally, a list of each mineral as present or absent was created for each sample. Minerals were generally identified in two larger categories, silicate-minerals and non-silicate minerals.

Silicate minerals include amphiboles: hornblende, micas: biotite, muscovite, and sericite; quartzes: quartz, as well as the metamorphosed versions quartzite and myrmekite, myrmekite with the addition of plagioclase; and feldspars: plagioclase feldspar (p-feldspar), potassium feldspar (k-feldspar), and microcline. Non-silicate minerals include carbonates: calcite; phosphates: apatite; and oxides: the opaque minerals (Perkins 1998). Table 4.2 displays the percentage of the minerals identified in each sample from this analysis.

Hornblende is an amphibole mineral identifiable by the pleochroism in Plane-Polarized Light (PPL) of various shades of yellow to green to brown. The mineral has cleavages at 56 and 124 degrees and extinction in Cross-Polarized Light (XPL) symmetrical to the cleavages (Perkins 1998).

The minerals in the mica group exhibit a perfect basal cleavage. Biotite is identifiable by the brownish to green pleochroism in PPL. Additionally, in XPL extinction occurs at ninety-degrees, or parallel. Often, the extinction exhibits a birds-eye appearance. Muscovite is usually colorless in PPL and may also show bird's eye extinction with more vivid colors in XPL. Sericite is a variety of muscovite visible as silky, narrow inclusions, often identified with plagioclase and quartz (Faithfull 1998; Perkins 1998)

The minerals identified in the quartz group include quartz, quartzite, and myrmekite. Quartz is colorless in PPL and easily recognized in XPL by the undulatory extinction and coloring, which usually ranges from white to dark gray or black in extinction. Quartzite is metamorphosed quartz, which appears similar to quartz in both PPL and XPL, but the grains of quartzite exhibit an interlocking structure. Myrmekite is the worm-like casts of quartz often

located in plagioclase crystals. In both PPL and XPL, the small inclusions appear similar to quartz grains (Perkins 1998).

Minerals in the feldspar group were identified as plagioclase feldspar, potassium-feldspar (k-feldspar), and microcline. Plagioclase feldspar is colorless without pleochroism in PPL. In XPL, plagioclase is white to gray with parallel twinning. K-feldspar is similar to plagioclase feldspar, however in XPL the twinning is simple, “carlsbad” twinning with half the mineral grain in extinction, while the other half remains illuminated (Nelson 2019). Microcline exhibits a combination of twinning in XPL which appears as a cross-hatched or “tartan” twinning (Perkins 1998; Strekeisen 2018a).

The non-silicate groups of minerals identified in this analysis include oxides, carbonates, and phosphates. Apatite is a phosphate mineral that is colorless in PPL and moderate relief, in XPL it exhibits parallel extinction and coloring ranging from white to gray. Calcite is a carbonate mineral that is colorless in PPL. Calcite appears similar to the feldspar group minerals in XPL; however, the lamellar twinning is parallel to the rhombohedral cleavage of the mineral (Perkins 1998; Strekeisen 2018b). The last group of minerals are the oxide groups, which are represented by the opaque minerals. These minerals do not pass light in either PPL or XPL (Perkins 1998).

TABLE 4.2 PERCENTAGE OF MINERALS IDENTIFIED IN EACH SAMPLE

Sample	Site Name (Number)	Percentage of Individual Minerals Identified in Each Sample												
		Apatite	Biotite	Calcite	Hornblende	Microcline	Muscovite	K-Feldspar	P-Feldspar	Quartz	Quartzite	Opaque	Myrmekite	Sericite
2019001	Peterson (47WK199)	0.00%	16.46%	15.19%	5.06%	0.00%	0.00%	2.53%	17.72%	16.46%	0.00%	12.66%	5.06%	8.86%
2019002	Peterson (47WK199)	4.17%	18.75%	14.58%	4.17%	1.04%	0.00%	0.00%	5.21%	20.83%	4.17%	12.50%	5.21%	9.38%
2019003	Peterson (47WK199)	0.00%	25.71%	16.19%	8.57%	0.00%	0.00%	0.00%	21.90%	6.67%	0.00%	12.38%	4.76%	3.81%
2019004	Peterson (47WK199)	0.00%	25.00%	19.00%	0.00%	3.00%	0.00%	0.00%	29.00%	9.00%	0.00%	10.00%	3.00%	2.00%
2019005	Peterson (47WK199)	0.00%	10.61%	22.73%	4.55%	4.55%	0.00%	0.00%	10.61%	22.73%	0.00%	3.03%	1.52%	19.70%
2019006	Peterson (47WK199)	0.00%	26.39%	15.28%	3.47%	0.00%	0.00%	0.00%	17.36%	8.33%	0.00%	13.89%	15.28%	0.00%
2019007	Peterson (47WK199)	0.00%	19.13%	15.65%	1.74%	0.00%	0.00%	0.00%	6.96%	16.52%	0.00%	20.00%	1.74%	18.26%
2019008	Finch (47IE902)	0.00%	22.31%	24.79%	0.83%	3.31%	0.00%	0.83%	13.22%	17.36%	0.00%	7.44%	0.83%	9.09%
2019009	Finch (47IE902)	0.00%	18.75%	15.00%	0.00%	10.00%	0.00%	7.50%	5.00%	26.25%	0.00%	11.25%	6.25%	0.00%
2019010	Finch (47IE902)	0.00%	19.28%	9.64%	8.43%	0.00%	0.00%	1.20%	28.92%	14.46%	3.61%	14.46%	0.00%	0.00%
2019011	Finch (47IE902)	0.00%	15.09%	18.87%	5.66%	0.00%	0.00%	0.00%	11.32%	33.96%	0.00%	15.09%	0.00%	0.00%
2019012	Finch (47IE902)	0.00%	9.68%	8.60%	4.30%	1.08%	0.00%	7.53%	17.20%	41.94%	0.00%	8.60%	1.08%	0.00%
2019013	Finch (47IE902)	0.00%	12.00%	6.00%	6.00%	0.00%	0.00%	0.00%	14.00%	52.00%	0.00%	10.00%	0.00%	0.00%
2019014	Sloan (11MC86)	0.00%	23.26%	11.63%	0.00%	6.98%	0.00%	6.98%	4.65%	27.91%	9.30%	0.00%	4.65%	4.65%
2019015	Sloan (11MC86)	0.00%	13.33%	15.56%	4.44%	2.22%	0.00%	2.22%	4.44%	42.22%	0.00%	0.00%	0.00%	15.56%
2019016	Sloan (11MC86)	0.00%	21.95%	14.63%	0.00%	4.88%	0.00%	2.44%	12.20%	29.27%	0.00%	2.44%	4.88%	7.32%
2019017	Sloan (11MC86)	0.00%	18.37%	12.24%	0.00%	0.00%	0.00%	6.12%	12.24%	28.57%	0.00%	0.00%	4.08%	18.37%
2019018	Sloan (11MC86)	0.00%	10.91%	1.82%	0.00%	1.82%	0.00%	0.00%	20.00%	54.55%	1.82%	3.64%	1.82%	1.82%
2019019	Sloan (11MC86)	0.00%	19.15%	16.31%	0.00%	2.84%	0.00%	0.71%	12.77%	31.21%	0.00%	5.67%	0.00%	11.35%
2019020	Sloan (11MC86)	0.00%	17.31%	16.35%	0.00%	2.88%	0.00%	0.00%	12.50%	27.88%	0.00%	6.73%	0.96%	15.38%
2019021	Sloan (11MC86)	0.00%	24.56%	10.53%	0.00%	3.51%	0.00%	5.26%	7.02%	21.05%	5.26%	5.26%	5.26%	12.28%
2019022	Albany Village (11WT1)	0.00%	23.08%	9.89%	0.00%	1.10%	0.00%	6.59%	13.19%	26.37%	0.00%	2.20%	4.40%	13.19%
2019023	Kautz (11DU46)	0.00%	22.62%	15.48%	11.90%	0.00%	0.00%	2.38%	17.86%	9.52%	0.00%	11.90%	3.57%	4.76%
2019024	Alberts (47IE887)	0.00%	19.15%	19.15%	4.26%	0.00%	0.00%	0.00%	12.77%	17.02%	4.26%	12.77%	6.38%	4.26%
2019025	CAP (47IE93)	0.00%	22.50%	15.00%	0.00%	0.00%	0.00%	5.00%	7.50%	15.00%	2.50%	15.00%	7.50%	10.00%
2019026	Bythe (11HA40)	0.00%	21.43%	10.71%	0.00%	0.00%	0.00%	7.14%	7.14%	39.29%	10.71%	3.57%	0.00%	0.00%
2019027	DeWitte/Liphardt	0.00%	27.66%	15.96%	0.00%	2.13%	0.00%	2.13%	6.38%	21.28%	3.19%	3.19%	3.19%	14.89%
	Total/Mean % of Mineral	0.15%	19.42%	14.33%	2.72%	1.90%	0.07%	2.47%	12.93%	25.10%	1.66%	8.28%	3.39%	7.59%

## Sample 1

In Sample 1, nine individual minerals were identified. These minerals include silicate mineral groups such as amphiboles, micas, quartzes, and feldspars, as well as non-silicate mineral groups including carbonates and oxides. Four points were identified as the amphibole hornblende. In the mica group, thirteen were biotite and seven were sericite. In the quartz mineral group, thirteen were quartz and four were myrmekite. In the feldspar group, fourteen were plagioclase feldspar, and two were k-feldspar. In the non-silicate mineral groups, twelve points were calcite and ten were opaque minerals. Figure 4.29 shows minerals identified in PPL and Figure 4.30 shows minerals identified in XPL from the thin section.

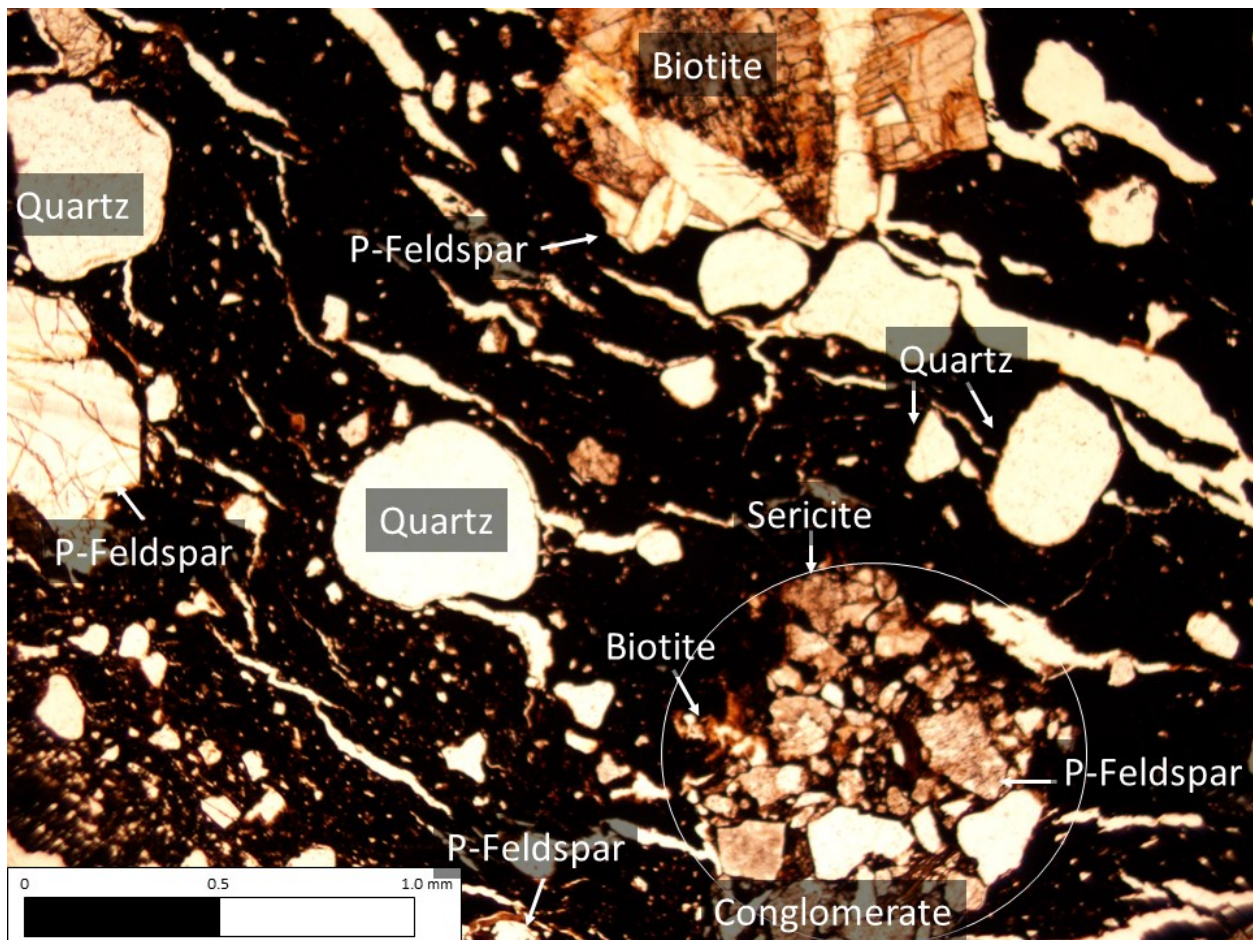


Figure 4.29 Thin section image of Sample 1 (Plane Polarized Light, 4X).

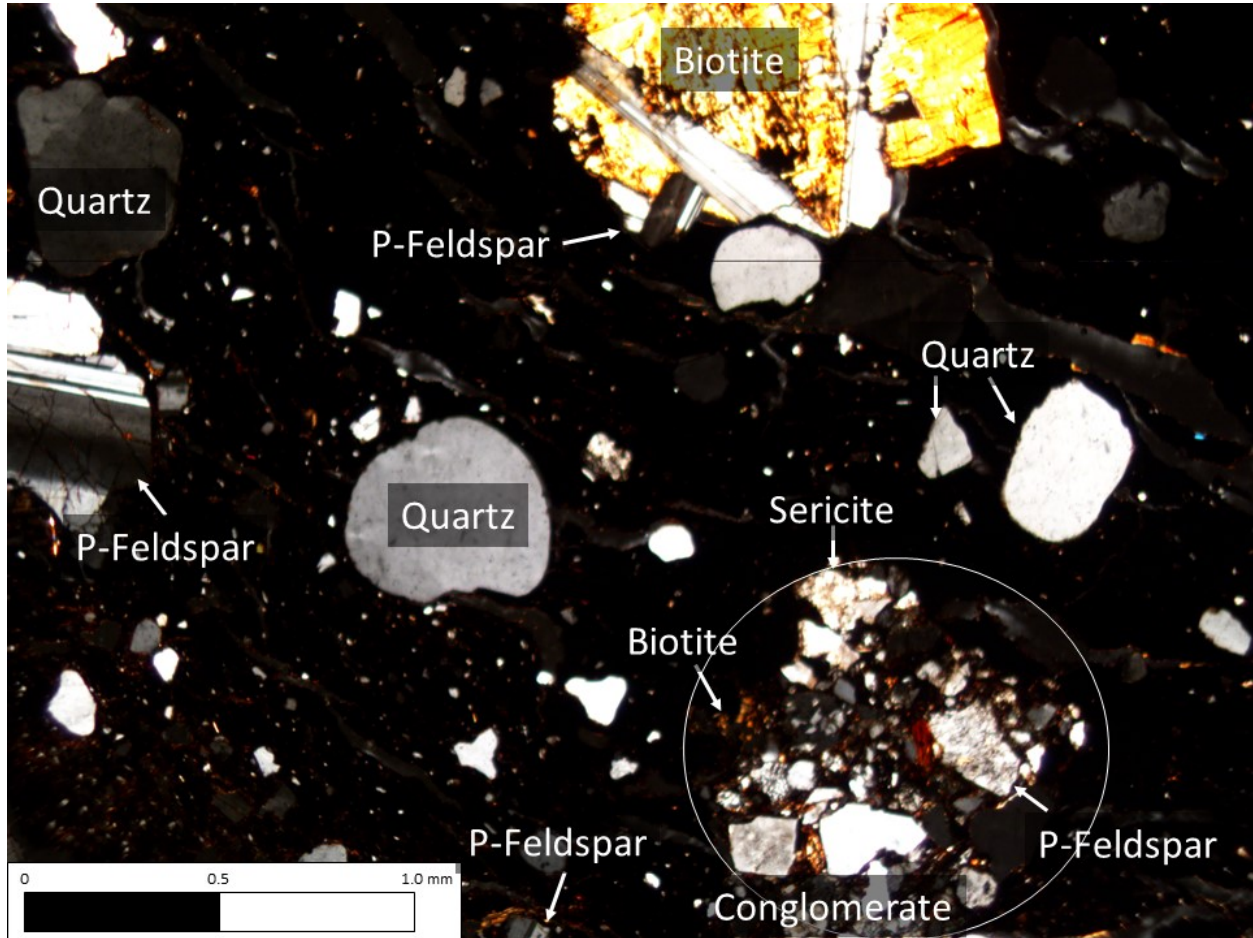


Figure 4.30 Thin section image of Sample 1 (Cross Polarized Light, 4X).

### *Sample 2*

In Sample 2, eleven individual minerals were identified. These minerals include silicate mineral groups such as amphiboles, micas, quartzes, and feldspars, as well as non-silicate mineral groups including phosphates, carbonates, and oxides. Four points were identified as hornblende in the amphibole group. In the mica group, eighteen points were biotite and nine were sericite. In the quartz mineral group, twenty were quartz, four were quartzite, and five were myrmekite. In the feldspar group, five were plagioclase feldspar, and one was microcline. In the



non-silicate mineral groups, four points were apatite, fourteen were calcite, and twelve were opaque minerals. Figure 4.31 shows minerals identified in PPL and Figure 4.32 shows minerals identified in XPL from the thin section.

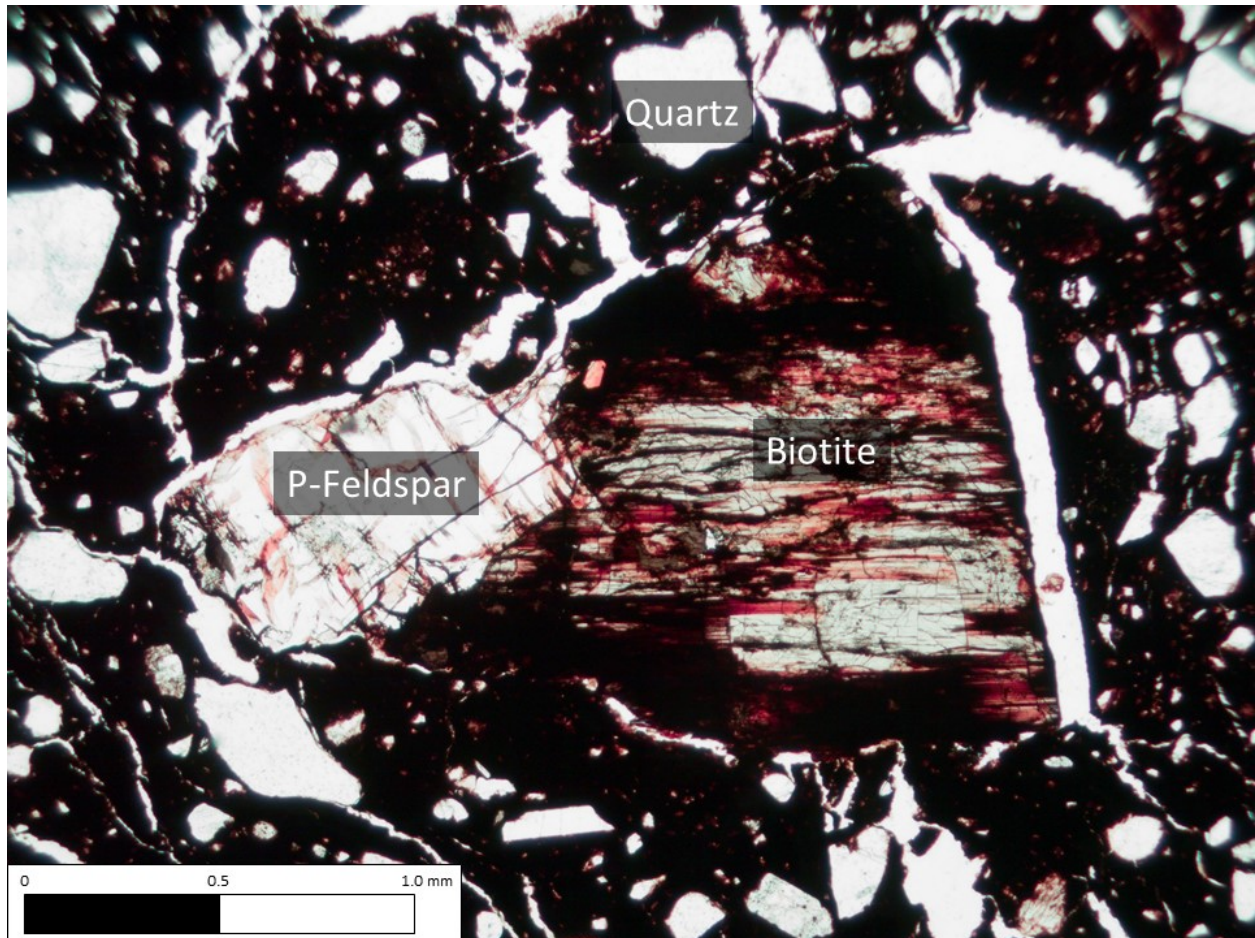


Figure 4.31 Thin section image of Sample 2 (Plane Polarized Light, 4X).

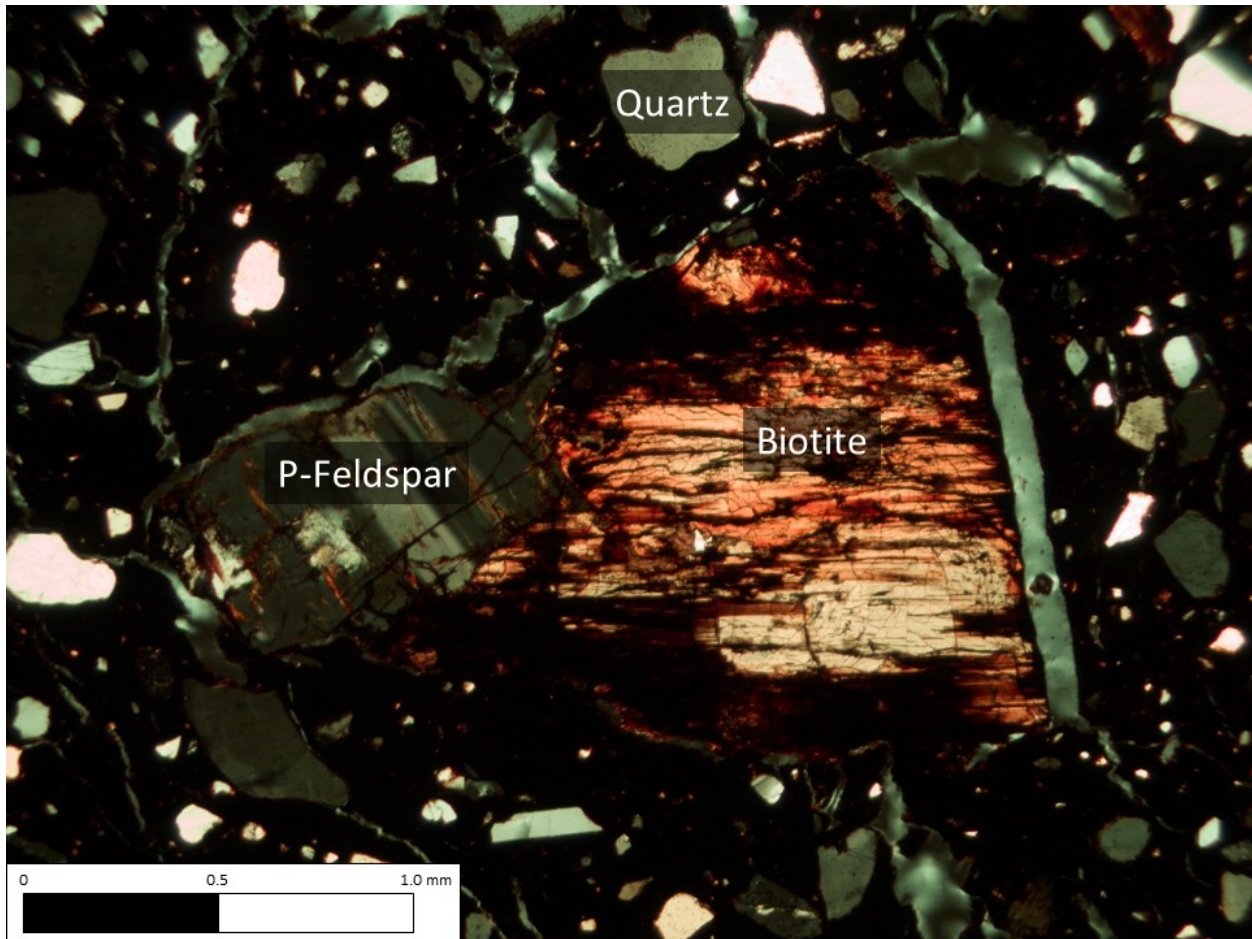


Figure 4.32 Thin section image of Sample 2 (Cross Polarized Light, 4X).

### *Sample 3*

In Sample 3, eight individual minerals were identified. These minerals include those in the silicate groups such as amphiboles, micas, quartzes, and feldspars, as well as non-silicate groups including carbonates and oxides. Nine points were identified as hornblende in the amphibole group. In the mica group, twenty-seven points were biotite and four were sericite. In the quartz mineral group, seven were quartz and five were myrmekite. In the feldspar group, twenty-three were plagioclase feldspar. Seventeen points were calcite in the carbonate group.

Thirteen points were opaque minerals. Figure 4.33 shows minerals identified in PPL and Figure 4.34 shows minerals identified in XPL from the thin section.

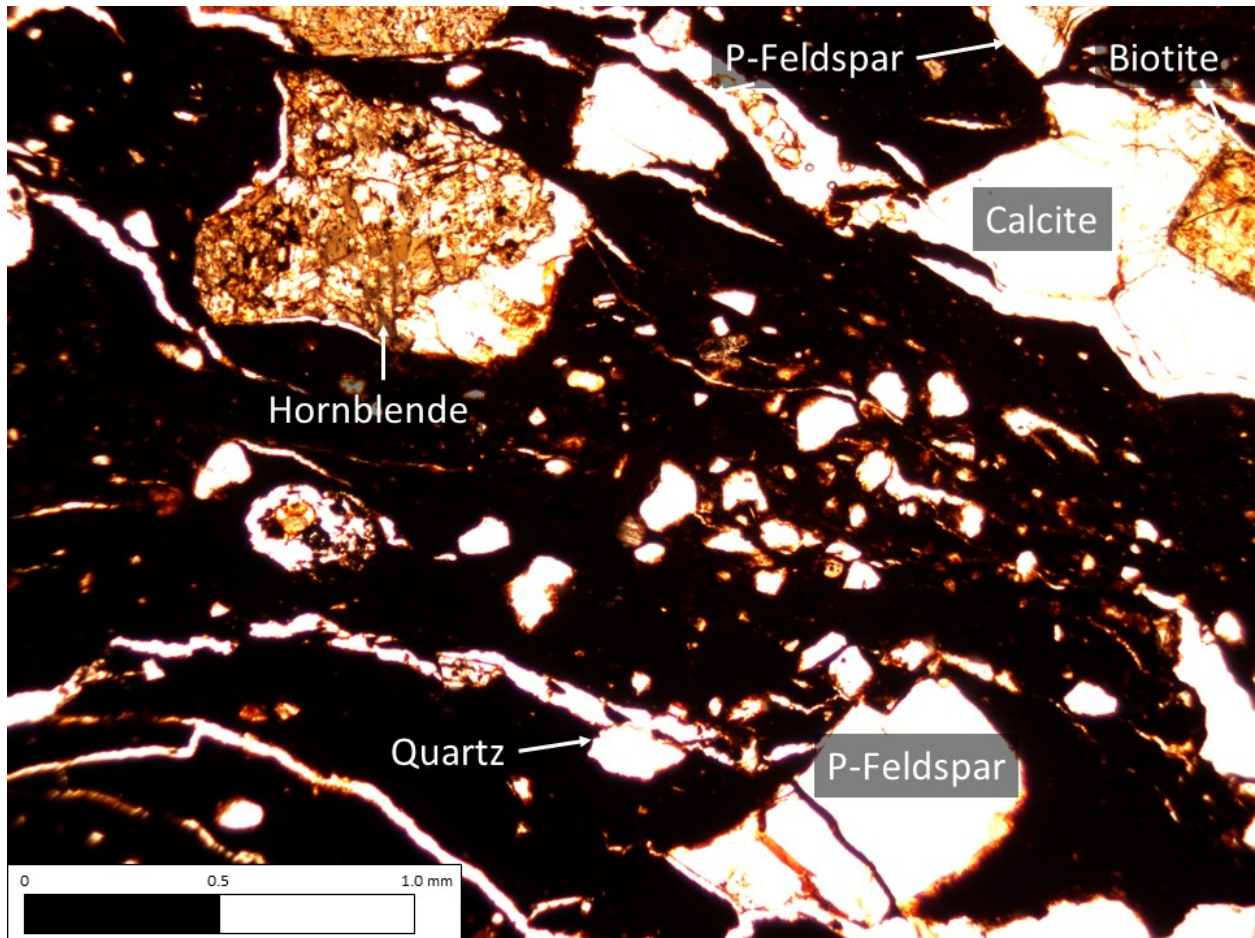


Figure 4.33 Thin section image of Sample 3 (Plane Polarized Light, 4X).

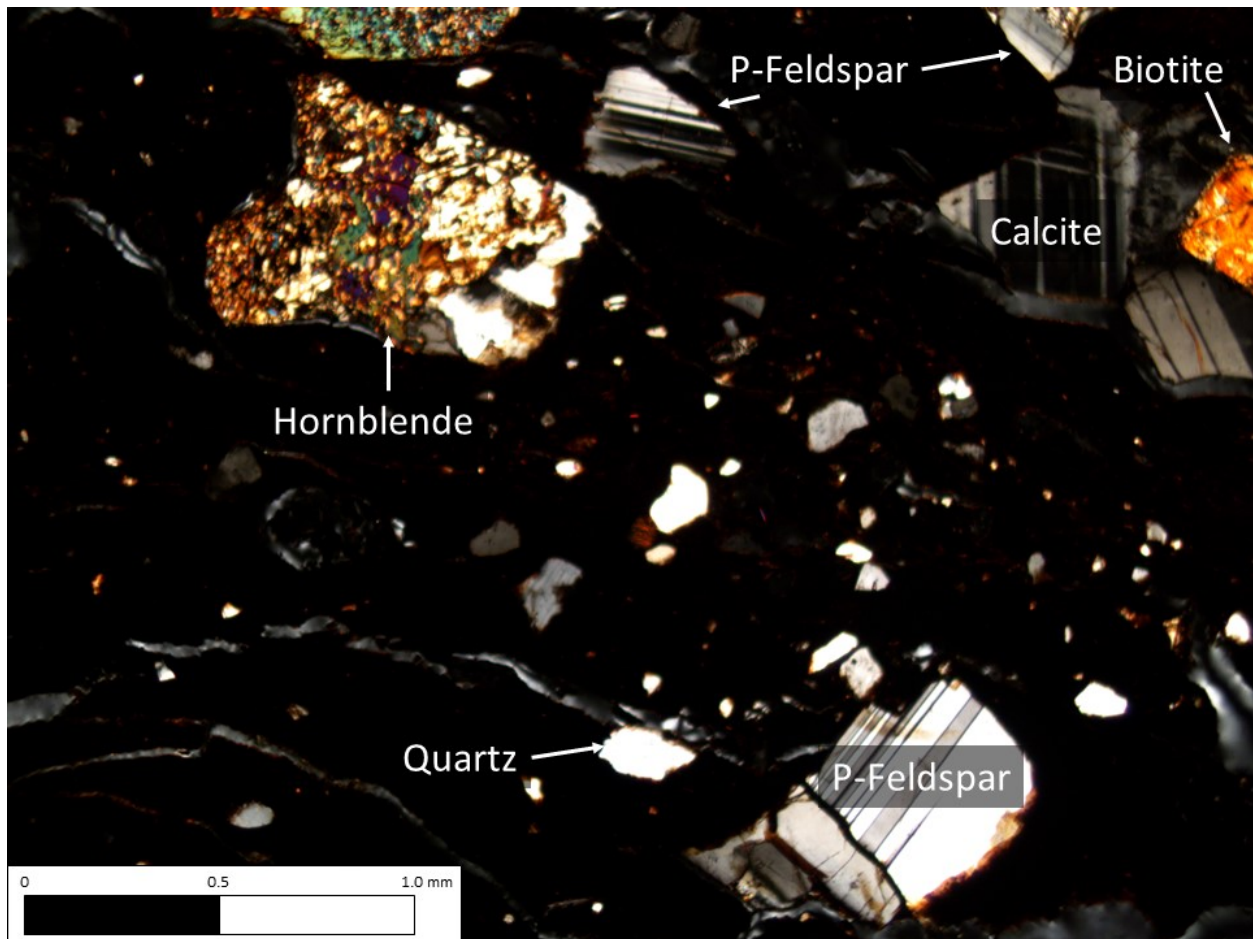


Figure 4.34 Thin section image of Sample 3 (Cross Polarized Light, 4X).

#### *Sample 4*

In Sample 4, eight individual minerals were identified. These minerals include those in the silicate groups such as micas, quartzes, and feldspars, as well as non-silicate groups including phosphates, carbonates, and oxides. In the mica group, twenty-five points were biotite and two were sericite. In the quartz mineral group, nine were quartz and three were myrmekite. In the feldspar group, twenty-nine points were plagioclase feldspar and three were microcline. In the non-silicate mineral groups, nineteen points were calcite and ten were opaque minerals. Figure

4.35 shows minerals identified in PPL and Figure 4.36 shows minerals identified in XPL from the thin section.

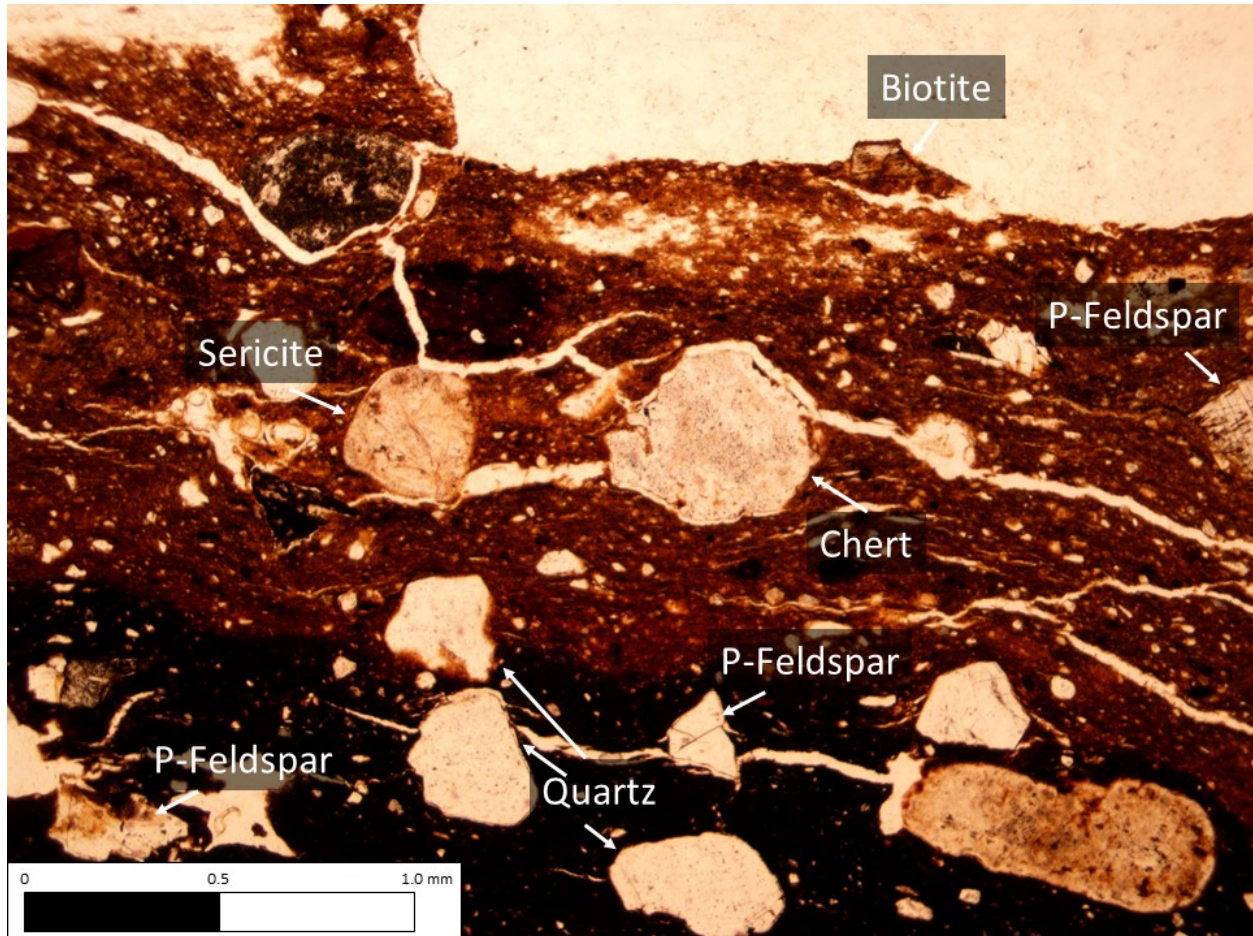


Figure 4.35 Thin section image of Sample 4 (Plane Polarized Light, 4X).

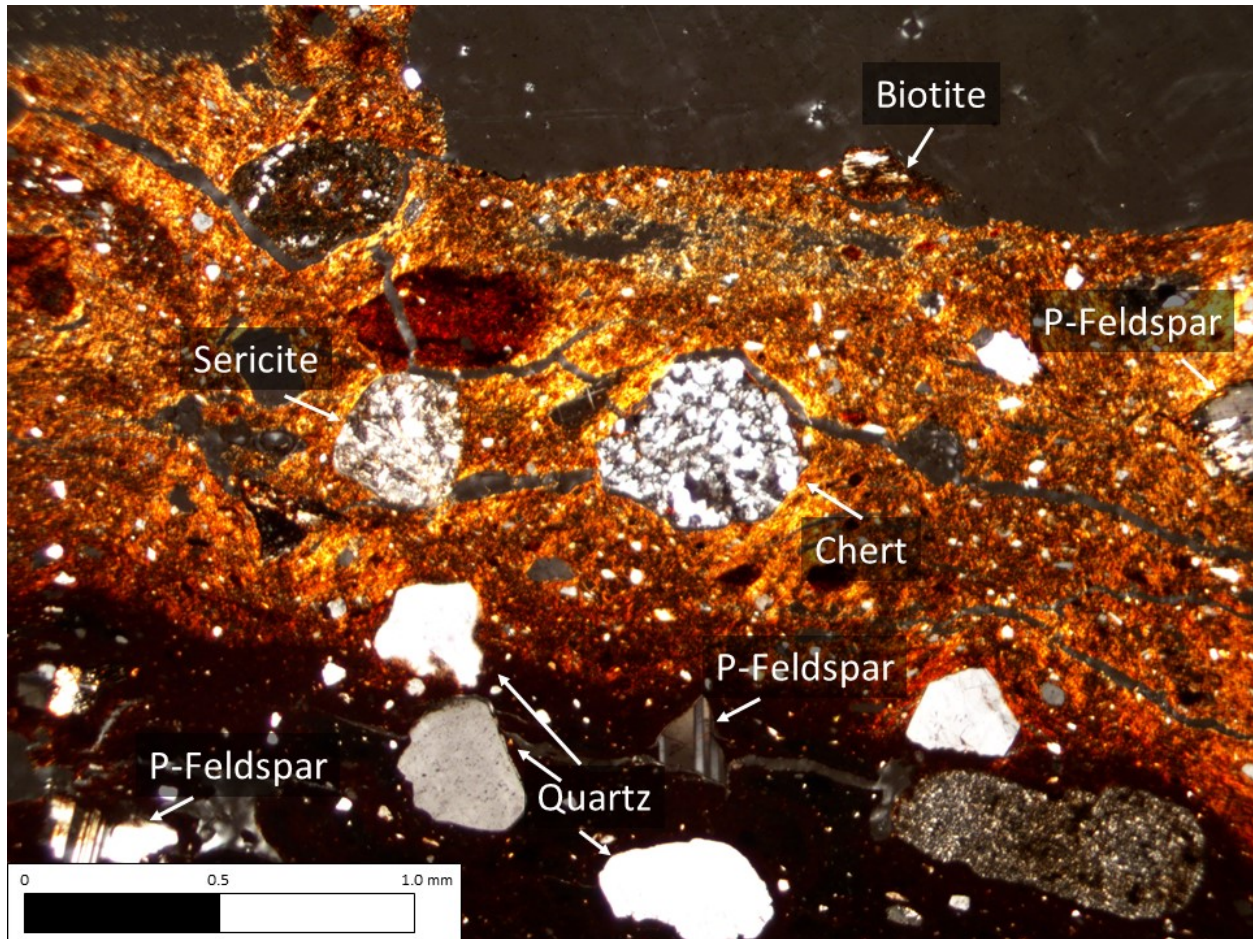


Figure 4.36 Thin section image of Sample 4 (Cross Polarized Light, 4X).

### *Sample 5*

In Sample 5, eight individual minerals were identified. These minerals include those in the silicate groups such as amphiboles, micas, quartzes, and feldspars, as well as non-silicate groups including carbonates and oxides. Three points were identified as hornblende in the amphibole group. In the mica group, seven points were biotite and thirteen were sericite. In the quartz mineral group, fifteen were quartz and one was myrmekite. In the feldspar group, seven points were plagioclase feldspar and three were microcline. In the carbonate group, fifteen points

were calcite. Two points were opaque minerals in the oxide group. Figure 4.37 shows minerals identified in PPL and Figure 4.38 shows minerals identified in XPL from the thin section.

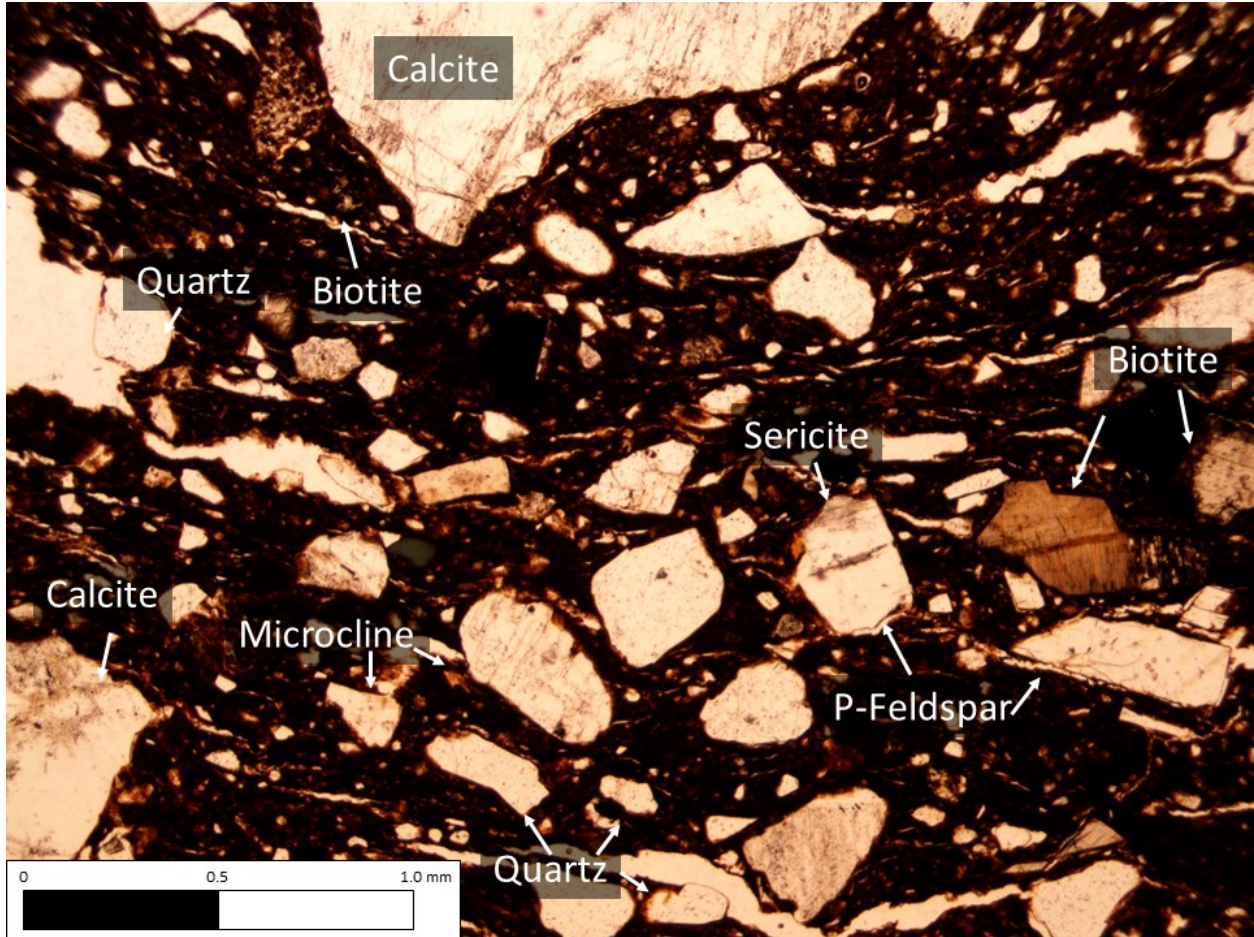


Figure 4.37 Thin section image of Sample 5 (Plane Polarized Light, 4X).

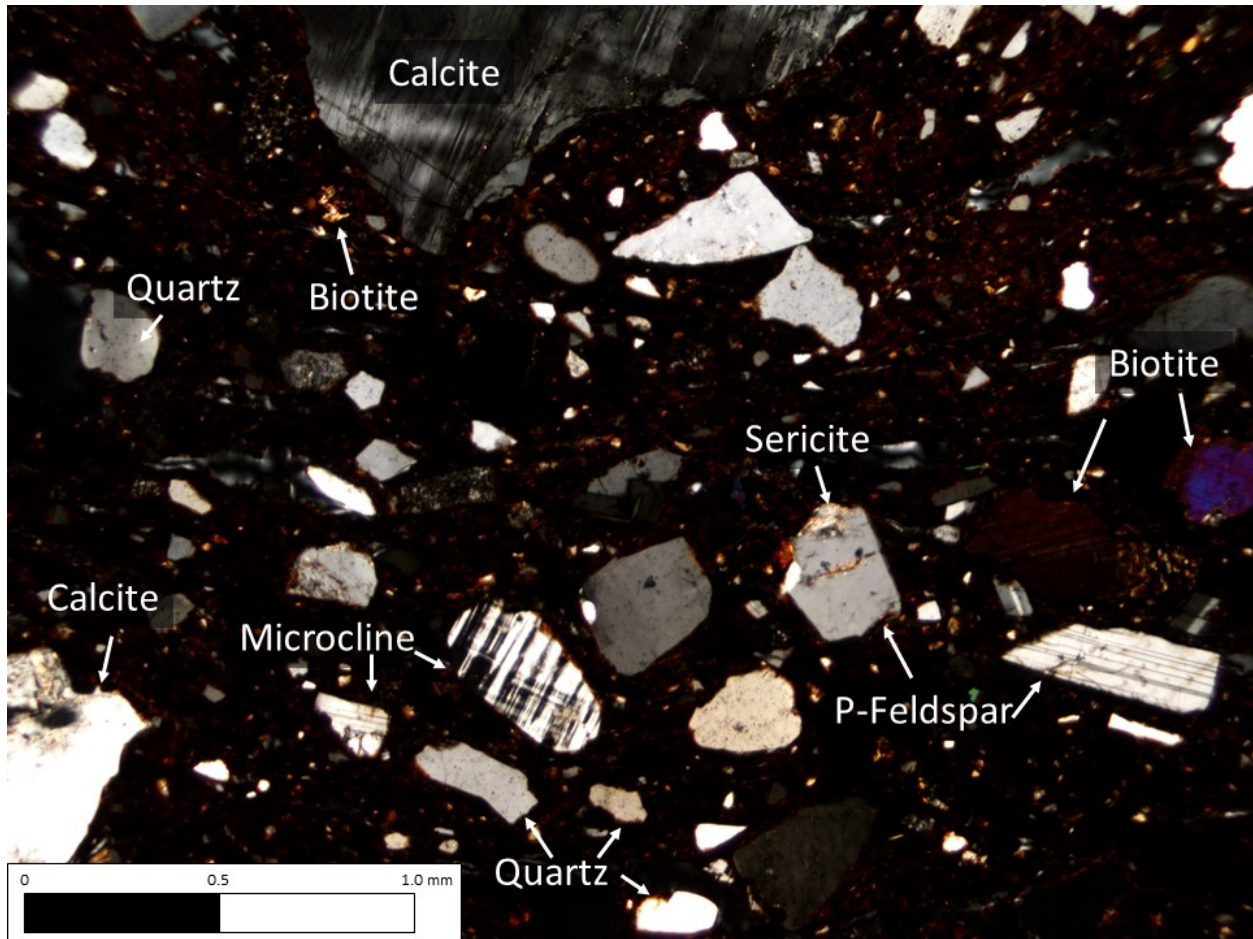


Figure 4.38 Thin section image of Sample 5 (Cross Polarized Light, 4X).

### *Sample 6*

In Sample 6, seven individual minerals were identified. These minerals include those in the silicate groups such as amphiboles, micas, quartzes, and feldspars, as well as non-silicate groups including carbonates and oxides. Five points were identified as hornblende in the amphibole group. In the mica group, thirty-eight points were biotite. In the quartz mineral group, twelve were quartz and twenty-two were myrmekite. In the feldspar group, twenty-five points were plagioclase feldspar. In the carbonate group, twenty-two points were calcite. Twenty-two



points were opaque minerals in the oxide group. Figure 4.39 shows minerals identified in PPL and Figure 4.40 shows minerals identified in XPL from the thin section.

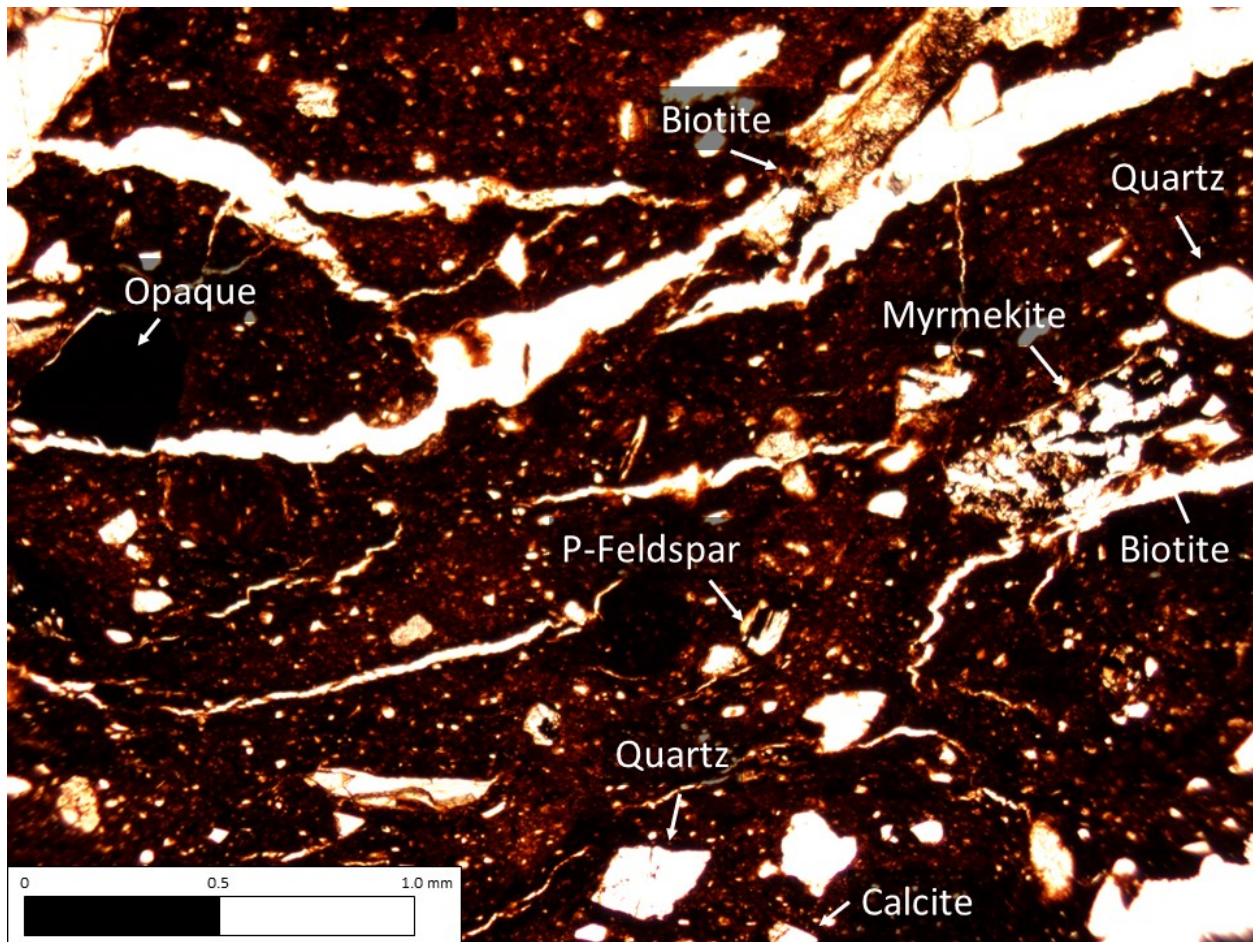


Figure 4.39 Thin section image of Sample 6 (Plane Polarized Light, 4X).

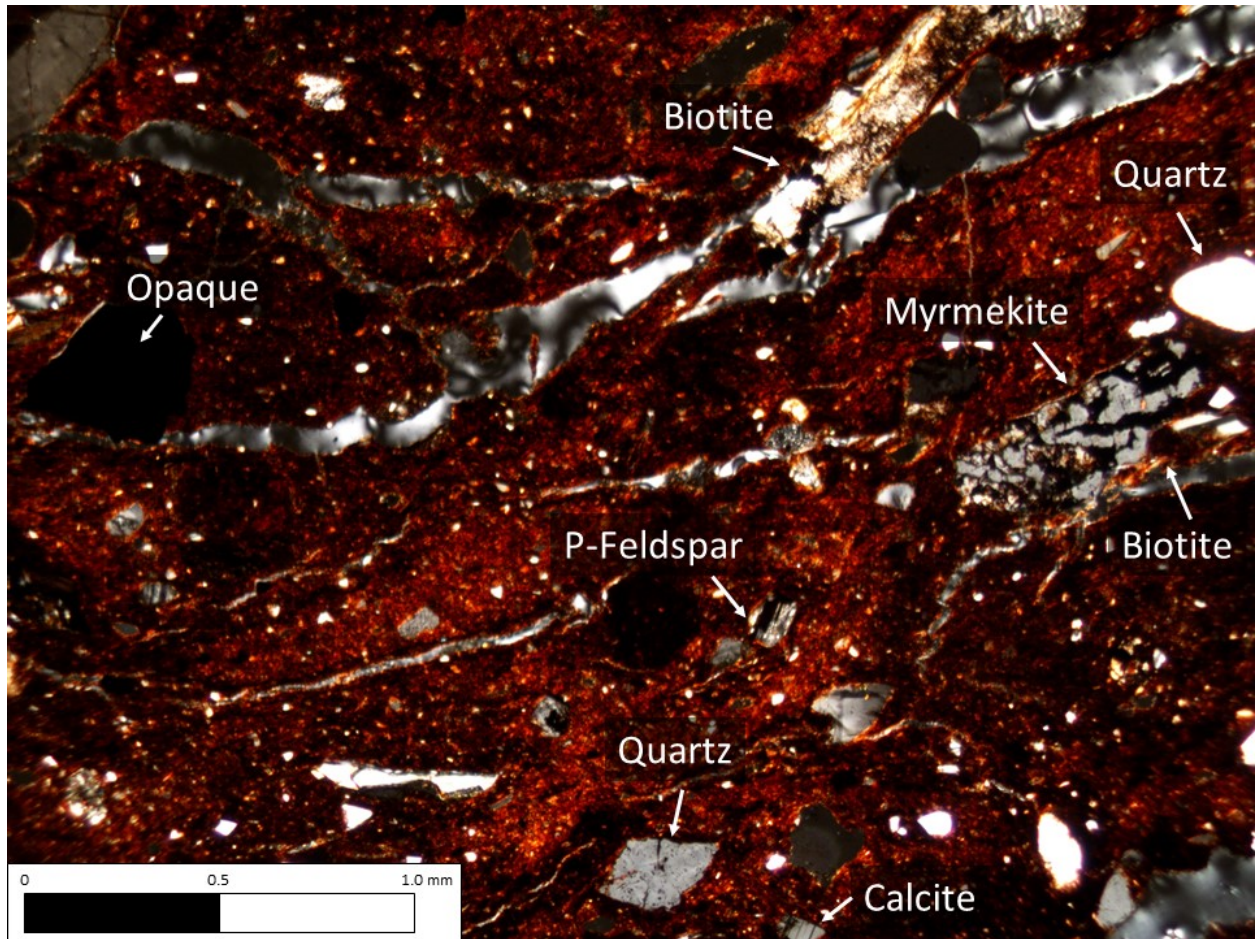


Figure 4.40 Thin section image of Sample 6 (Cross Polarized Light, 4X).

### *Sample 7*

In Sample 7, eight individual mineral types were identified. These include those in the silicate groups such as amphiboles, micas, quartzes, and feldspars, as well as non-silicate groups including carbonates and oxides. Two points were identified as hornblende in the amphibole group. In the mica group, twenty-two points were biotite and twenty-one were sericite. In the quartz mineral group, nineteen were quartz and two were myrmekite. In the feldspar group, eight points were plagioclase feldspar. In the carbonate group, eighteen points were calcite. Twenty-

three points were opaque minerals in the oxide group. Figure 4.41 shows minerals identified in PPL and Figure 4.42 shows minerals identified in XPL from the thin section.

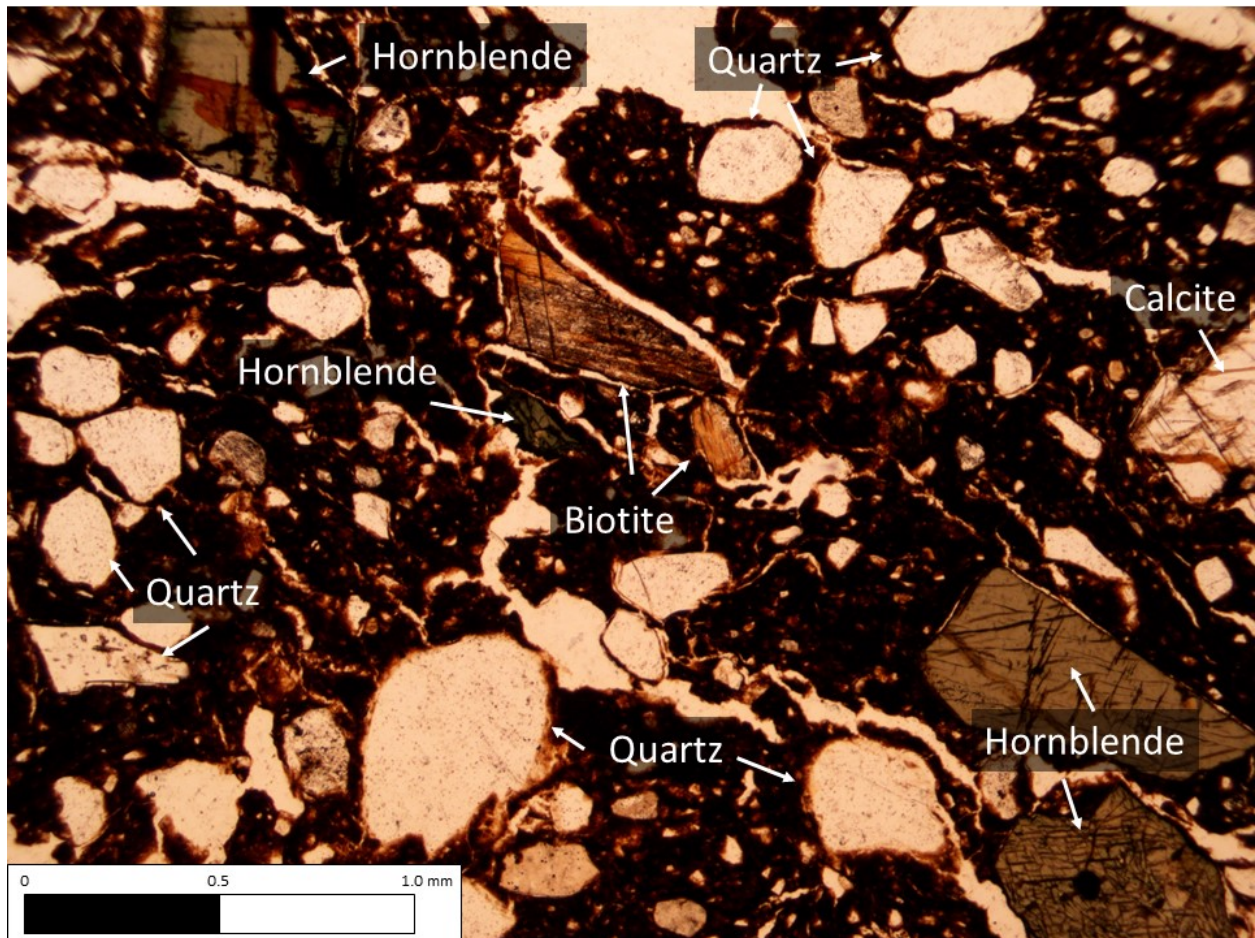


Figure 4.41 Thin section image of Sample 7 (Plane Polarized Light, 4X).

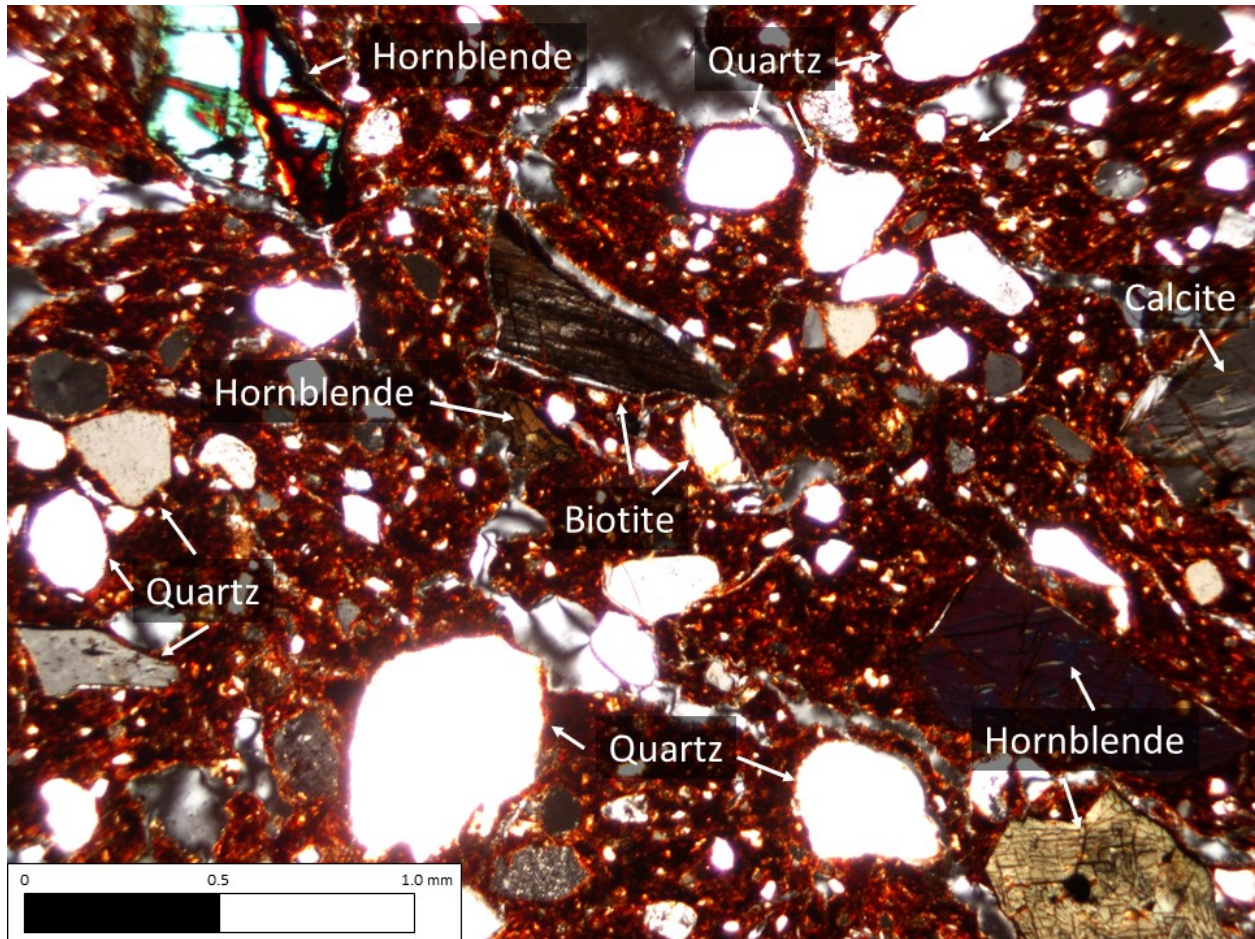


Figure 4.42 Thin section image of Sample 7 (Cross Polarized Light, 4X).

### *Sample 8*

In Sample 8, ten individual mineral types were identified. These include those in the silicate groups such as amphiboles, micas, quartzes, and feldspars, as well as non-silicate groups including carbonates and oxides. One point was identified as hornblende in the amphibole group. In the mica group, twenty-seven points were biotite and eleven were sericite. In the quartz mineral group, twenty-one were quartz and one was myrmekite. In the feldspar group, sixteen points were plagioclase feldspar, one was k-feldspar, and four were microcline. In the carbonate group, thirty points were calcite. Nine points were opaque minerals in the oxide group. Figure

4.43 shows minerals identified in PPL and Figure 4.44 shows minerals identified in XPL from the thin section.

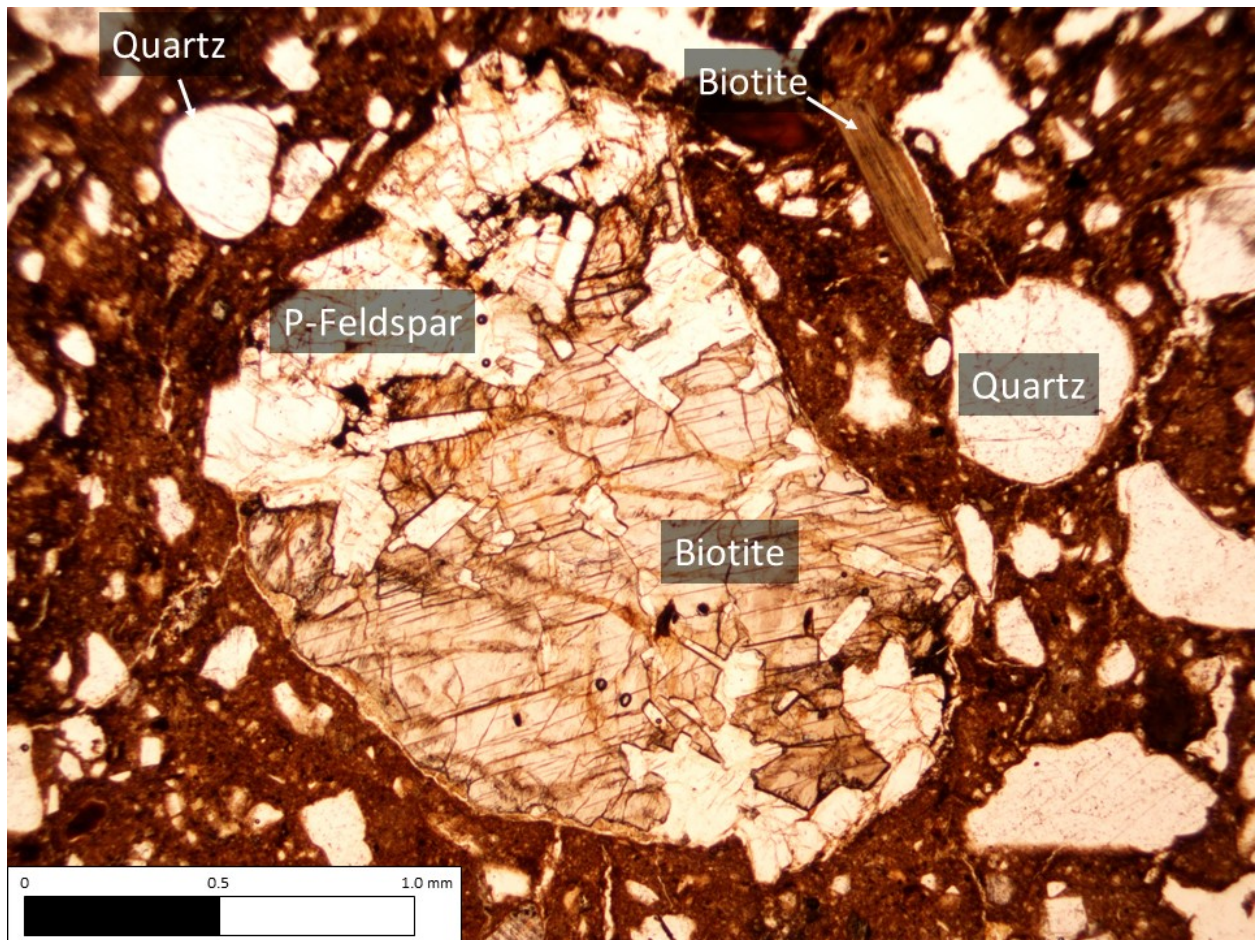


Figure 4.43 Thin section image of Sample 8 (Plane Polarized Light, 4X).

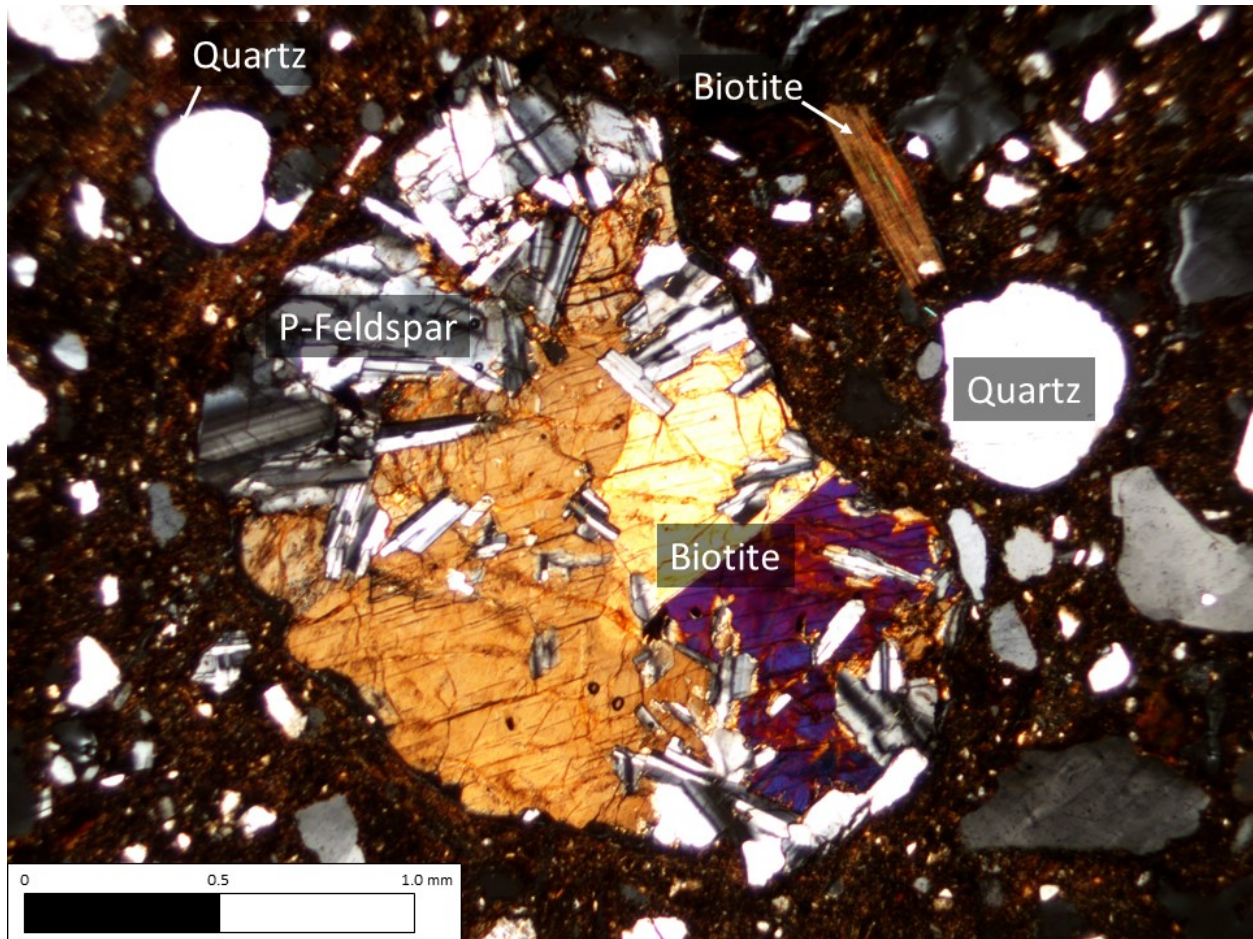


Figure 4.44 Thin section image of Sample 8 (Cross Polarized Light, 4X).

### *Sample 9*

In Sample 9, eight individual mineral types were identified. These include those in the silicate groups such as micas, quartzes, and feldspars, as well as non-silicate groups such as carbonates and oxides. In the mica group, fifteen points were biotite. In the quartz mineral group, twenty-one were quartz and five were myrmekite. In the feldspar group, four points were plagioclase feldspar, six were k-feldspar, and eight were microcline. In the carbonate group, twelve points were calcite. Nine points were opaque minerals in the oxide group. Figure 4.45

shows minerals identified in PPL and Figure 4.46 shows minerals identified in XPL from the thin section.

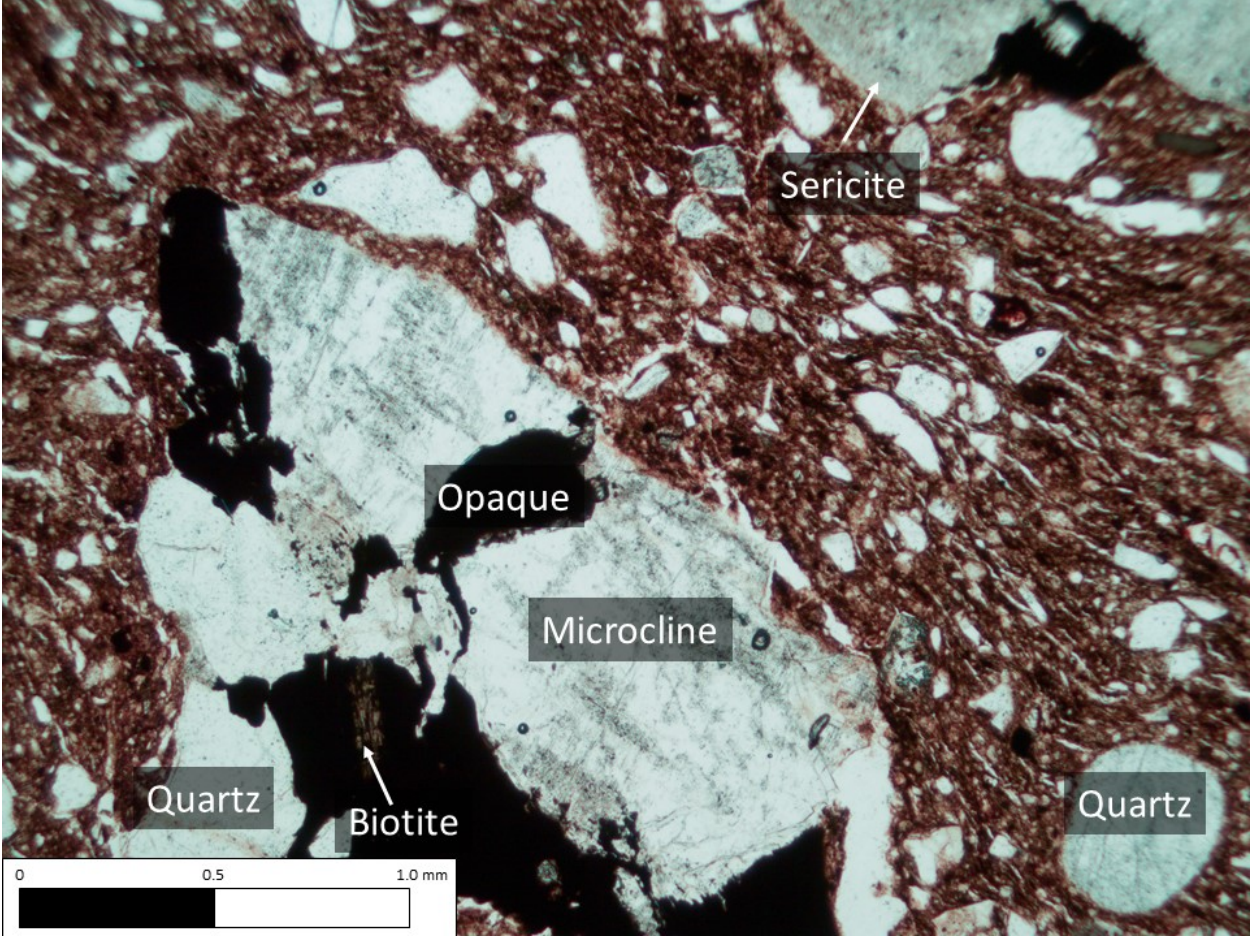


Figure 4.45 Thin section image of Sample 9 (Plane Polarized Light, 4X).

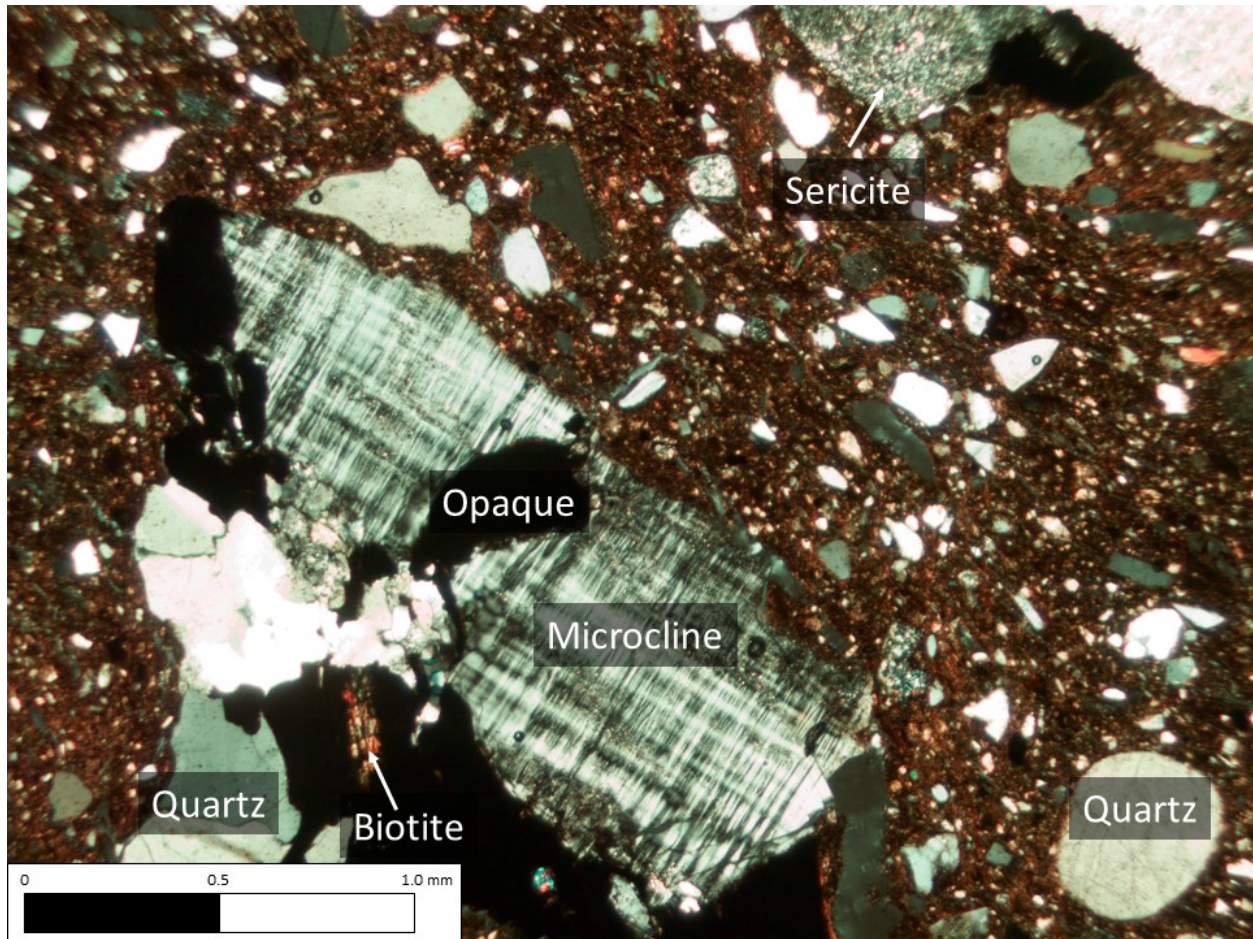


Figure 4.46 Thin section image of Sample 9 (Cross Polarized Light, 4X).

### *Sample 10*

In Sample 10, eight individual mineral types were identified. These include those in the silicate groups such as amphiboles, micas, quartzes, and feldspars, as well as non-silicate groups such as carbonates and oxides. Seven points were identified as hornblende in the amphibole group. In the mica group, sixteen points were biotite. In the quartz mineral group, twelve were quartz and three were quartzite. In the feldspar group, twenty-four points were plagioclase feldspar and one was k-feldspar. In the carbonate group, eight points were calcite. Twelve points



were opaque minerals in the oxide group. Figure 4.47 shows minerals identified in PPL and Figure 4.48 shows minerals identified in XPL from the thin section.

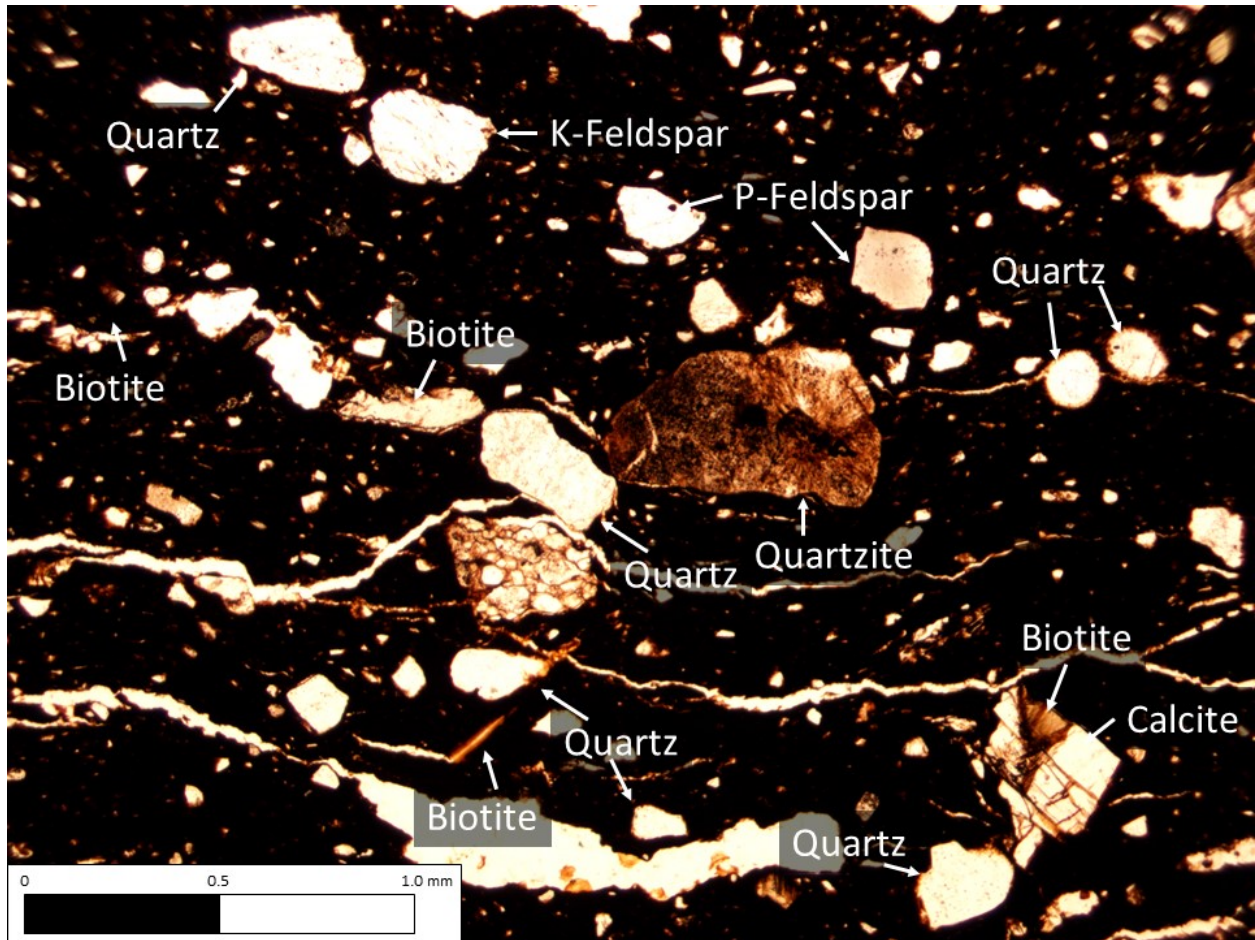


Figure 4.47 Thin section image of Sample 10 (Plane Polarized Light, 4X).

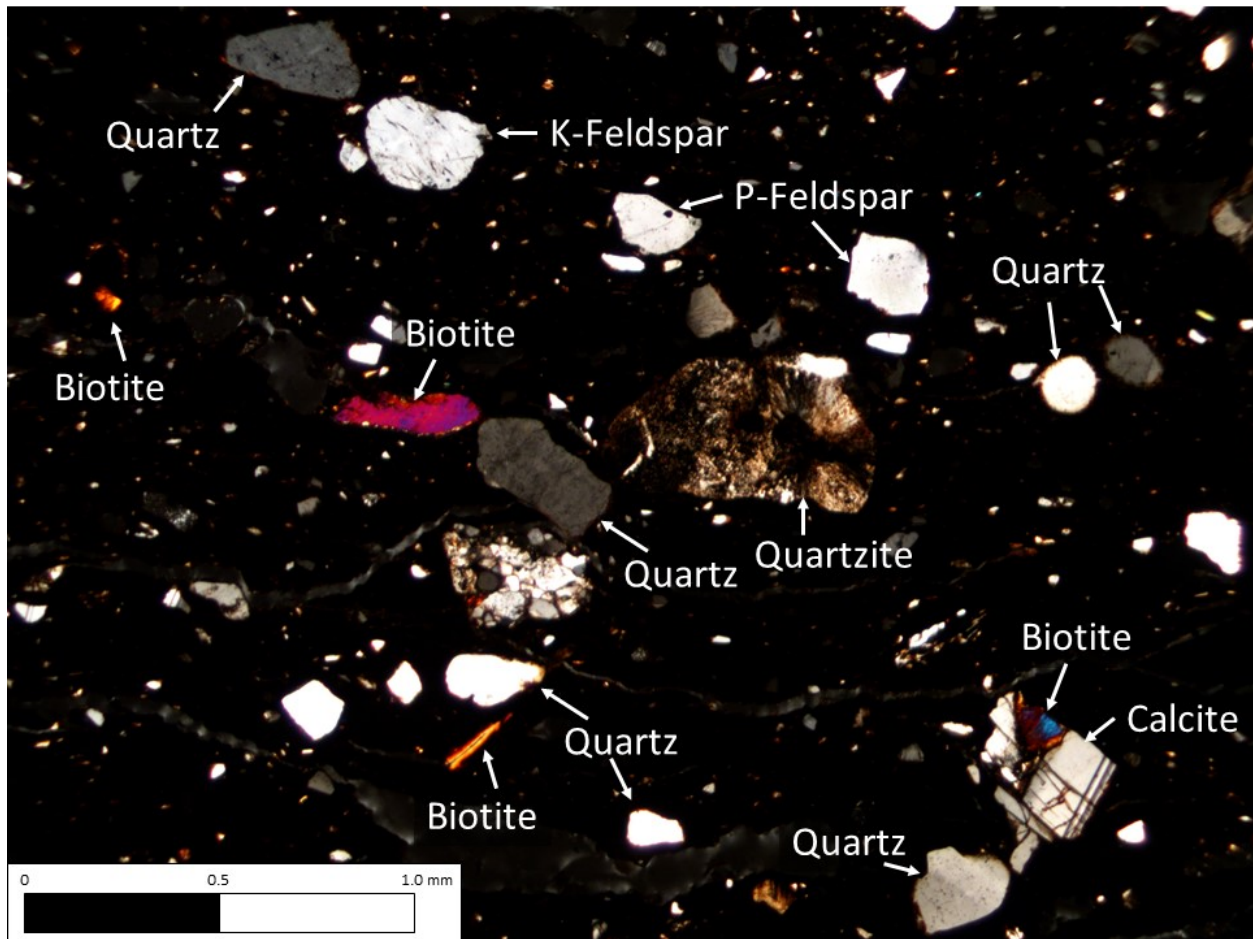


Figure 4.48 Thin section image of Sample 10 (Plane Polarized Light, 4X).

### *Sample 11*

In Sample 11, six individual mineral types were identified. These include those in the silicate groups such as amphiboles, micas, quartzes, and feldspars, as well as non-silicate groups such as carbonates and oxides. Three points were identified as hornblende in the amphibole group. In the mica group, eight points were biotite. In the quartz mineral group, eighteen were quartz. In the feldspar group, six points were plagioclase feldspar. In the carbonate group, ten points were calcite. Eight points were opaque minerals in the oxide group. Figure 4.49 shows

minerals identified in PPL and Figure 4.50 shows minerals identified in XPL from the thin section.

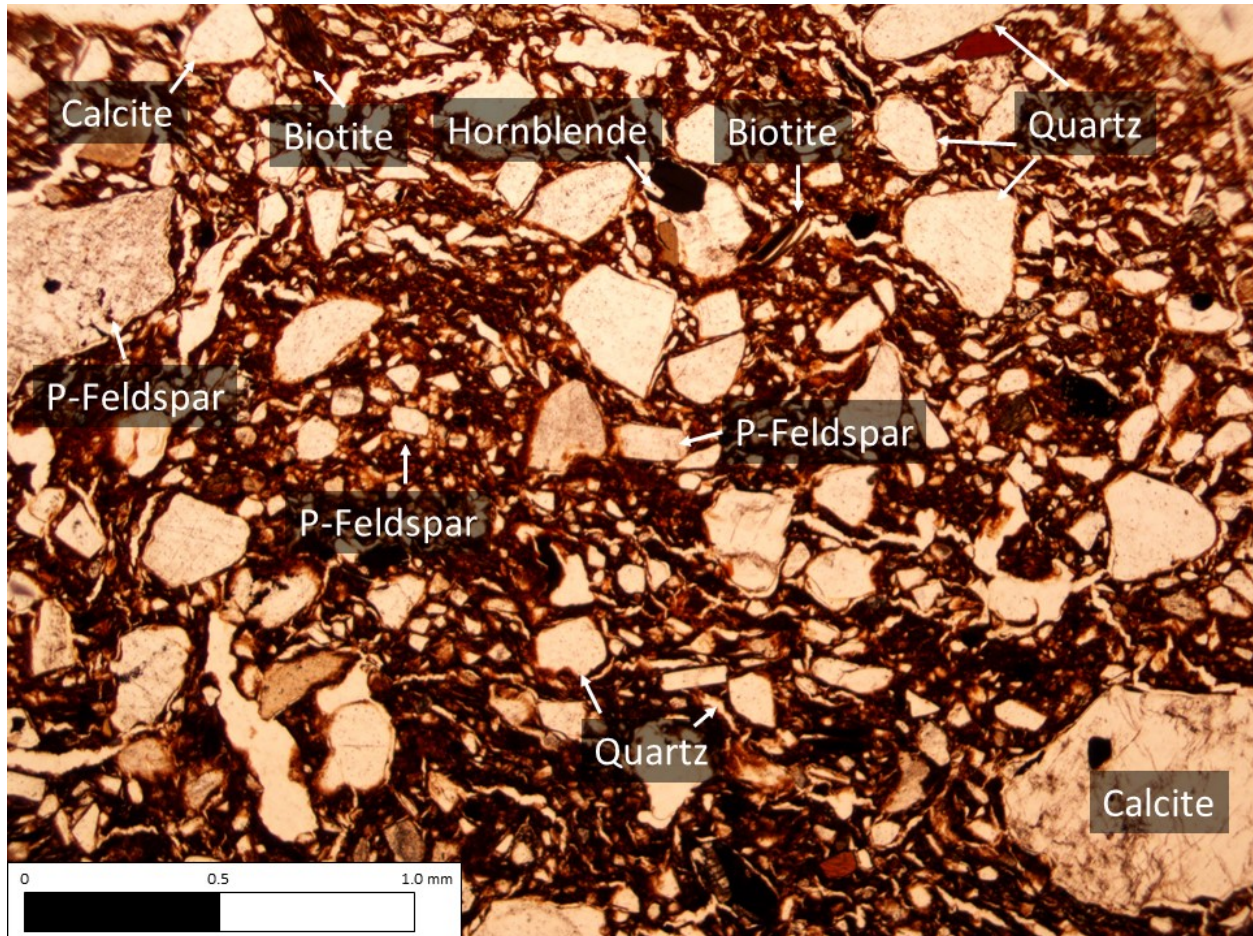


Figure 4.49 Thin section image of Sample 11 (Plane Polarized Light, 4X).

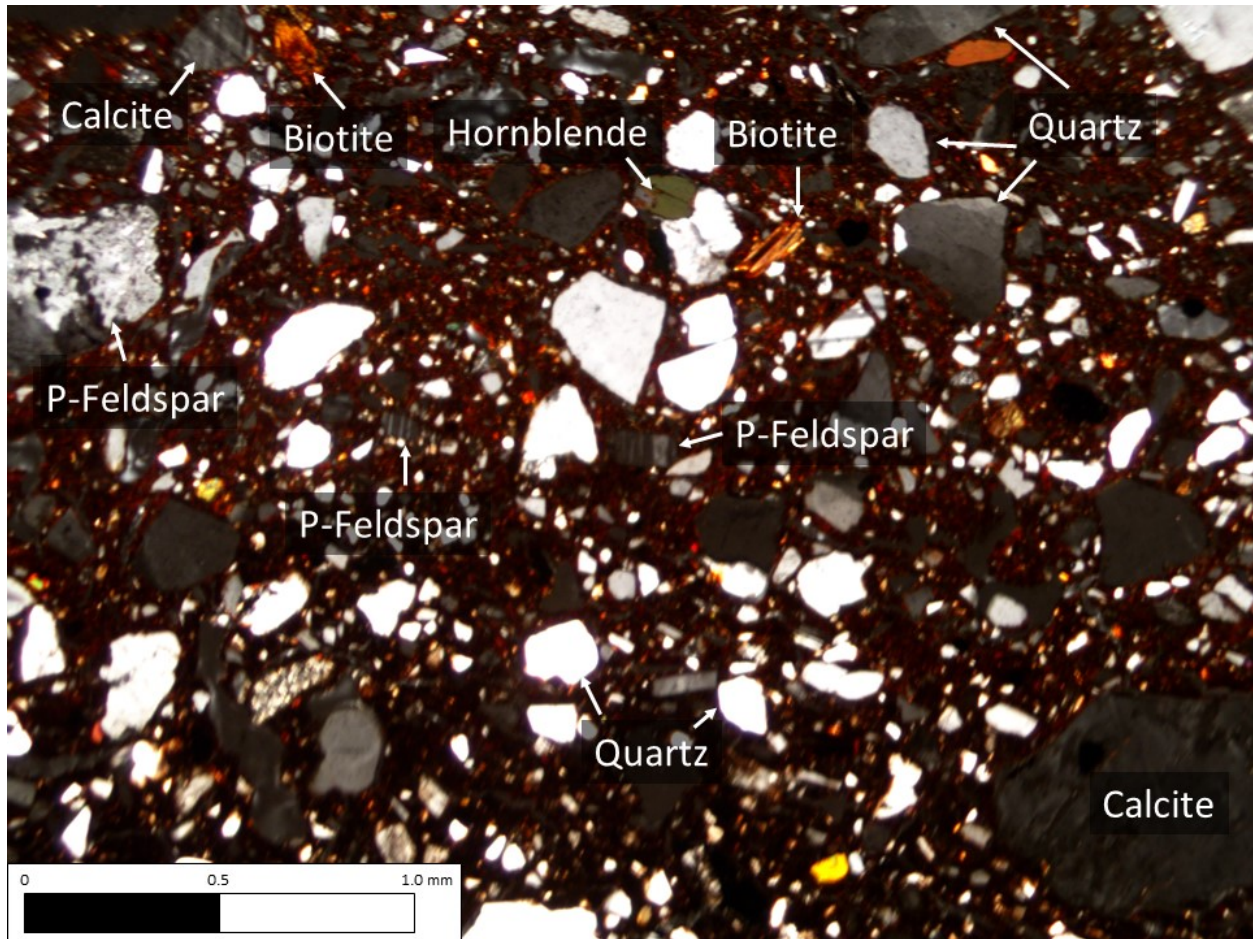


Figure 4.50 Thin section image of Sample 11 (Cross Polarized Light, 4X).

### *Sample 12*

In Sample 12, nine individual mineral types were identified. These include those in the silicate groups such as amphiboles, micas, quartzes, and feldspars, as well as non-silicate groups such as carbonates and oxides. Four points were identified as hornblende in the amphibole group. In the mica group, nine points were biotite. In the quartz mineral group, thirty-nine were quartz and one was myrmekite. In the feldspar group, sixteen points were plagioclase feldspar, seven were k-feldspar, and one was microcline. In the carbonate group, eight points were calcite. Eight

points were opaque minerals in the oxide group. Figure 4.51 shows minerals identified in PPL and Figure 4.52 shows minerals identified in XPL from the thin section.

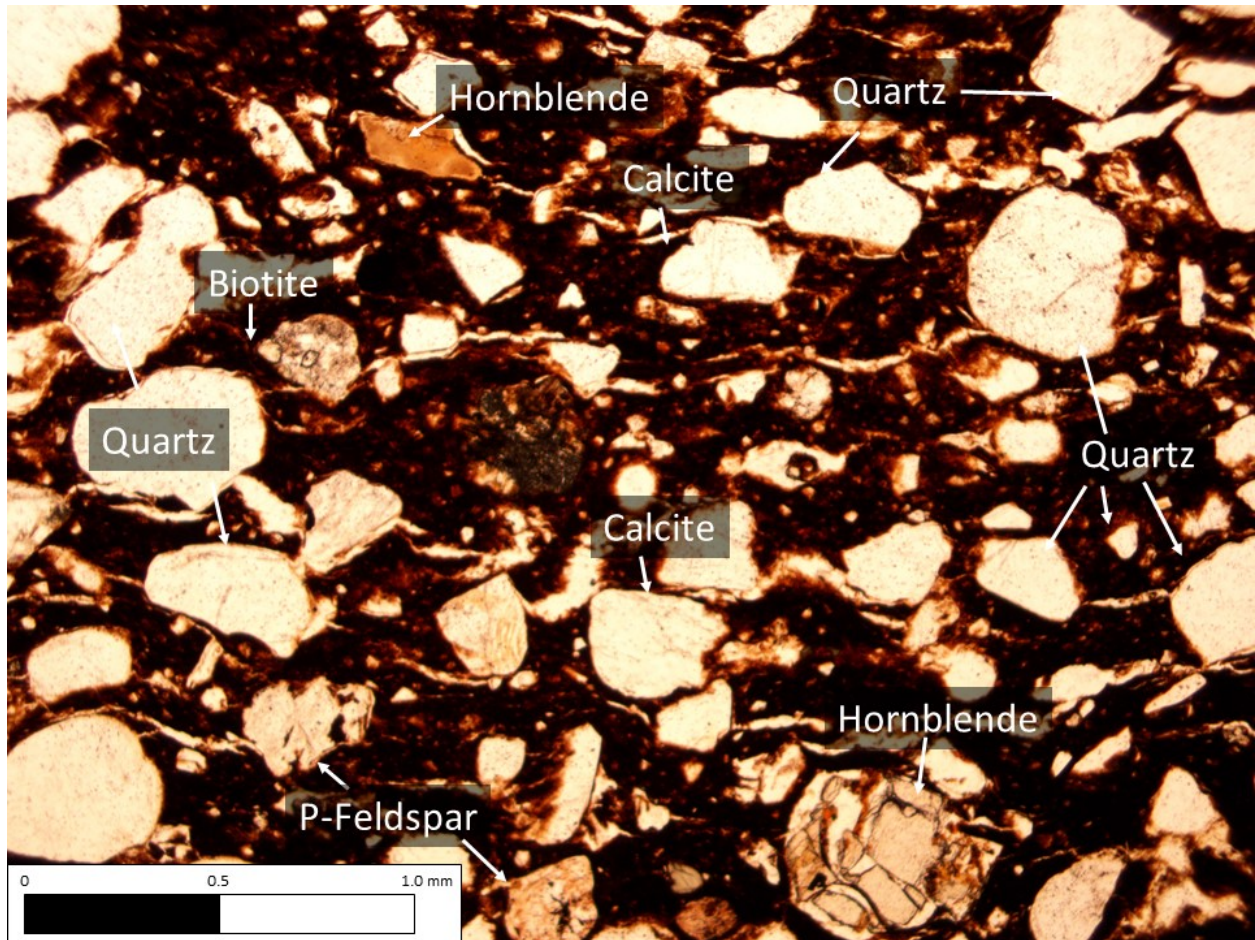


Figure 4.51 Thin section image of Sample 12 (Plane Polarized Light, 4X).

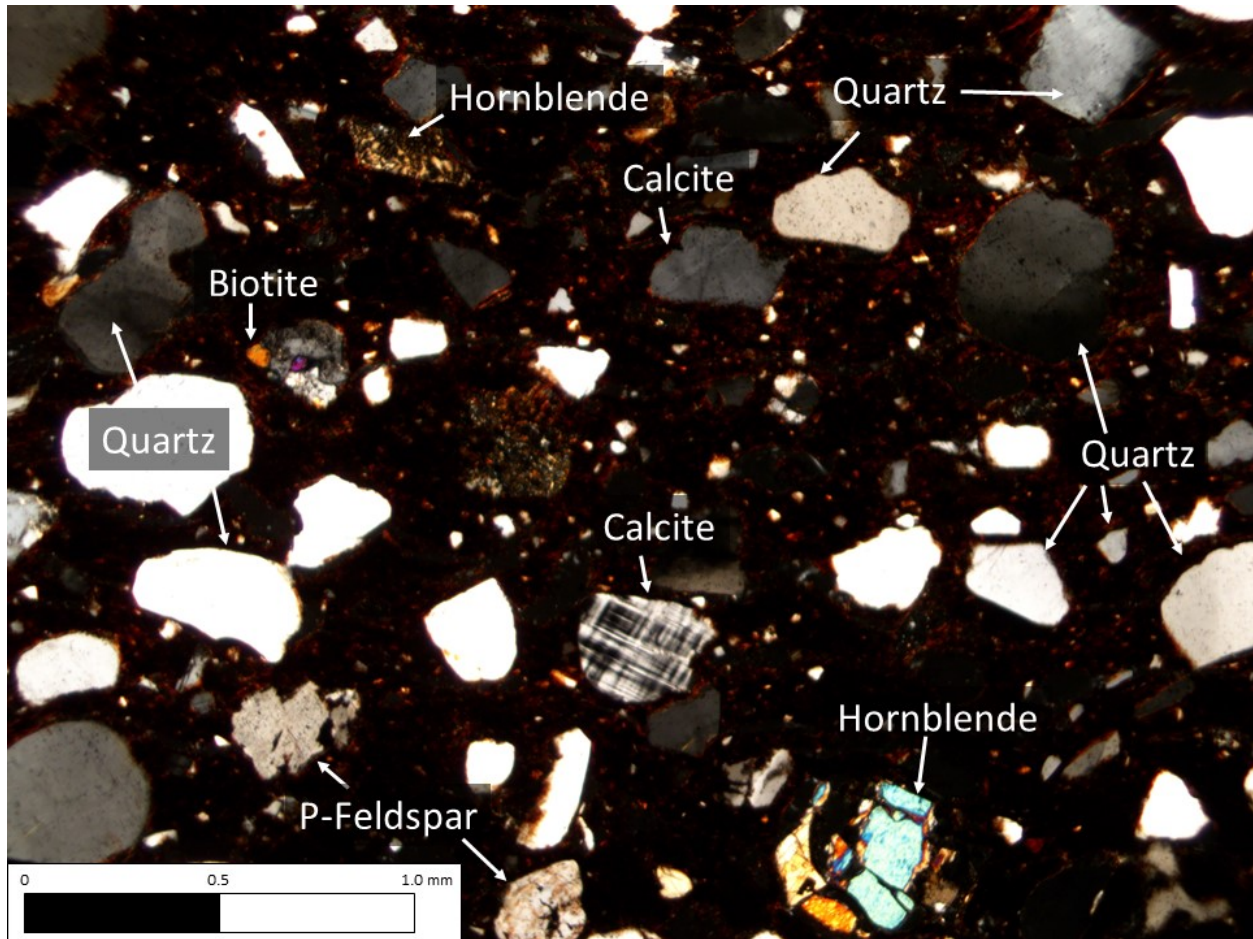


Figure 4.52 Thin section image of Sample 12 (Cross Polarized Light, 4X).

### *Sample 13*

In Sample 13, six individual mineral types were identified. These include those in the silicate groups such as amphiboles, micas, quartzes, and feldspars, as well as non-silicate groups such as carbonates and oxides. Three points were identified as hornblende in the amphibole group. In the mica group, six points were biotite. In the quartz mineral group, twenty-six were quartz. In the feldspar group, seven points were plagioclase feldspar. In the carbonate group, three points were calcite. Five points were opaque minerals in the oxide group. Figure 4.53

shows minerals identified in PPL and Figure 4.54 shows minerals identified in XPL from the thin section.

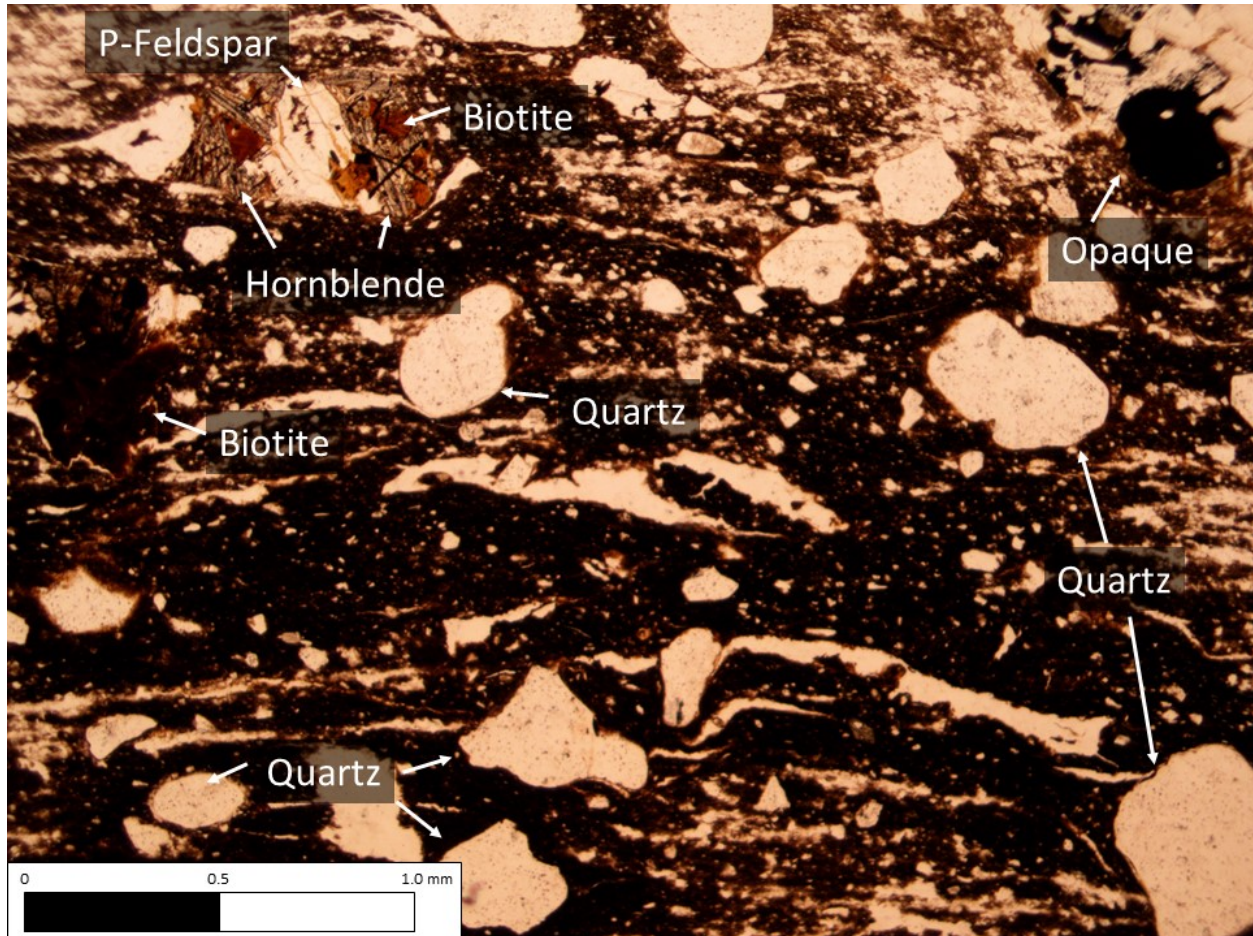


Figure 4.53 Thin section image of Sample 13 (Plane Polarized Light, 4X).

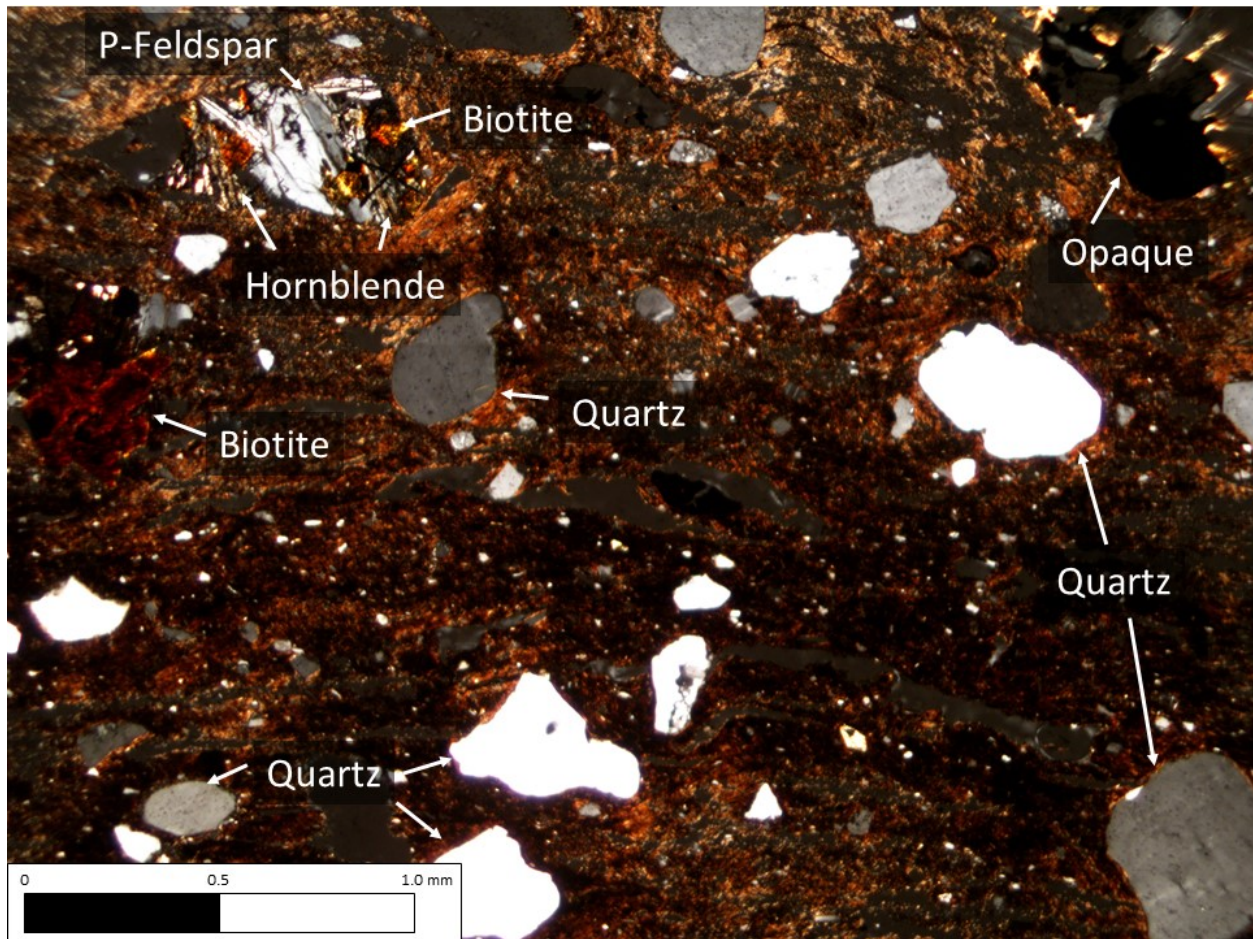


Figure 4.54 Thin section image of Sample 13 (Cross Polarized Light, 4X).

### *Sample 14*

In Sample 14, nine individual mineral types were identified. These include those in the silicate groups such as micas, quartzes, and feldspars, as well as carbonates in the non-silicate groups. In the mica group, ten points were biotite and two were sericite. In the quartz mineral group, twelve were quartz, four were quartzite, and two were myrmekite. In the feldspar group, two points were plagioclase feldspar, three were k-feldspar, and three were microcline. In the carbonate group, five points were calcite. Figure 4.55 shows minerals identified in PPL and Figure 4.56 shows minerals identified in XPL from the thin section.



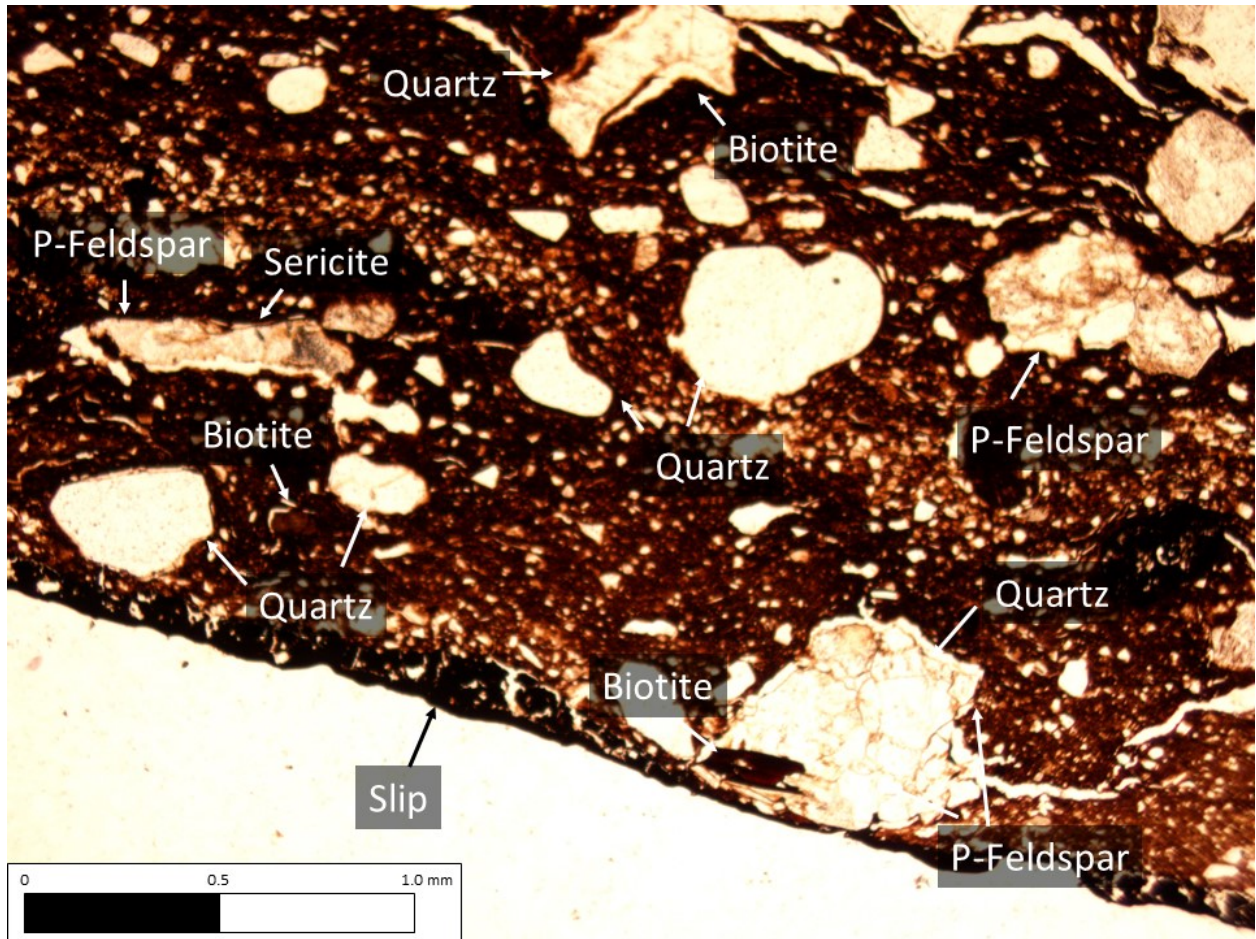


Figure 4.55 Thin section image of Sample 14 (Plane Polarized Light, 4X).

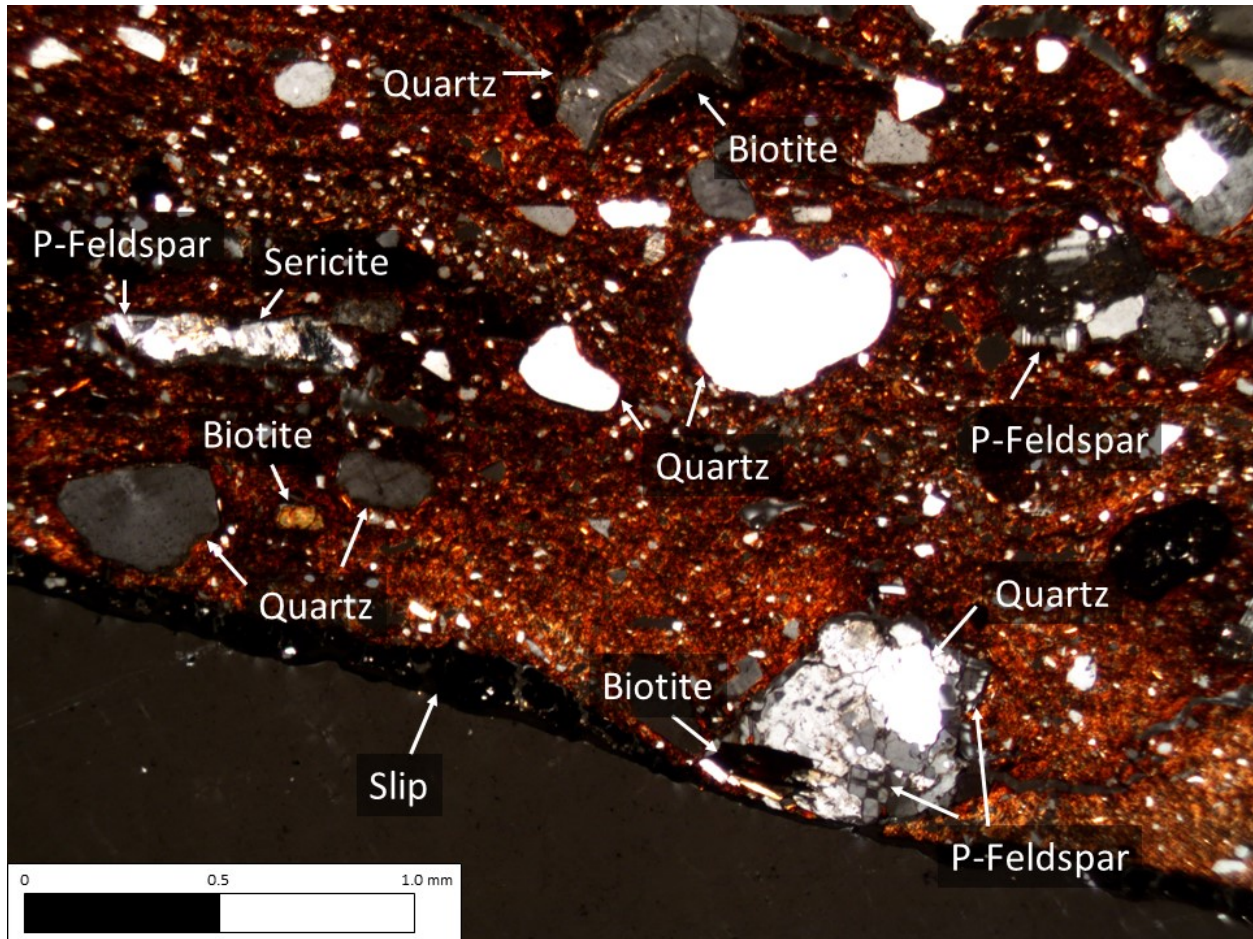


Figure 4.56 Thin section image of Sample 14 (Cross Polarized Light, 4X).

### Sample 15

In Sample 15, eight individual mineral types were identified. These include those in the silicate groups such as amphiboles, micas, quartzes, and feldspars, as well as carbonates in the non-silicate groups. Two points were identified as hornblende in the amphibole group. In the mica group, six points were biotite and seven were sericite. In the quartz mineral group, nineteen were quartz. In the feldspar group, two points were plagioclase feldspar, one was k-feldspar, and one was microcline. In the carbonate group, seven points were calcite. Figure 4.57 shows

minerals identified in PPL and Figure 4.58 shows minerals identified in XPL from the thin section.

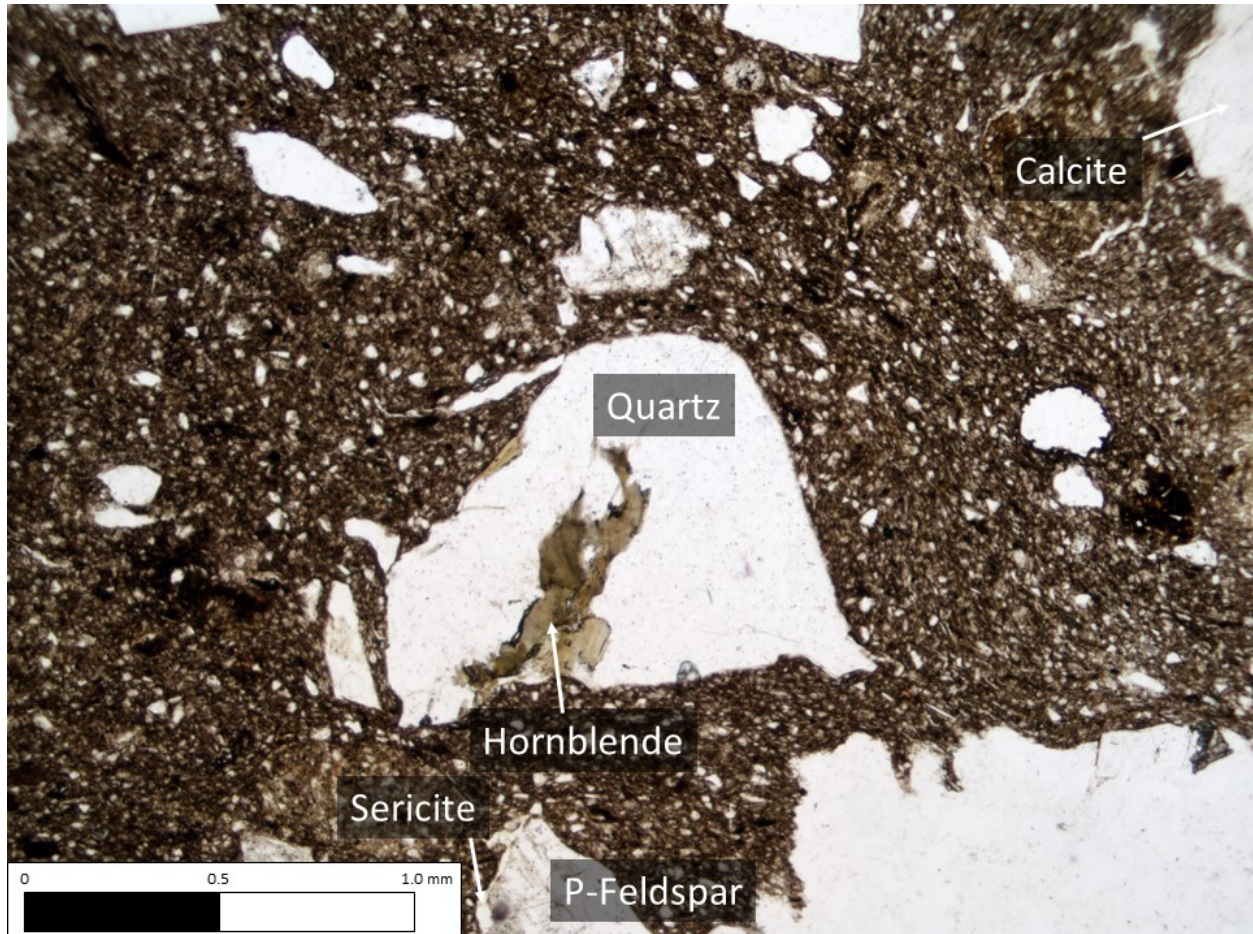


Figure 4.57 Thin section image of Sample 15 (Plane Polarized Light, 4X).

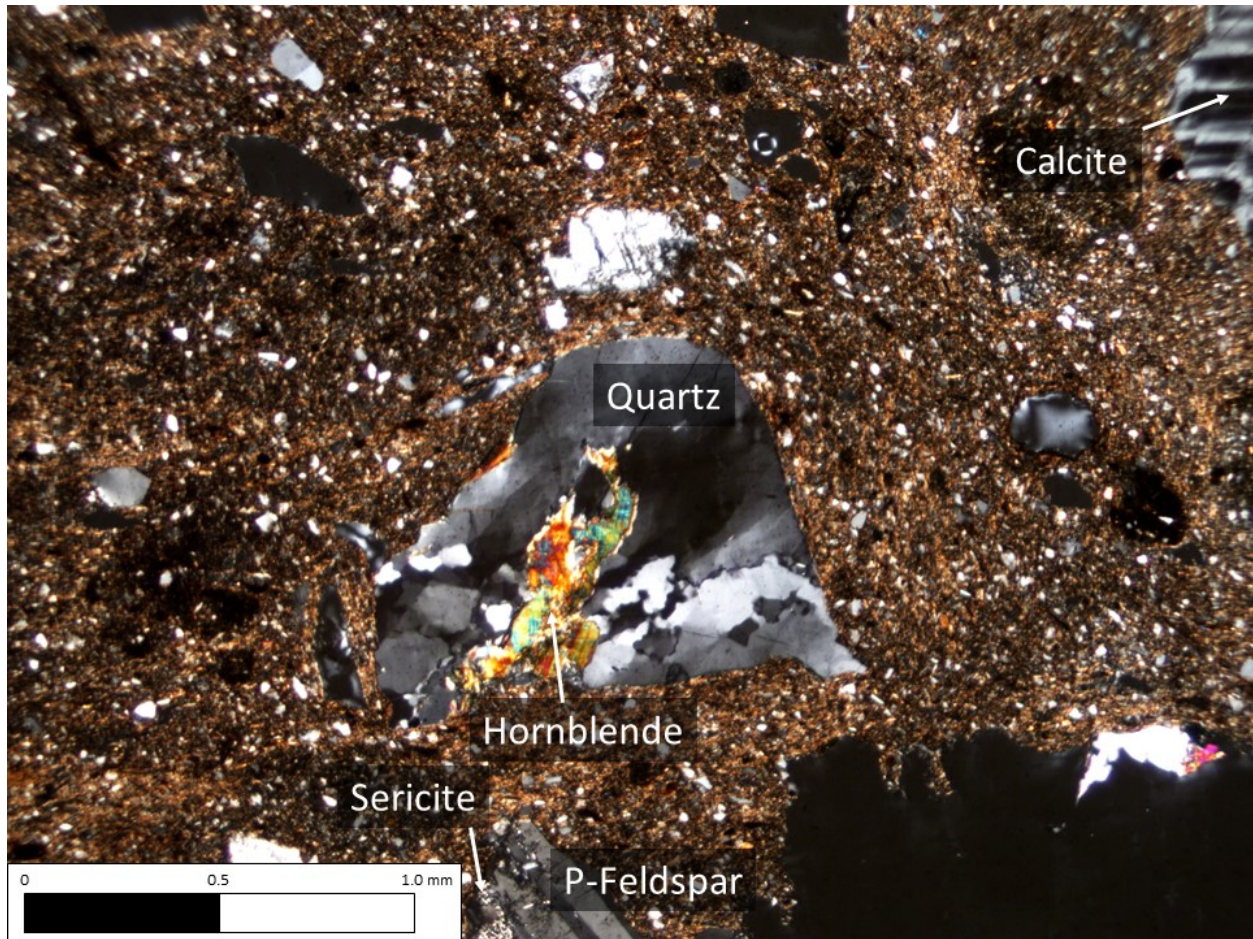


Figure 4.58 Thin section image of Sample 15 (Cross Polarized Light, 4X).

### *Sample 16*

In Sample 16, nine individual mineral types were identified. These include those in the silicate groups such as micas, quartzes, and feldspars, as well as non-silicate groups such as carbonates and oxides. In the mica group, nine points were biotite and three points were sericite. In the quartz mineral group, twelve were quartz and two were myrmekite. In the feldspar group, five points were plagioclase feldspar, one was k-feldspar, and two were microcline. In the carbonate group, six points were calcite. One point was an opaque mineral in the oxide group.

Figure 4.59 shows minerals identified in PPL and Figure 4.60 shows minerals identified in XPL from the thin section.

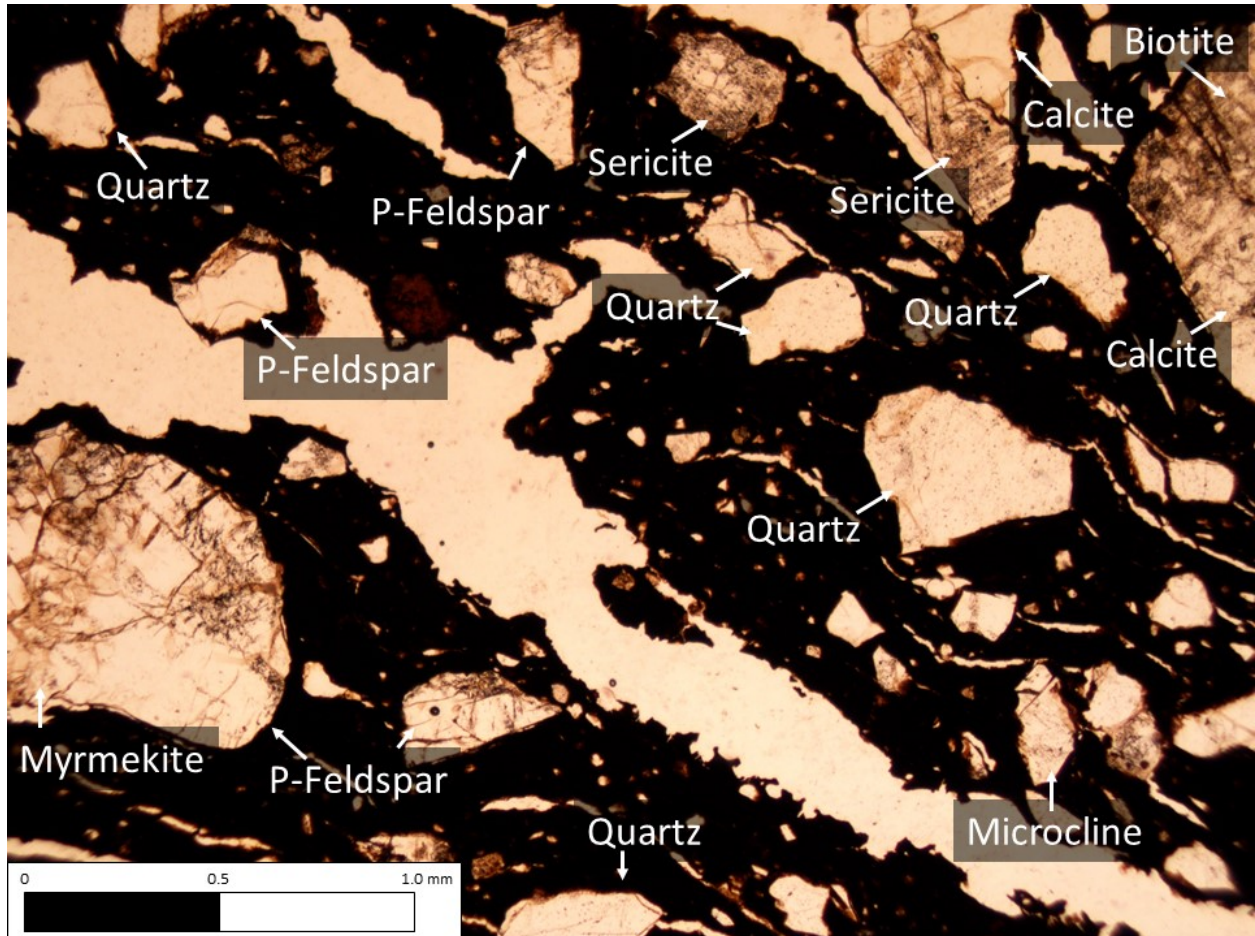


Figure 4.59 Thin section image of Sample 16 (Plane Polarized Light, 4X).

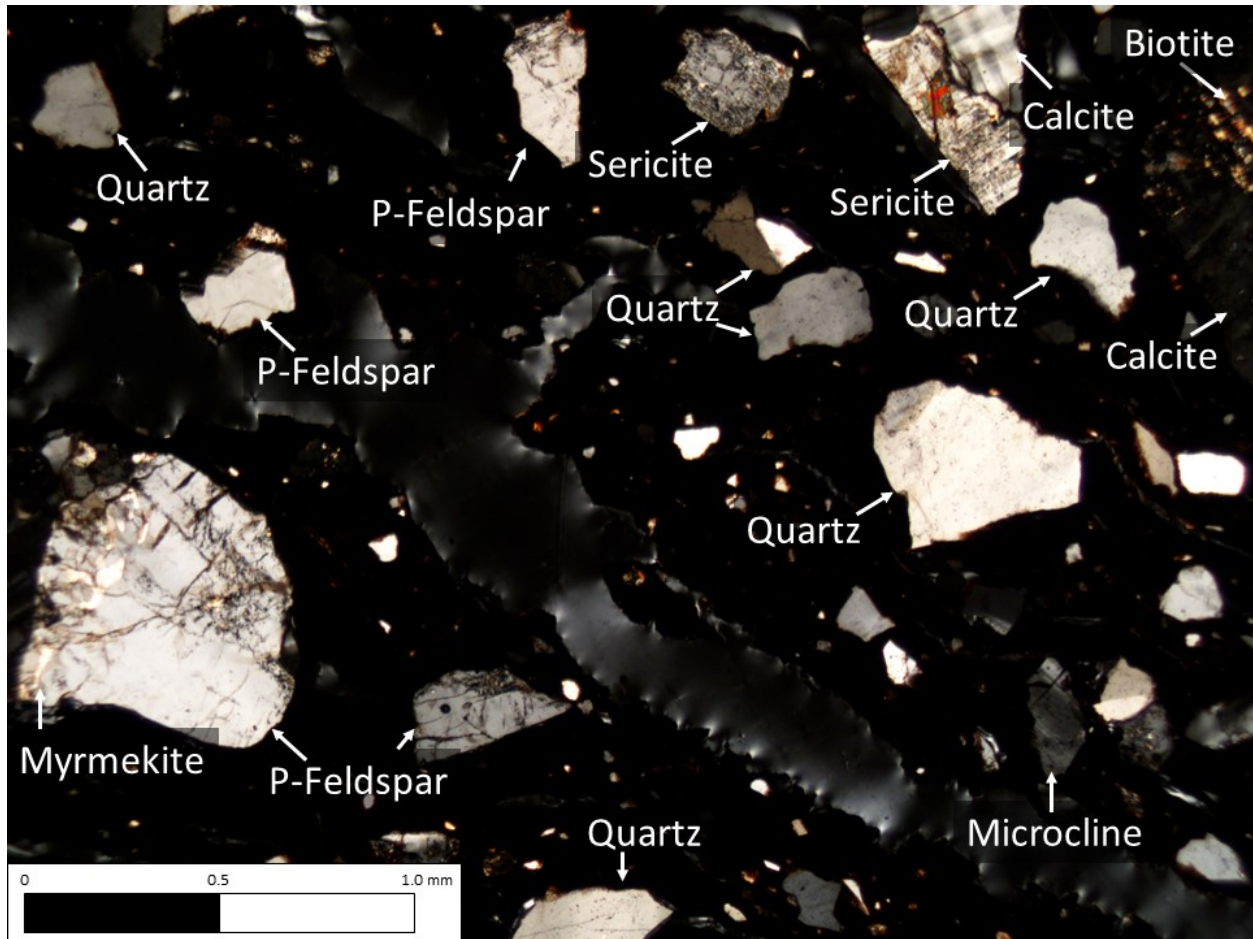


Figure 4.60 Thin section image of Sample 16 (Cross Polarized Light, 4X).

### *Sample 17*

In Sample 17, seven individual mineral types were identified. These include those in the silicate groups such as micas, quartzes, and feldspars, as well as carbonates in the non-silicate groups. In the mica group, nine points were biotite and nine points were sericite. In the quartz mineral group, fourteen were quartz and two were myrmekite. In the feldspar group, six points were plagioclase feldspar and three were k-feldspar. In the carbonate group, six points were calcite. Figure 4.61 shows minerals identified in PPL and Figure 4.62 shows minerals identified in XPL from the thin section.

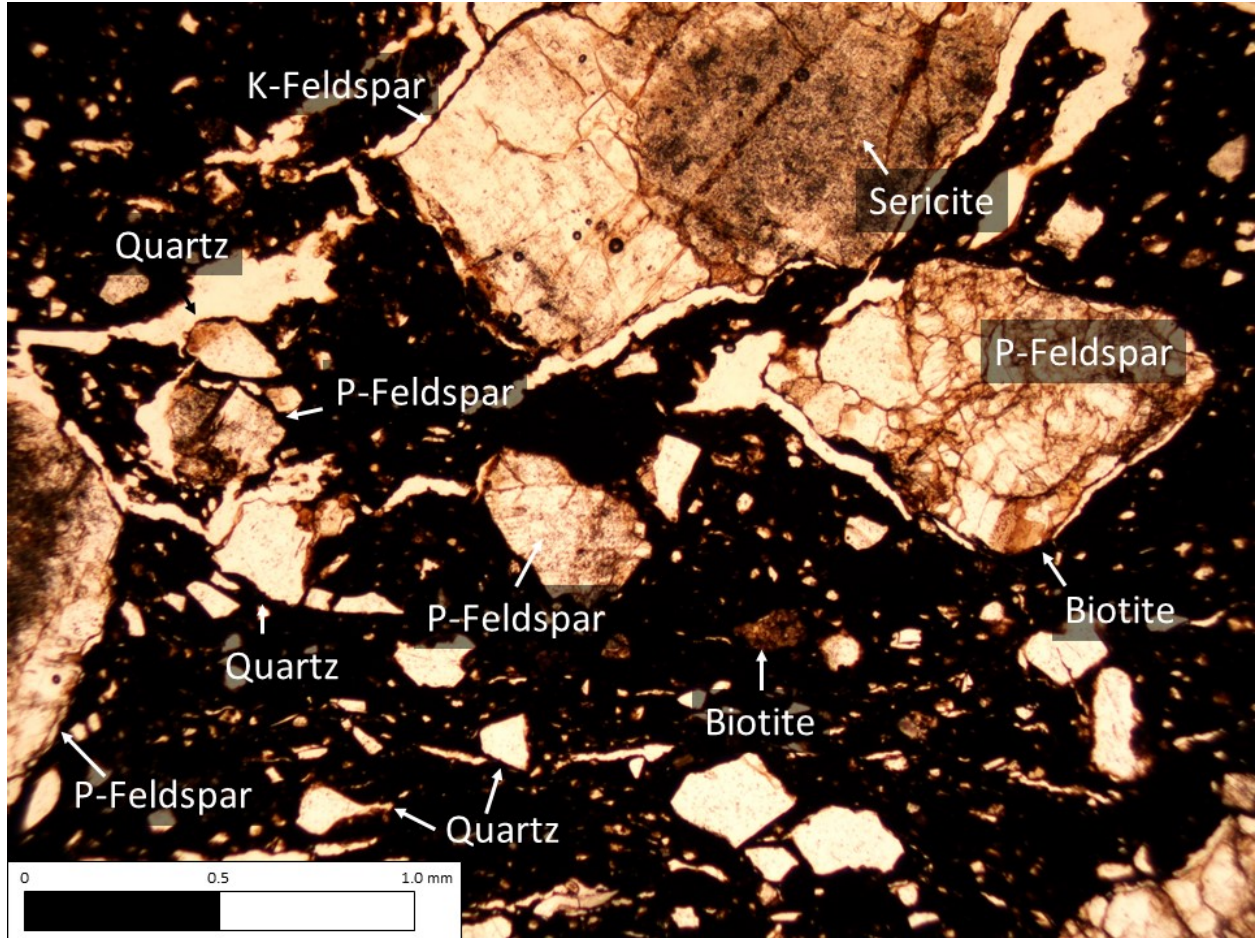


Figure 4.61 Thin section image of Sample 17 (Plane Polarized Light, 4X).

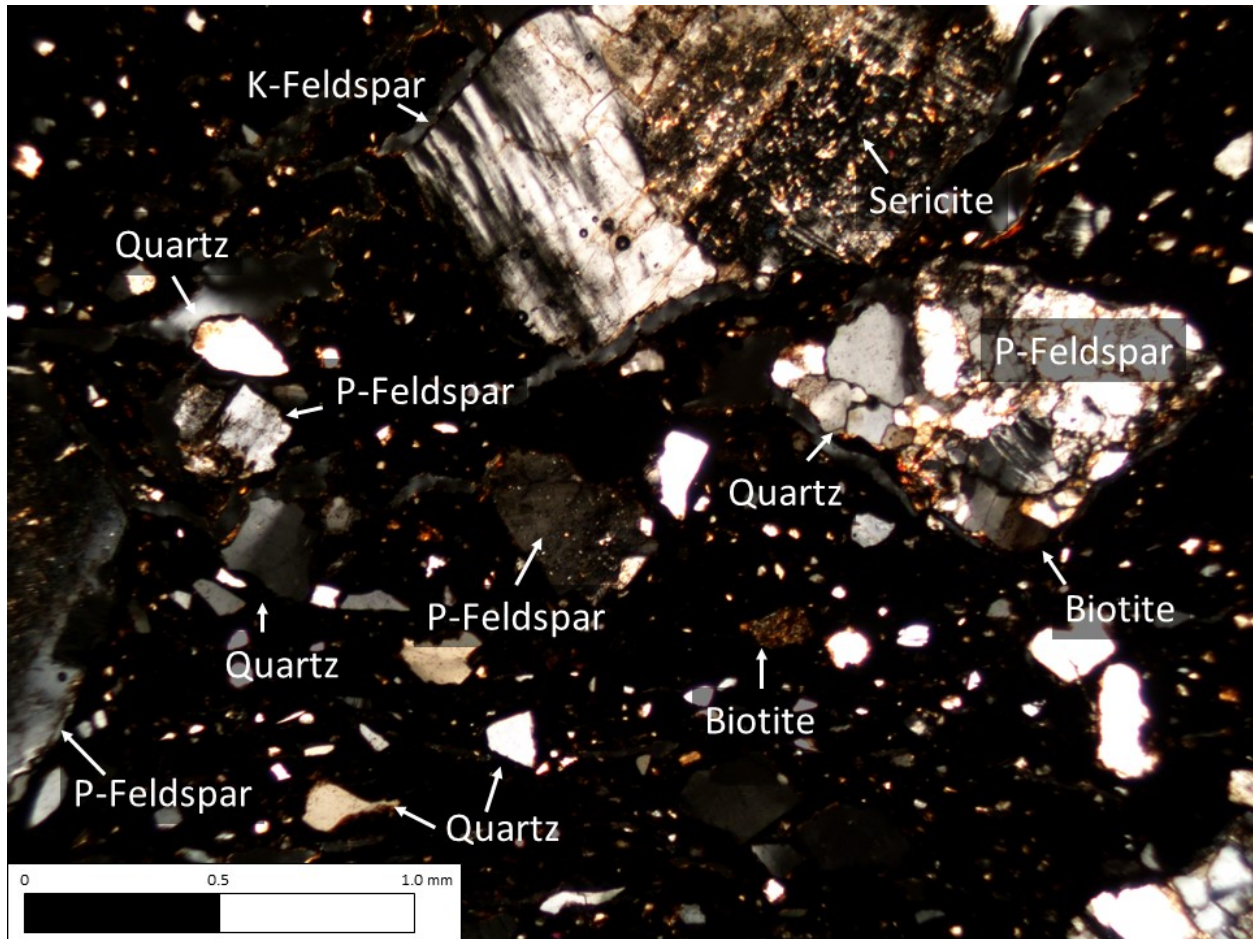


Figure 4.62 Thin section image of Sample 17 (Cross Polarized Light, 4X).

### *Sample 18*

In Sample 18, ten individual mineral types were identified. These include those in the silicate groups such as micas, quartzes, and feldspars, as well as non-silicate groups such as carbonates and oxides. In the mica group, six points were biotite, one point was muscovite, and one point was sericite. In the quartz mineral group, thirty were quartz, one was quartzite, and one was myrmekite. In the feldspar group, eleven points were plagioclase feldspar and one was microcline. In the carbonate group, one point was calcite. Two points were opaque minerals in



the oxide group. Figure 4.63 shows minerals identified in PPL and Figure 4.64 shows minerals identified in XPL from the thin section.

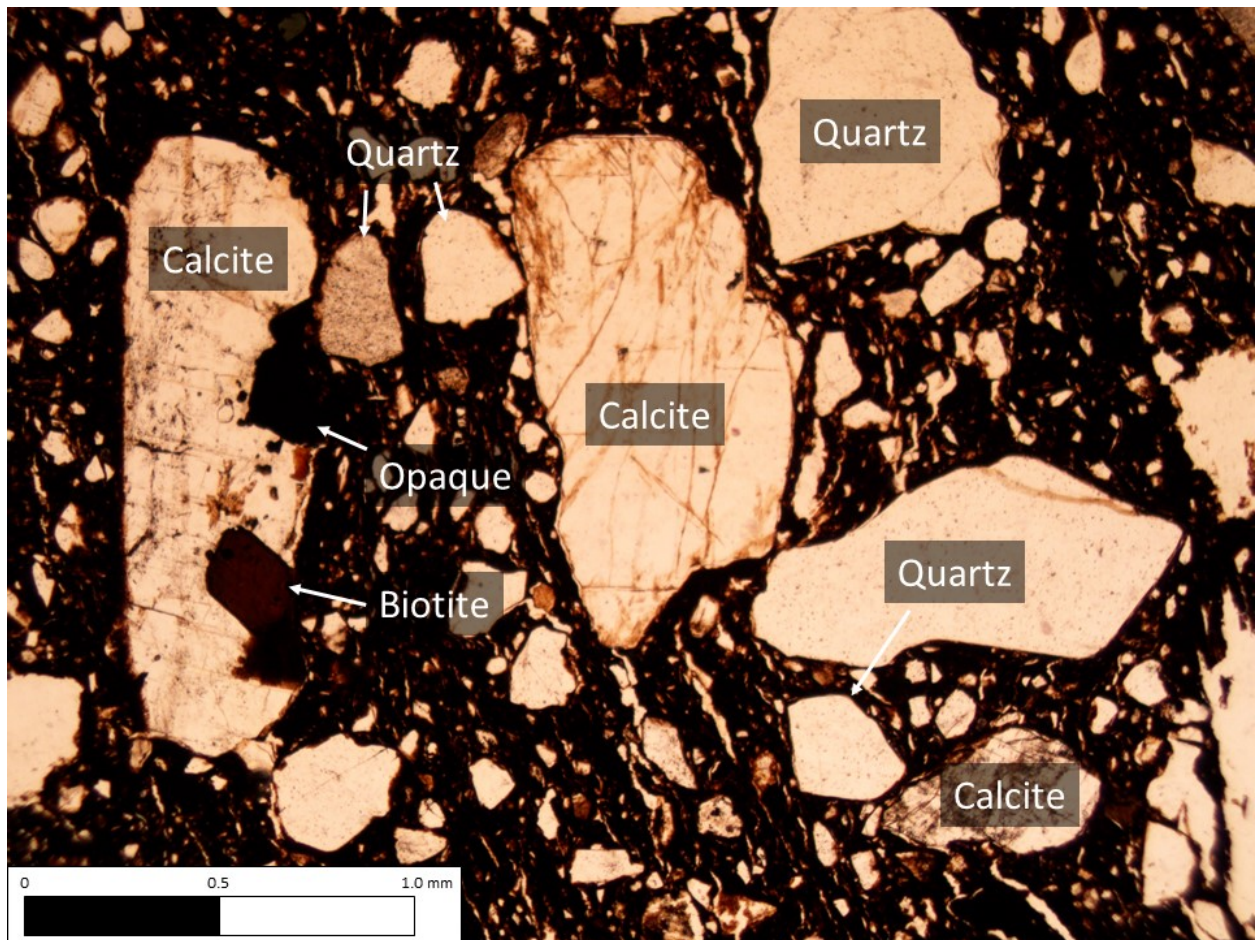


Figure 4.63 Thin section image of Sample 18 (Plane Polarized Light, 4X).

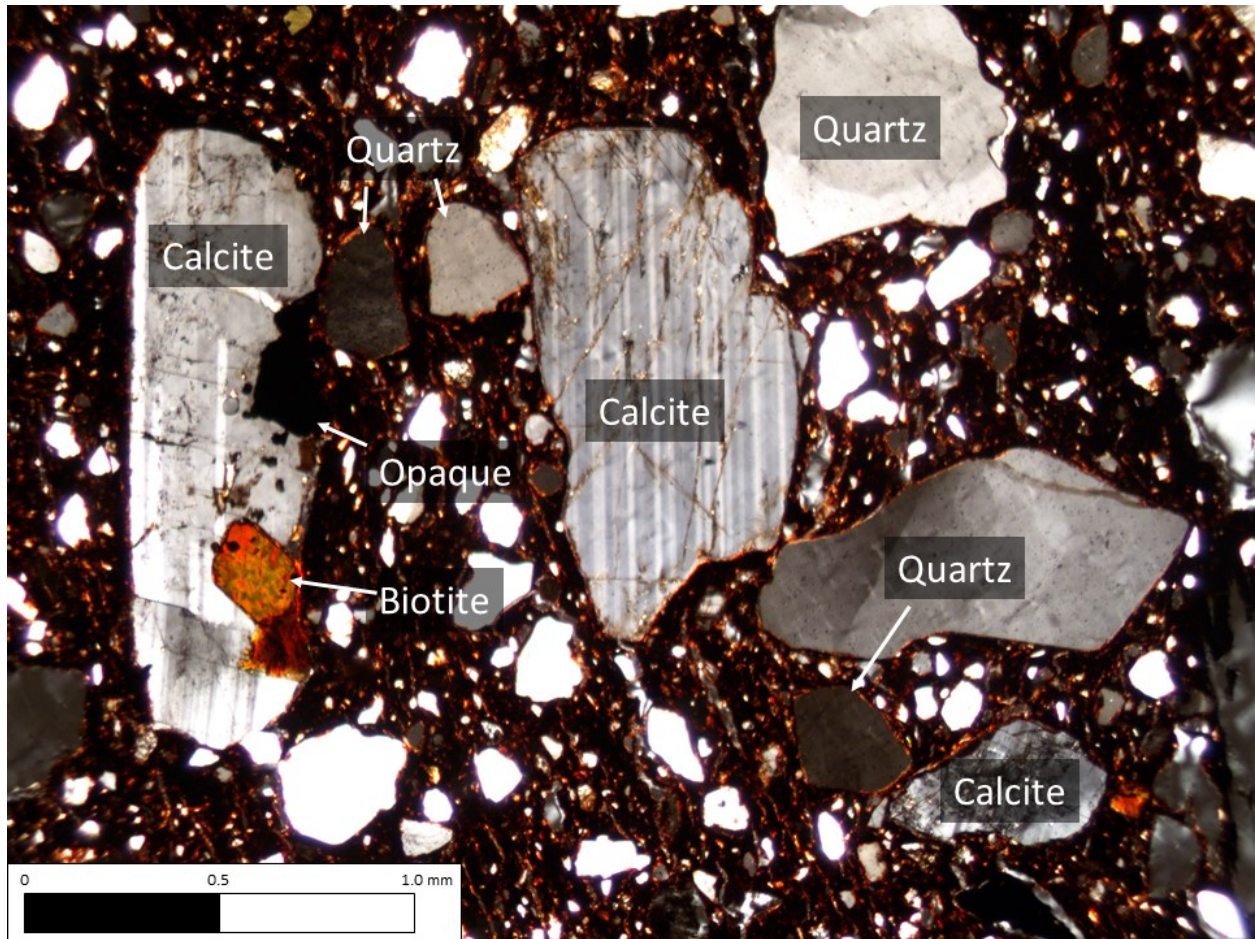


Figure 4.64 Thin section image of Sample 18 (Cross Polarized Light, 4X).

### *Sample 19*

In Sample 19, eight individual mineral types were identified. These include those in the silicate groups such as micas, quartzes, and feldspars, as well as non-silicate groups such as carbonates and oxides. In the mica group, twenty-seven points were biotite and sixteen points were sericite. In the quartz mineral group, forty-four were quartz. In the feldspar group, eighteen points were plagioclase feldspar, one was k-feldspar, and four were microcline. In the carbonate group, twenty-three points were calcite. Eight points were opaque minerals in the oxide group.

Figure 4.65 shows minerals identified in PPL and Figure 4.66 shows minerals identified in XPL from the thin section.

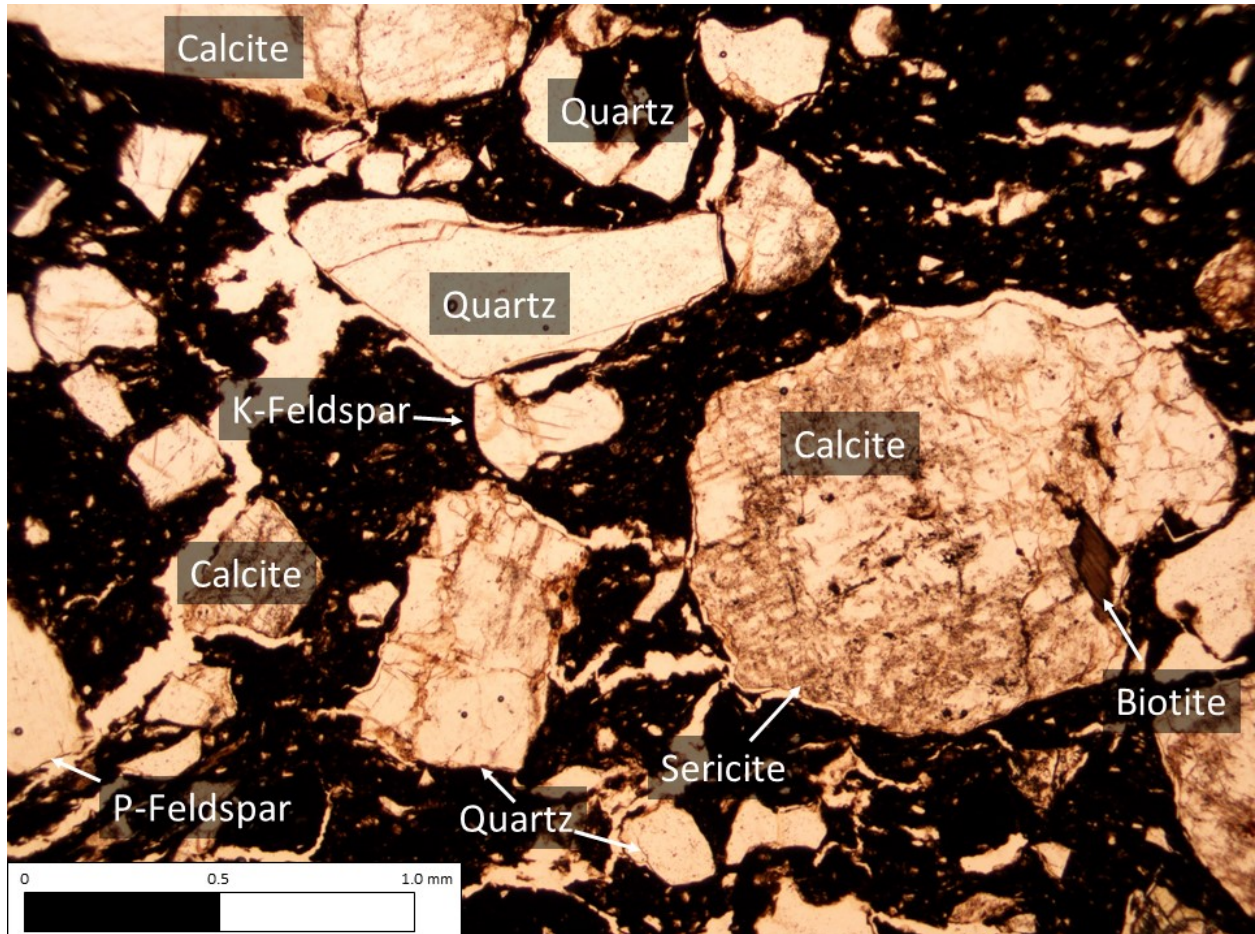


Figure 4.65 Thin section image of Sample 19 (Plane Polarized Light, 4X).

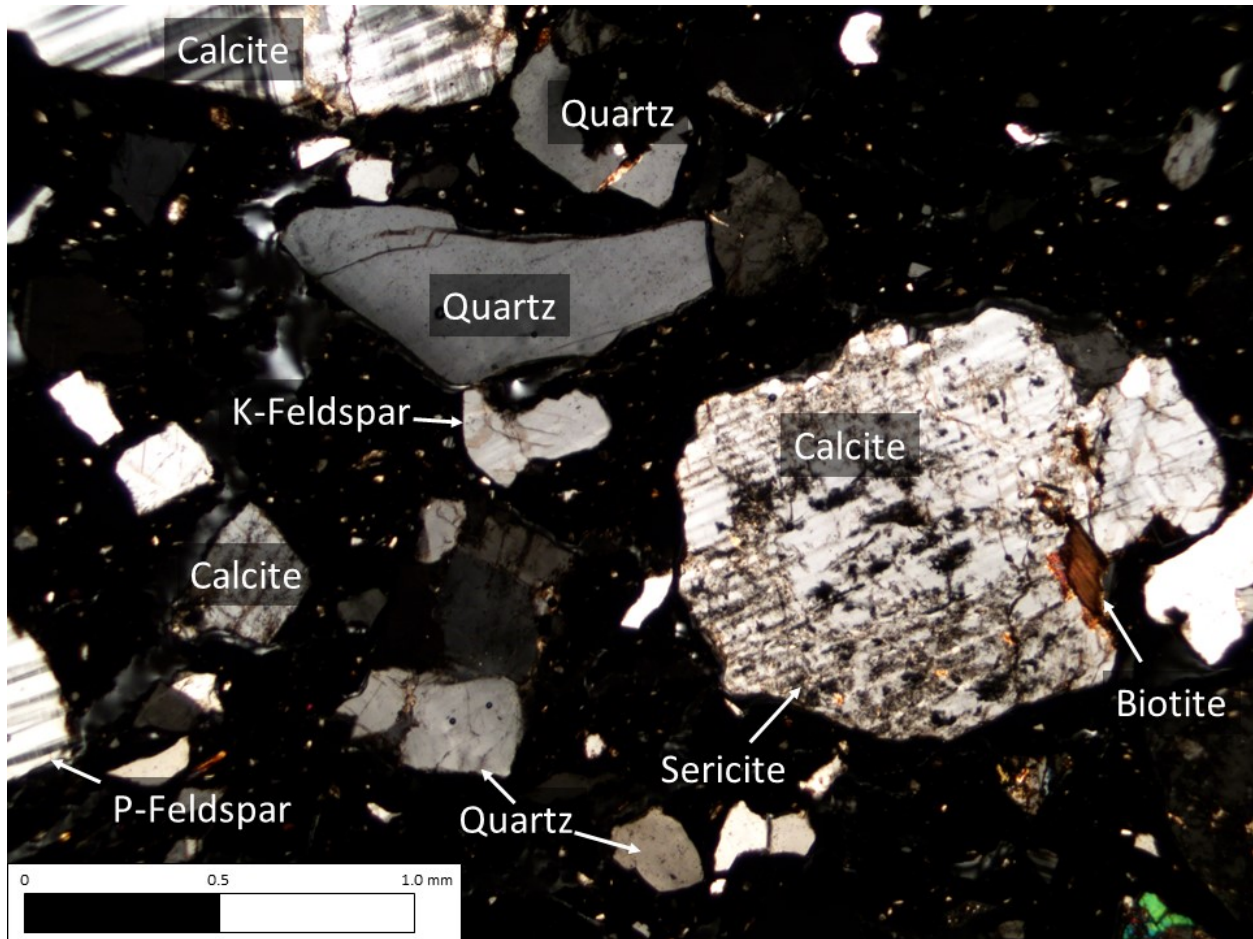


Figure 4.66 Thin section image of Sample 19 (Cross Polarized Light, 4X).

### *Sample 20*

In Sample 20, eight individual mineral types were identified. These include those in the silicate groups such as micas, quartzes, and feldspars, as well as non-silicate groups such as carbonates and oxides. In the mica group, eighteen points were biotite and sixteen points were sericite. In the quartz mineral group, twenty-nine were quartz and one was myrmekite. In the feldspar group, thirteen points were plagioclase feldspar and three were microcline. In the carbonate group, seventeen points were calcite. Seven points were opaque minerals in the oxide

group. Figure 4.67 shows minerals identified in PPL and Figure 4.68 shows minerals identified in XPL from the thin section.

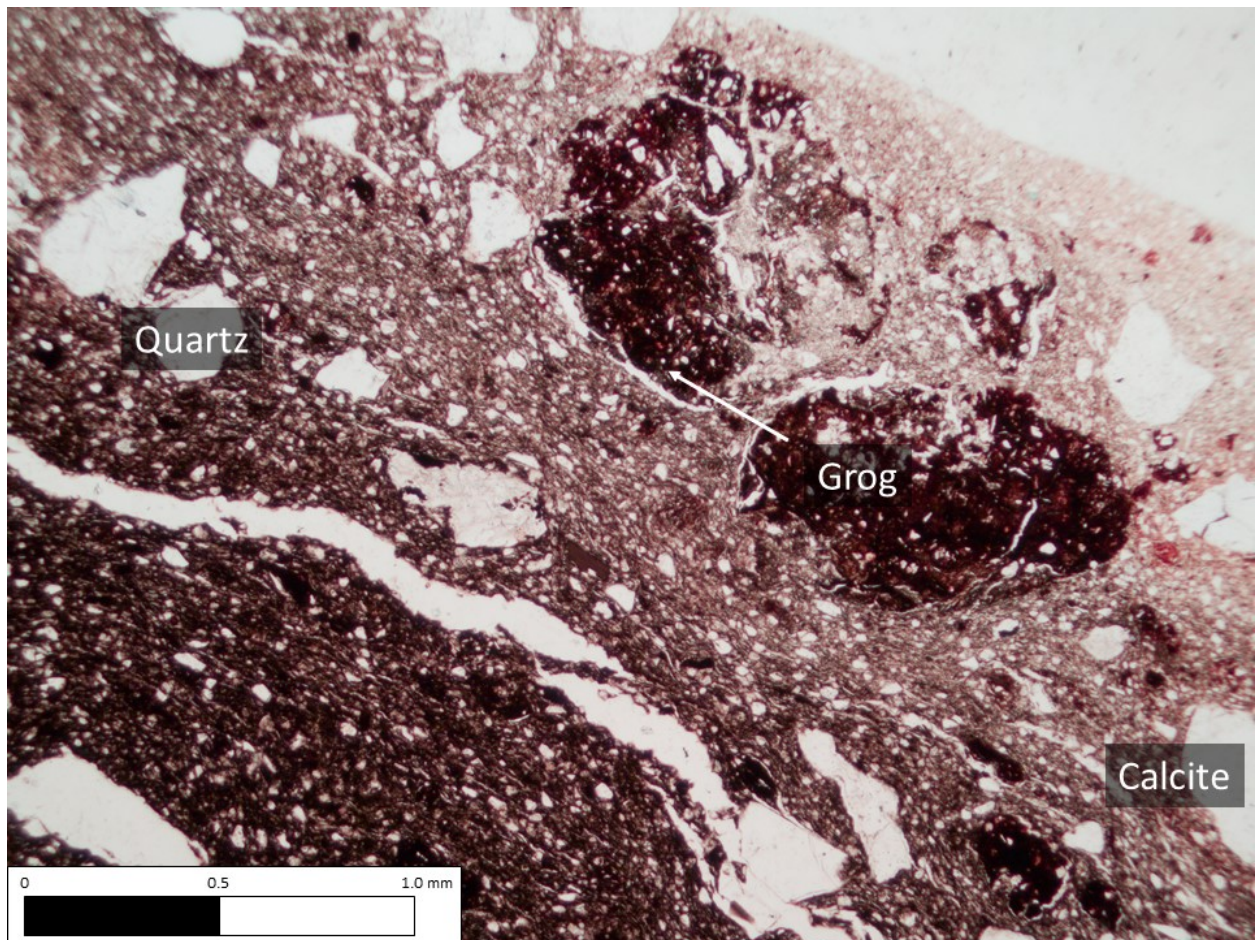


Figure 4.67 Thin section image of Sample 20 (Plane Polarized Light, 4X).

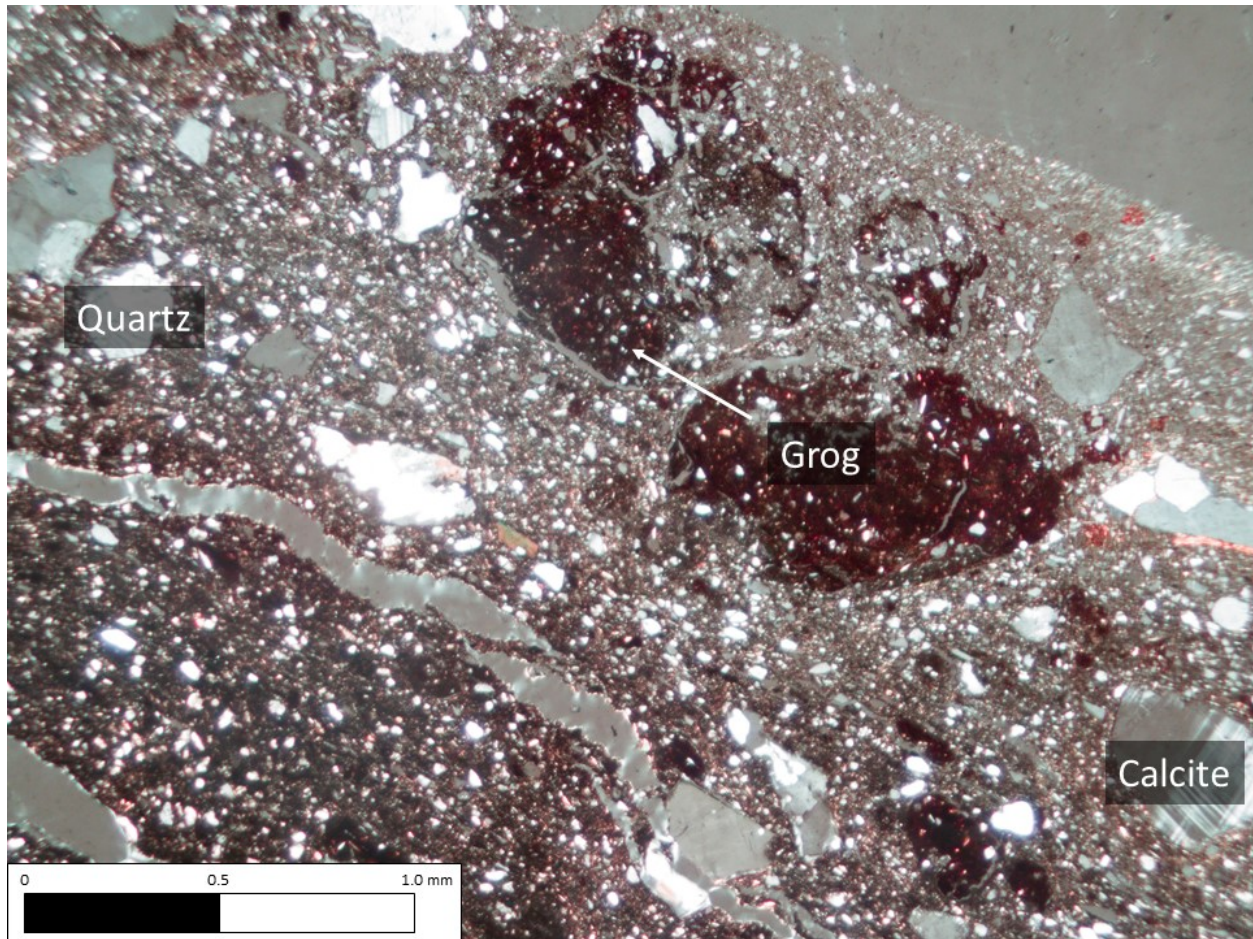


Figure 4.68 Thin section image of Sample 20 (Cross Polarized Light, 4X).

### *Sample 21*

In Sample 21, ten individual mineral types were identified. These include those in the silicate groups such as micas, quartzes, and feldspars, as well as non-silicate groups such as carbonates and oxides. In the mica group, fourteen points were biotite and seven points were sericite. In the quartz mineral group, twelve were quartz, three were quartzite and three were myrmekite. In the feldspar group, four points were plagioclase feldspar, three were k-feldspar, and two were microcline. In the carbonate group, six points were calcite. Three points were

opaque minerals in the oxide group. Figure 4.69 shows minerals identified in PPL and Figure 4.70 shows minerals identified in XPL from the thin section.

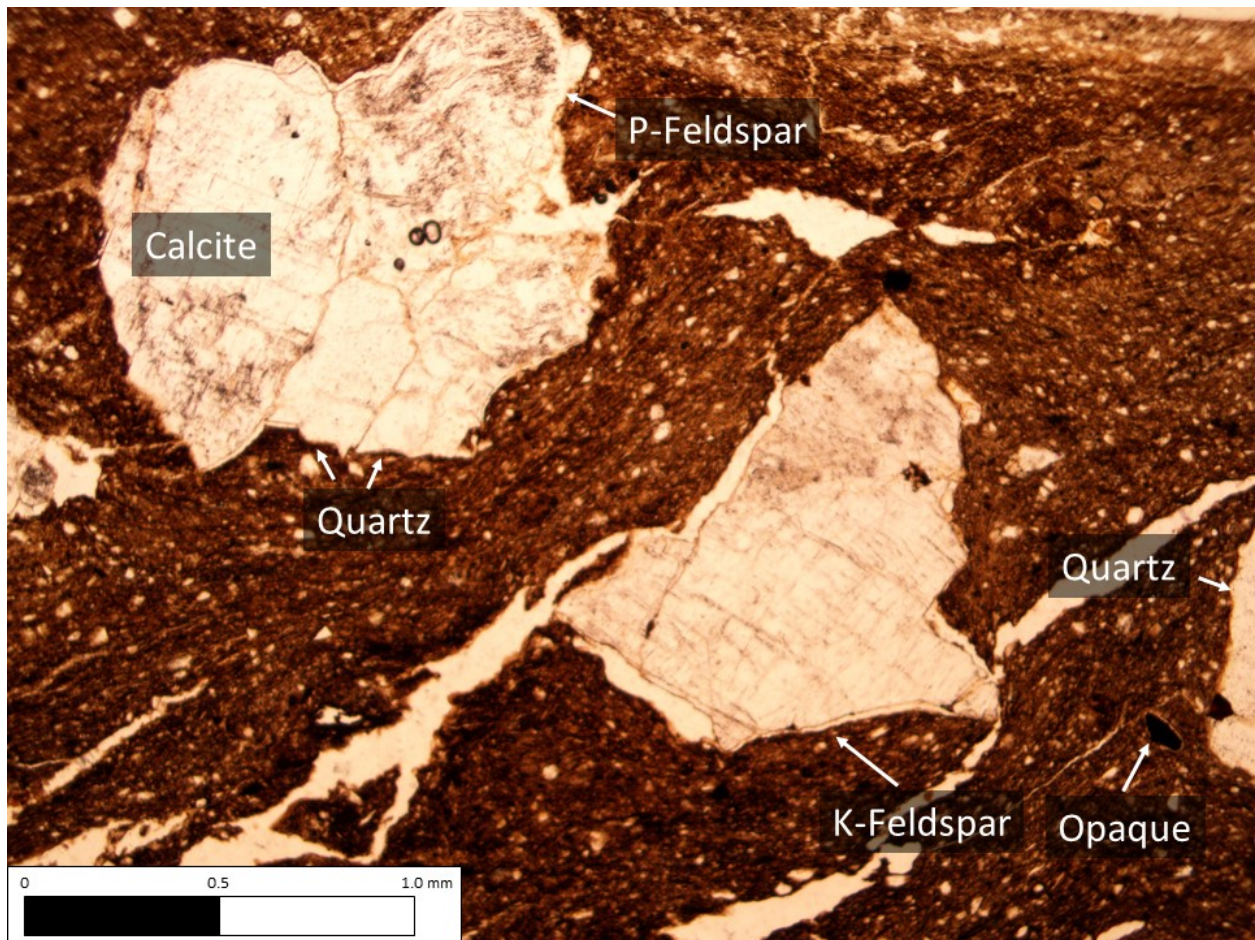


Figure 4.69 Thin section image of Sample 21 (Plane Polarized Light, 4X).

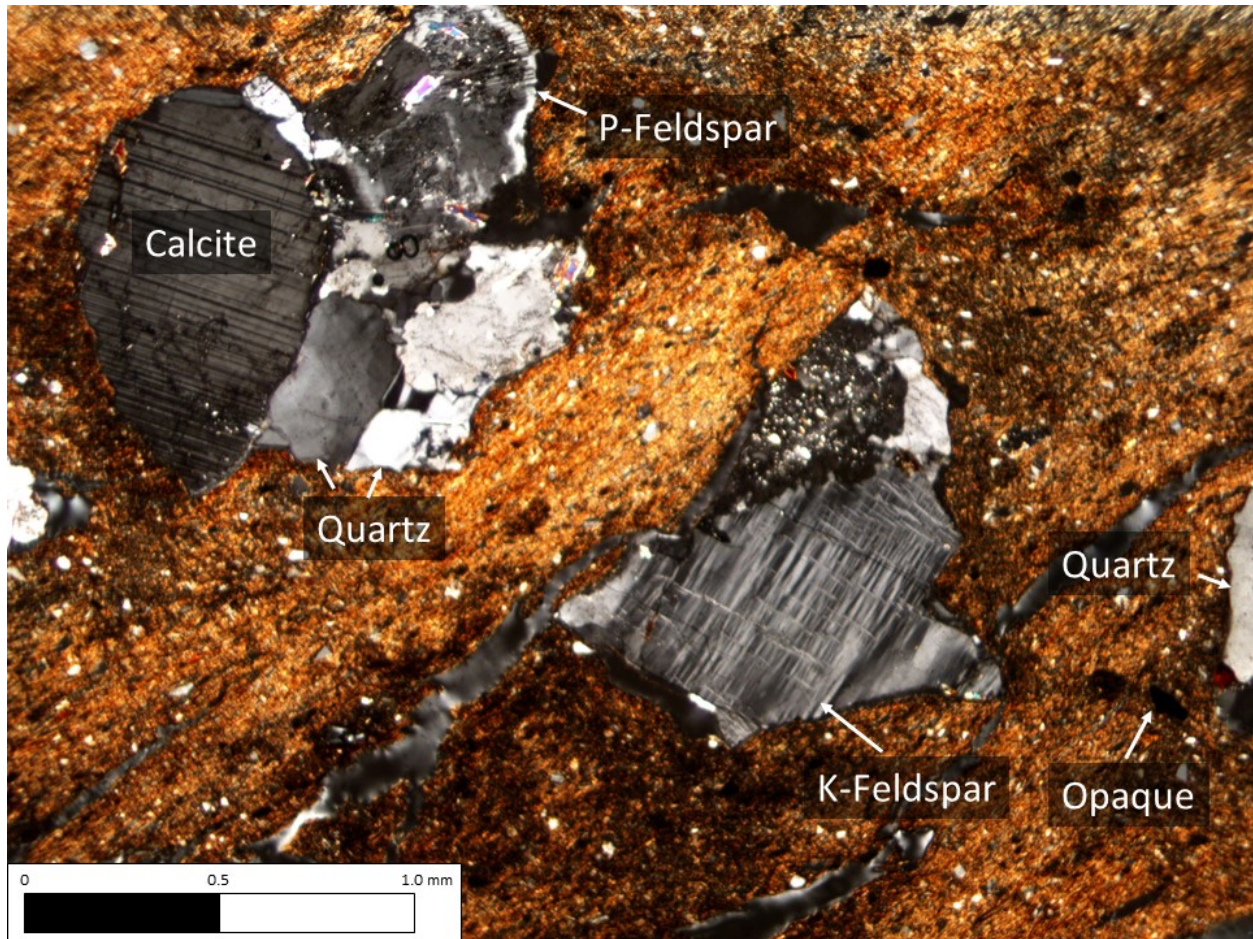


Figure 4.70 Thin section image of Sample 21 (Cross Polarized Light, 4X).

### *Sample 22*

In Sample 22, nine individual mineral types were identified. These include those in the silicate groups such as micas, quartzes, and feldspars, as well as non-silicate groups such as carbonates and oxides. In the mica group, twenty-one points were biotite and twelve points were sericite. In the quartz mineral group, twenty-four were quartz and four were myrmekite. In the feldspar group, twelve points were plagioclase feldspar, six were k-feldspar, and one was microcline. In the carbonate group, nine points were calcite. Two points were opaque minerals in



the oxide group. Figure 4.71 shows minerals identified in PPL and Figure 4.72 shows minerals identified in XPL from the thin section.

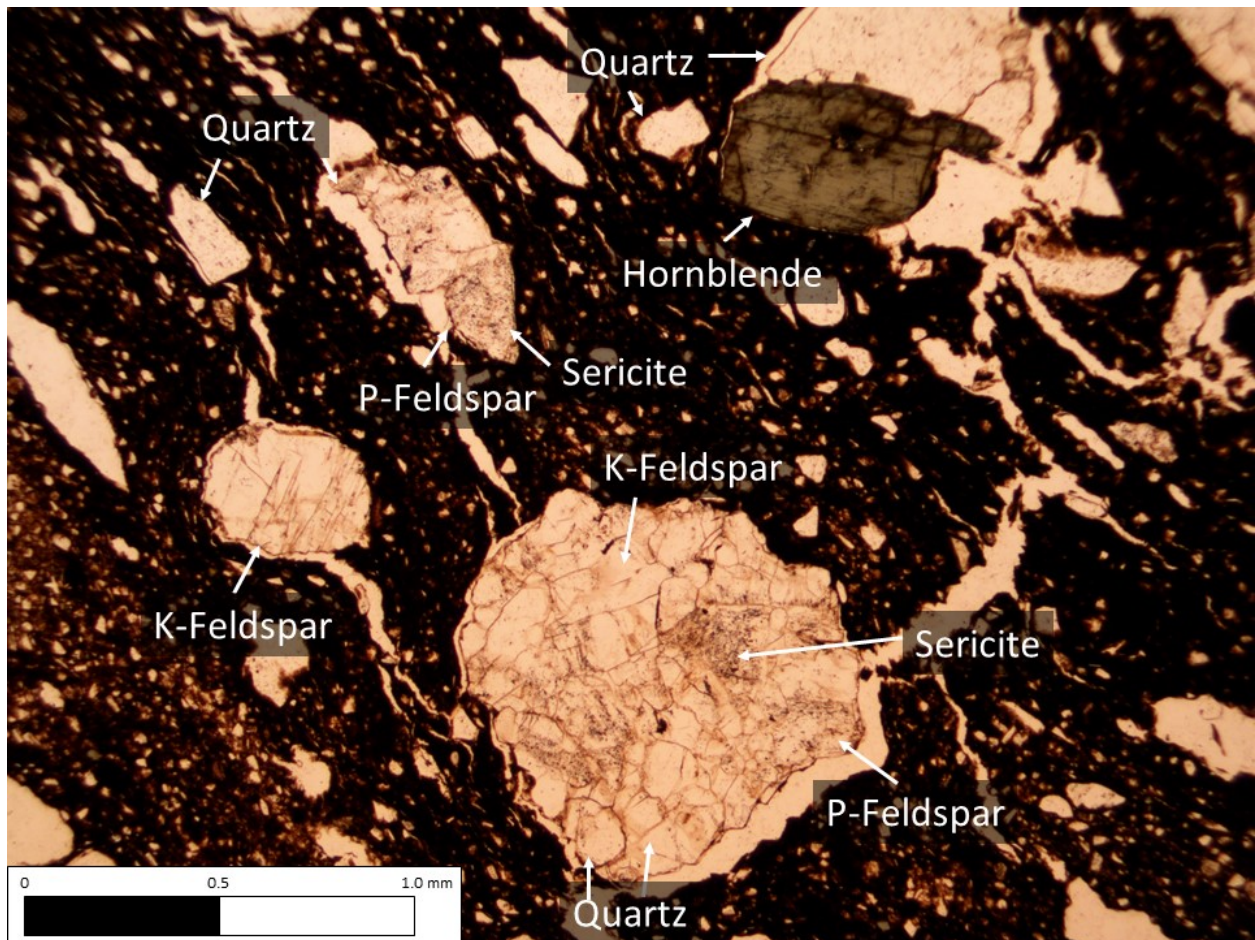


Figure 4.71 Thin section image of Sample 22 (Plane Polarized Light, 4X).

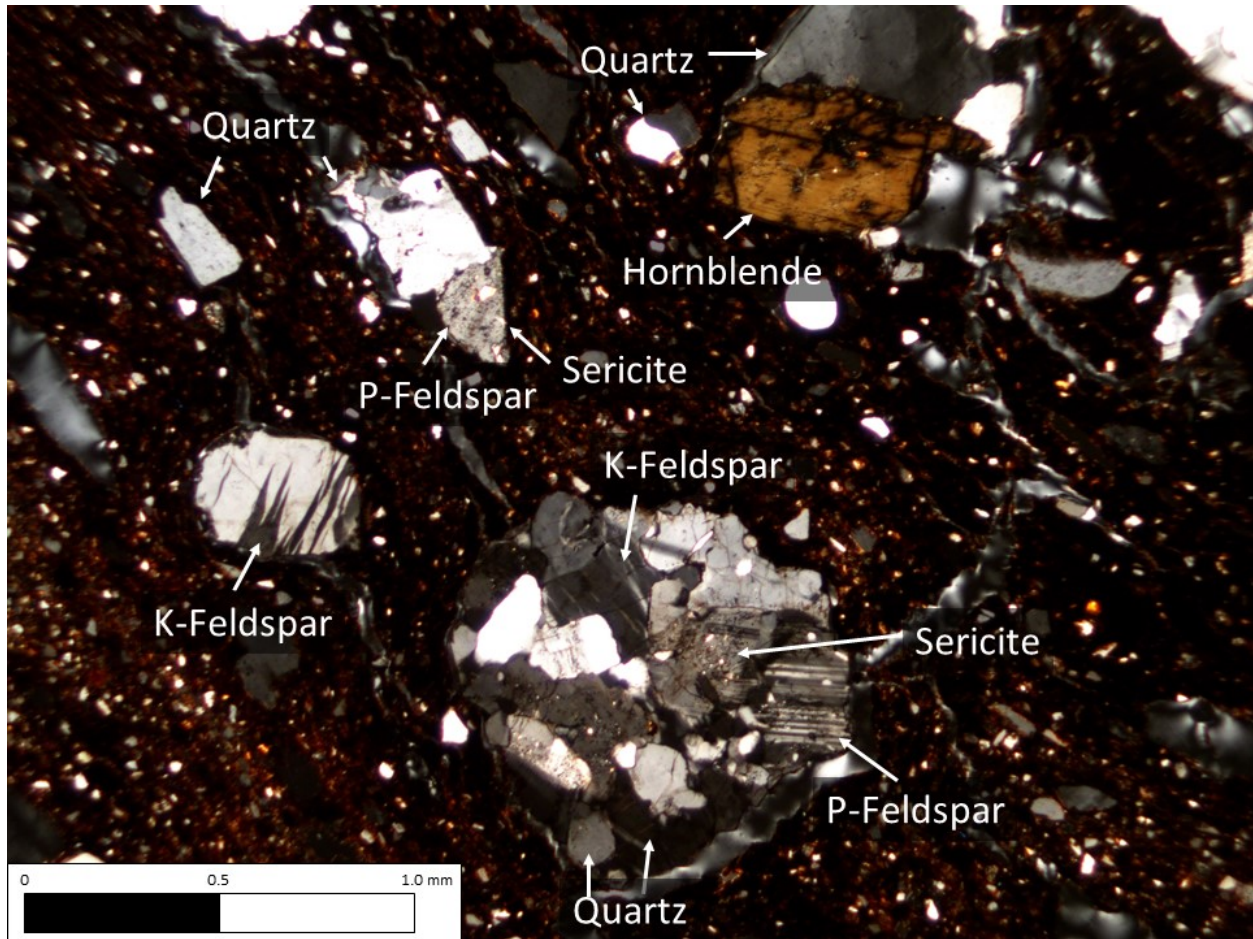


Figure 4.72 Thin section image of Sample 22 (Cross Polarized Light, 4X).

### *Sample 23*

In Sample 23, nine individual mineral types were identified. These include those in the silicate groups such as amphiboles, micas, quartzes, and feldspars, as well as non-silicate groups such as carbonates and oxides. Ten points were identified as hornblende in the amphibole group. In the mica group, nineteen points were biotite and four points were sericite. In the quartz mineral group, eight were quartz and three were myrmekite. In the feldspar group, fifteen points were plagioclase feldspar and two were k-feldspar. In the carbonate group, thirteen points were

calcite. Ten points were opaque minerals in the oxide group. Figure 4.73 shows minerals identified in PPL and Figure 4.74 shows minerals identified in XPL from the thin section.

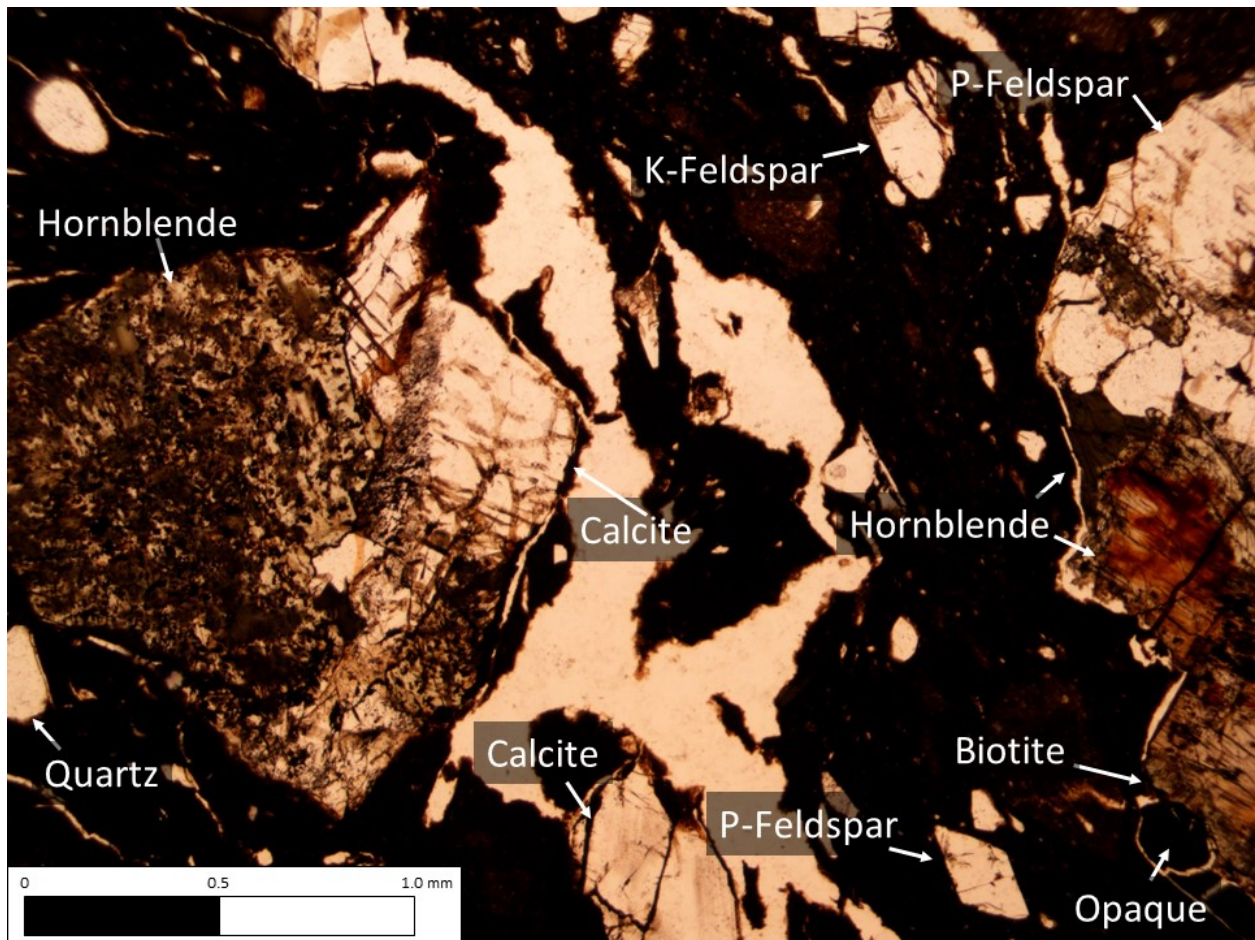


Figure 4.73 Thin section image of Sample 23 (Plane Polarized Light, 4X).

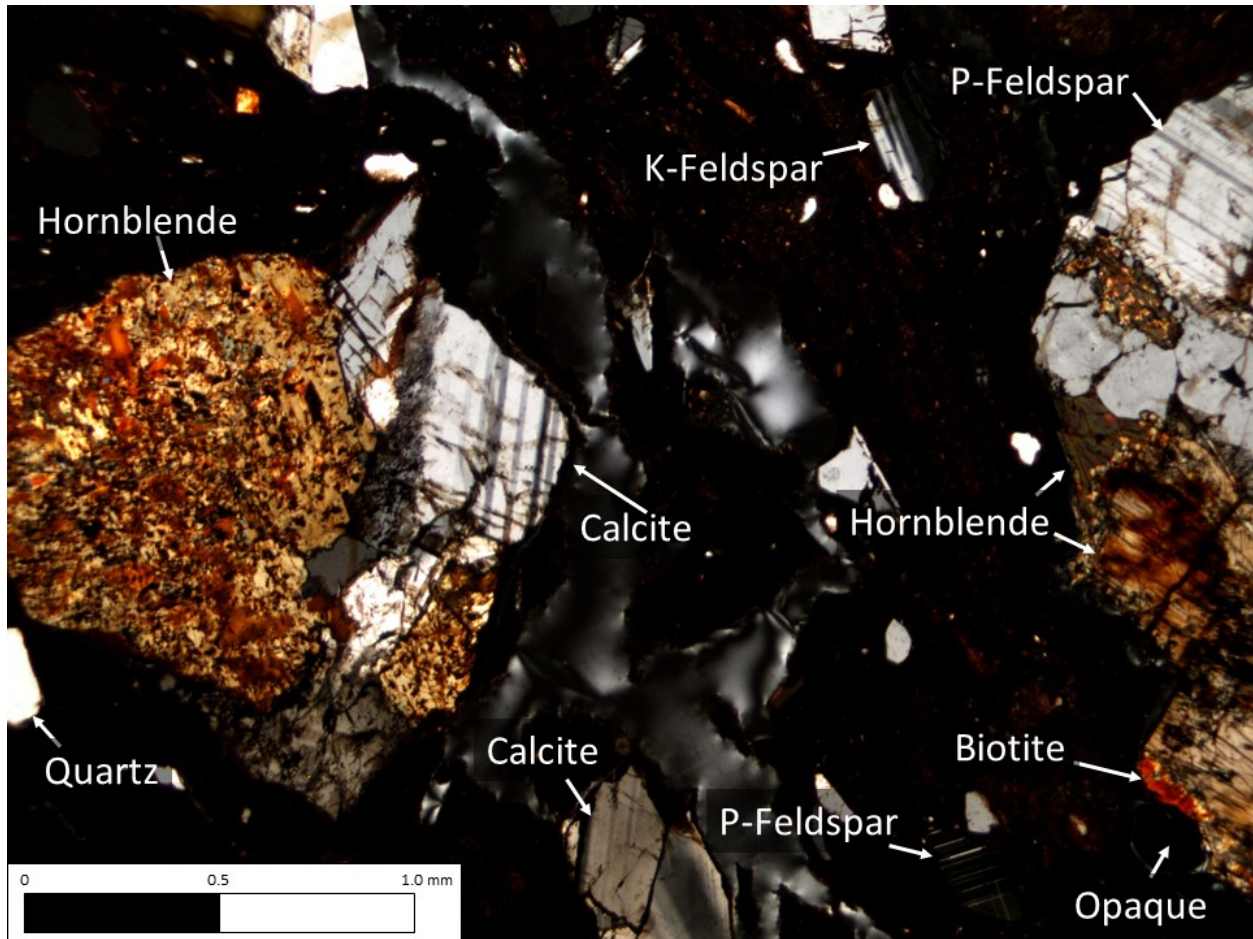


Figure 4.74 Thin section image of Sample 23 (Cross Polarized Light, 4X).

### *Sample 24*

In Sample 24, nine individual mineral types were identified. These include those in the silicate groups such as amphiboles, micas, quartzes, and feldspars, as well as non-silicate groups such as carbonates and oxides. Two points were identified as hornblende in the amphibole group. In the mica group, nine points were biotite and two points were sericite. In the quartz mineral group, eight were quartz, two were quartzite, and three were myrmekite. In the feldspar group, six points were identified as plagioclase feldspar. In the carbonate group, nine points were

calcite. Six points were opaque minerals in the oxide group. Figure 4.75 shows minerals identified in PPL and Figure 4.76 shows minerals identified in XPL from the thin section.

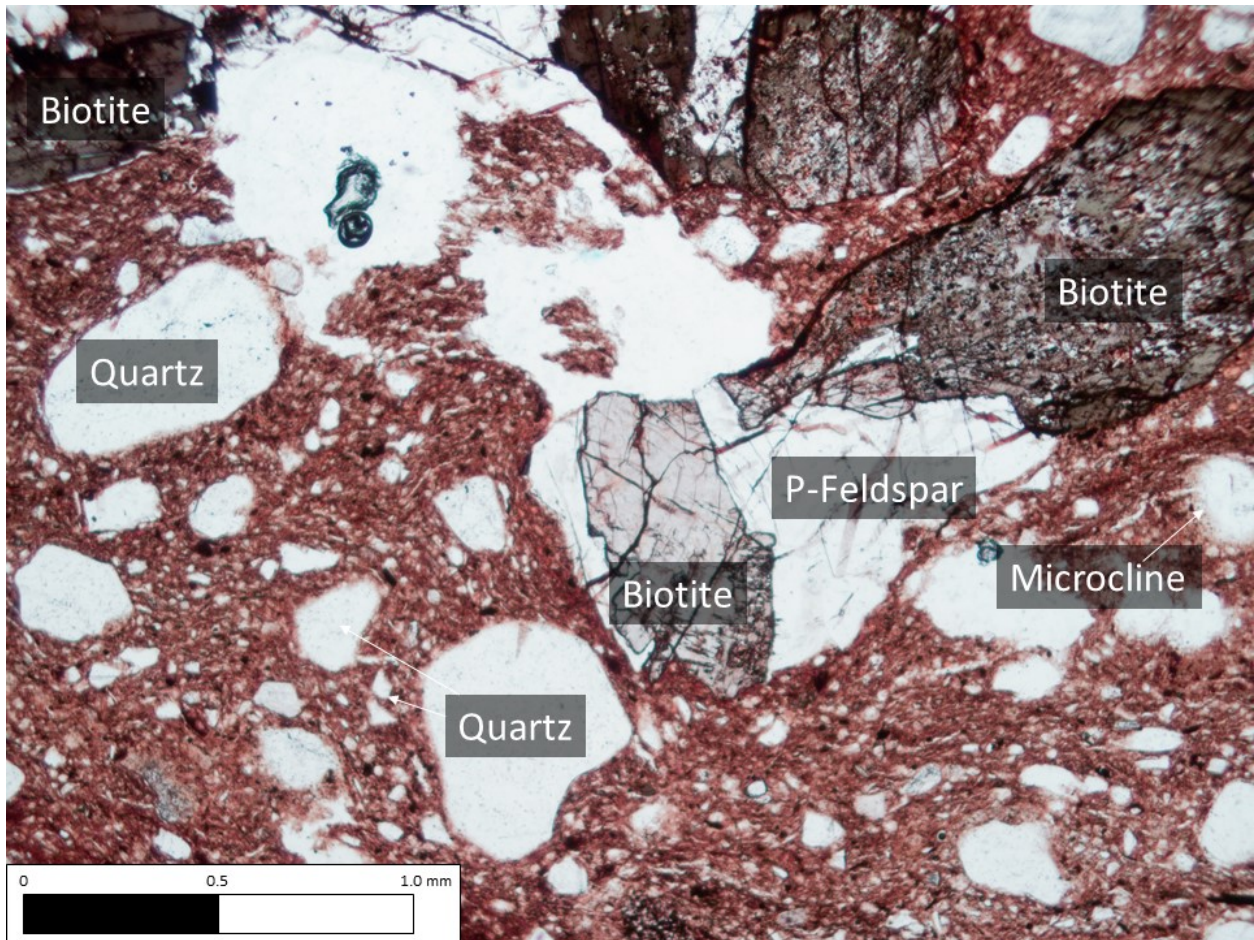


Figure 4.75 Thin section image of Sample 24 (Plane Polarized Light, 4X).

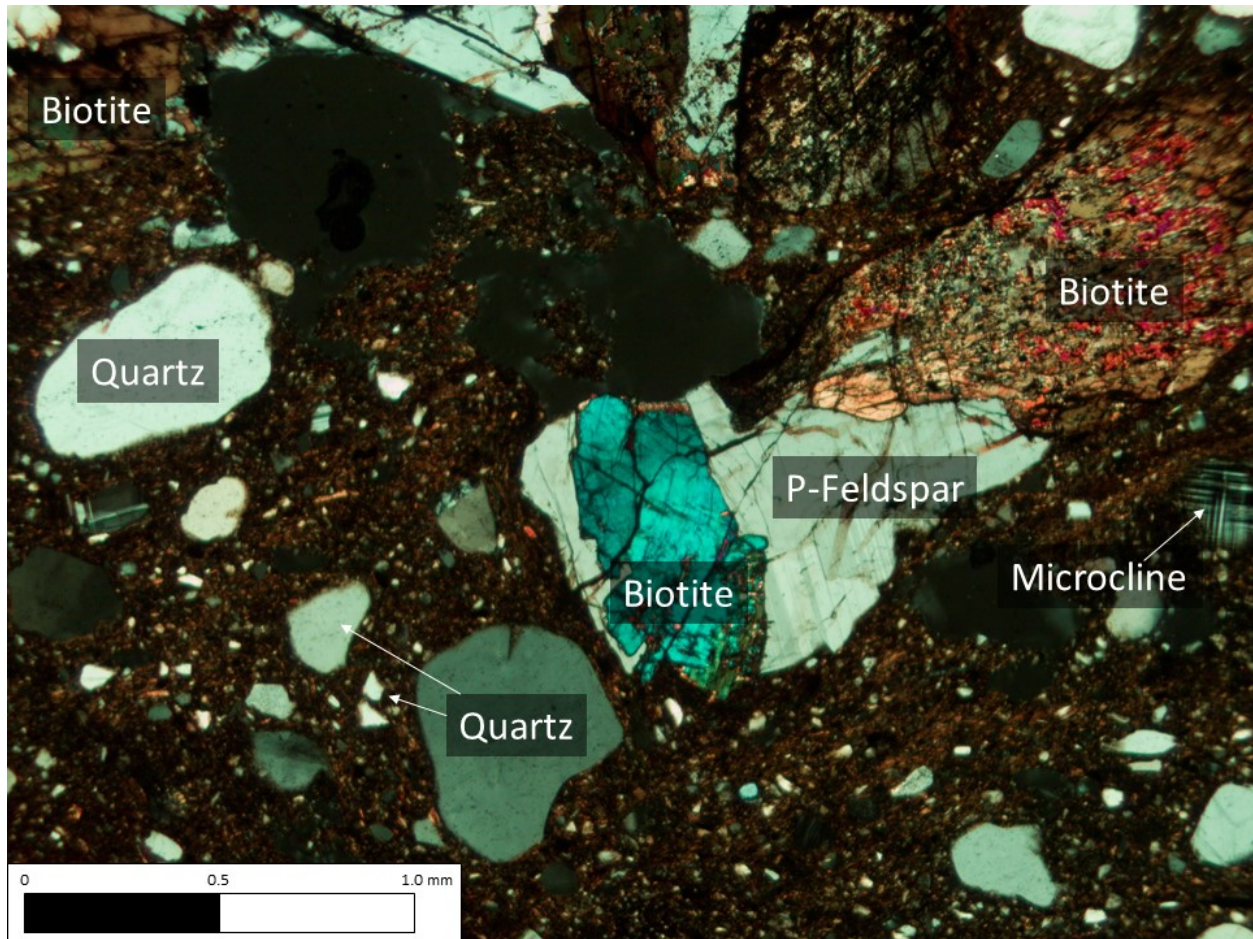


Figure 4.76 Thin section image of Sample 24 (Cross Polarized Light, 4X).

### *Sample 25*

In Sample 25, nine individual mineral types were identified. These include those in the silicate groups such as micas, quartzes, and feldspars, as well as non-silicate groups such as carbonates and oxides. In the mica group, nine points were biotite and four points were sericite. In the quartz mineral group, six were quartz, one was quartzite, and three were myrmekite. In the feldspar group, three points were identified as plagioclase feldspar and two were k-feldspar. In the carbonate group, six points were calcite. Six points were opaque minerals in the oxide group.

Figure 4.77 shows minerals identified in PPL and Figure 4.78 shows minerals identified in XPL from the thin section.

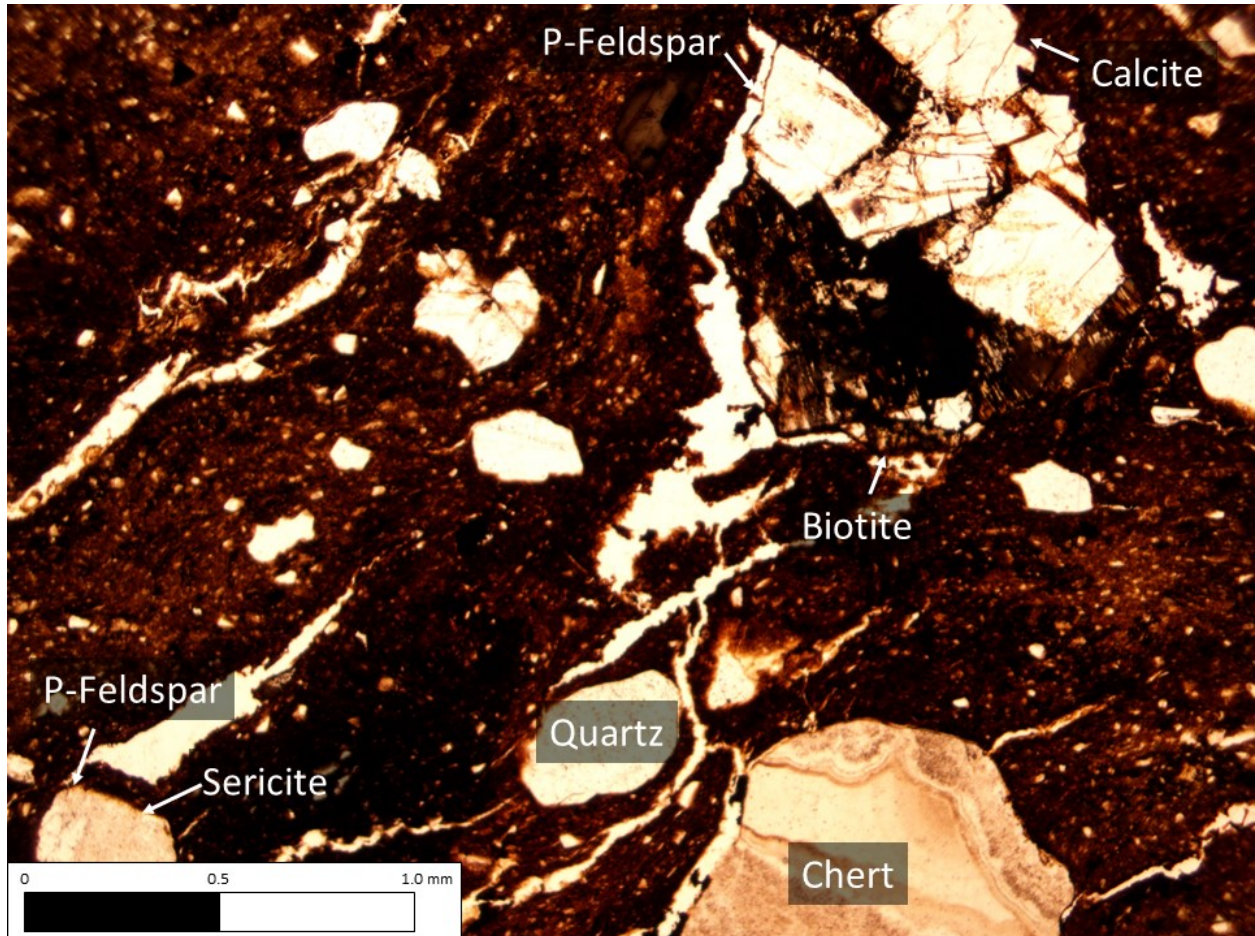


Figure 4.77 Thin section image of Sample 25 (Plane Polarized Light, 4X).

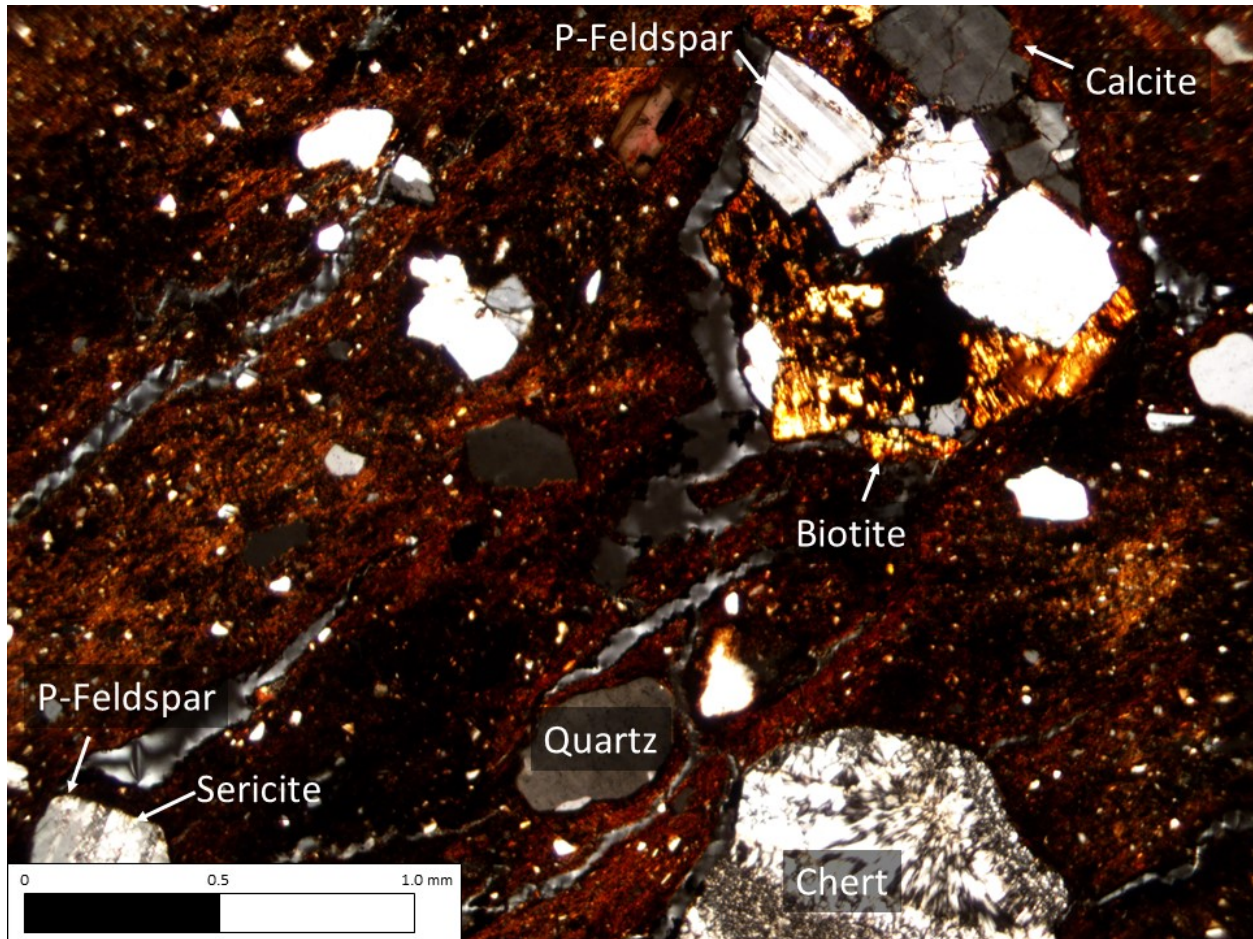


Figure 4.78 Thin section image of Sample 25 (Cross Polarized Light, 4X).

### *Sample 26*

In Sample 26, seven individual mineral types were identified. These include those in the silicate groups such as micas, quartzes, and feldspars, as well as non-silicate groups such as carbonates and oxides. In the mica group, six points were biotite. In the quartz mineral group, eleven were quartz and three were quartzite. In the feldspar group, two points were identified as plagioclase feldspar and two were k-feldspar. In the carbonate group, three points were calcite. One point was an opaque mineral in the oxide group. Figure 4.79 shows minerals identified in PPL and Figure 4.80 shows minerals identified in XPL from the thin section.



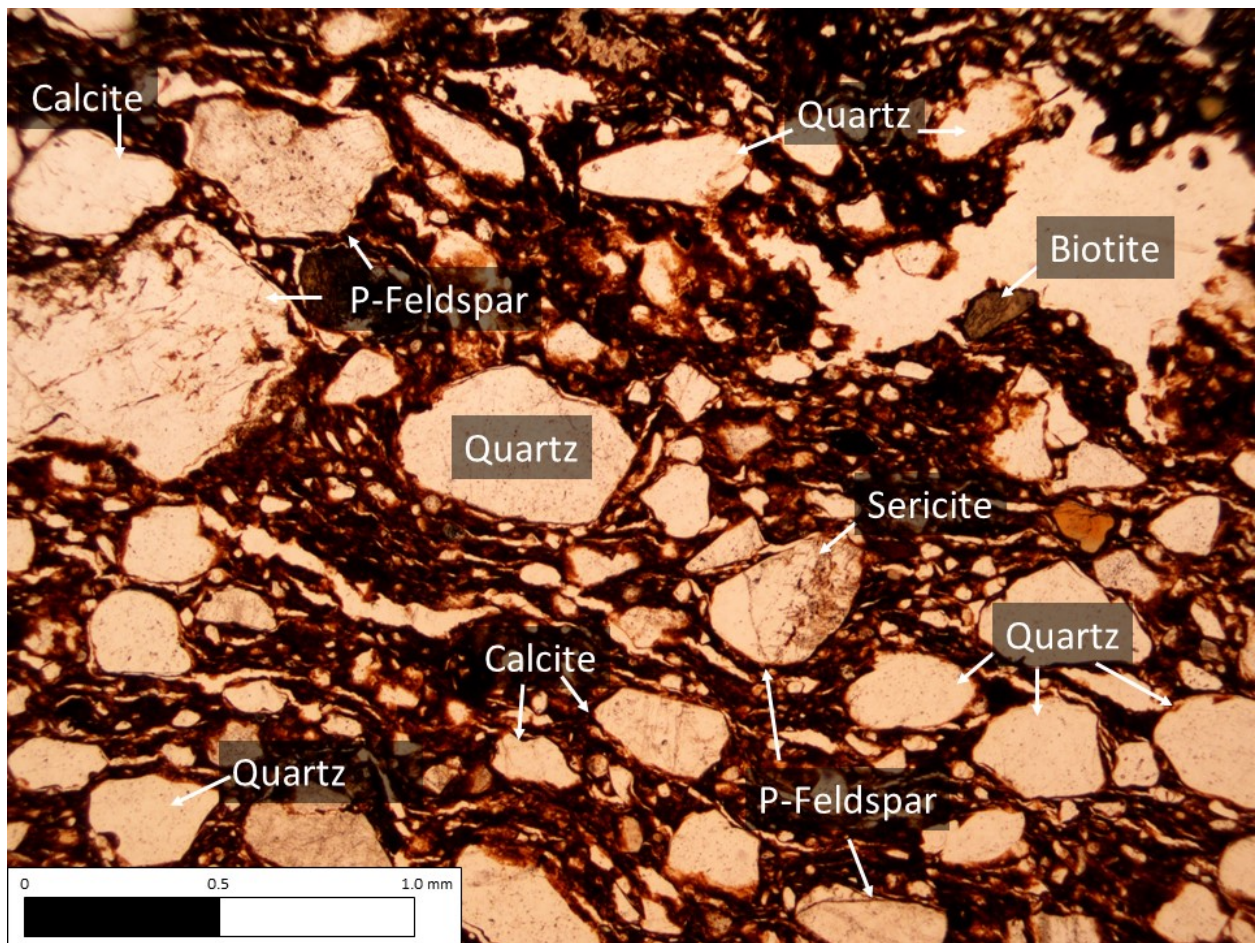


Figure 4.79 Thin section image of Sample 26 (Plane Polarized Light, 4X).

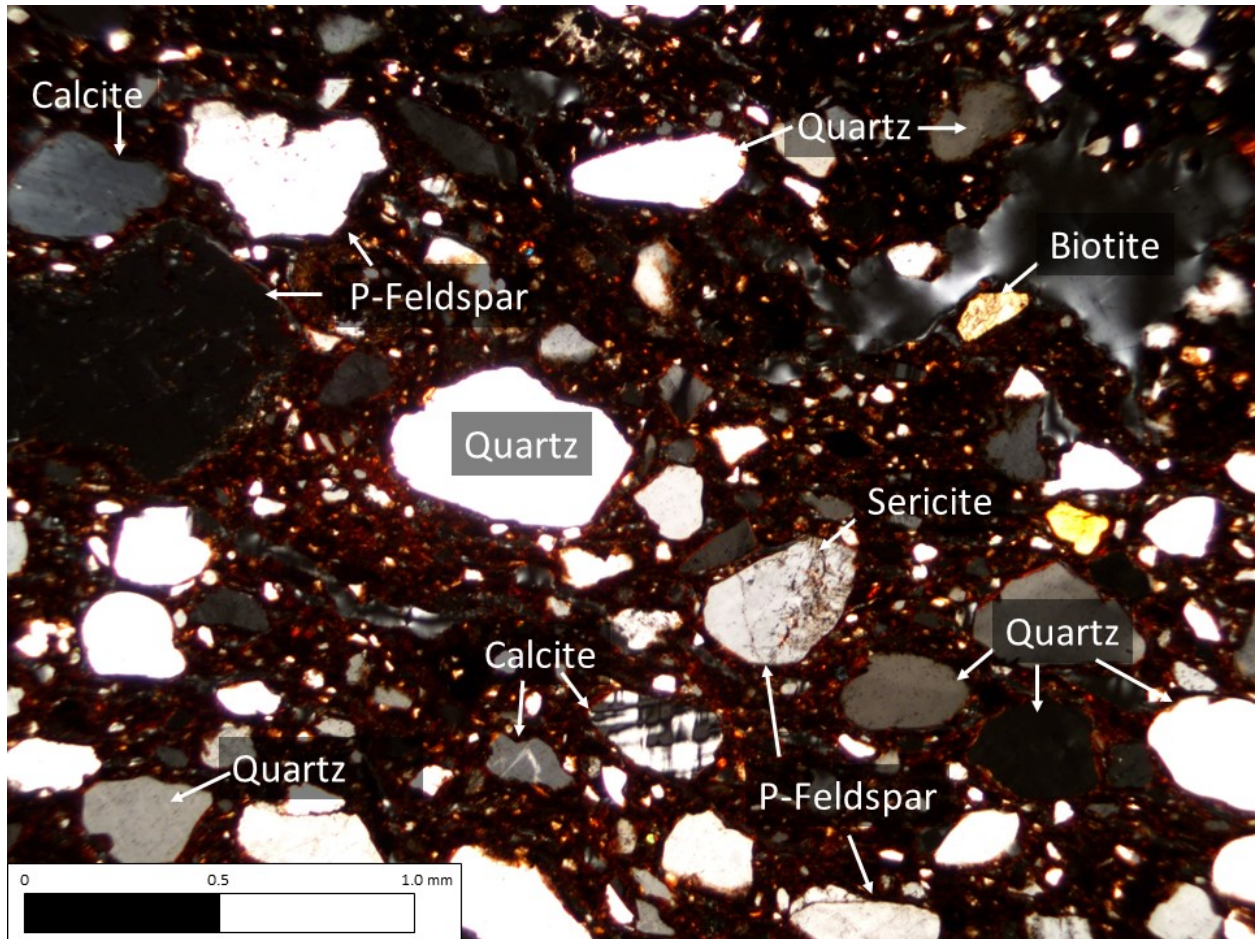


Figure 4.80 Thin section image of Sample 26 (Cross Polarized Light, 4X).

### *Sample 27*

In Sample 27, ten individual mineral types were identified. These include those in the silicate groups such as micas, quartzes, and feldspars, as well as non-silicate groups such as carbonates and oxides. In the mica group, twenty-six points were biotite and fourteen were sericite. In the quartz mineral group, twenty were quartz, three were quartzite, and three were myrmekite. In the feldspar group, six points were identified as plagioclase feldspar, two were k-feldspar, and two were microcline. In the carbonate group, fifteen points were calcite. Three

points were opaque minerals in the oxide group. Figure 4.81 shows minerals identified in PPL and Figure 4.82 shows minerals identified in XPL from the thin section.

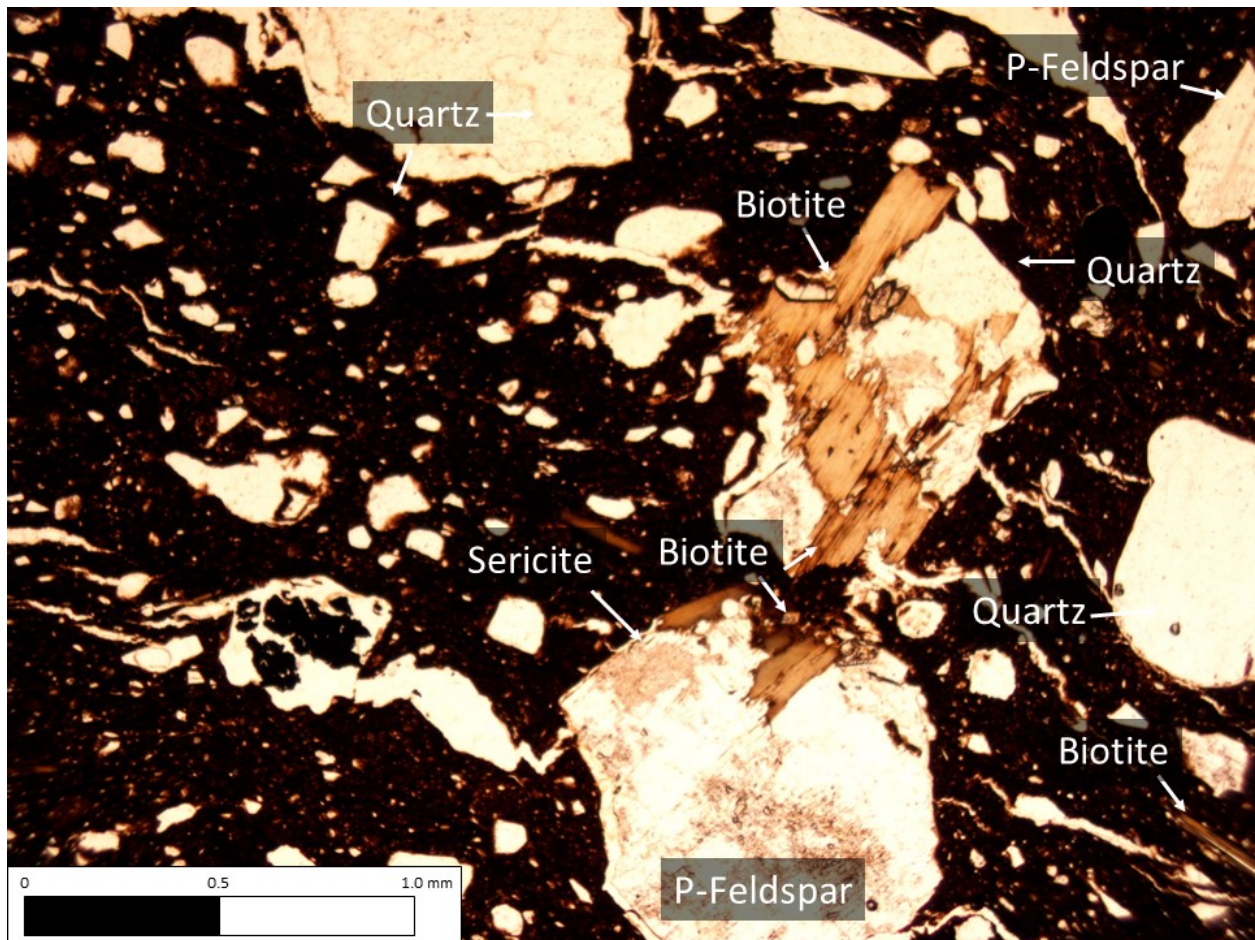


Figure 4.81 Thin section image of Sample 27 (Plane Polarized Light, 4X).

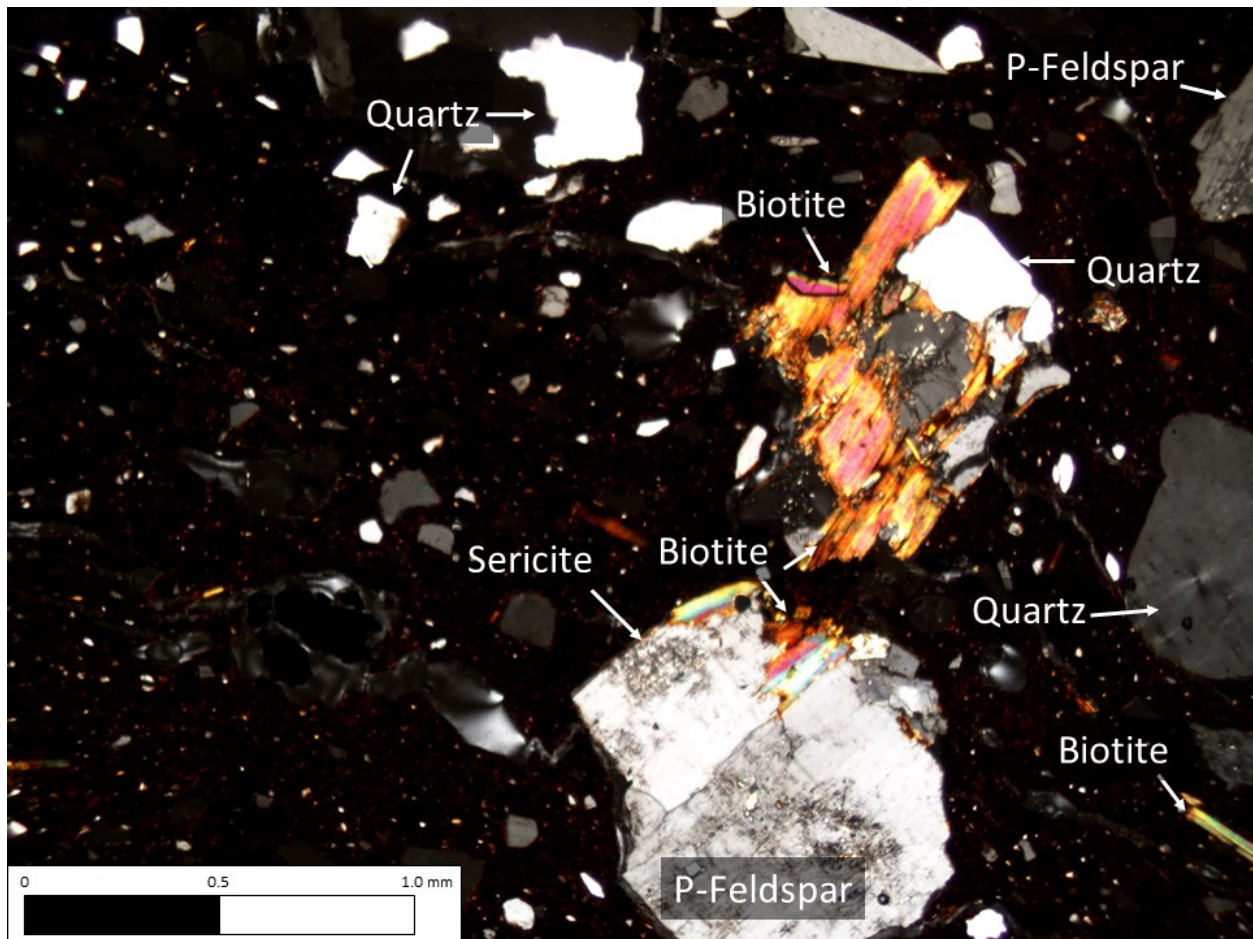


Figure 4.82 Thin section image of Sample 27 (Cross Polarized Light, 4X).

### **Petrographic Analysis: Body Composition**

The paste of a vessel is the combination of the clay, the sand, and the silt. These naturally occurring ingredients constitute the clay used to construct ceramic vessels, excluding the human-added temper. In the petrographic analysis, the number of clay, silt, and sand particles were counted and the percentage of each was calculated for each sample. Additionally, a sand-size index was calculated to attempt to characterize regional clay types.

The body of a vessel is the combination of the natural clay, the sand, and the added temper. These ingredients constitute the recipe of the ceramic paste used for construction. In the

petrographic analysis, the sand and temper were counted, and the silt and matrix counts were combined to calculate the clay.

For the grains identified as sand and temper, a sand-size index and temper-size index was calculated using an ordinal scale based on the measurement of maximum grain diameter under the microscope: fine (0.00625-0.249 mm), medium (0.25-0.499 mm), coarse, (0.5-0.99 mm), very coarse (1.0-1.99 mm), and gravel (>2.0 mm). The fine grains were then assigned a value of 1, medium grains = 2, coarse grains = 3, very coarse grains = 4, and gravel = 5. The calculation requires multiplication of all grains in each class by the weighted value for that size grade, and then adding the totals together and dividing by total grains for all size classes combined to calculate a mean size-index for each sample (Stoltman 1991, 1999, 2001, 2009, 2011). Table 4.3 exhibits the compositional data of temper, sand, clay, and silt counts, percentages, and the sand-size and temper-size indices.

TABLE 4.3 BODY AND PASTE COUNTS, PERCENTAGES, AND SIZE INDICES

Sample	Site Name (Number)	Body						Paste							
		Temper Count	Sand Count	Clay Count	Temper (%)	Sand (%)	Clay (%)	Temper Size Index	Silt Count	Sand Count	Clay Count	Silt (%)	Sand (%)	Clay (%)	Sand Size Index
2019001	Peterson (47WK199)	19	5	80	18.27	4.81	76.92	1.00	12	5	68	14.12	5.88	80.00	1.00
2019002	Peterson (47WK199)	21	9	175	10.24	4.39	85.37	1.14	31	9	144	16.85	4.89	78.26	1.00
2019003	Peterson (47WK199)	15	1	135	9.93	0.66	89.40	1.13	9	1	126	6.62	0.74	92.65	1.00
2019004	Peterson (47WK199)	20	4	239	7.60	1.52	90.87	1.05	13	4	226	5.35	1.65	93.00	1.00
2019005	Peterson (47WK199)	21	1	146	12.50	0.60	86.90	1.05	39	1	107	26.53	0.68	72.79	1.00
2019006	Peterson (47WK199)	29	2	156	15.51	1.07	83.42	1.21	10	2	146	6.33	1.27	92.41	1.00
2019007	Peterson (47WK199)	35	0	188	15.70	0.00	84.30	1.26	35	0	153	18.62	0.00	81.38	N/A
2019008	Finch (47IE902)	31	1	183	14.42	0.47	85.12	1.13	30	1	153	16.30	0.54	83.15	1.00
2019009	Finch (47IE902)	30	5	231	11.28	1.88	86.84	1.07	34	5	197	14.41	2.12	83.47	1.00
2019010	Finch (47IE902)	13	0	180	6.74	0.00	93.26	1.23	25	0	155	13.89	0.00	86.11	N/A
2019011	Finch (47IE902)	14	3	143	8.75	1.88	89.38	1.29	41	3	102	28.08	2.05	69.86	1.00
2019012	Finch (47IE902)	15	4	221	6.25	1.67	92.08	1.19	58	4	163	25.78	1.78	72.44	1.00
2019013	Finch (47IE902)	9	1	202	4.25	0.47	95.28	1.11	31	1	171	15.27	0.49	84.24	1.00
2019014	Sloan (11MC86)	11	5	103	9.24	4.20	86.55	1.18	15	5	88	13.89	4.63	81.48	1.00
2019015	Sloan (11MC86)	11	2	286	3.24	0.59	84.37	1.09	11	2	275	3.82	0.69	95.49	1.00
2019016	Sloan (11MC86)	10	3	127	7.14	2.14	90.71	1.00	20	3	107	15.38	2.31	82.31	1.00
2019017	Sloan (11MC86)	16	2	84	15.69	1.96	82.35	1.13	7	2	77	8.14	2.33	89.53	1.00
2019018	Sloan (11MC86)	12	5	204	5.43	2.26	92.31	1.30	39	5	165	18.66	2.39	78.95	1.80
2019019	Sloan (11MC86)	34	6	225	12.83	2.26	84.91	1.00	35	6	190	15.15	2.60	82.25	1.00
2019020	Sloan (11MC86)	32	5	246	11.31	1.77	86.93	1.17	11	5	235	4.38	1.99	93.63	1.00
2019021	Sloan (11MC86)	14	2	233	5.62	0.80	93.57	1.00	6	2	227	2.55	0.85	96.60	1.00
2019022	Albany Village (11WT1)	15	7	155	8.47	3.95	87.57	1.07	20	7	135	12.35	4.32	83.33	1.00
2019023	Kautz (11DU46)	23	0	131	14.94	0.00	85.06	1.26	8	0	123	6.11	0.00	93.89	N/A
2019024	Alberts (47IE887)	14	4	312	4.24	1.21	94.55	1.14	66	4	246	20.89	1.27	77.85	1.00
2019025	CAP (47IE93)	7	3	108	5.93	2.54	91.53	1.00	15	3	93	13.51	2.70	83.78	1.67
2019026	Blythe (11HA40)	5	6	184	2.56	3.08	94.36	1.00	54	6	130	28.42	3.16	68.42	1.33
2019027	DeWitte/Liphardt Habitation (11RI57)	31	4	170	15.12	1.95	82.93	1.00	14	4	156	8.05	2.30	89.66	1.00

### *Sample 1*

The points identified in the clay, silt, and sand categories were used to calculate the paste composition of the sample. Petrographic analysis on Sample 1 identified a total of eighty-five points in the natural paste categories. Sixty-eight of the points were clay, twelve were silt, and five were sand. The overall percentages of the paste category are represented as 80.0% clay, 14.1% silt, and 5.9% sand (Figure 4.83). The sand particles were only classed in the fine-grain size category; therefore, the sand-size index is 1.0.

The total number of points counted on the sample were used to calculate the body composition of the sample. A total of 104 points were counted on Sample 1. Of these, 80 were clay, nineteen were temper, and five were sand. The overall percentages of the body categories are 76.9% clay, 18.3% temper, and 4.8% sand (Figure 4.84). All temper particles were fine-size grit pieces. The temper-size index is 1.0.

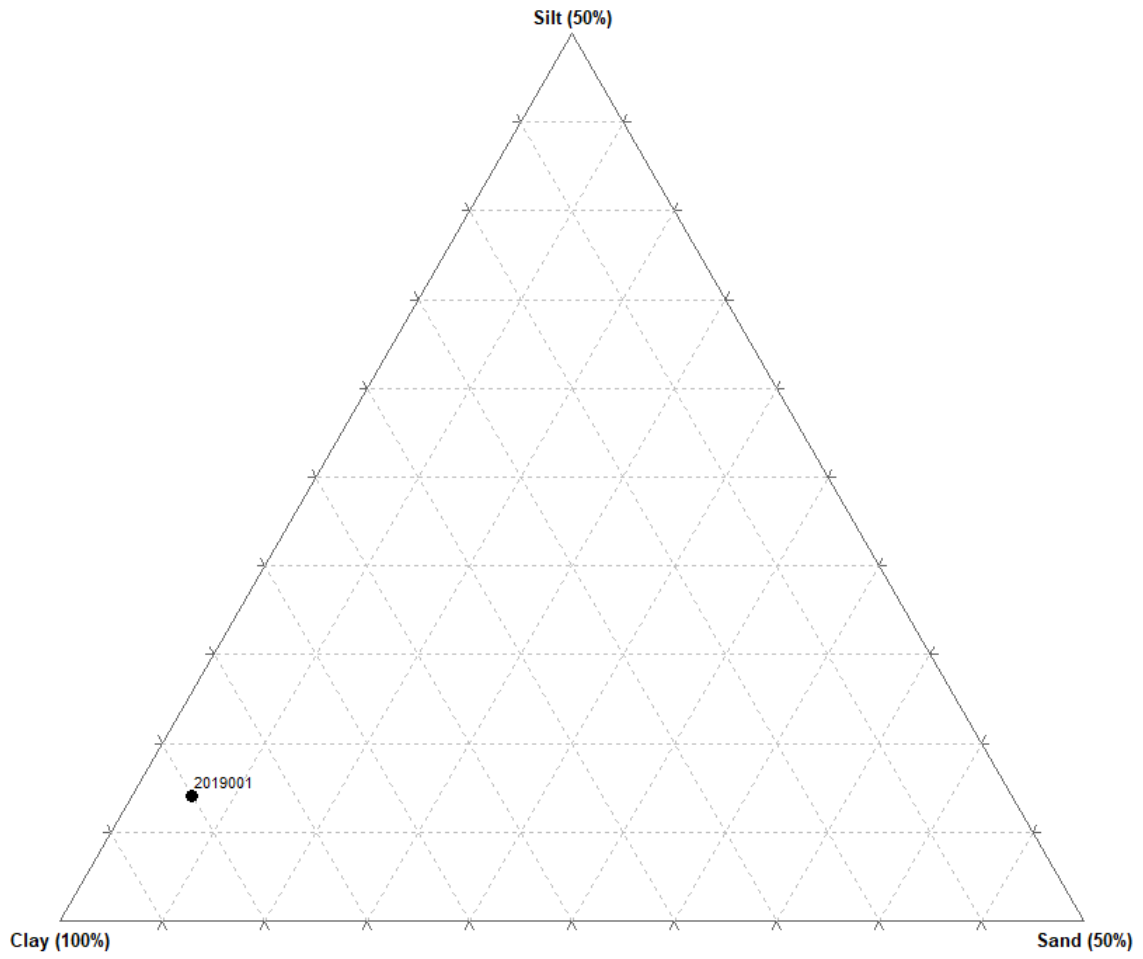


Figure 4.83 Ternary diagram of Sample 1 paste composition.



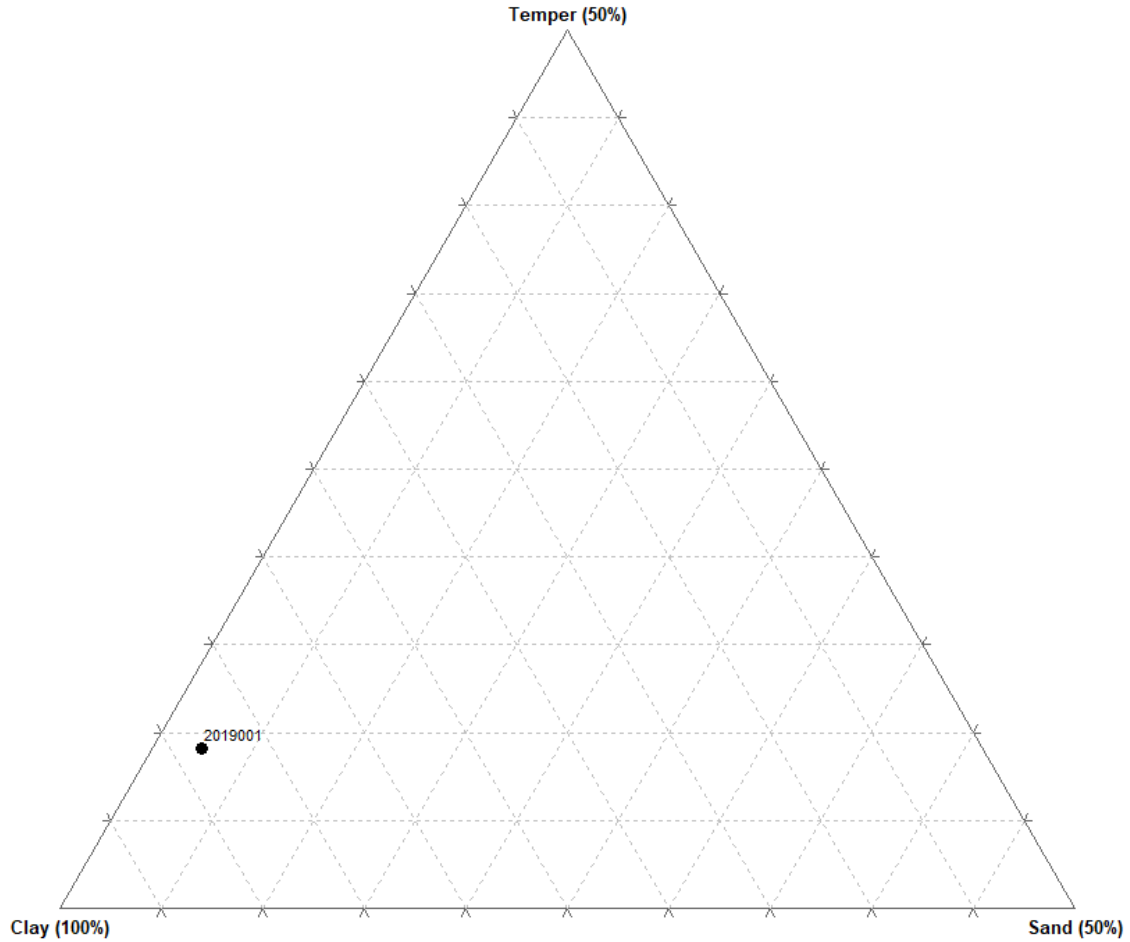


Figure 4.84 Ternary diagram of Sample 1 body composition.

### *Sample 2*

Petrographic analysis on Sample 2 identified a total of 184 points in the natural paste categories. Of these, 144 were clay, thirty-one were silt, and nine were sand. The overall percentages of the paste category are represented as 78.3% clay, 16.8% silt, and 4.9% sand (Figure 4.85). The sand particles were only classed in the fine-grain size category; therefore, the sand-size index is 1.0.

The total number of points counted on the sample were used to calculate the body composition of the sample. A total of 205 points were counted on Sample 2. Of these, 175 were

clay, twenty-one were temper, and nine were sand. The overall percentages of the body categories are 85.4% clay, 10.2 % temper, and 4.4% sand (Figure 4.86). All temper particles were grit pieces. Three grit pieces were classed in the medium-grain size category, and eighteen were classed in the fine-grain size category. The temper-size index is calculated at 1.14.

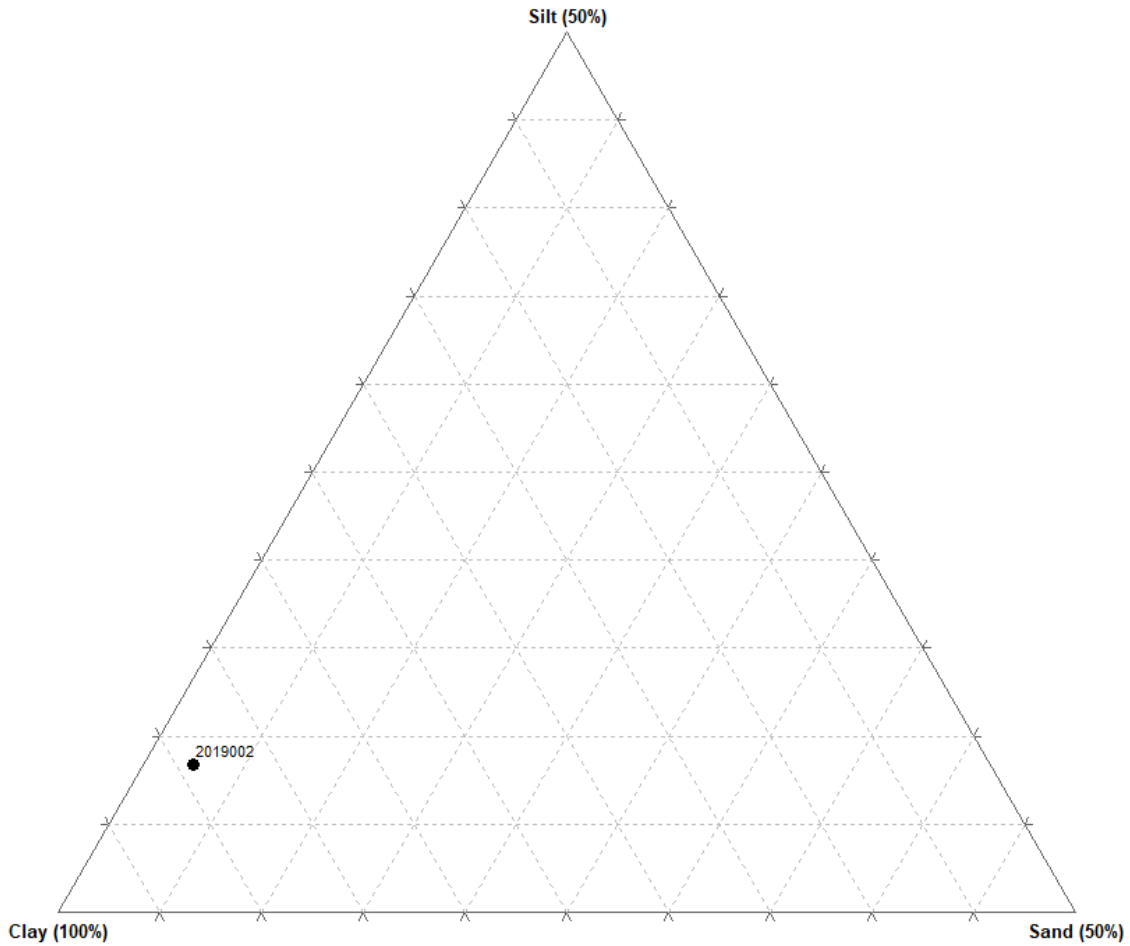


Figure 4.85 Ternary diagram of Sample 2 paste composition.

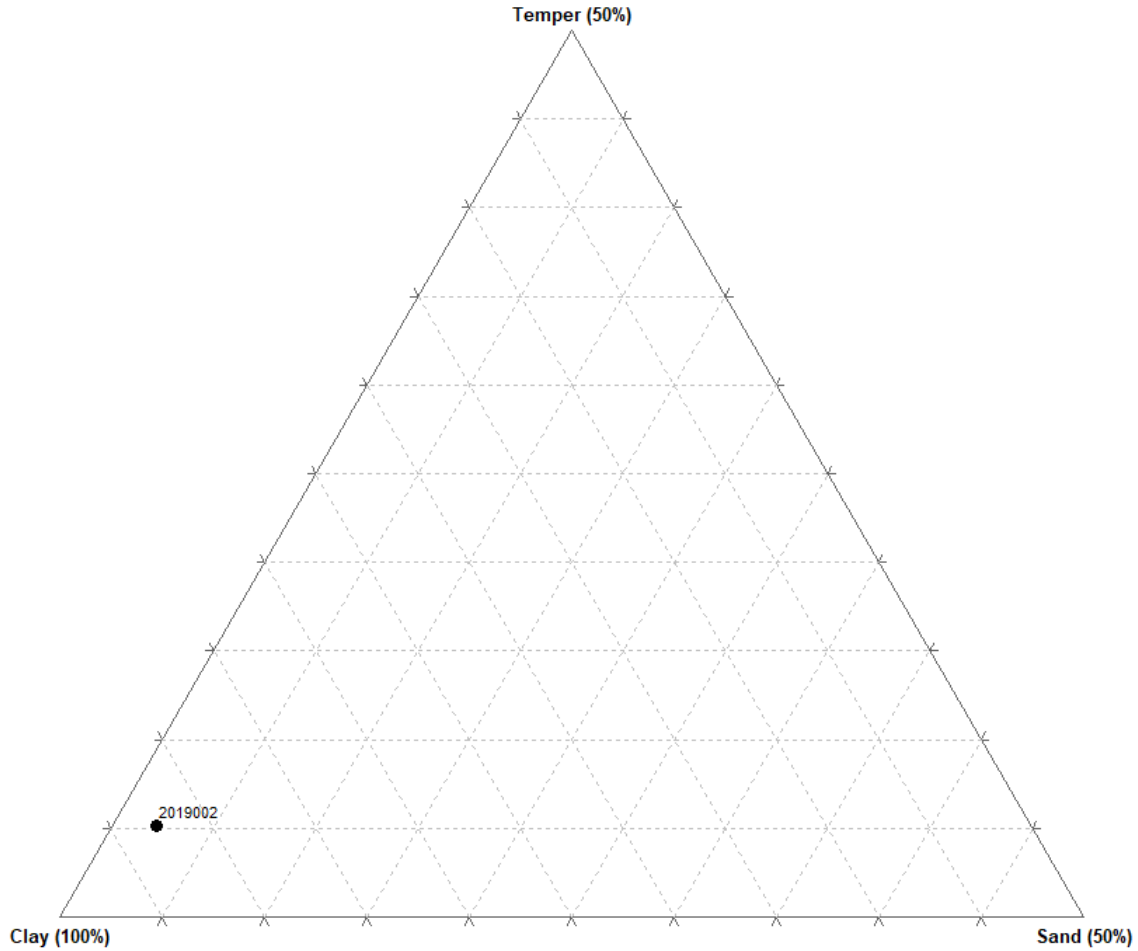


Figure 4.86 Ternary diagram of Sample 2 body composition.

### Sample 3

Petrographic analysis on Sample 3 identified 136 points in the natural paste categories. Of these, 126 were clay, nine were silt, and one was sand. The overall percentages of the paste category are represented as 92.7% clay, 6.6% silt, and 0.7% sand (Figure 4.87). The sand particle was classed in the fine-grain size category; therefore, the sand-size index is 1.0.

The total number of points counted on the sample were used to calculate the body composition of the sample. A total of 151 points were counted on Sample 3. Of these, 135 were clay, fifteen were temper, and one was sand. The overall percentages of the body categories are

89.4% clay, 9.9% temper, and 0.7% sand (Figure 4.88). All temper particles were grit pieces.

Two grit pieces were classed in the medium-grain size category, and thirteen were classed in the fine-grain size category. The temper-size index is calculated at 1.13.

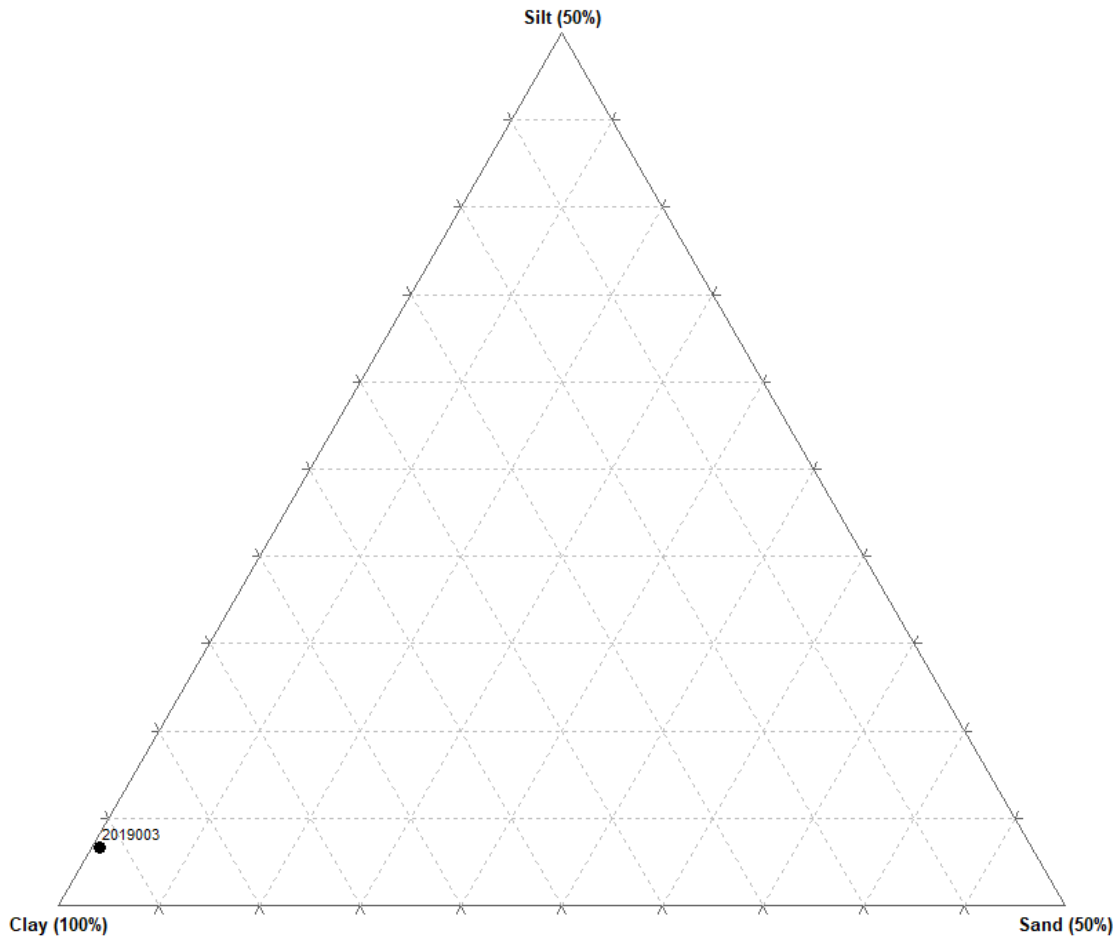


Figure 4.87 Ternary diagrams of Sample 3 paste composition.

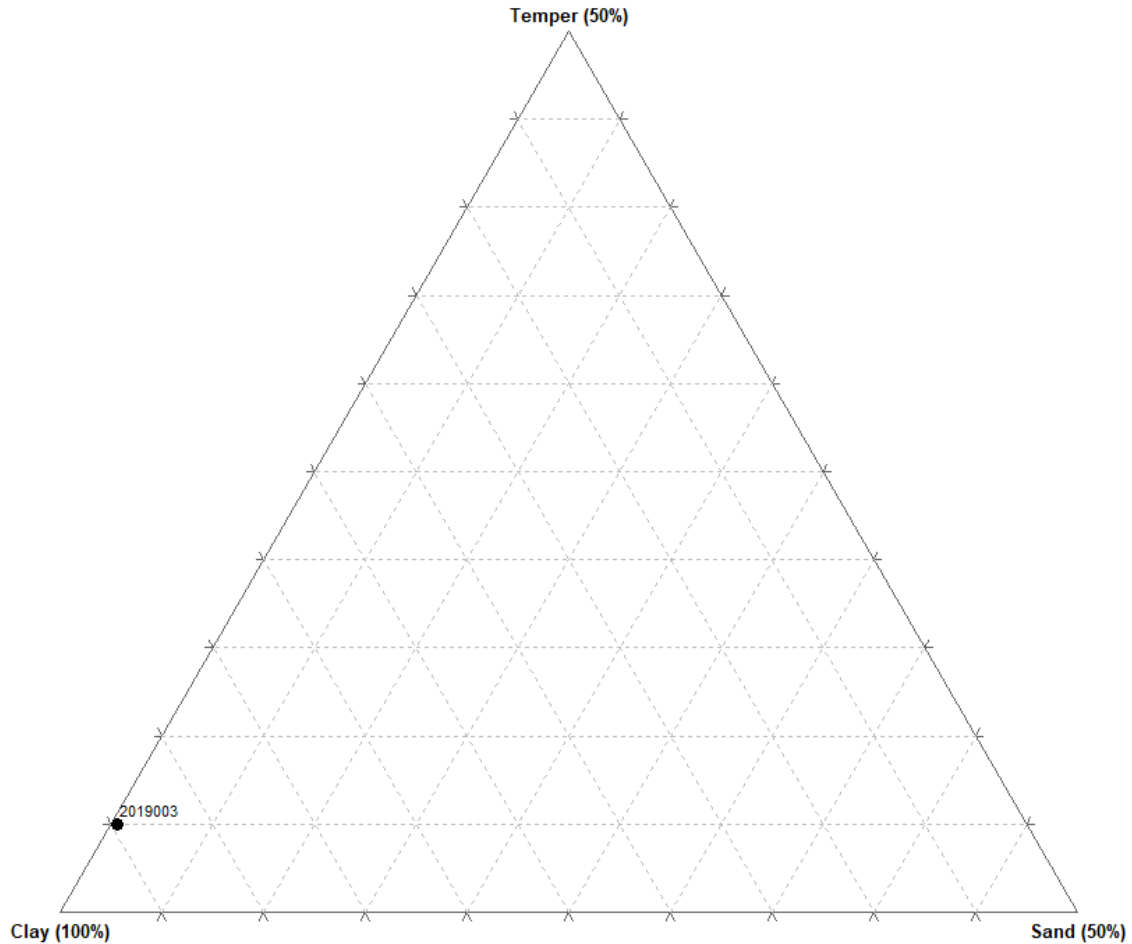


Figure 4.88 Ternary diagrams of Sample 3 body composition.

#### *Sample 4*

Petrographic analysis on Sample 4 identified 243 points in the natural paste categories. Of these, 226 were clay, thirteen were silt, and four were sand. The overall percentages of the paste category are represented as 93.0% clay, 5.3% silt, and 1.7% sand (Figure 4.89). The sand particles were classed in the fine-grain size category; therefore, the sand-size index is 1.0.

The total number of points counted on the sample were used to calculate the body composition of the sample. A total of 263 points were counted on Sample 4. Of these, 239 were clay, twenty were temper, and four were sand. The overall percentages of the body categories are

90.9% clay, 7.6% temper, and 1.5% sand (Figure 4.90). All temper particles were grit pieces. One grit piece was classed in the medium-grain size category, and nineteen were classed in the fine-grain size category. The temper-size index is calculated at 1.05.

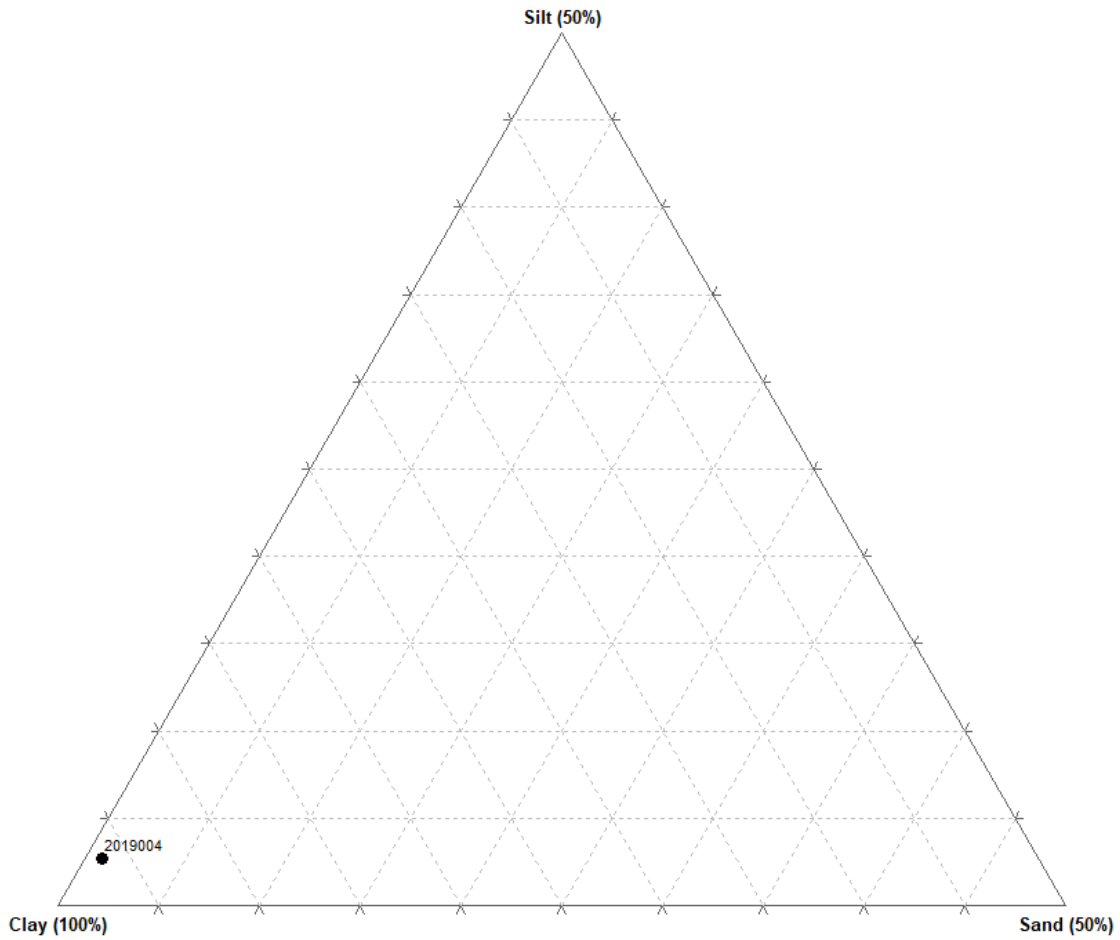


Figure 4.89 Ternary diagram of Sample 4 paste composition.

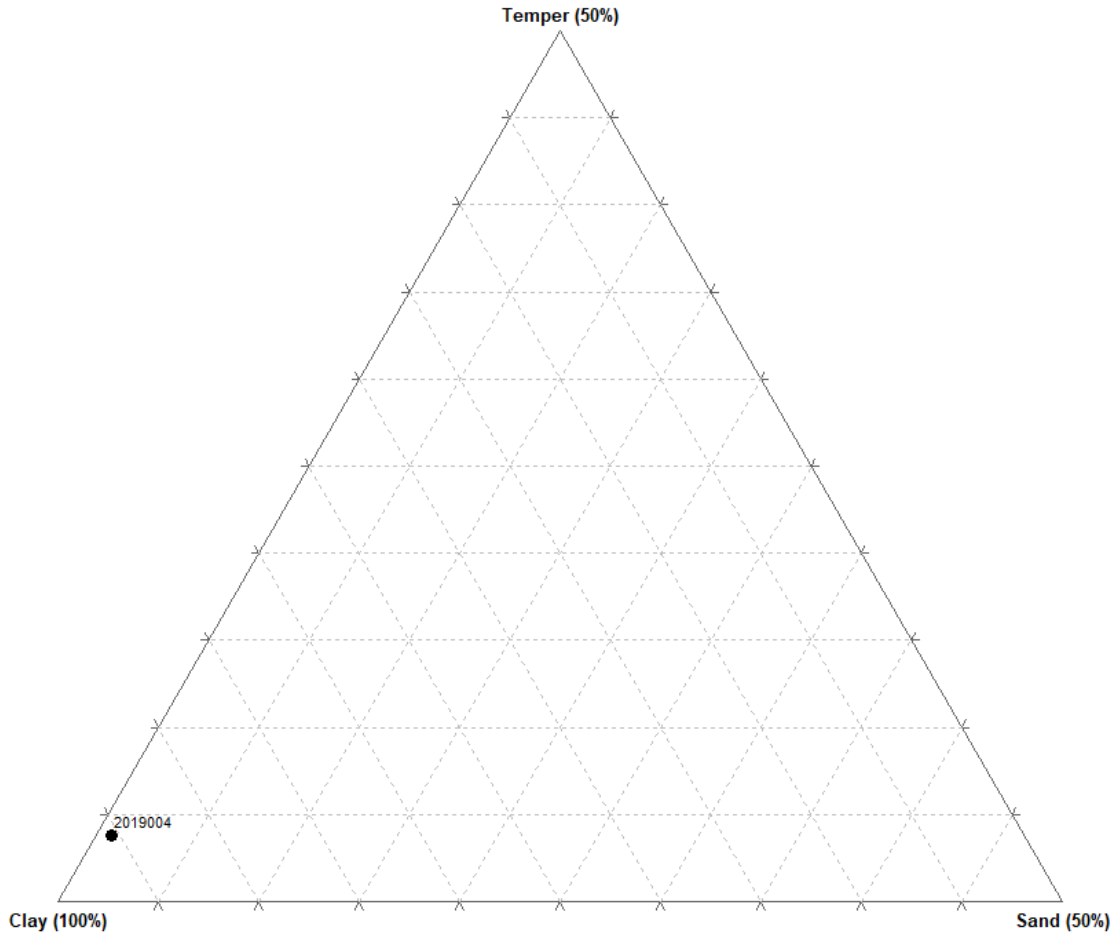


Figure 4.90 Ternary diagram of Sample 4 body composition.

**Sample 5**

Petrographic analysis on Sample 5 identified 147 points in the natural paste categories. Of these, 107 were clay, thirty-nine were silt, and one was sand. The overall percentages of the paste category are represented as 72.8% clay, 26.5% silt, and 0.7% sand (Figure 4.91). The sand particle was classed in the fine-grain size category; therefore, the sand-size index is 1.0.

The total number of points counted on the sample were used to calculate the body composition of the sample. A total of 168 points were counted on Sample 5. Of these, 146 were clay, twenty-one were temper, and one was sand. The overall percentages of the body categories

are 86.9% clay, 12.5% temper, and 0.6% sand (Figure 4.92). All temper particles were grit pieces. One grit piece was classed in the medium-grain size category, and twenty were classed in the fine-grain size category. The temper-size index is calculated at 1.05.

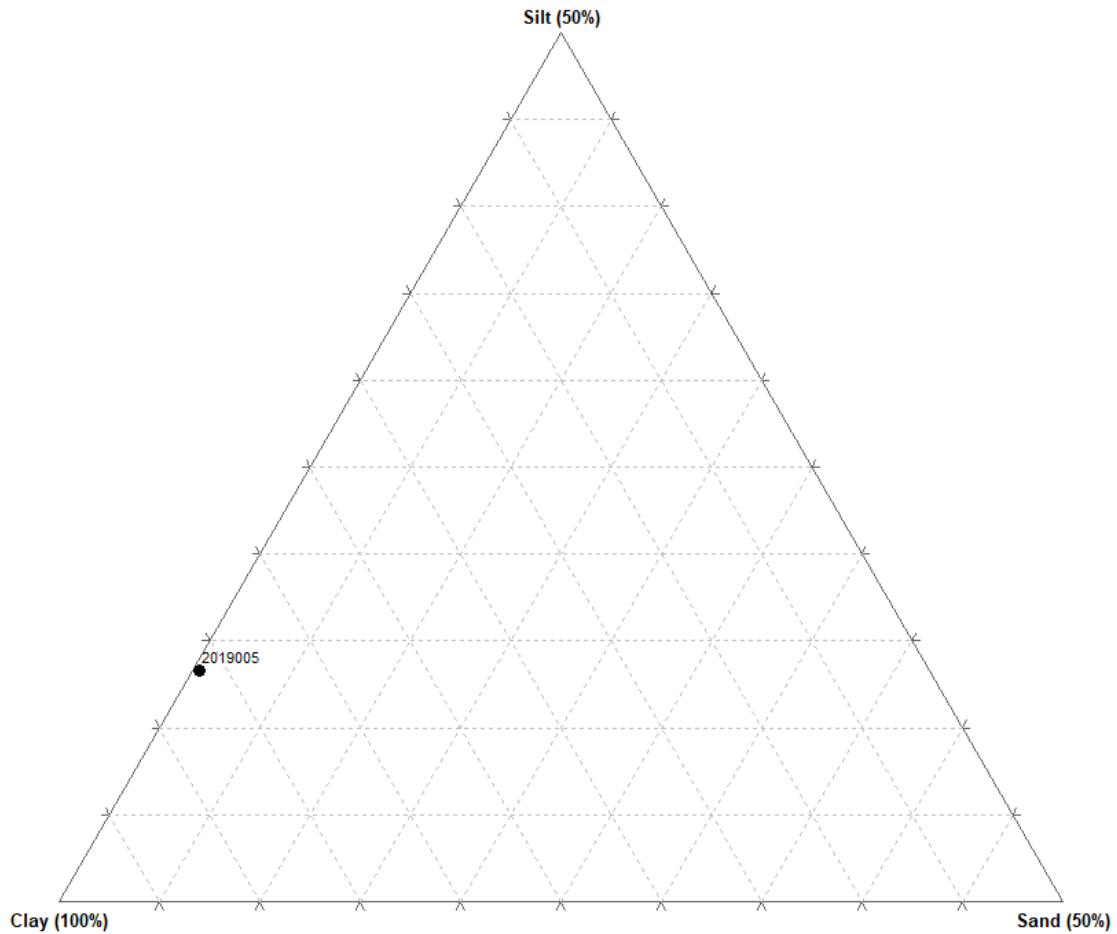


Figure 4.91 Ternary diagram of Sample 5 paste composition.



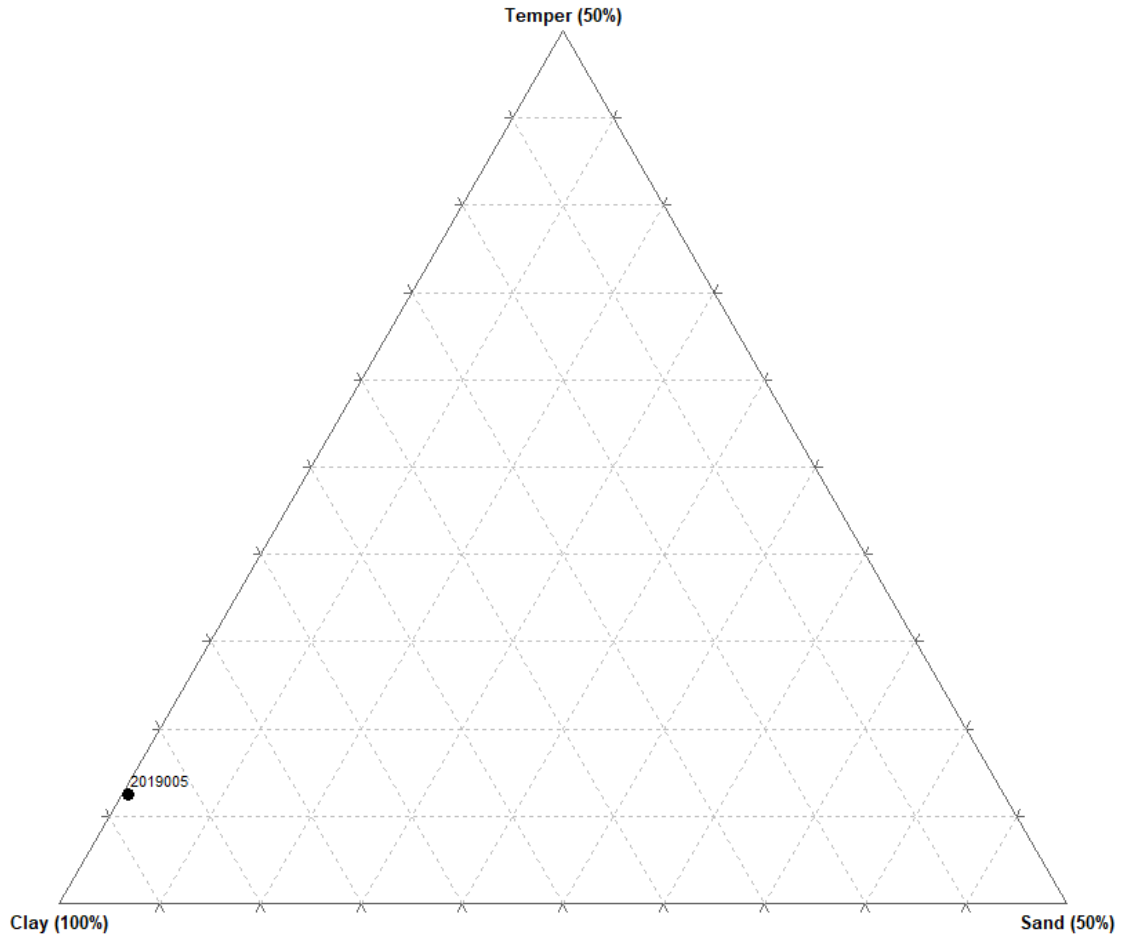


Figure 4.92 Ternary diagram of Sample 5 body composition.

### Sample 6

Petrographic analysis on Sample 6 identified 158 points in the natural paste categories. Of these, 146 were clay, ten were silt, and two were sand. The overall percentages of the paste category are represented as 92.4% clay, 6.3% silt, and 1.3% sand (Figure 4.93). The sand particles were classed in the fine-grain size category; therefore, the sand-size index is 1.0.

The total number of points counted on the sample were used to calculate the body composition of the sample. A total of 187 points were counted on Sample 6. Of these, 156 were clay, twenty-nine were temper, and two were sand. The overall percentages of the body

categories are 83.4% clay, 15.5% temper, and 1.1% sand (Figure 4.94). All temper particles were grit pieces. Six grit pieces were classed in the medium-grain size category, and twenty-three were classed in the fine-grain size category. The temper-size index is calculated at 1.21.

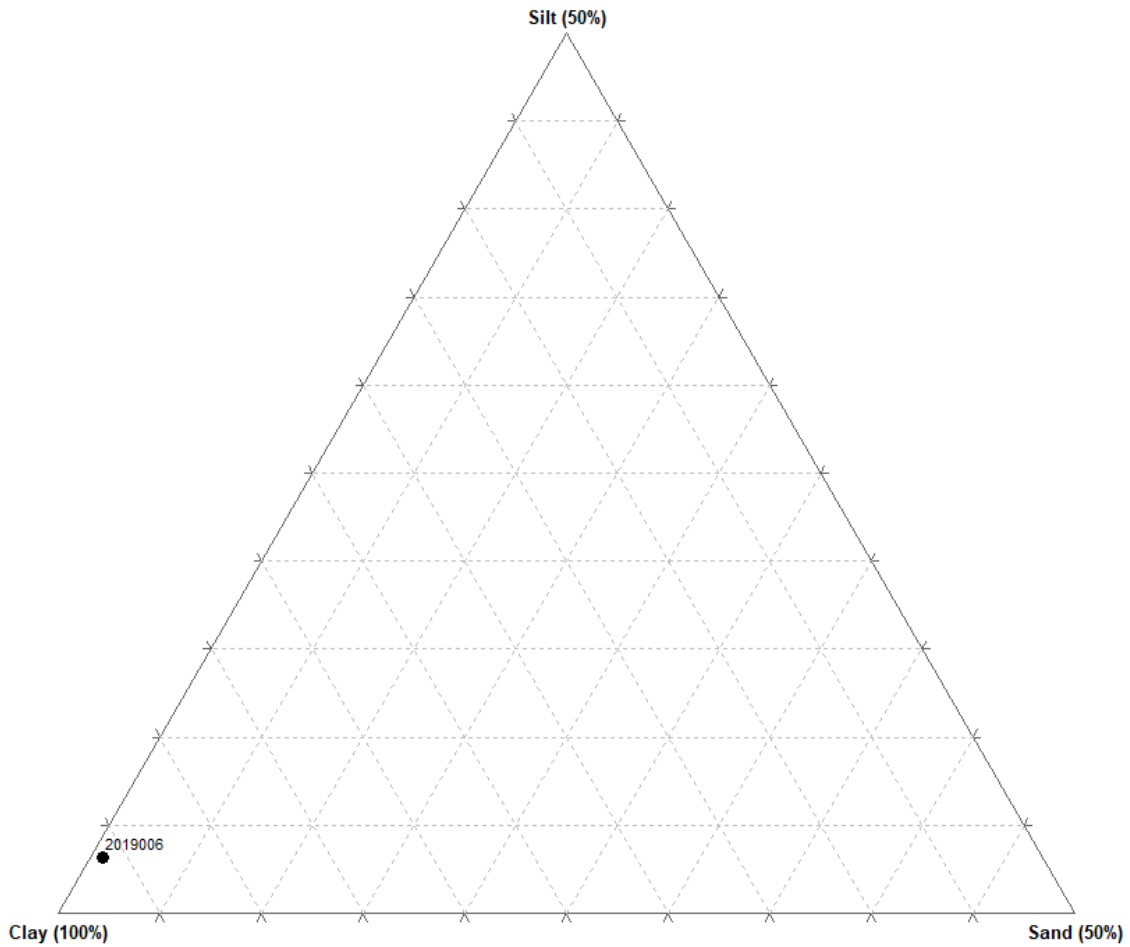


Figure 4.93 Ternary diagram of Sample 6 paste composition

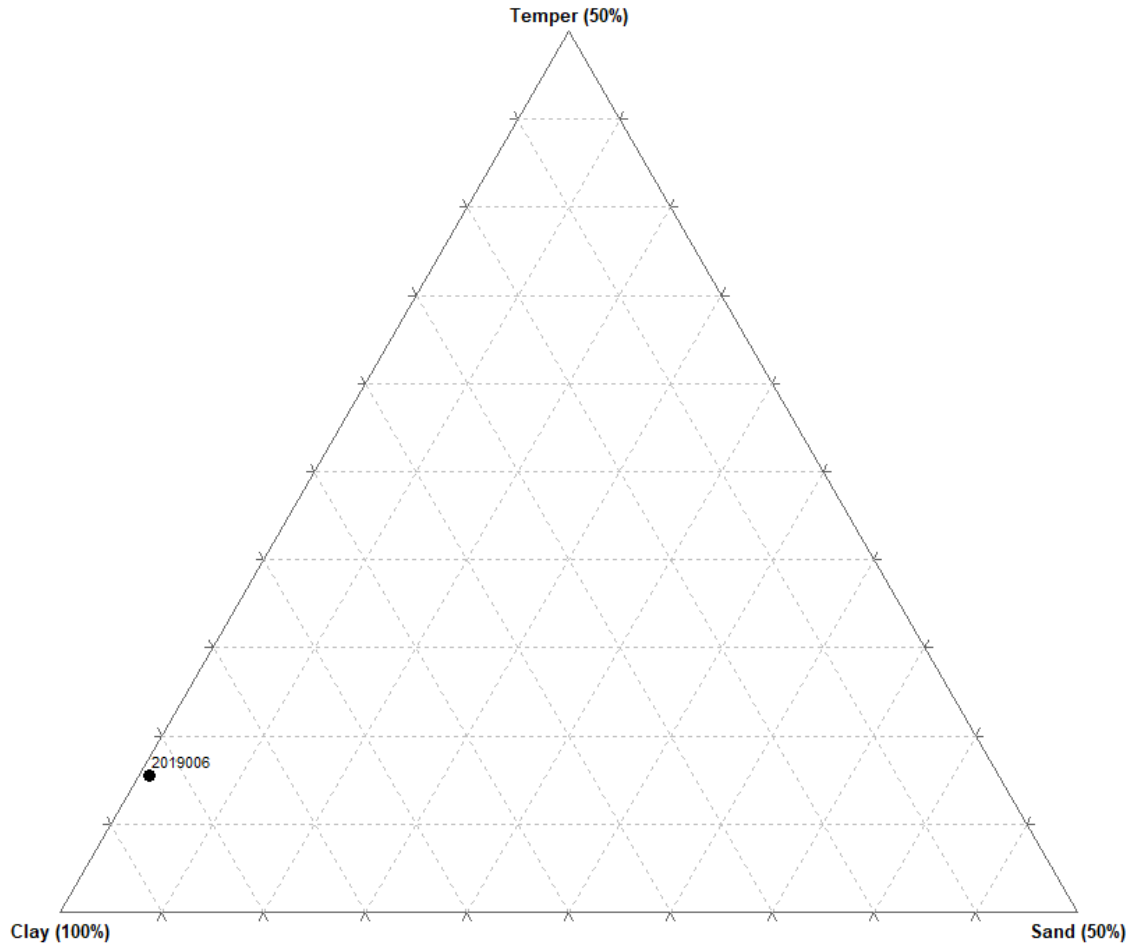


Figure 4.94 Ternary diagram of Sample 6 body composition.

### *Sample 7*

Petrographic analysis on sample 7 identified a total of 188 points in the natural paste categories. Of these, 153 were clay, thirty-five were silt, and no natural particles were identified in the sand-size category. The overall percentages of the paste category are represented as 81.4% clay and 18.6% silt (Figure 4.95). As there were no minerals in the sand-size category, the sand-size index was not calculated.

The total number of points counted on the sample were used to calculate the body composition of the sample. A total of 223 points were counted on Sample 7. Of these, 188 were

clay and thirty-five were temper. The overall percentages of the body categories are 84.3% clay and 15.7% temper (Figure 4.96). All temper particles were grit pieces. Nine grit pieces were classed in the medium-grain size category, and twenty-six were classed in the fine-grain size category. The temper-size index is calculated at 1.26.

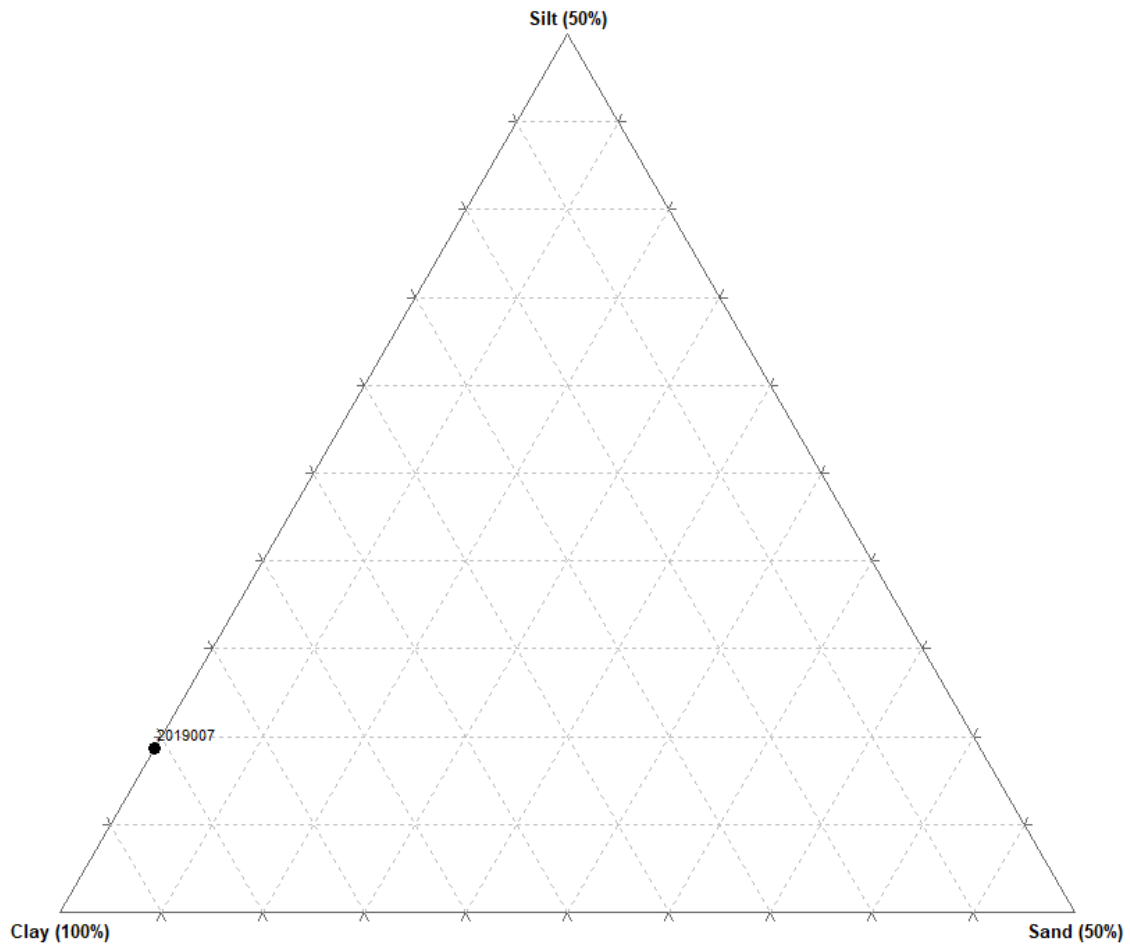


Figure 4.95 Ternary diagram of Sample 7 paste composition.

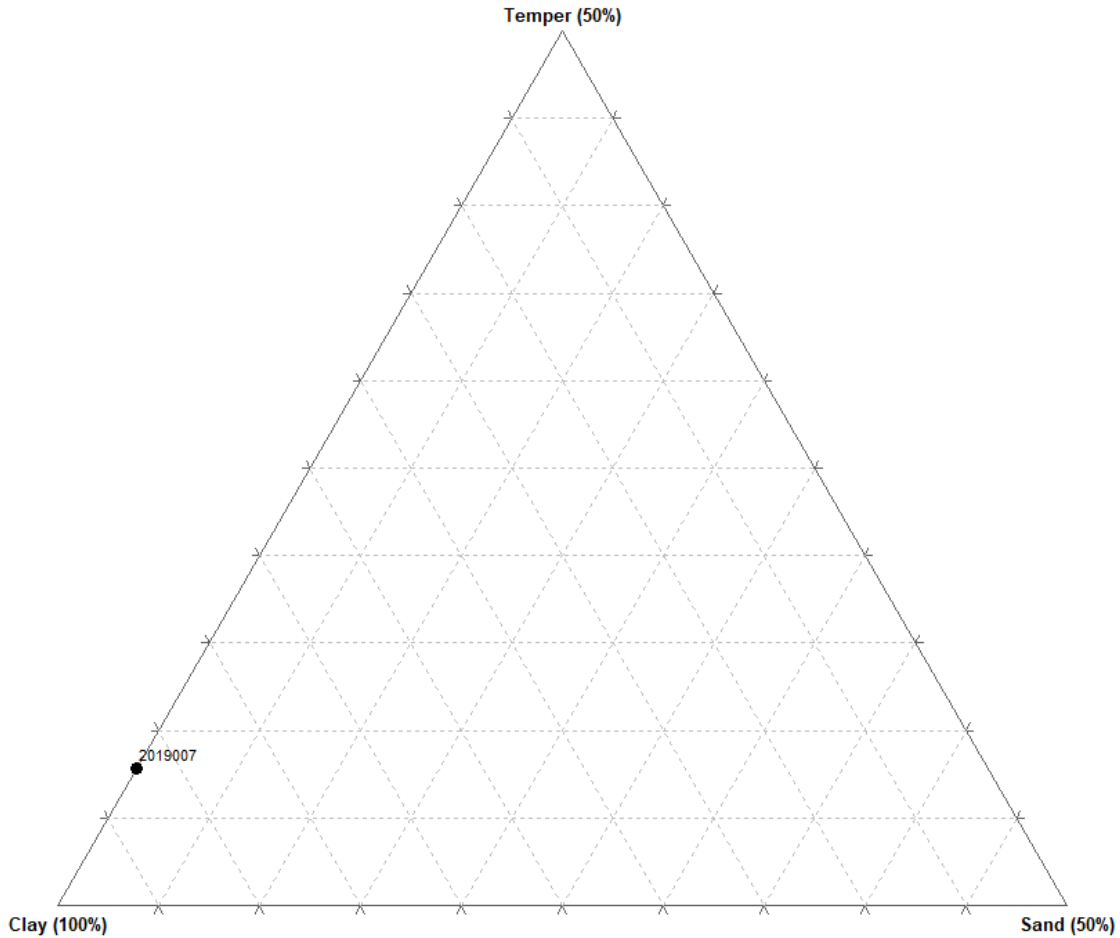


Figure 4.96 Ternary diagram of Sample 7 body composition.

### *Sample 8*

Petrographic analysis on Sample 8 identified 184 points in the natural paste categories. Of these, 153 were clay, thirty were silt, and one was sand. The overall percentages of the paste category are represented as 83.2% clay, 16.3% silt, and 0.5% sand (Figure 4.97). The sand particles were classed in the fine-grain size category; therefore, the sand-size index is 1.0.

The total number of points counted on the sample were used to calculate the body composition of the sample. A total of 215 points were counted on Sample 8. Of these, 183 were clay, thirty-one were temper, and one was sand. The overall percentages of the body categories

are 85.1% clay, 14.4% temper, and 0.5% sand (Figure 4.98). All temper particles were grit pieces. Four grit pieces were classed in the medium-grain size category, and twenty-seven were classed in the fine-grain size category. The temper-size index is calculated at 1.13.

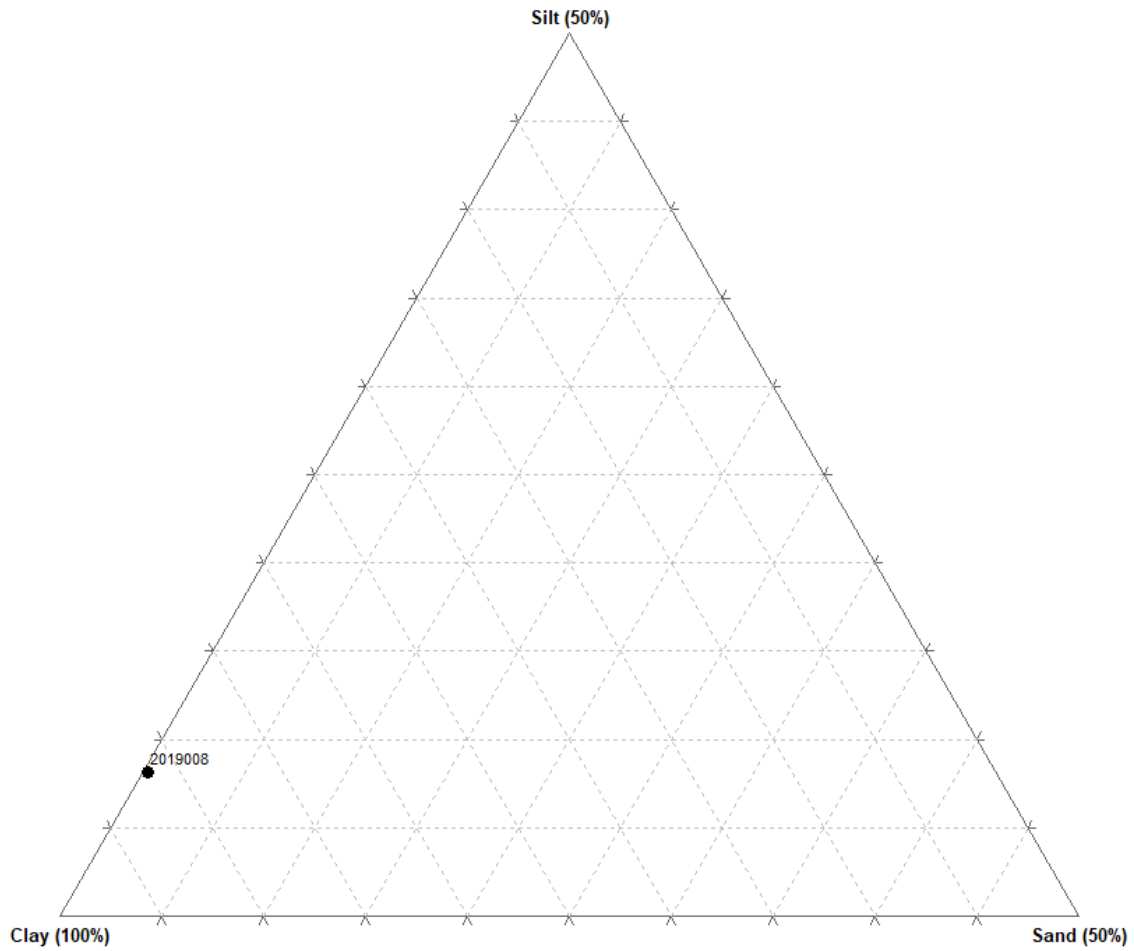


Figure 4.97 Ternary diagram of Sample 8 paste composition.

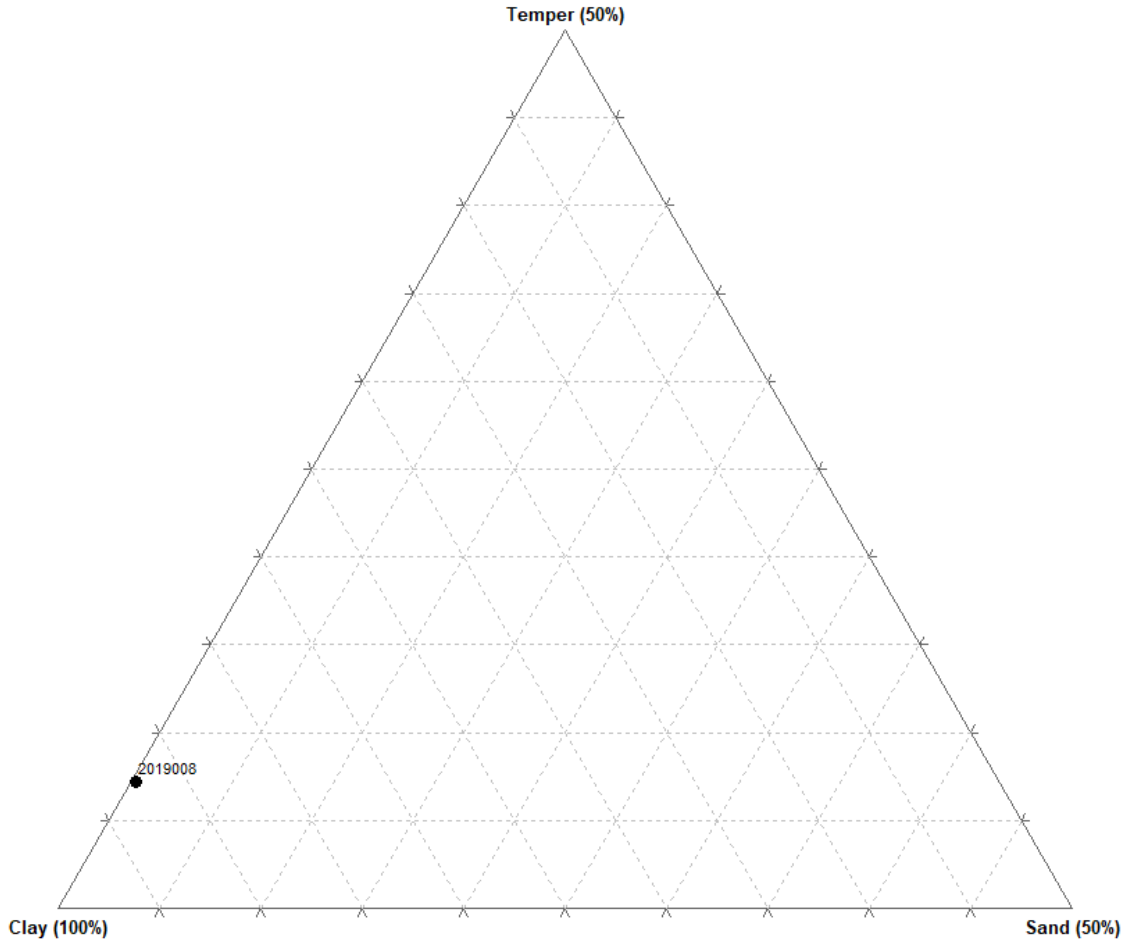


Figure 4.98 Ternary diagram of Sample 8 body composition.

### *Sample 9*

Petrographic analysis on Sample 9 identified 236 points in the natural paste categories. Of these, 197 were clay, thirty-four were silt, and five were sand. The overall percentages of the paste category are represented as 83.5% clay, 14.4% silt, and 2.1% sand (Figure 4.99). The sand particles were classed in the fine-grain size category; therefore, the sand-size index is 1.0.

The total number of points counted on the sample were used to calculate the body composition of the sample. A total of 266 points were counted on Sample 9. Of these, 231 were clay, thirty were temper, and five were sand. The overall percentages of the body categories are

86.8% clay, 11.3% temper, and 1.9% sand (Figure 4.100). All temper particles were grit pieces. Two grit pieces were classed in the medium-grain size category, and twenty-eight were classed in the fine-grain size category. The temper-size index is calculated at 1.07.

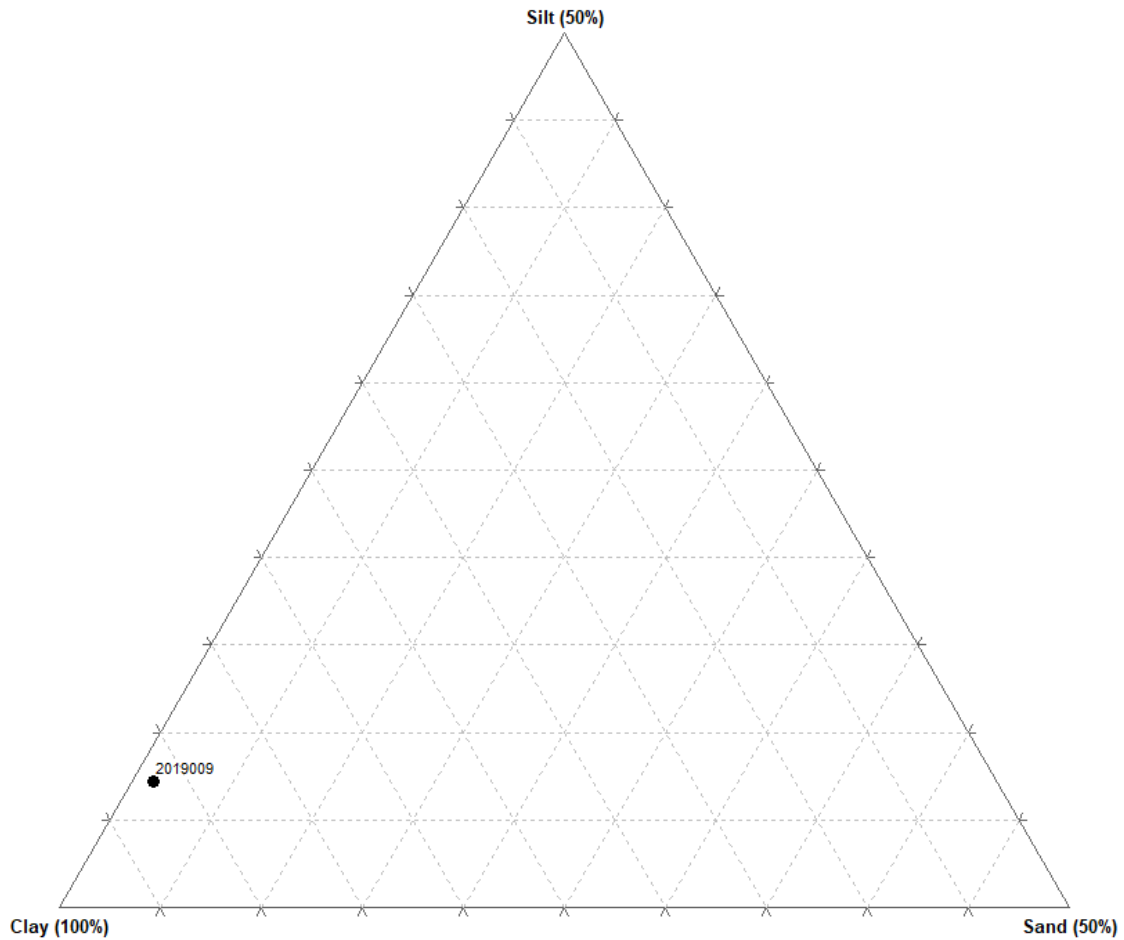


Figure 4.99 Ternary diagram of Sample 9 paste composition.



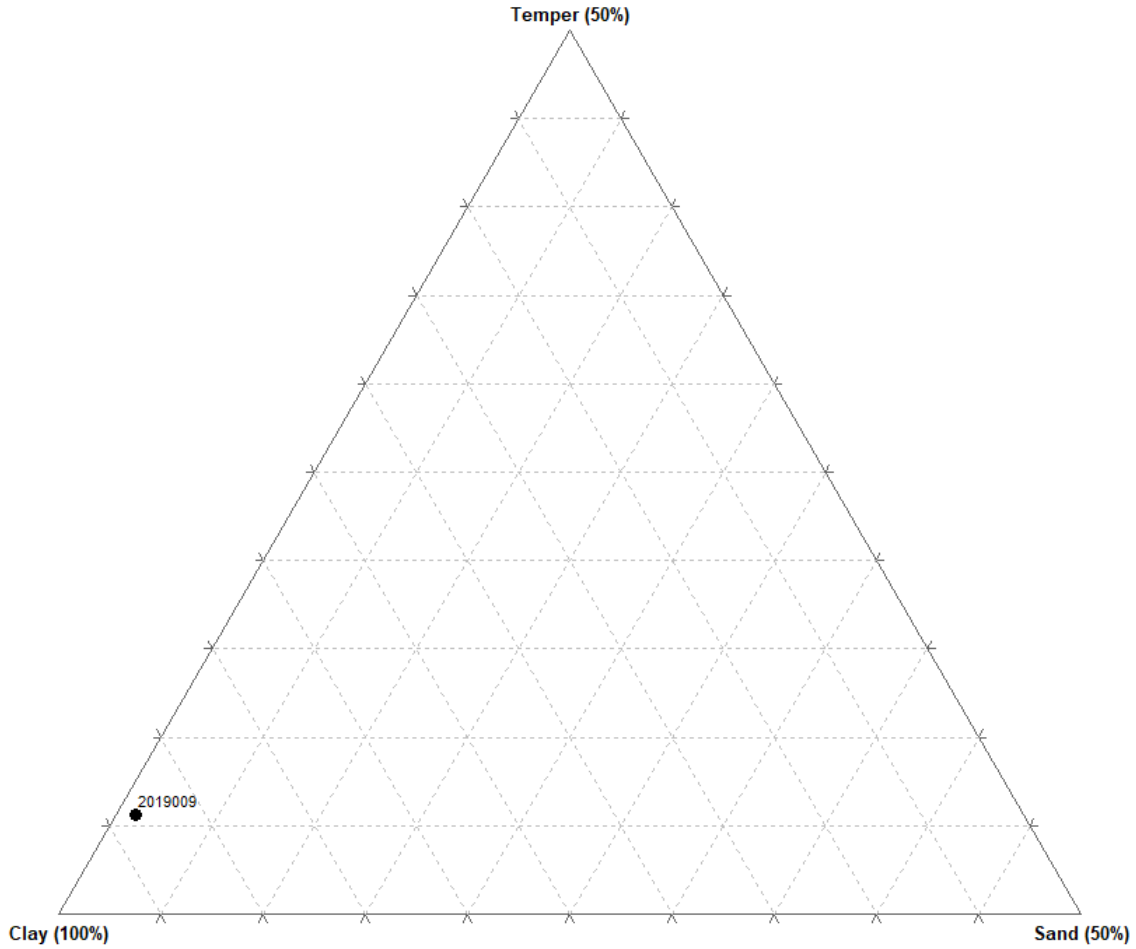


Figure 4.100 Ternary diagram of Sample 9 body composition.

**Sample 10**

Petrographic analysis on Sample 10 identified 180 points in the natural paste categories. Of these, 155 were clay, twenty-five were silt, and no natural particles were in the sand-size category. The overall percentages of the paste category are represented as 86.1% clay and 13.9% silt (Figure 4.101). As there were no minerals in the sand-size category, the sand-size index was not calculated.

The total number of points counted on the sample were used to calculate the body composition of the sample. A total of 193 points were counted on Sample 10. Of these, 180 were

clay and thirteen were temper. The overall percentages of the body categories are 93.3% clay and 6.7% temper (Figure 4.102). All temper particles were grit pieces. Three grit pieces were classed in the medium-grain size category, and ten were classed in the fine-grain size category. The temper-size index is calculated at 1.23.

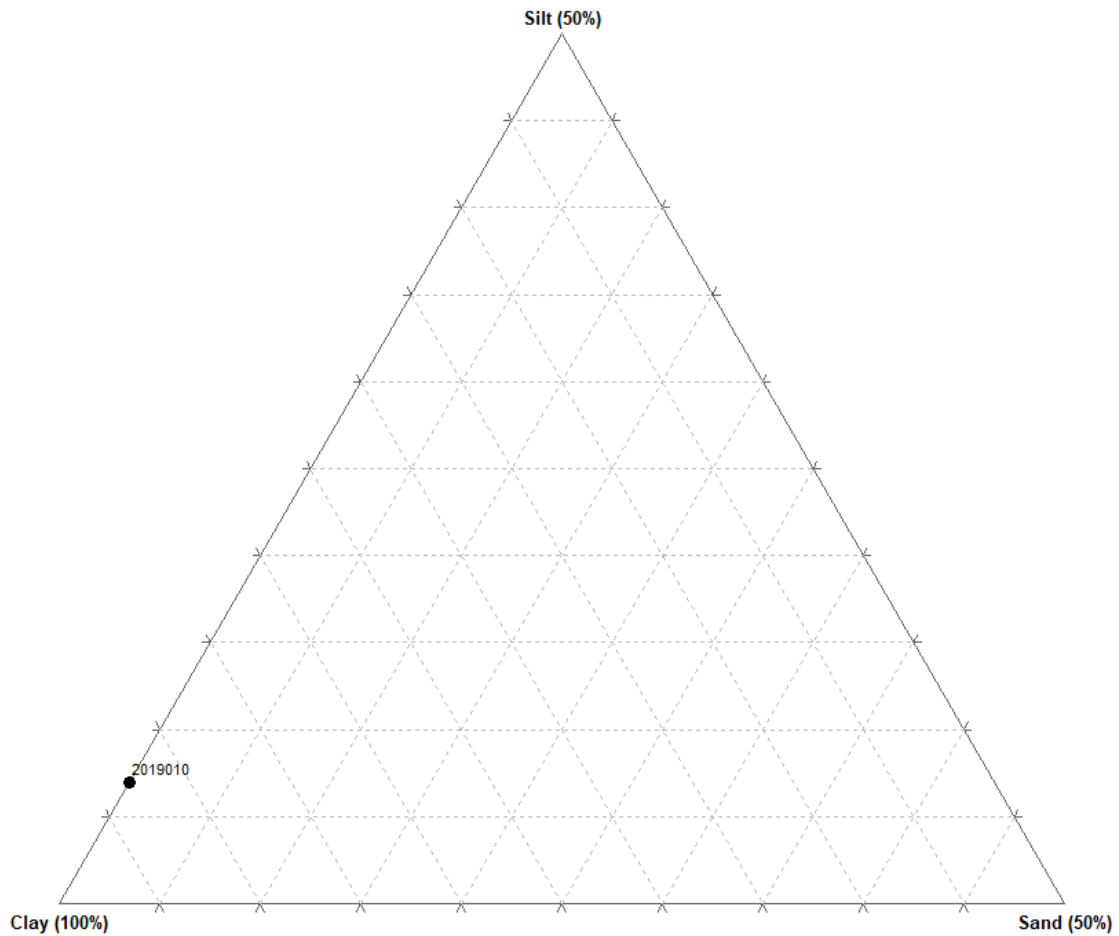


Figure 4.101 Ternary diagram of Sample 10 paste composition.

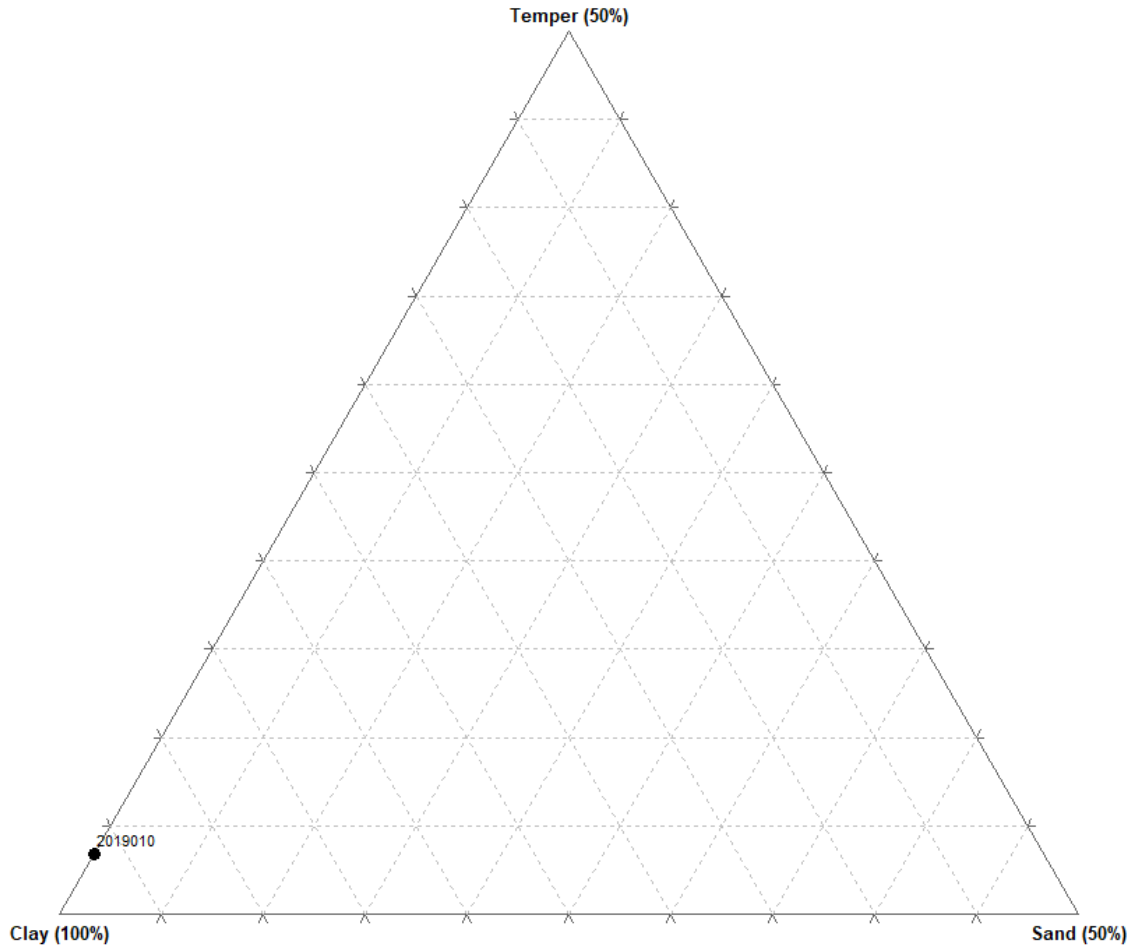


Figure 4.102 Ternary diagram of Sample 10 body composition.

### *Sample 11*

Petrographic analysis on Sample 11 identified 146 points in the natural paste categories. Of these, 102 were clay, forty-one were silt, and three were sand. The overall percentages of the paste category are represented as 69.9% clay, 28.1% silt, and 2.0% sand (Figure 4.103). The sand particles were classed in the fine-grain size category; therefore, the sand-size index is 1.0.

The total number of points counted on the sample were used to calculate the body composition of the sample. A total of 160 points were counted on Sample 11. Of these, 143 were clay, fourteen were temper, and three were sand. The overall percentages of the body categories

are 89.4% clay, 8.8% temper, and 1.9% sand (Figure 4.104). All temper particles were grit pieces. Three grit pieces were classed in the coarse-grain size category, two were classed in the medium-grain size category, and nine were classed in the fine-grain size category. The temper-size index is calculated at 1.29.

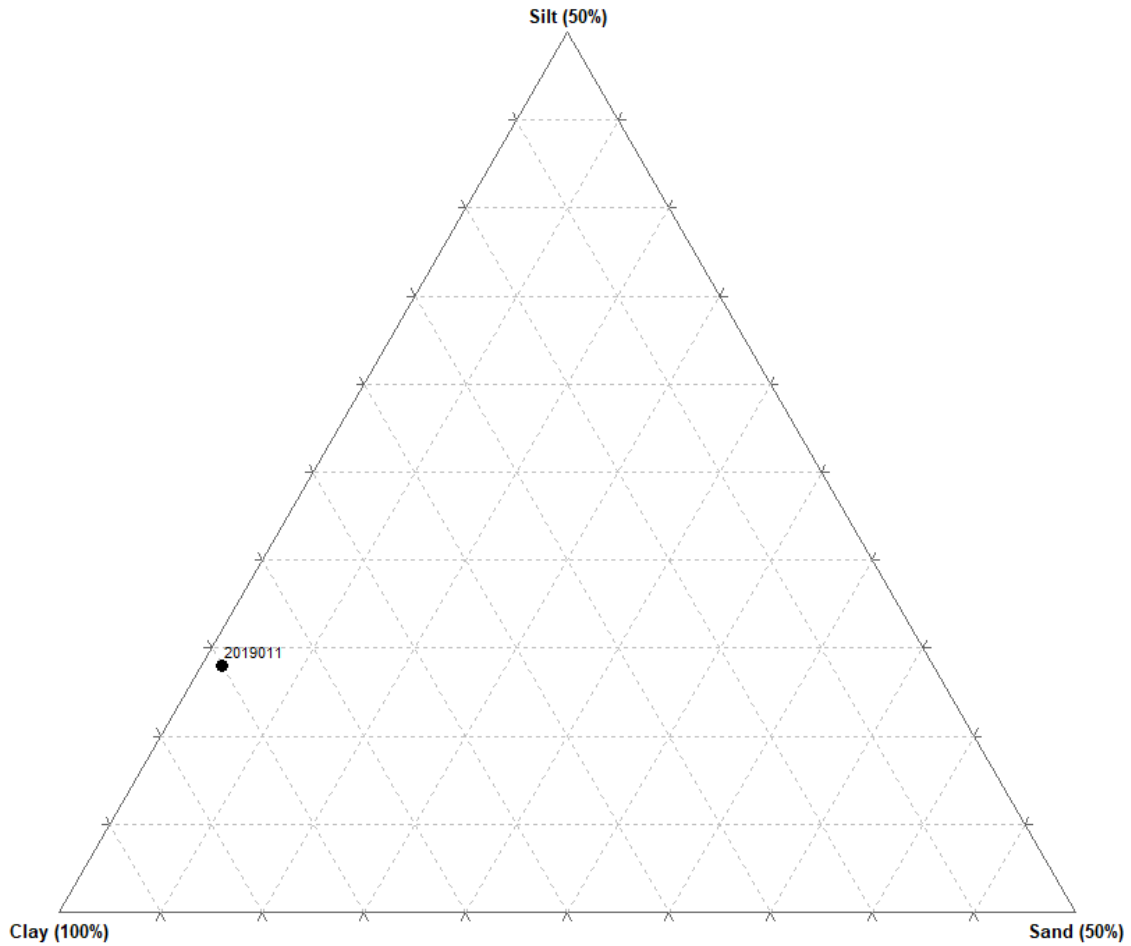


Figure 4.103 Ternary diagram of Sample 11 paste composition.

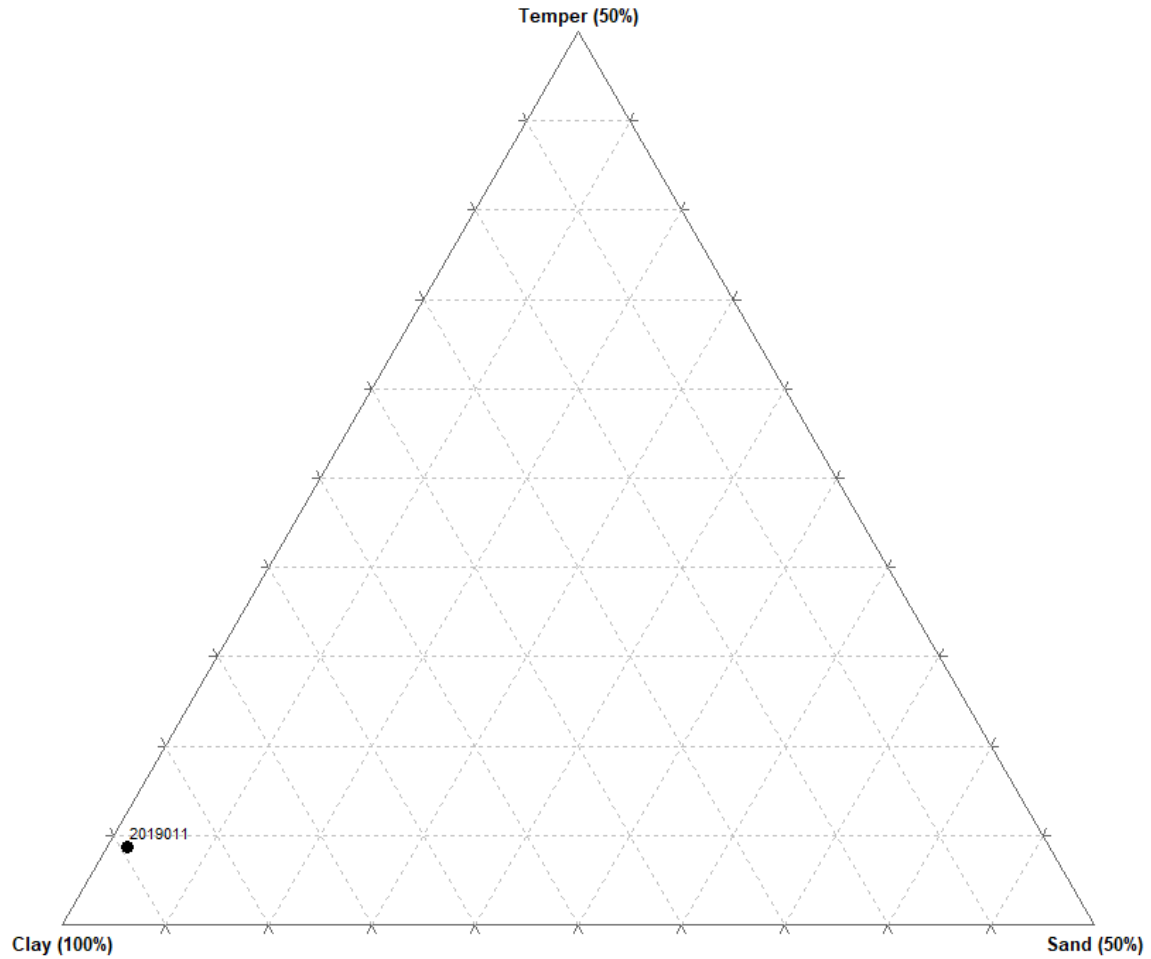


Figure 4.104 Ternary diagram of Sample 11 body composition.

### *Sample 12*

Petrographic analysis on Sample 12 identified 225 points in the natural paste categories. Of these, 163 were clay, fifty-eight were silt, and four were sand. The overall percentages of the paste category are represented as 72.4% clay, 25.8% silt, and 1.8% sand (Figure 4.105). The sand particles were classed in the fine-grain size category; therefore, the sand-size index is 1.0.

The total number of points counted on the sample were used to calculate the body composition of the sample. A total of 240 points were counted on Sample 12. Of these, 221 were

clay, fifteen were temper, and four were sand. The overall percentages of the body categories are 92.1% clay, 6.2% temper, and 1.7% sand (Figure 4.106). All temper particles were grit pieces. One grit piece was classed in the coarse-grain size category, two were classed in the medium-grain size category, and twelve were classed in the fine-grain size category. The temper-size index is calculated at 1.19.

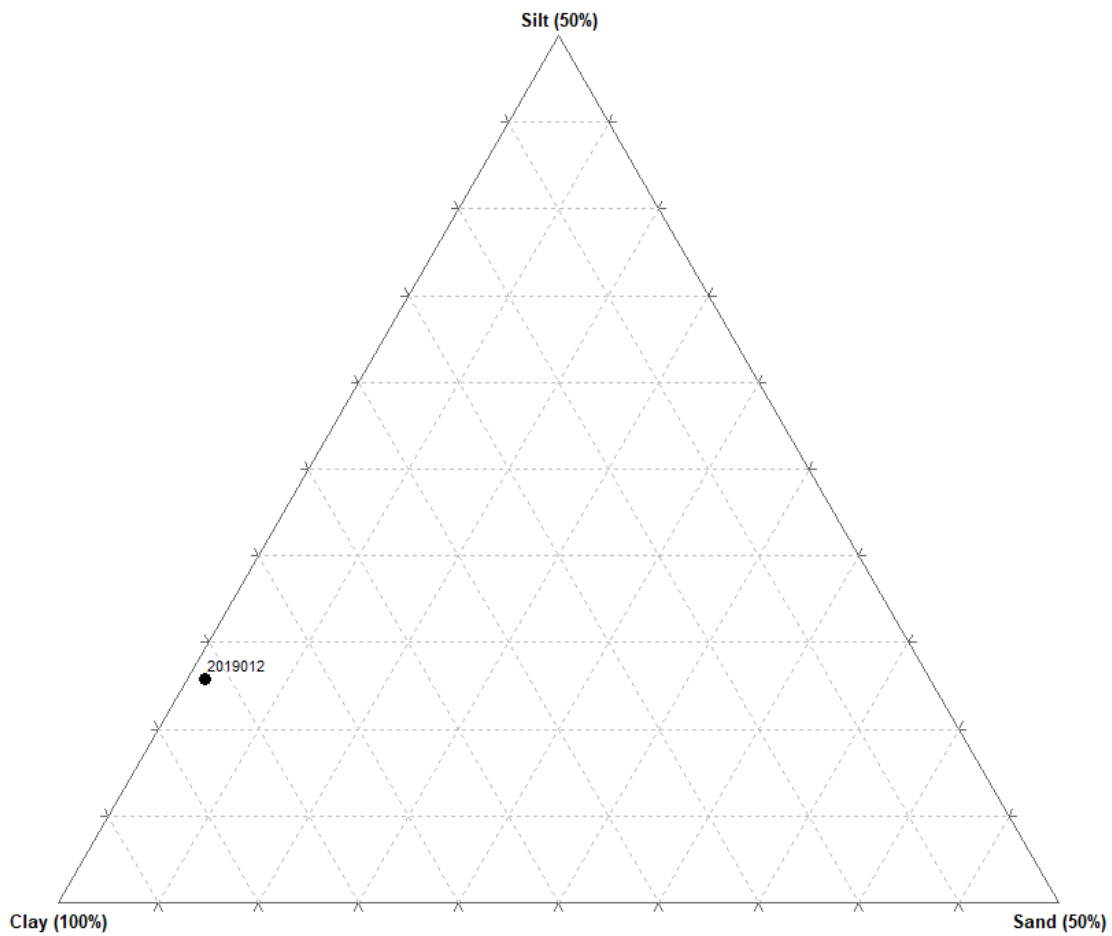


Figure 4.105 Ternary diagram of Sample 12 paste composition.

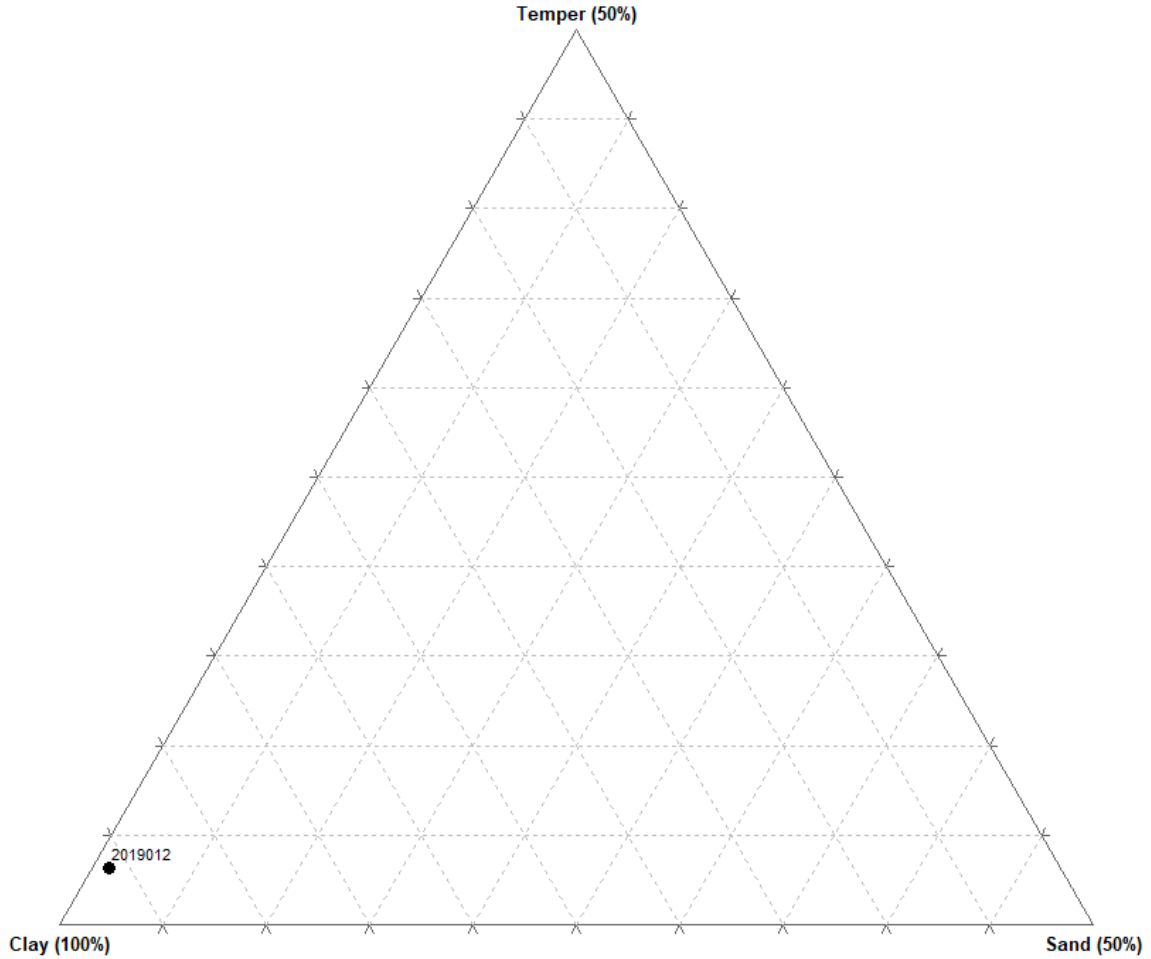


Figure 4.106 Ternary diagram of Sample 12 body composition.

**Sample 13**

Petrographic analysis on Sample 13 identified 203 points in the natural paste categories. Of these, 171 were clay, thirty-one were silt, and one were sand. The overall percentages of the paste category are represented as 84.2% clay, 15.3% silt, and 0.5% sand (Figure 4.107). The sand particle was classed in the fine-grain size category; therefore, the sand-size index is 1.0.

The total number of points counted on the sample were used to calculate the body composition of the sample. A total of 212 points were counted on Sample 13. Of these, 202 were

clay, nine were temper, and one was sand. The overall percentages of the body categories are 95.3% clay, 4.2% temper, and 0.5% sand (Figure 4.108). All temper particles were grit pieces. One grit piece was classed in the medium-grain size category, and eight were classed in the fine-grain size category. The temper-size index is calculated at 1.11.

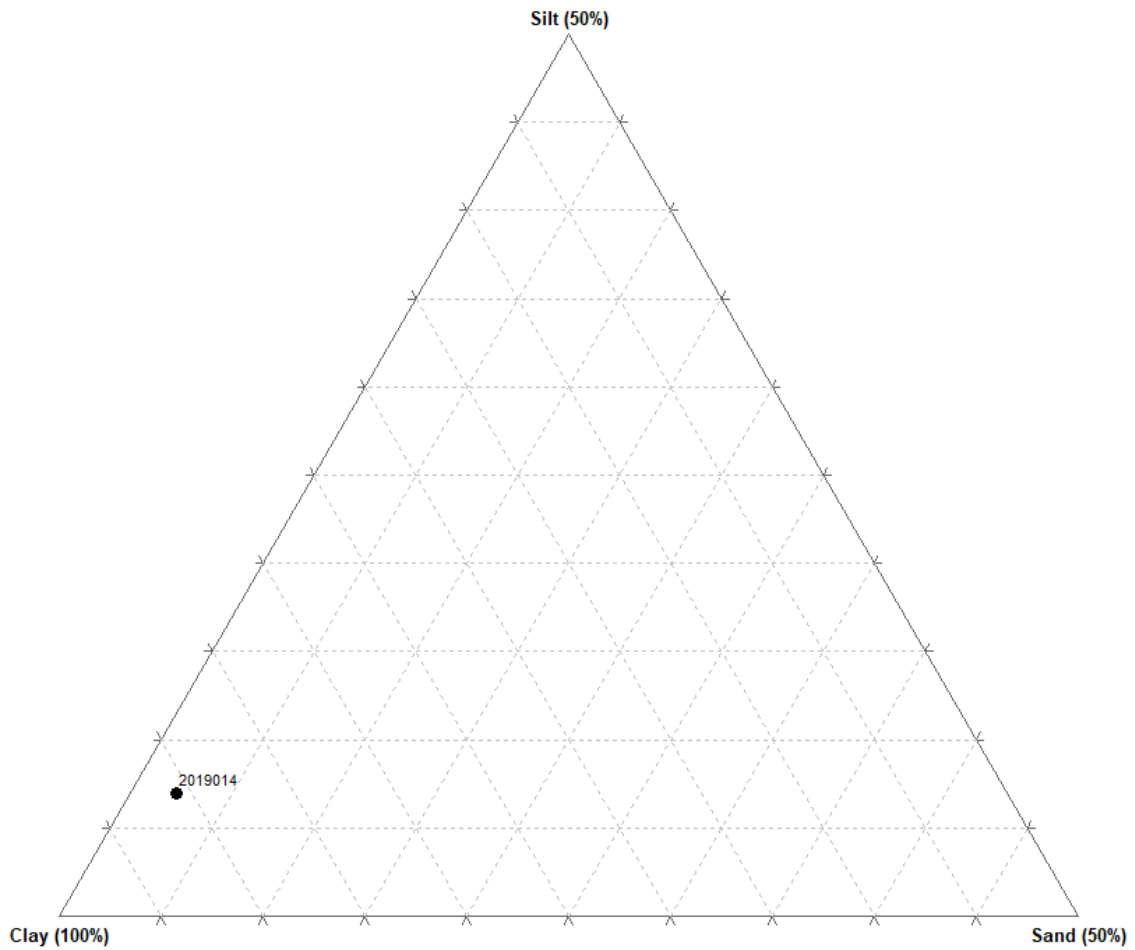


Figure 4.107 Ternary diagram of Sample 13 paste composition.



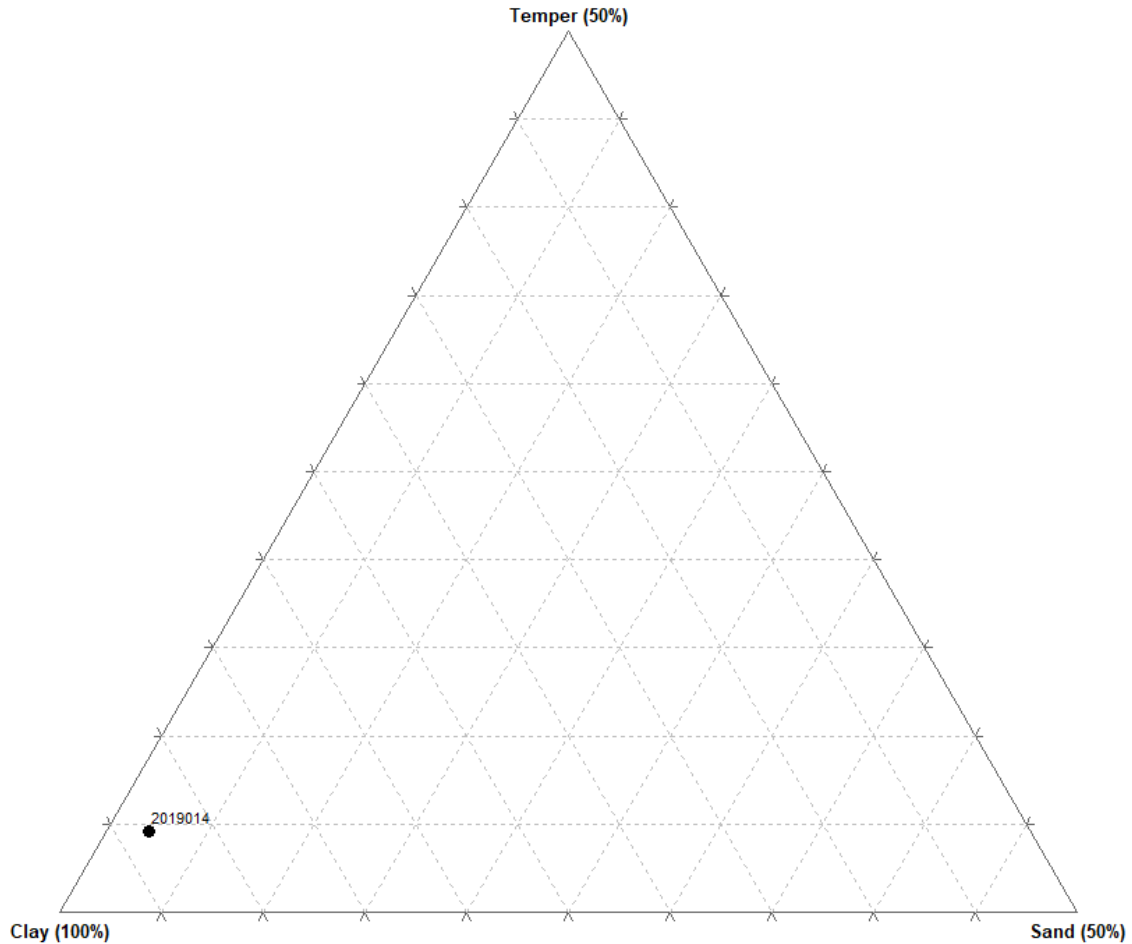


Figure 4.108 Ternary diagram of Sample 13 body composition.

### *Sample 14*

Petrographic analysis on Sample 14 identified 108 points in the natural paste categories. Of these, 88 were clay, fifteen were silt, and five were sand. The overall percentages of the paste category are represented as 81.5% clay, 13.9% silt, and 4.6% sand (Figure 4.109). The sand particles were classed in the fine-grain size category; therefore, the sand-size index is 1.0.

The total number of points counted on the sample were used to calculate the body composition of the sample. A total of 119 points were counted on Sample 14. Of these, 103 were clay, eleven were temper, and five were sand. The overall percentages of the body categories are

86.6% clay, 9.2% temper, and 4.2% sand (Figure 4.110). All temper particles were grit pieces. Two grit pieces were classed in the medium-grain size category, and nine were classed in the fine-grain size category. The temper-size index is calculated at 1.18.

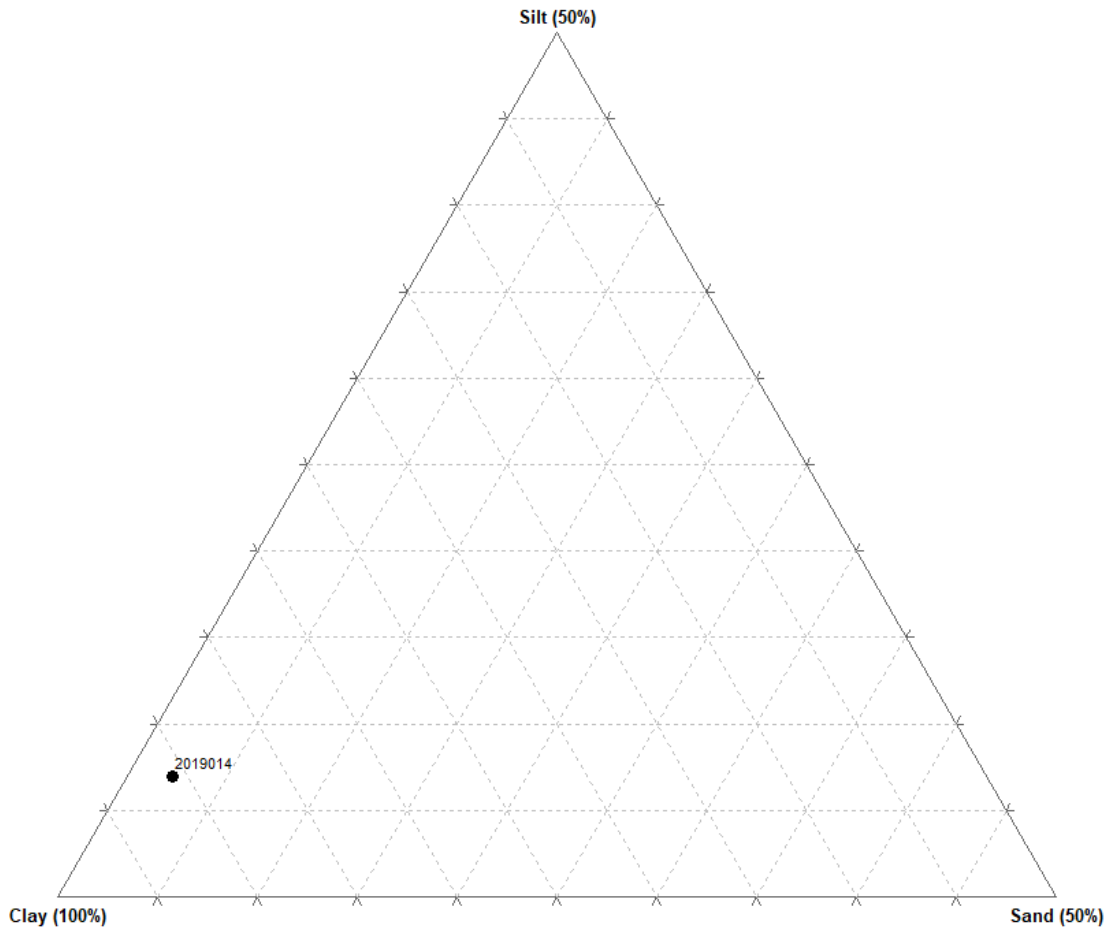


Figure 4.109 Ternary diagram of Sample 14 paste composition.

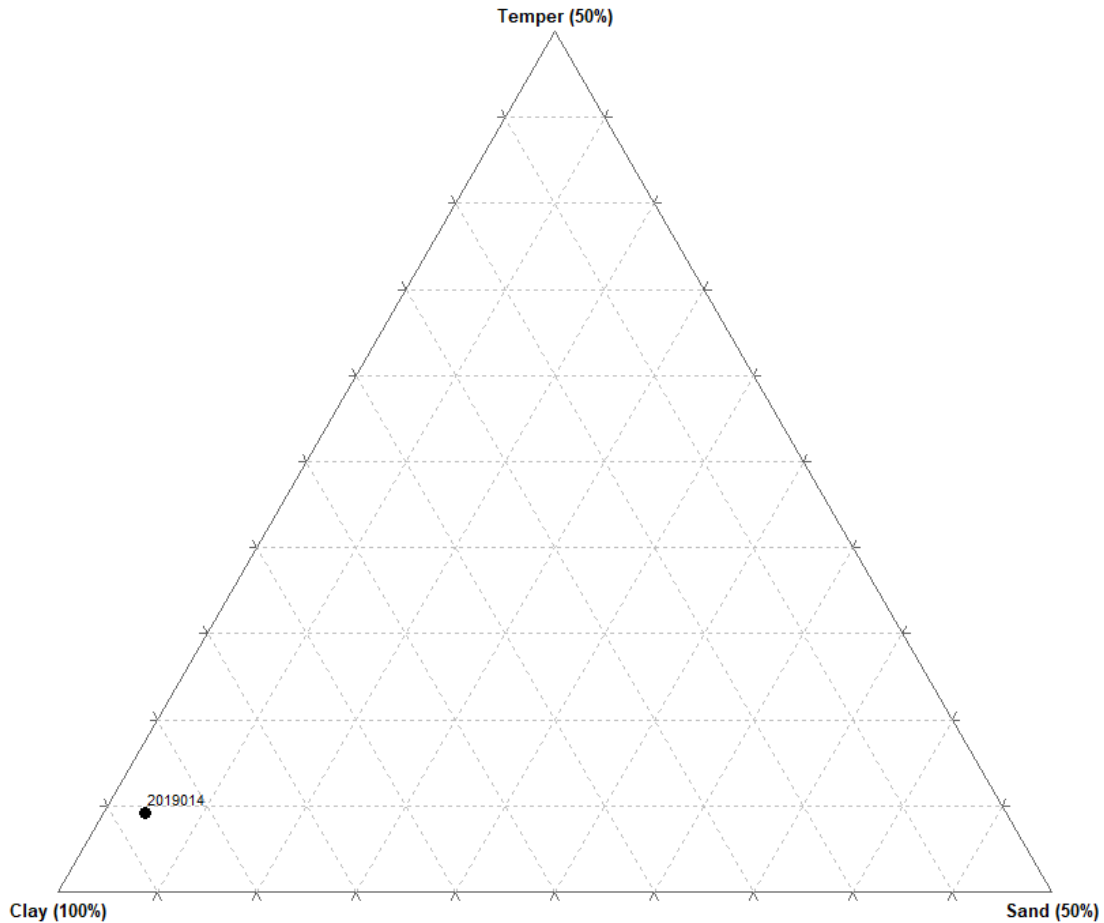


Figure 4.110 Ternary diagram of Sample 14 body composition.

### *Sample 15*

Petrographic analysis on Sample 15 identified 288 points in the natural paste categories. Of these, 275 were clay, eleven were silt, and two were sand. The overall percentages of the paste category are represented as 95.5% clay, 3.8% silt, and 0.7% sand (Figure 4.111). The sand particles were classed in the fine-grain size category; therefore, the sand-size index is 1.0.

The total number of points counted on the sample were used to calculate the body composition of the sample. A total of 299 points were counted on Sample 15. Of these, 286 were clay, eleven were temper, and two were sand. The overall percentages of the body categories are

95.7% clay, 3.7% temper, and 0.7% sand (Figure 4.112). Although grog was identified in the paste at a macro-level, all temper particles that were counted in the petrographic analysis were grit pieces. One grit piece was classed in the medium-grain size category, and ten were classed in the fine-grain size category. The temper-size index is calculated at 1.09.

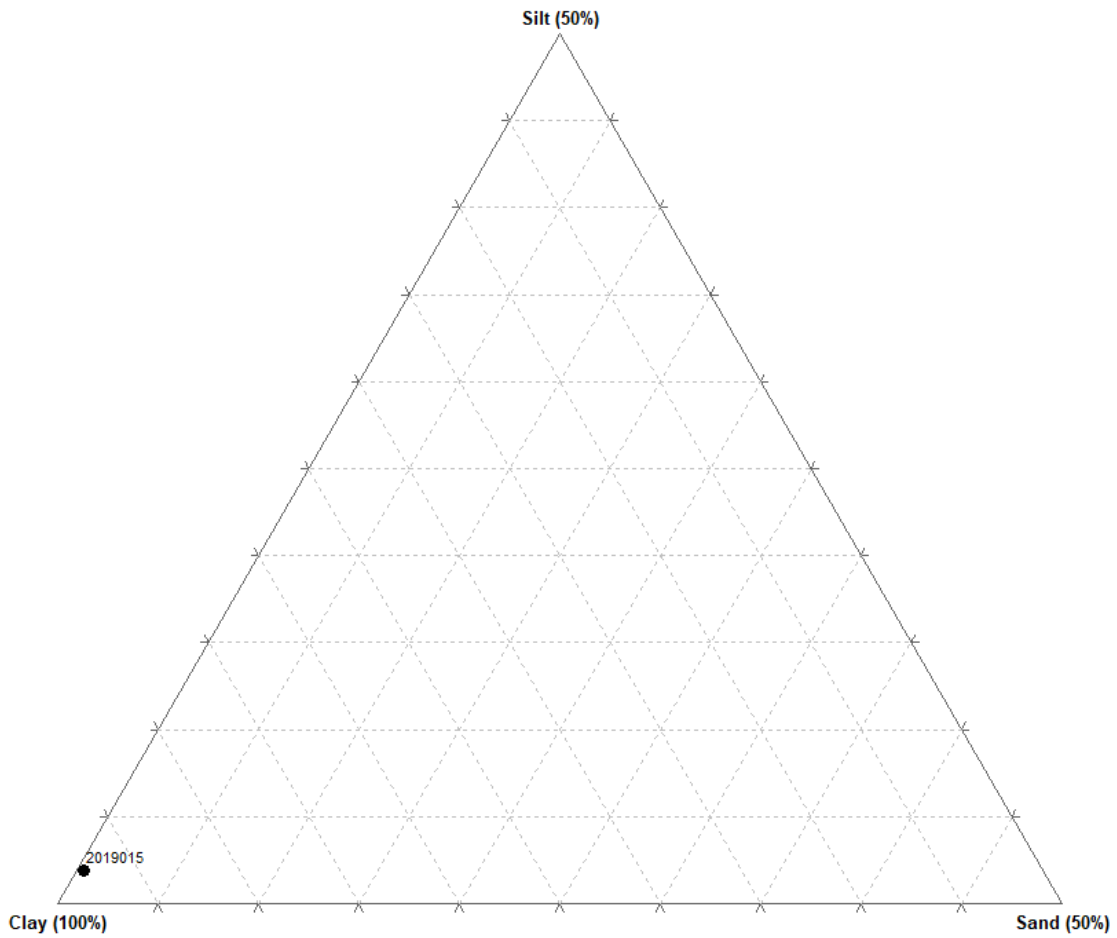


Figure 4.111 Ternary diagram of Sample 15 paste composition.

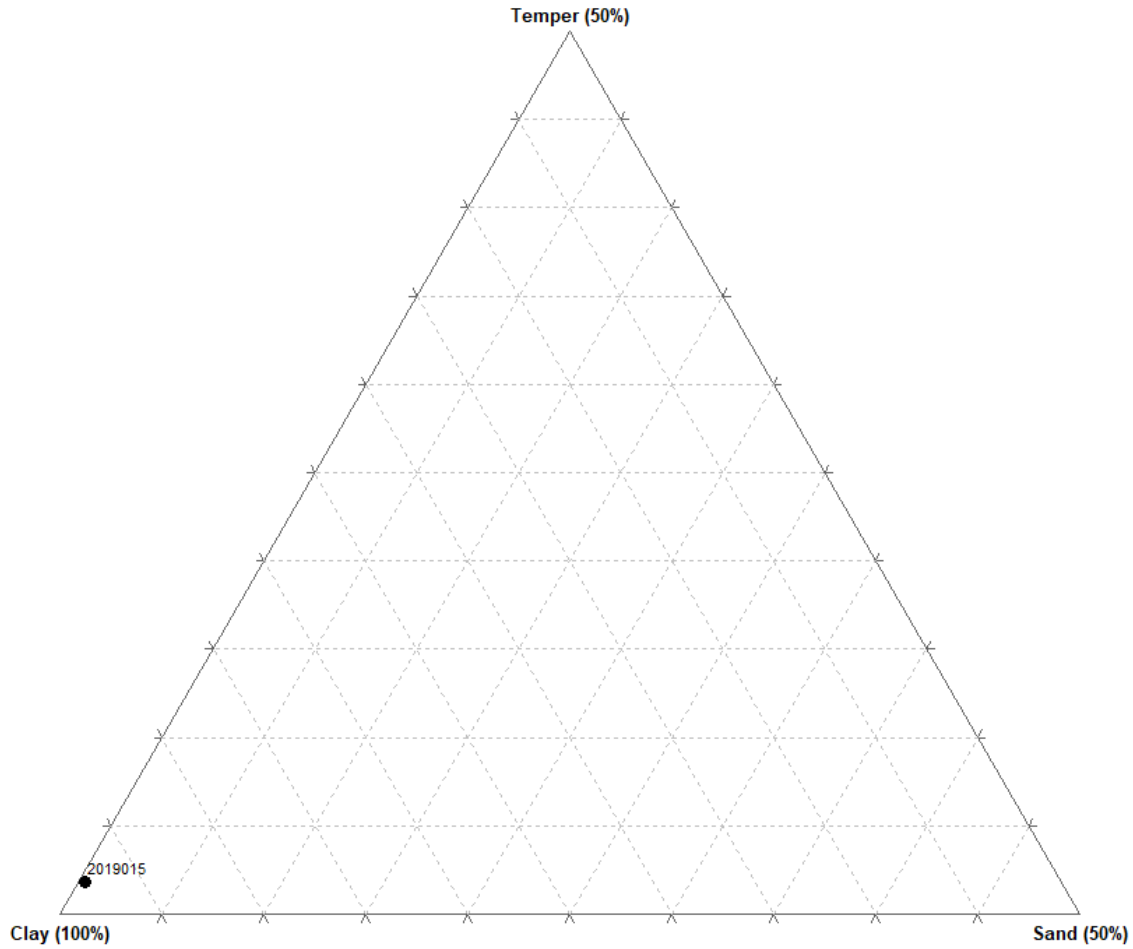


Figure 4.112 Ternary diagram of Sample 15 body composition.

### *Sample 16*

Petrographic analysis on Sample 16 identified 130 points in the natural paste categories. Of these, 107 were clay, twenty were silt, and three were sand. The overall percentages of the paste category are represented as 82.3% clay, 15.4% silt, and 2.3% sand (Figure 4.113). The sand particles were classed in the fine-grain size category; therefore, the sand-size index is 1.0.

The total number of points counted on the sample were used to calculate the body composition of the sample. A total of 140 points were counted on Sample 16. Of these, 127 were clay, ten were temper, and three were sand. The overall percentages of the body categories are

90.7% clay, 7.1% temper, and 2.1% sand (Figure 4.114). All temper particles were fine-size grit pieces. The temper-size index is 1.0.

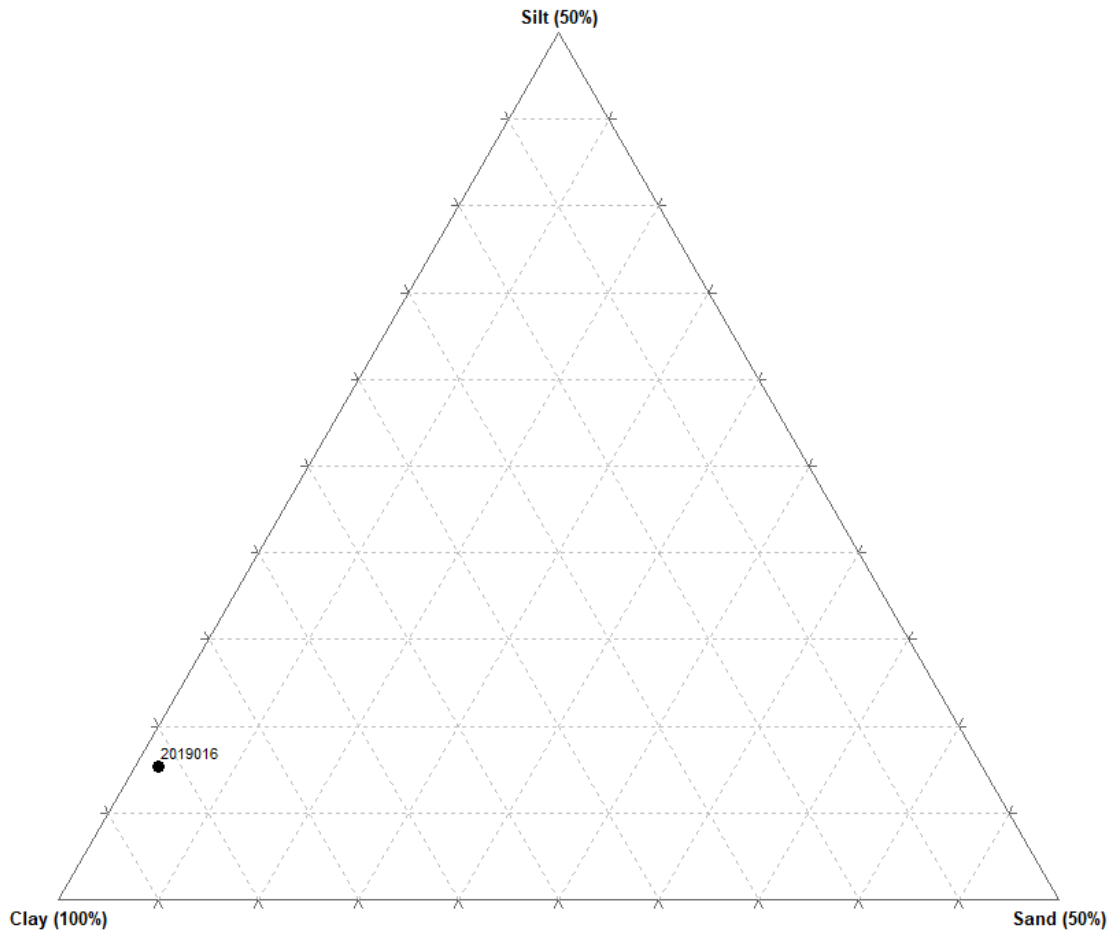


Figure 4.113 Ternary diagram of Sample 16 paste composition.

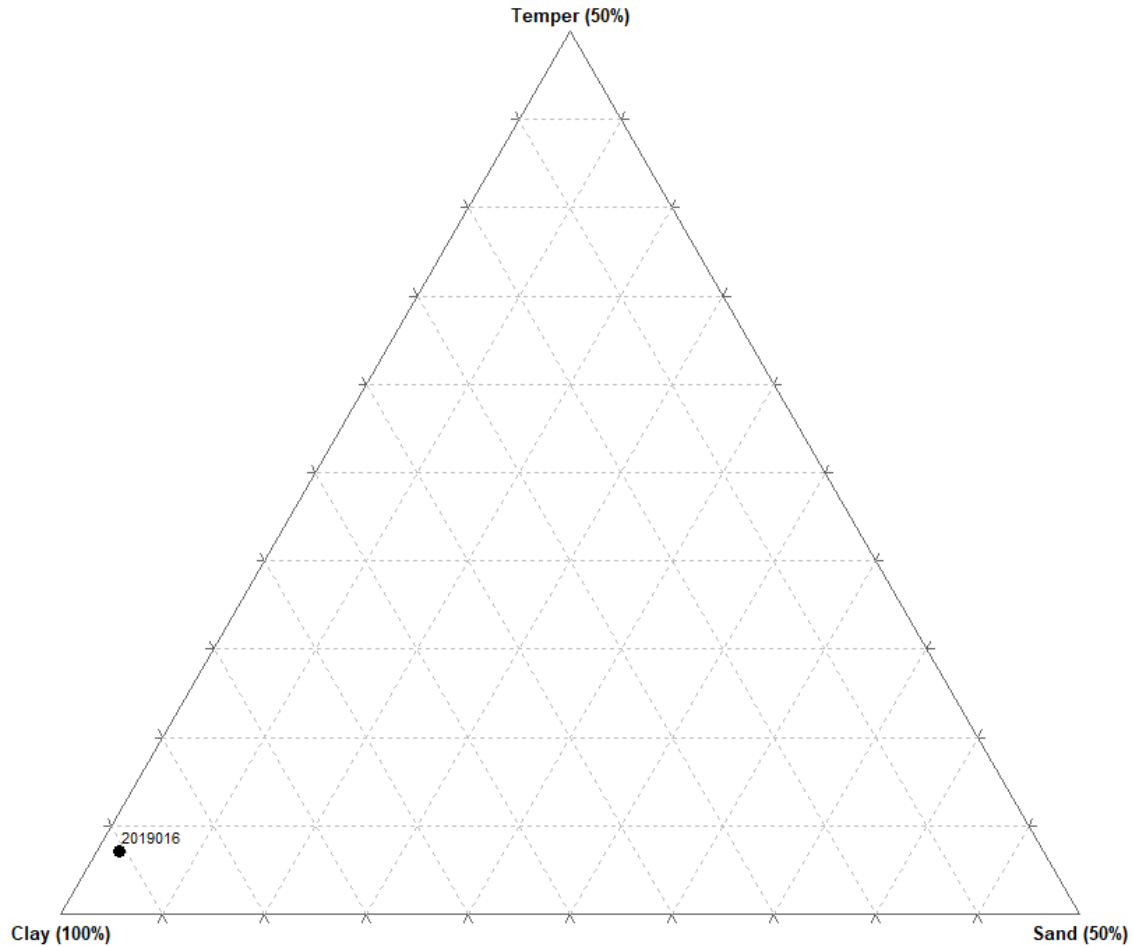


Figure 4.114 Ternary diagram of Sample 16 body composition.

### Sample 17

Petrographic analysis on Sample 17 identified 86 points in the natural paste categories. Of these, 77 were clay, seven were silt, and two were sand. The overall percentages of the paste category are represented as 89.5% clay, 8.1% silt, and 2.3% sand (Figure 4.115). The sand particles were classed in the fine-grain size category; therefore, the sand-size index is 1.0.

The total number of points counted on the sample were used to calculate the body composition of the sample. A total of 102 points were counted on Sample 17. Of these, eighty-four were clay, sixteen were temper, and two were sand. The overall percentages of the body

categories are 82.4% clay, 15.7% temper, and 1.9% sand (Figure 4.116). All temper particles were grit pieces. Two grit pieces were classed in the medium-grain size category, and fourteen were classed in the fine-grain size category. The temper-size index is calculated at 1.13.

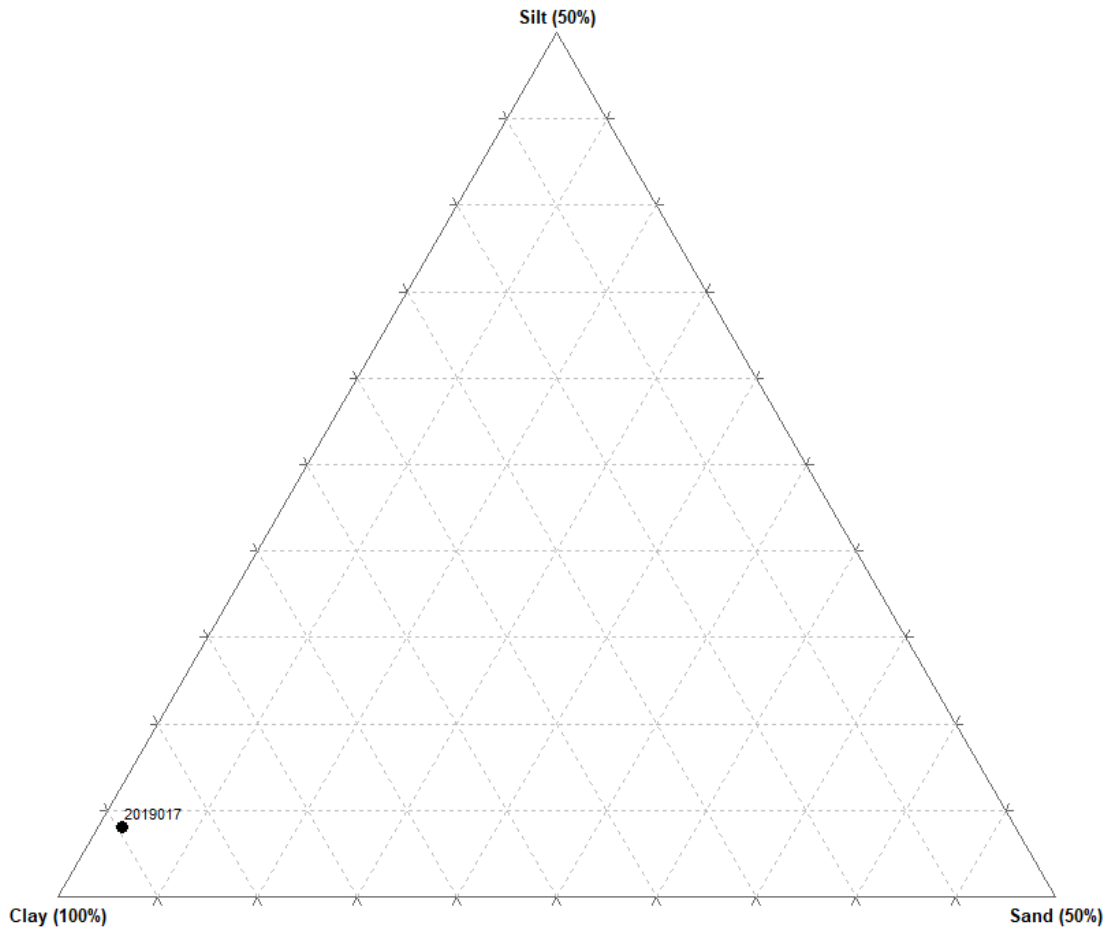


Figure 4.115 Ternary diagram of Sample 17 paste composition.



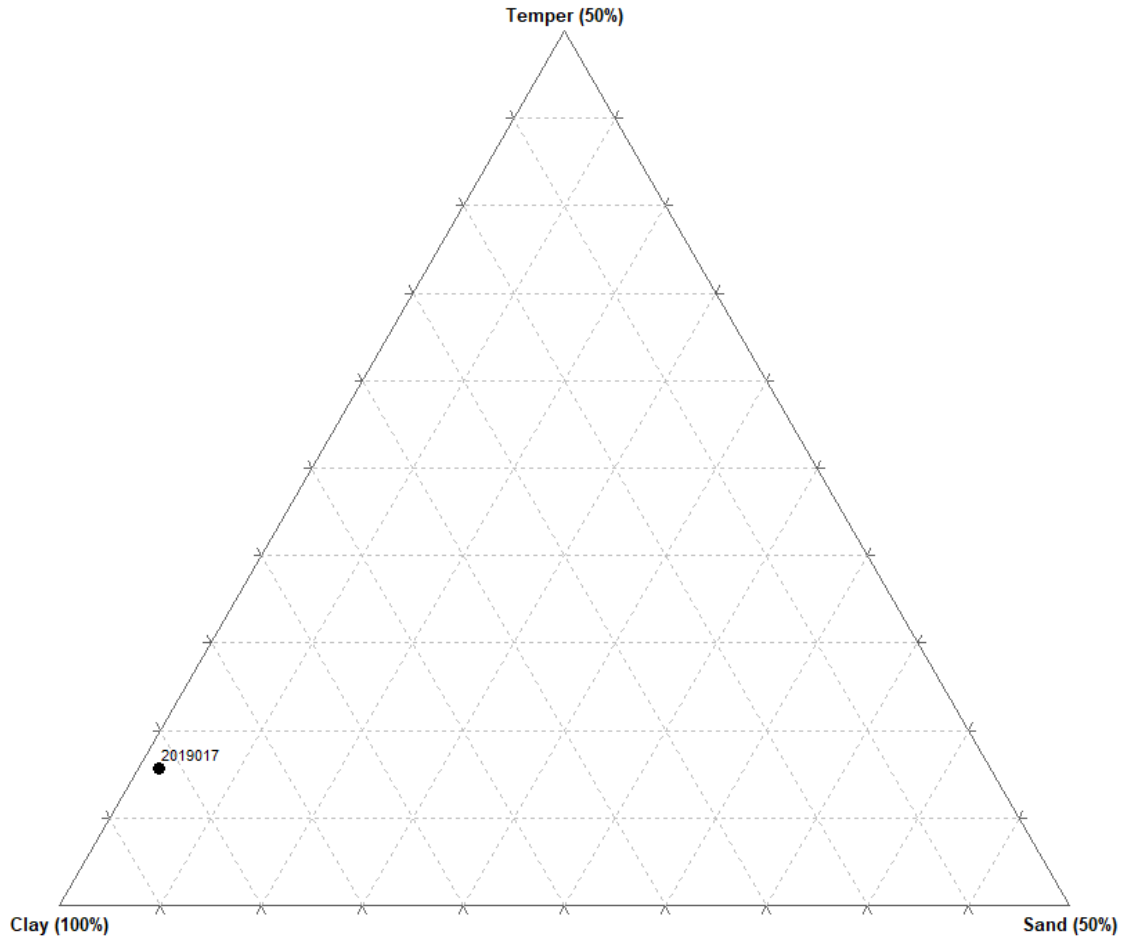


Figure 4.116 Ternary diagram of Sample 17 body composition.

### *Sample 18*

Petrographic analysis on Sample 18 identified 209 points in the natural paste categories. Of these, 165 were clay, thirty-nine were silt, and five were sand. The overall percentages of the paste category are represented as 78.9% clay, 18.7% silt, and 2.4% sand (Figure 4.117). Two sand particles were classed in the medium-grain size category and three sand particles were classed in the fine-grain size category; therefore, the sand-size index is 1.8.

The total number of points counted on the sample were used to calculate the body composition of the sample. A total of 221 points were counted on Sample 18. Of these, 204 were

clay, twelve were temper, and five were sand. The overall percentages of the body categories are 92.3% clay, 5.4% temper, and 2.3% sand (Figure 4.118). Two temper particles were grog pieces, ten temper particles were grit pieces. The grog pieces were classed in the fine-grain size category, one grit piece was classed in the medium-grain size category, and nine were classed in the fine-grain size category. The temper-size index is calculated at 1.3.

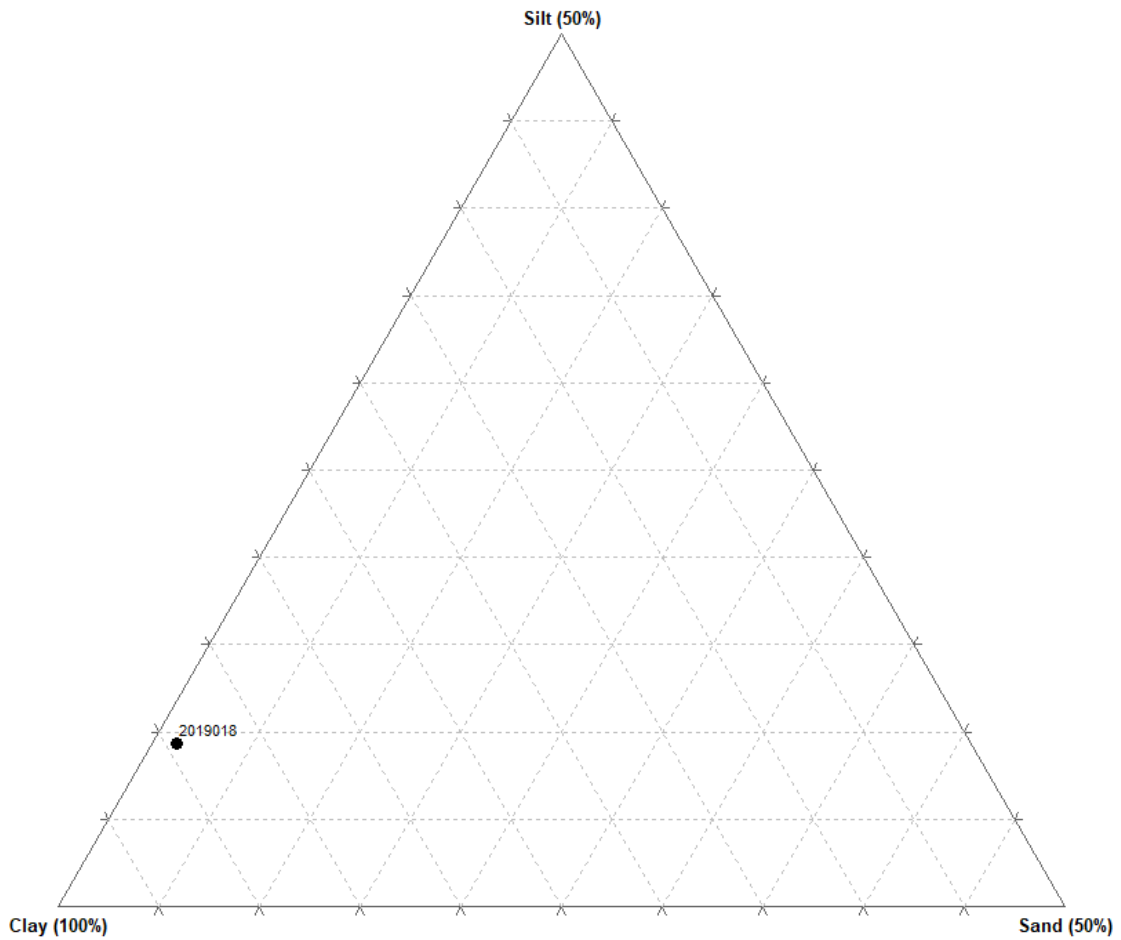


Figure 4.117 Ternary diagram of Sample 18 paste composition.

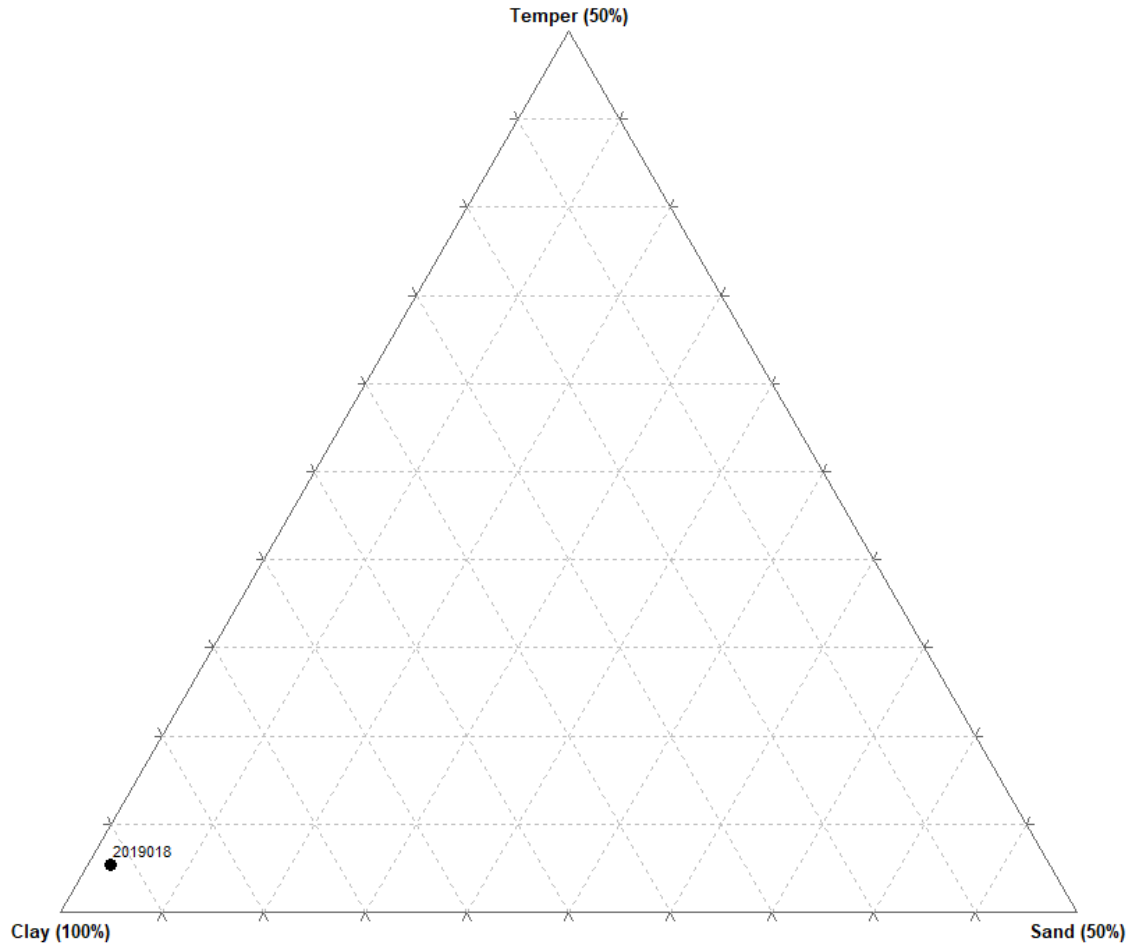


Figure 4.118 Ternary diagram of Sample 18 body composition.

### *Sample 19*

Petrographic analysis on Sample 19 identified 231 points in the natural paste categories. Of these, 190 were clay, thirty-five were silt, and six were sand. The overall percentages of the paste category are represented as 82.3% clay, 15.2% silt, and 2.6% sand (Figure 4.119). The sand particles were classed in the fine-grain size category; therefore, the sand-size index is 1.0.

The total number of points counted on the sample were used to calculate the body composition of the sample. A total of 265 points were counted on Sample 19. Of these, 225 were clay, thirty-four were temper, and six were sand. The overall percentages of the body categories

are 84.9% clay, 12.8% temper, and 2.3% sand (Figure 4.120). All temper particles were fine-size grit pieces. The temper-size index is 1.0.

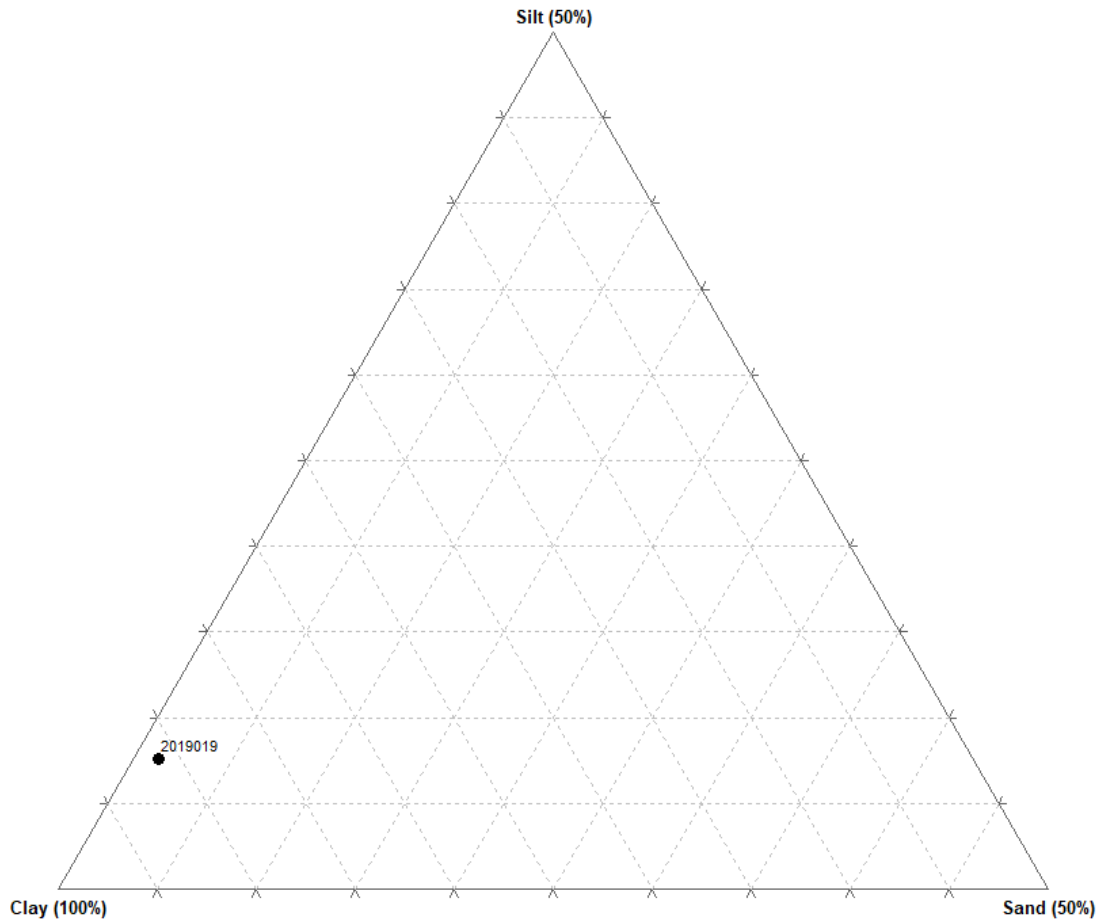


Figure 4.119 Ternary diagram of Sample 19 paste composition.

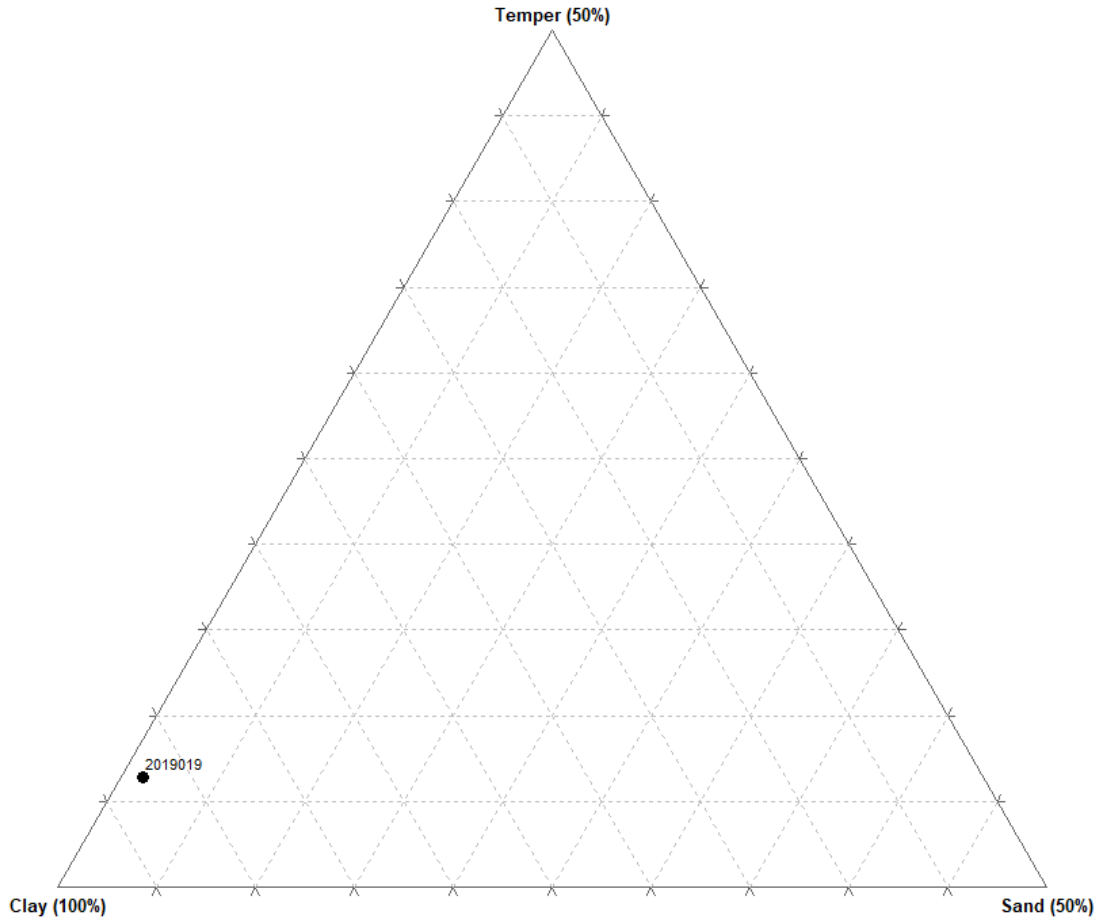


Figure 4.120 Ternary diagram of Sample 19 body composition.

**Sample 20**

Petrographic analysis on Sample 20 identified 251 points in the natural paste categories. Of these, 235 were clay, eleven were silt, and five were sand. The overall percentages of the paste category are represented as 93.6% clay, 4.4% silt, and 2.0% sand (Figure 4.121). The sand particles were classed in the fine-grain size category; therefore, the sand-size index is 1.0.

The total number of points counted on the sample were used to calculate the body composition of the sample. A total of 283 points were counted on Sample 20. Of these, 246 were clay, thirty-two were temper, and five were sand. The overall percentages of the body categories

are 86.9% clay, 11.3% temper, and 1.8% sand (Figure 4.122). Three temper particles were grog pieces, twenty-nine temper particles were grit pieces. The grog pieces were classed in the fine-grain size category, two grit pieces were classed in the medium-grain size category, and twenty-seven were classed in the fine-grain size category. The temper-size index is calculated at 1.17.

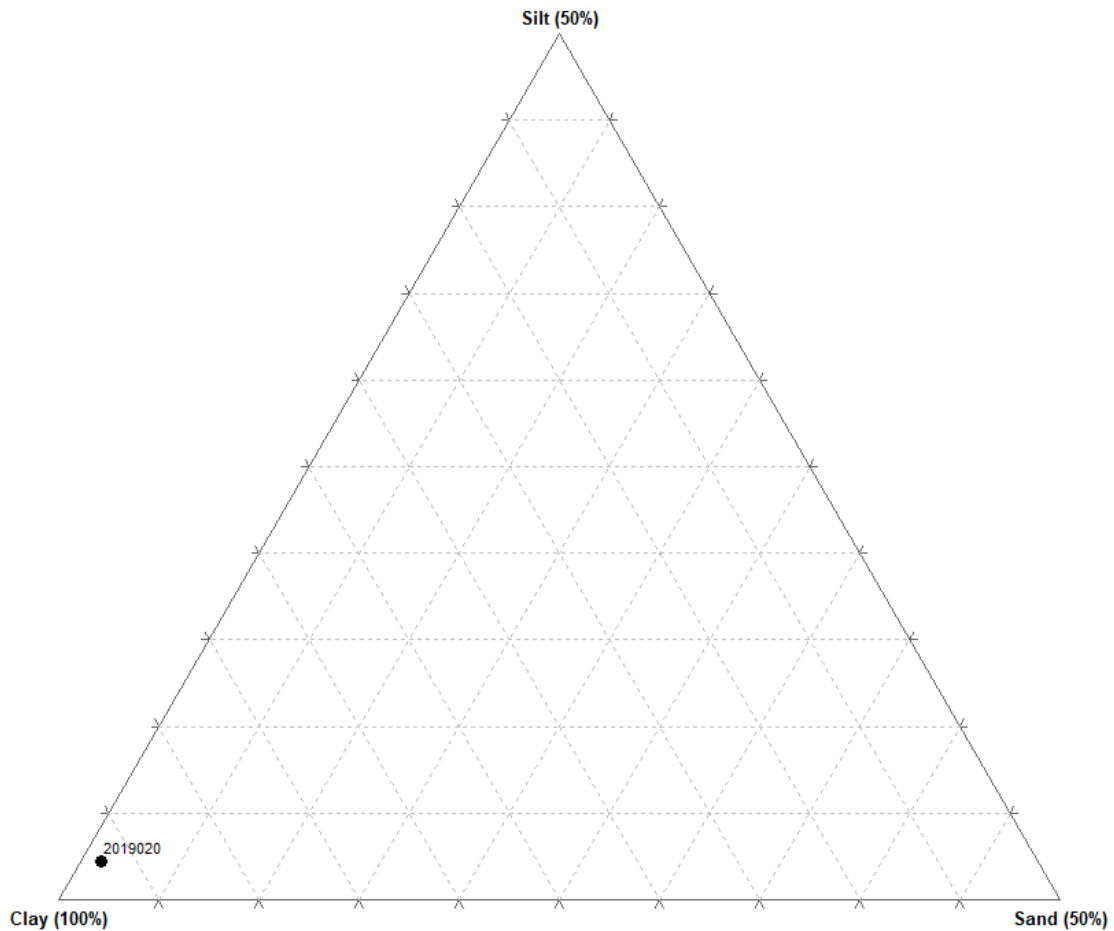


Figure 4.121 Ternary diagram of Sample 20 paste composition.

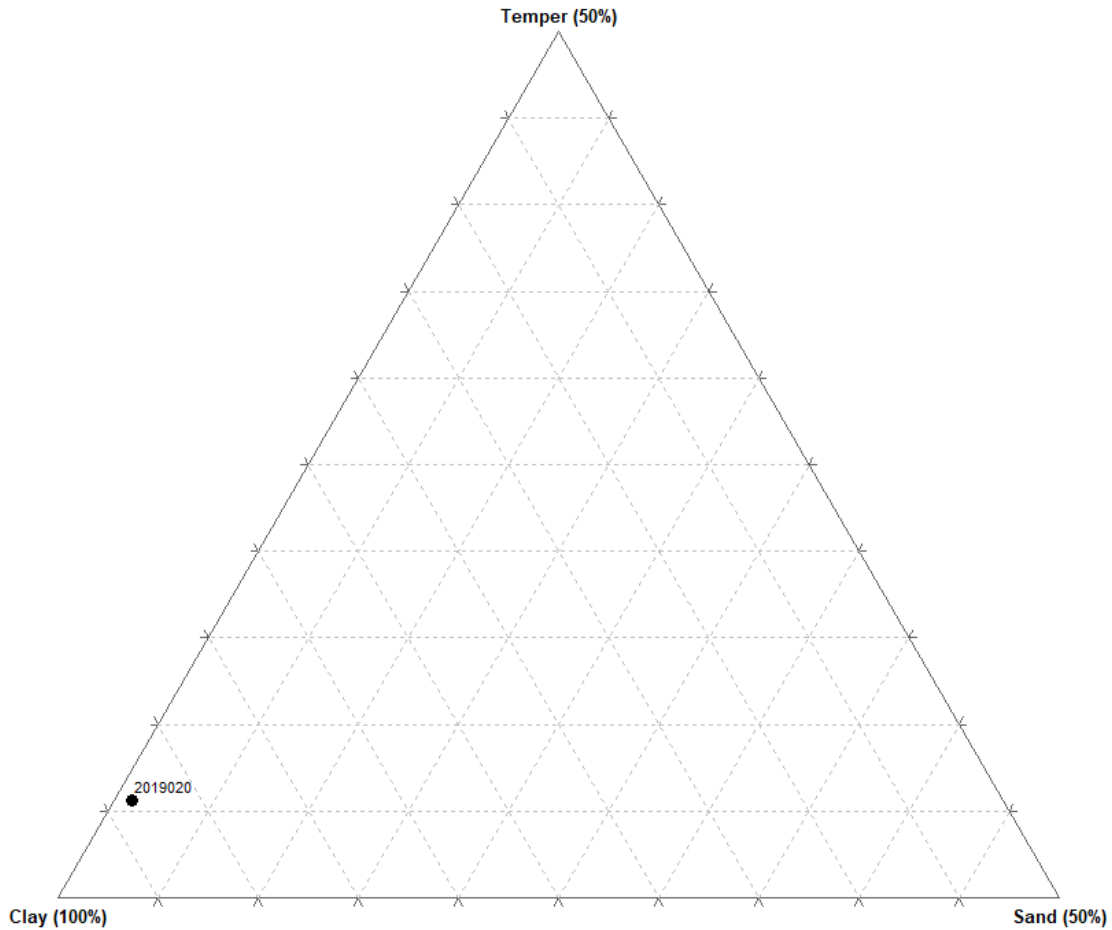


Figure 4.122 Ternary diagram of Sample 20 body composition.

### Sample 21

Petrographic analysis on Sample 21 identified 235 points in the natural paste categories. Of these, 227 were clay, six were silt, and two were sand. The overall percentages of the paste category are represented as 96.6% clay, 2.6% silt, and 0.9% sand (Figure 4.123). The sand particles were classed in the fine-grain size category; therefore, the sand-size index is 1.0.

The total number of points counted on the sample were used to calculate the body composition of the sample. A total of 249 points were counted on Sample 21. Of these, 233 were clay, fourteen were temper, and two were sand. The overall percentages of the body categories

are 93.6% clay, 5.6% temper, and 0.8% sand (Figure 4.124). All temper particles were fine-size grit pieces. The temper-size index is 1.0.

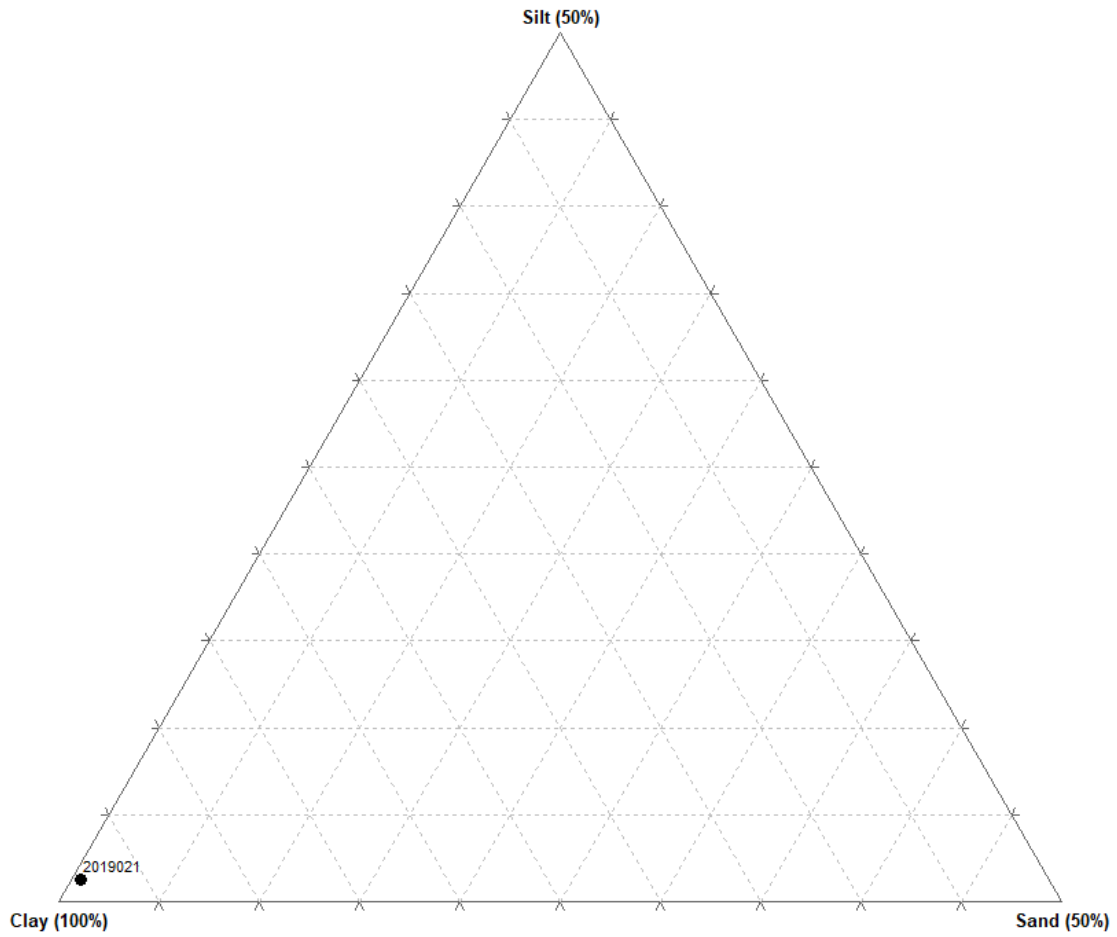


Figure 4.123 Ternary diagram of Sample 21 paste composition.



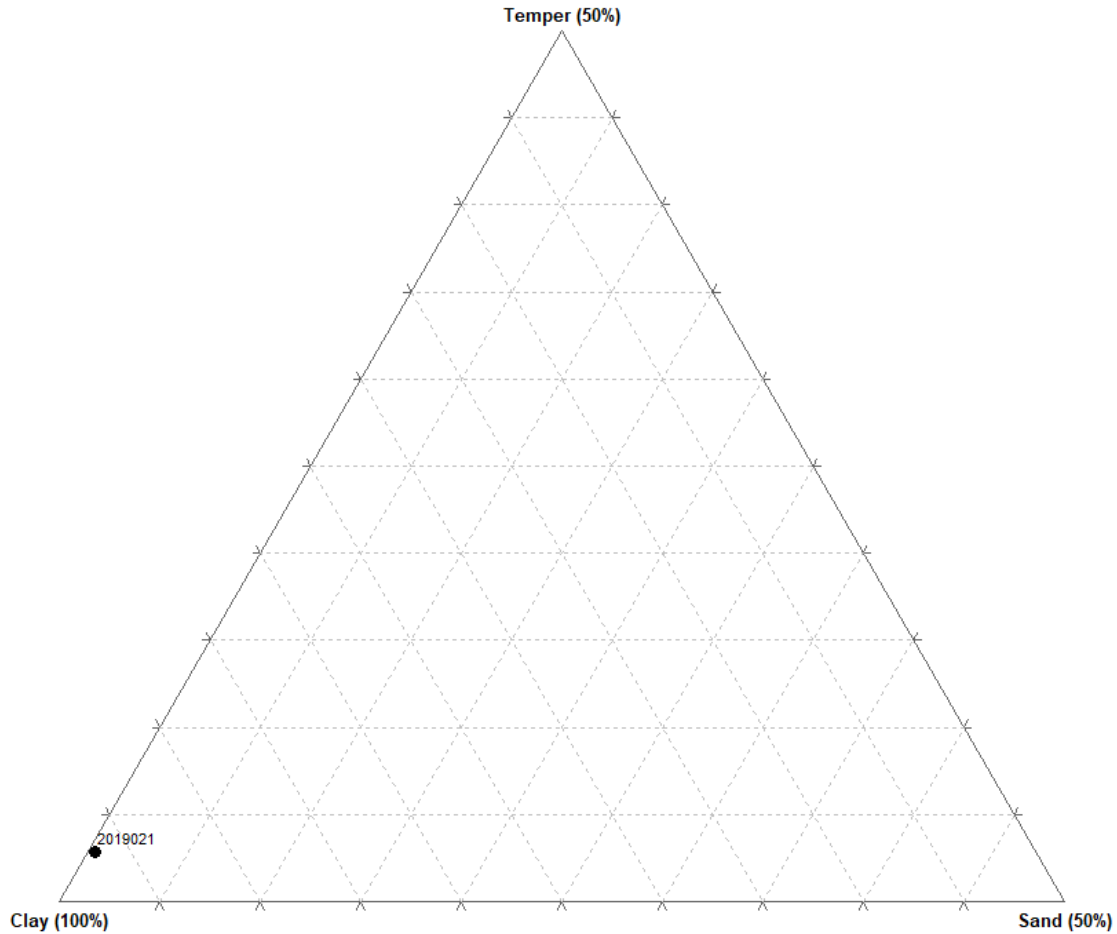


Figure 4.124 Ternary diagram of Sample 21 body composition.

### Sample 22

Petrographic analysis on Sample 22 identified 162 points in the natural paste categories. Of these, 135 were clay, twenty were silt, and seven were sand. The overall percentages of the paste category are represented as 83.3% clay, 12.3% silt, and 4.3% sand (Figure 4.125). The sand particles were classed in the fine-grain size category; therefore, the sand-size index is 1.0.

The total number of points counted on the sample were used to calculate the body composition of the sample. A total of 177 points were counted on Sample 22. Of these, 155 were clay, fifteen were temper, and seven were sand. The overall percentages of the body categories

are 87.6% clay, 8.5% temper, and 3.9% sand (Figure 4.126). All temper particles were grit pieces. One grit piece was classed in the medium-grain size category, and fourteen were classed in the fine-grain size category. The temper-size index is calculated at 1.07.

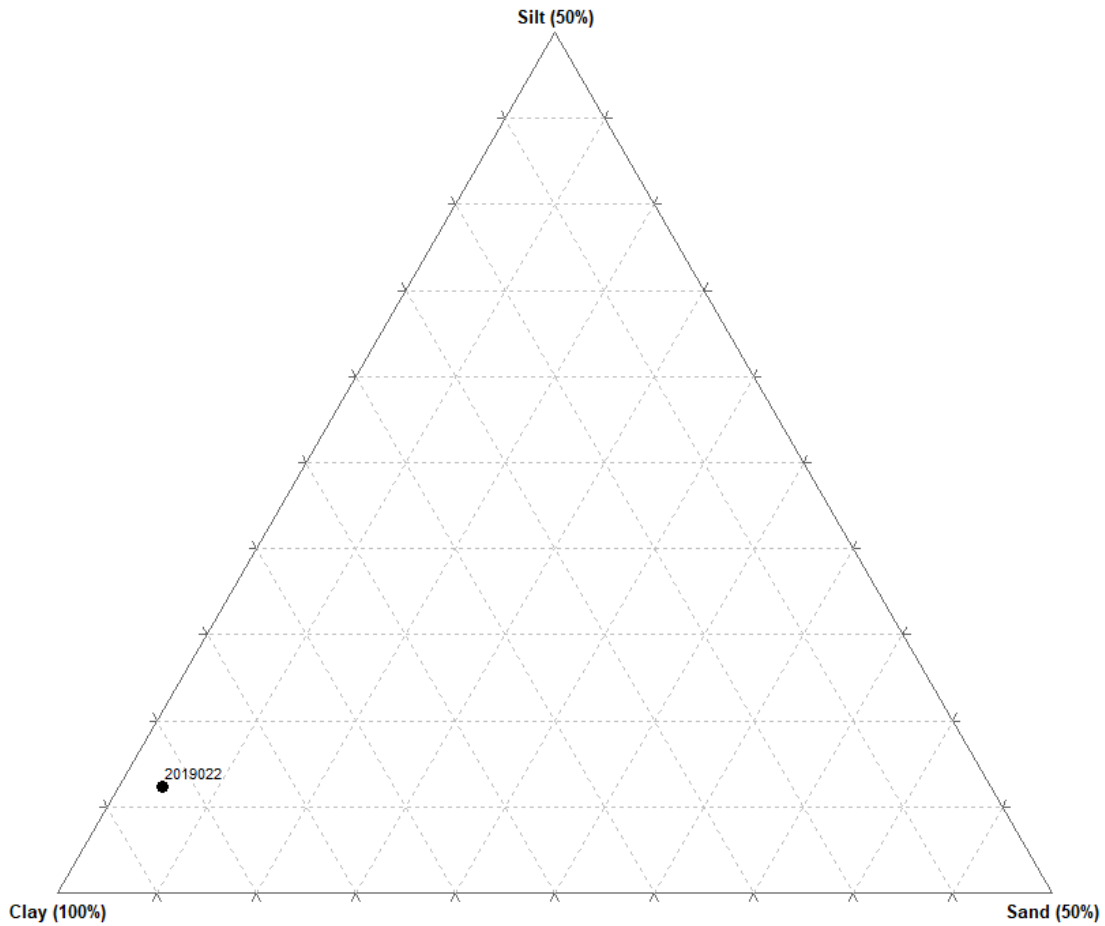


Figure 4.125 Ternary diagram of Sample 22 paste composition.

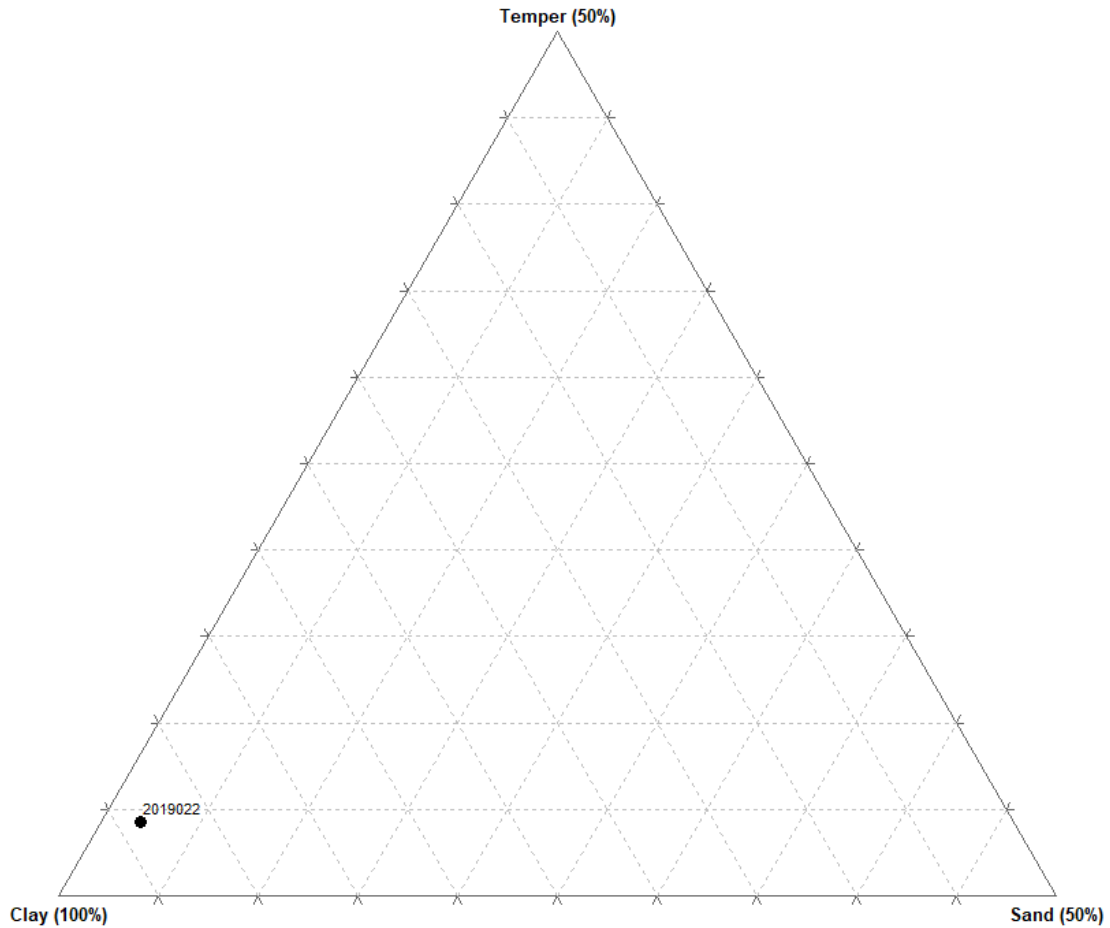


Figure 4.126 Ternary diagram of Sample 22 body composition.

### Sample 23

Petrographic analysis on Sample 23 identified 131 points in the natural paste categories. Of these, 123 were clay, eight were silt, and no natural particles were in the sand-sized category. The overall percentages of the paste category are represented as 93.9% clay and 6.1% silt (Figure 4.127). As there were no minerals in the sand-size category, the sand-size index was not calculated.

The total number of points counted on the sample were used to calculate the body composition of the sample. A total of 154 points were counted on Sample 23. Of these, 131 were

clay and twenty-three were temper. The overall percentages of the body categories are 85.1% clay and 14.9% temper (Figure 4.128). All temper particles were grit pieces. Six grit pieces were classed in the medium-grain size category, and seventeen were classed in the fine-grain size category. The temper-size index is calculated at 1.26.

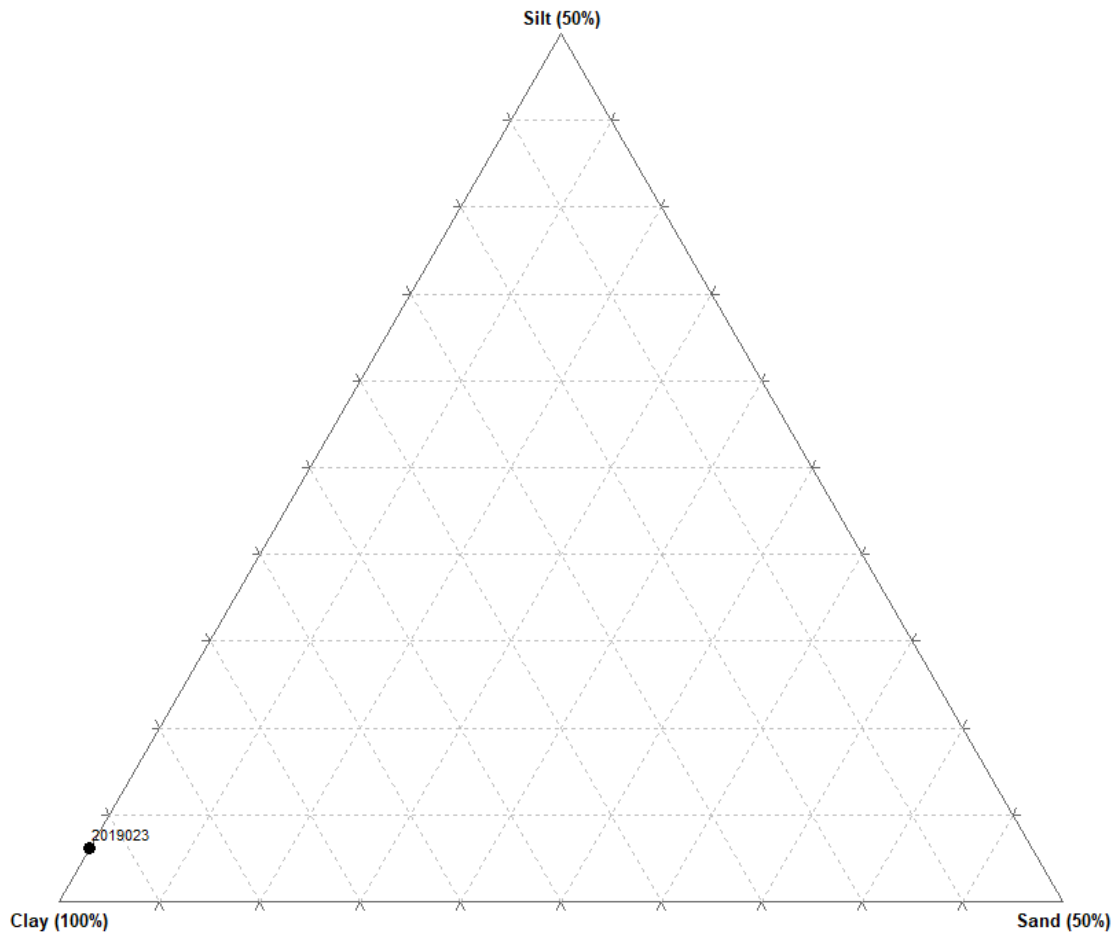


Figure 4.127 Ternary diagram of Sample 23 paste composition.

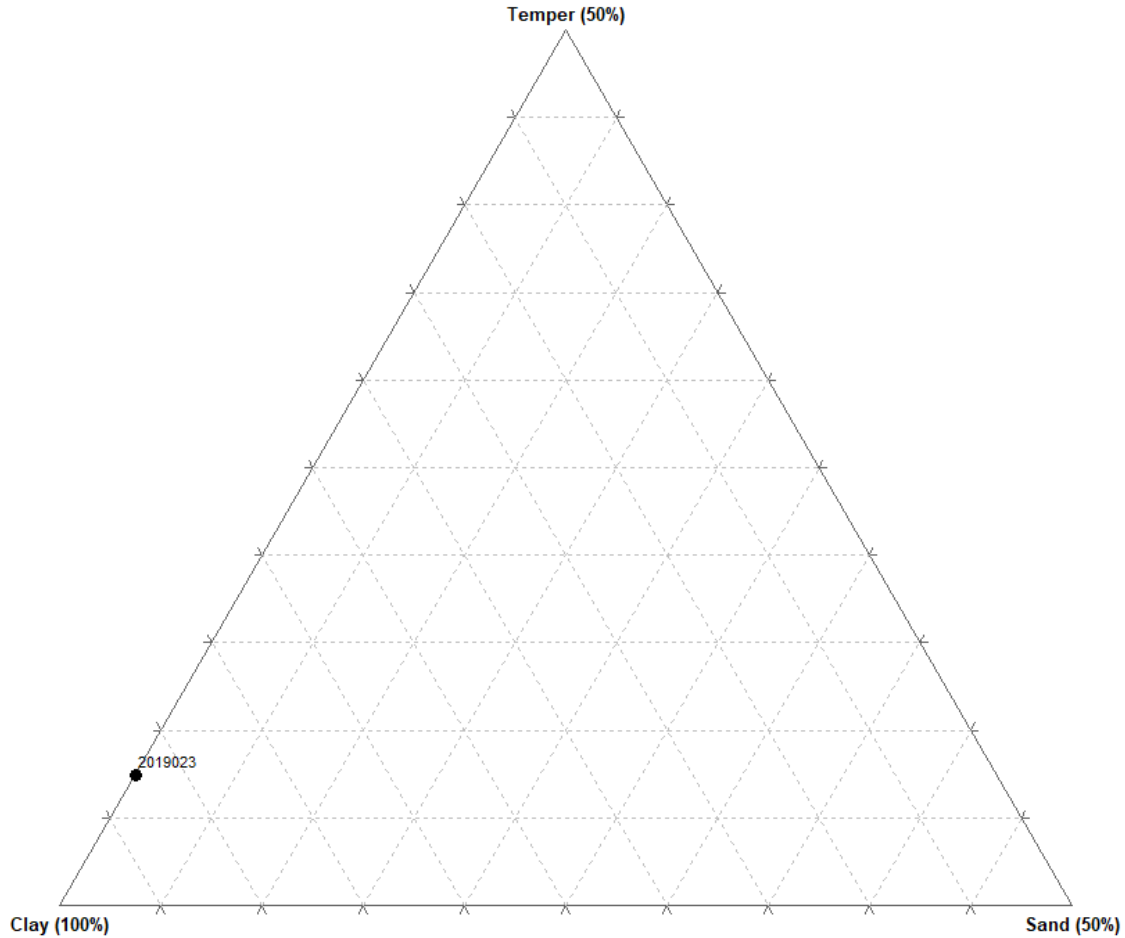


Figure 4.128 Ternary diagram of Sample 23 body composition.

### *Sample 24*

Petrographic analysis on Sample 24 identified 316 points in the natural paste categories. Of these, 246 were clay, sixty-six were silt, and four were sand. The overall percentages of the paste category are represented as 77.8% clay, 20.9% silt, and 1.3% sand (Figure 4.129). The sand particles were classed in the fine-grain size category; therefore, the sand-size index is 1.0.

The total number of points counted on the sample were used to calculate the body composition of the sample. A total of 330 points were counted on Sample 24. Of these, 312 were clay, fourteen were temper, and four were sand. The overall percentages of the body categories

are 94.5% clay, 4.2% temper, and 1.2% sand (Figure 4.130). All temper particles were grit pieces. Two grit pieces were classed in the medium-grain size category, and twelve were classed in the fine-grain size category. The temper-size index is calculated at 1.14.

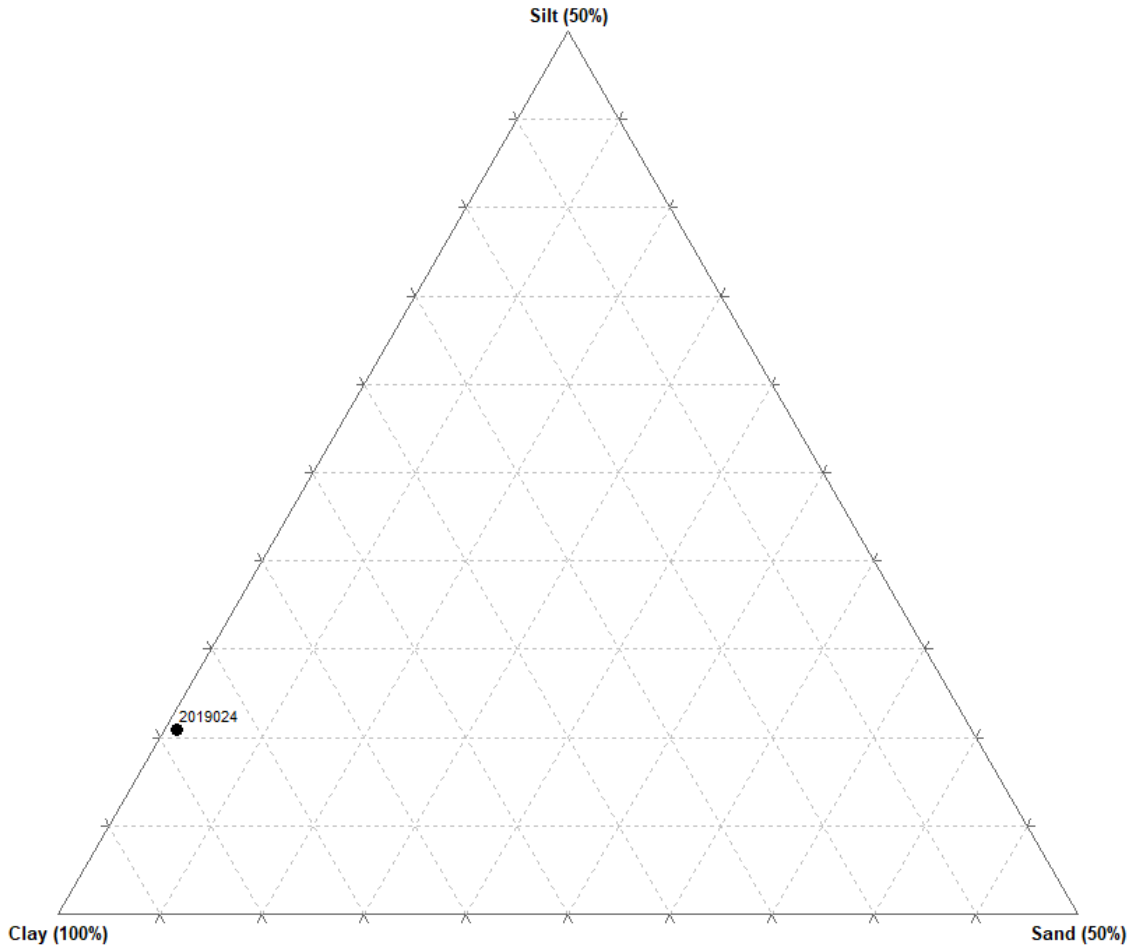


Figure 4.129 Ternary diagram of Sample 24 paste composition.

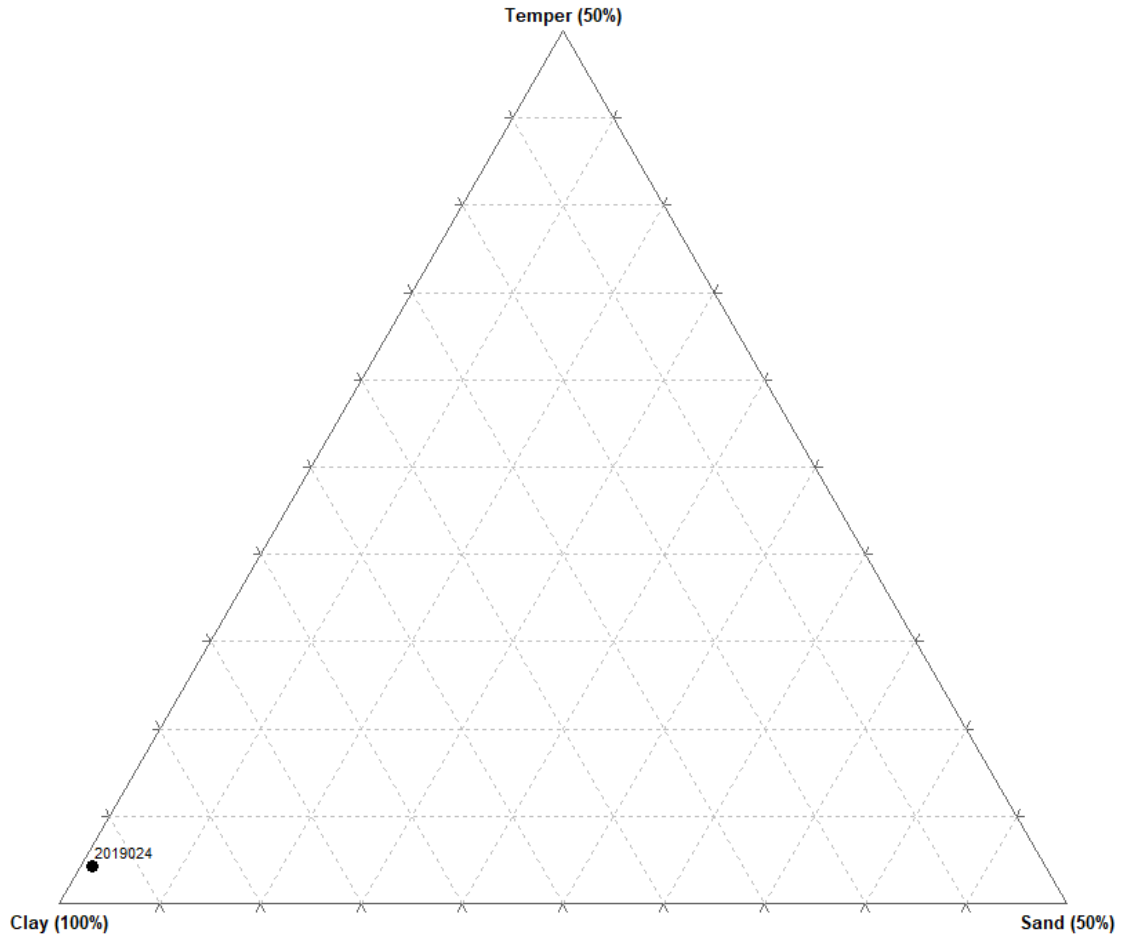


Figure 4.130 Ternary diagram of Sample 24 body composition.

**Sample 25**

Petrographic analysis on Sample 25 identified 111 points in the natural paste categories. Of these, ninety-three were clay, fifteen were silt, and three were sand. The overall percentages of the paste category are represented as 83.8% clay, 13.5% silt, and 2.7% sand (Figure 4.131). One sand particle was classed in the medium-grain size category and two sand particles were classed in the fine-grain size category; therefore, the sand-size index is 1.67.

The total number of points counted on the sample were used to calculate the body composition of the sample. A total of 118 points were counted on Sample 25. Of these, 108 were

clay, seven were temper, and three were sand. The overall percentages of the body categories are 91.5% clay, 5.9% temper, and 2.5% sand (Figure 4.132). All temper particles were grit pieces. All temper particles were fine-size grit pieces. The temper-size index is 1.0.

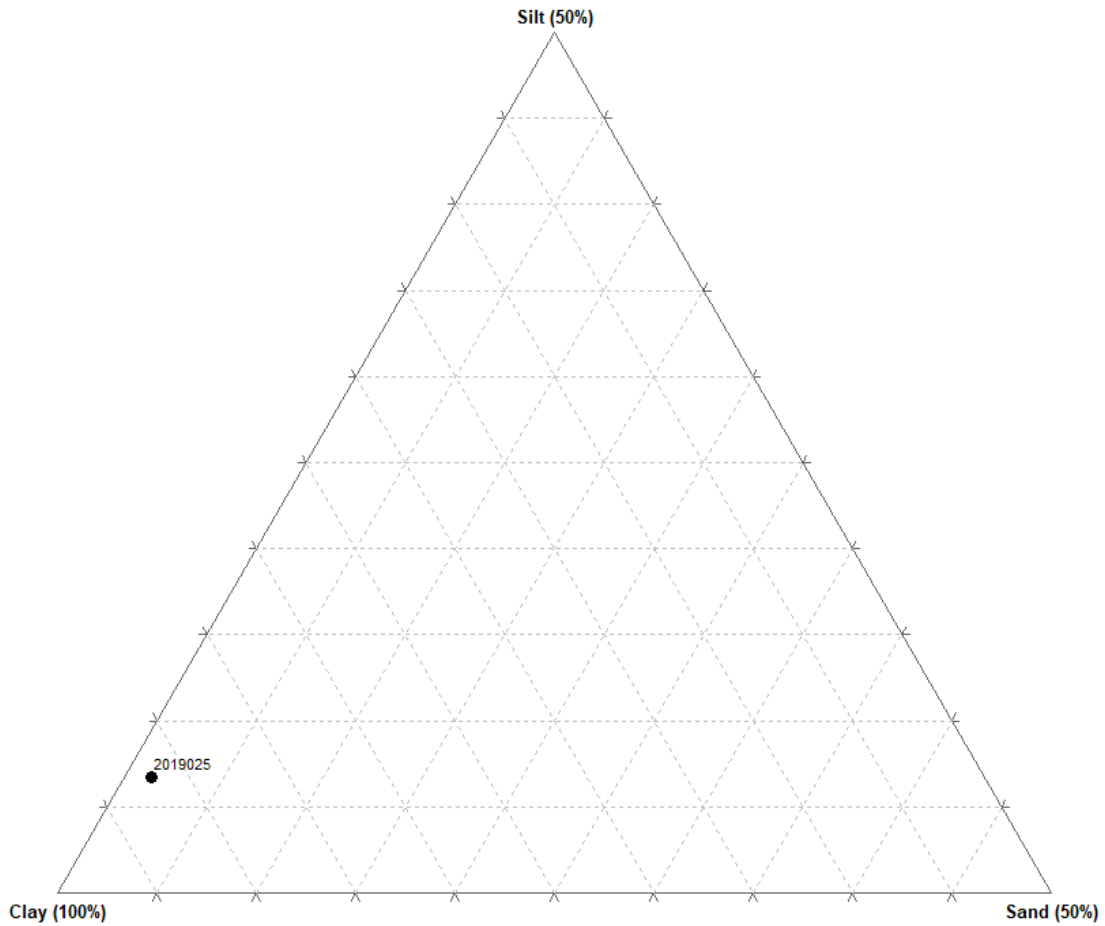


Figure 4.131 Ternary diagram of Sample 25 paste composition.



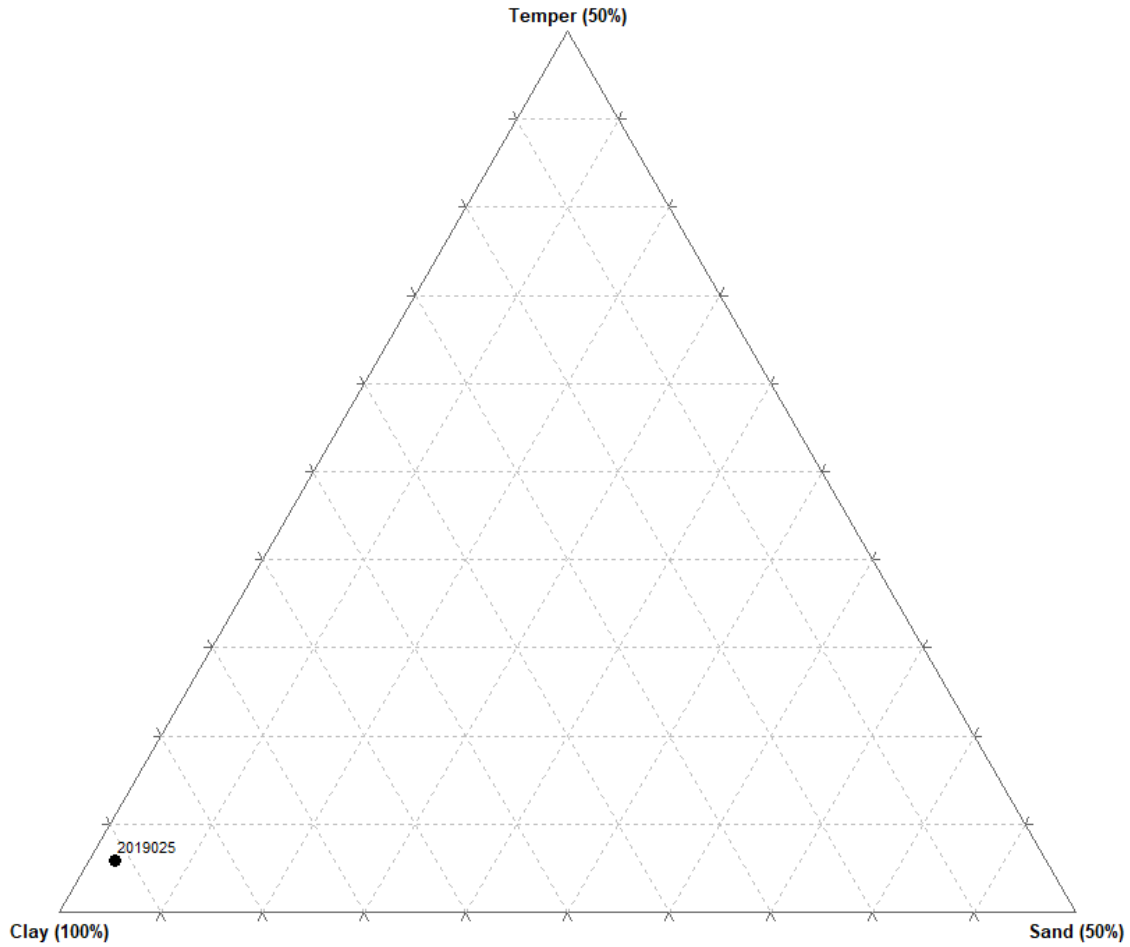


Figure 4.132 Ternary diagram of Sample 25 body composition.

### *Sample 26*

Petrographic analysis on Sample 26 identified 190 points in the natural paste categories. Of these, 130 were clay, fifty-four were silt, and six were sand. The overall percentages of the paste category are represented as 68.4% clay, 28.4% silt, and 3.2% sand (Figure 4.133). One sand particle was classed in the medium-grain size category and three sand particles were classed in the fine-grain size category; therefore, the sand-size index is 1.33.

The total number of points counted on the sample were used to calculate the body composition of the sample. A total of 195 points were counted on Sample 26. Of these, 184 were

clay, five were temper, and six were sand. The overall percentages of the body categories are 94.4% clay, 2.6% temper, and 3.0% sand (Figure 4.134). All temper particles were grit pieces. All temper particles were fine-size grit pieces. The temper-size index is 1.0.

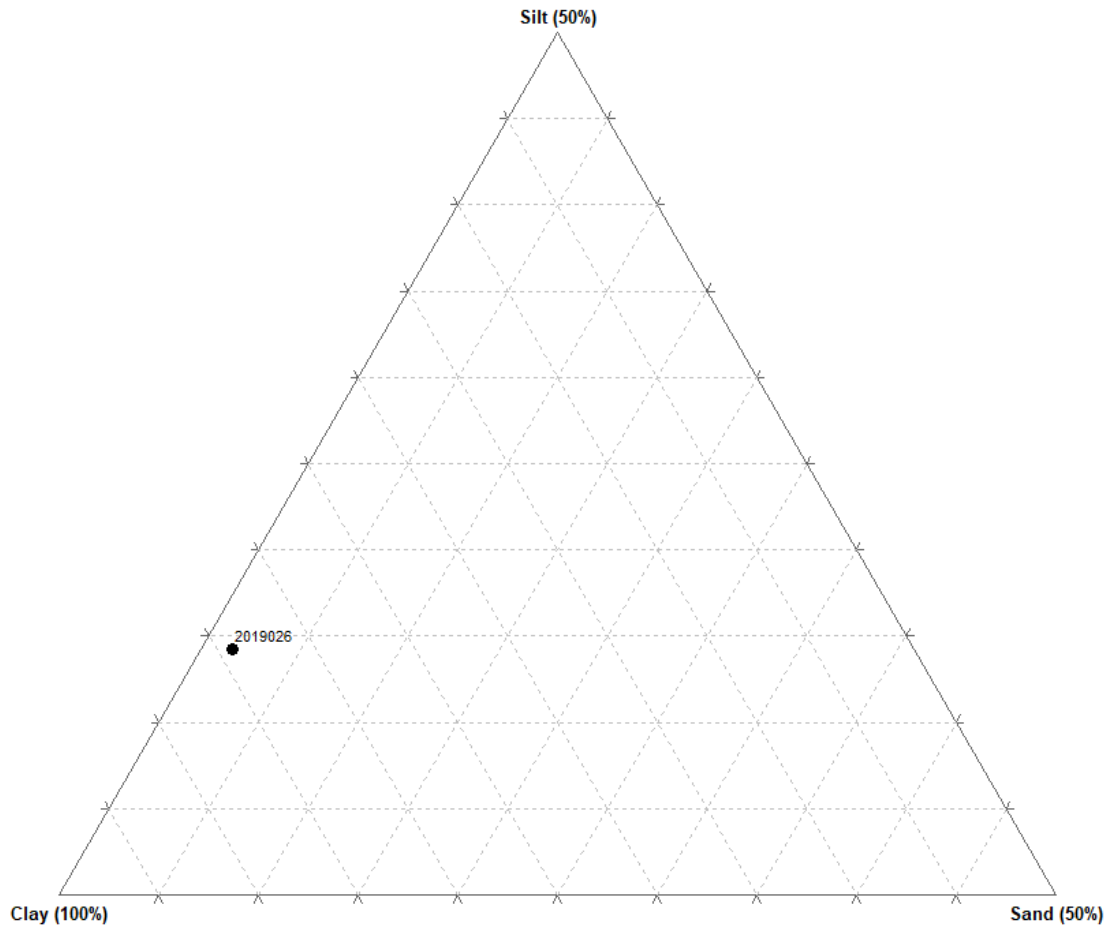


Figure 4.133 Ternary diagram of Sample 26 paste composition.

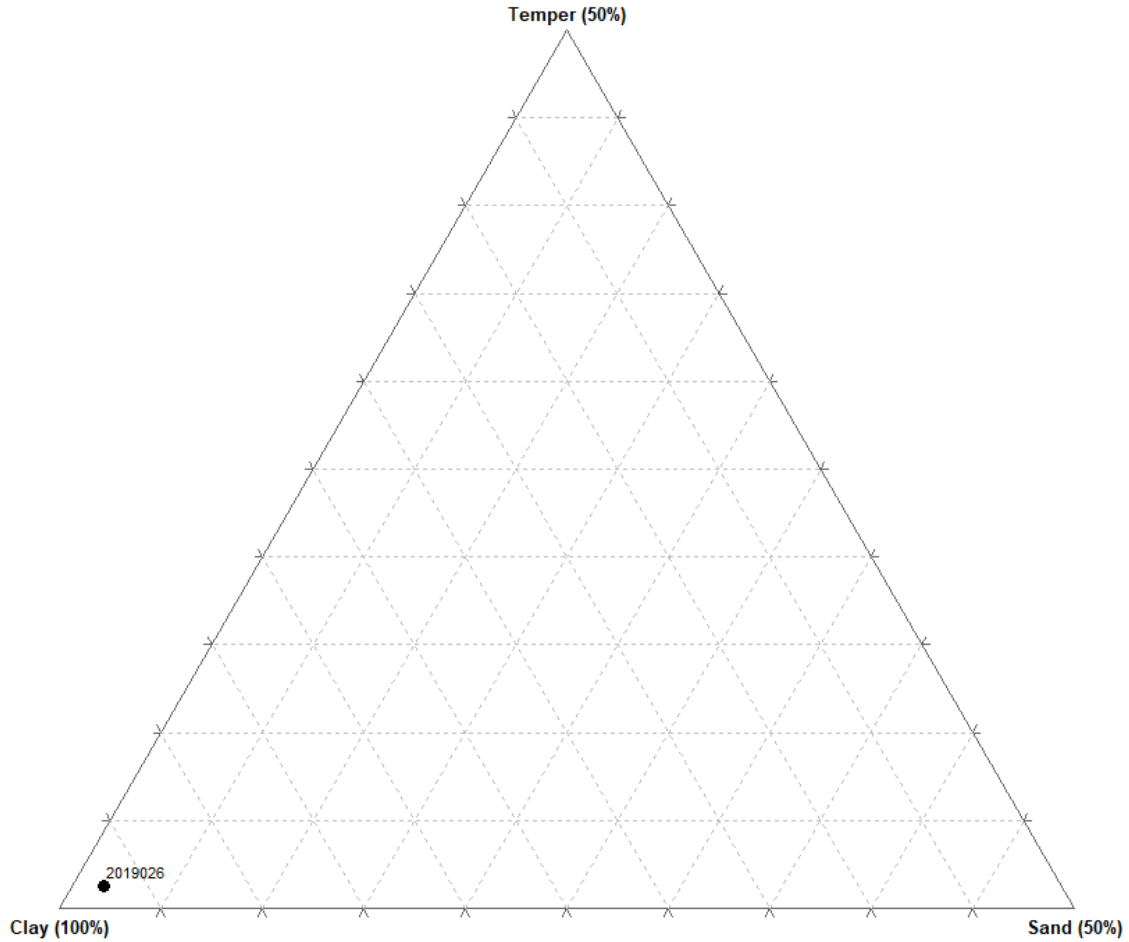


Figure 4.134 Ternary diagram of Sample 26 body composition.

**Sample 27**

Petrographic analysis on Sample 27 identified 174 points in the natural paste categories. Of these, 156 were clay, fourteen were silt, and four were sand. The overall percentages of the paste category are represented as 89.7% clay, 8.0% silt, and 2.3% sand (Figure 4.135). The sand particles were classed in the fine-grain size category; therefore, the sand-size index is 1.0.

The total number of points counted on the sample were used to calculate the body composition of the sample. A total of 205 points were counted on Sample 27. Of these, 170 were clay, thirty-one were temper, and four were sand. The overall percentages of the body categories

are 82.9% clay, 15.1% temper, and 2.0% sand (Figure 4.136). All temper particles were grit pieces. All temper particles were fine-size grit pieces. The temper-size index is 1.0.

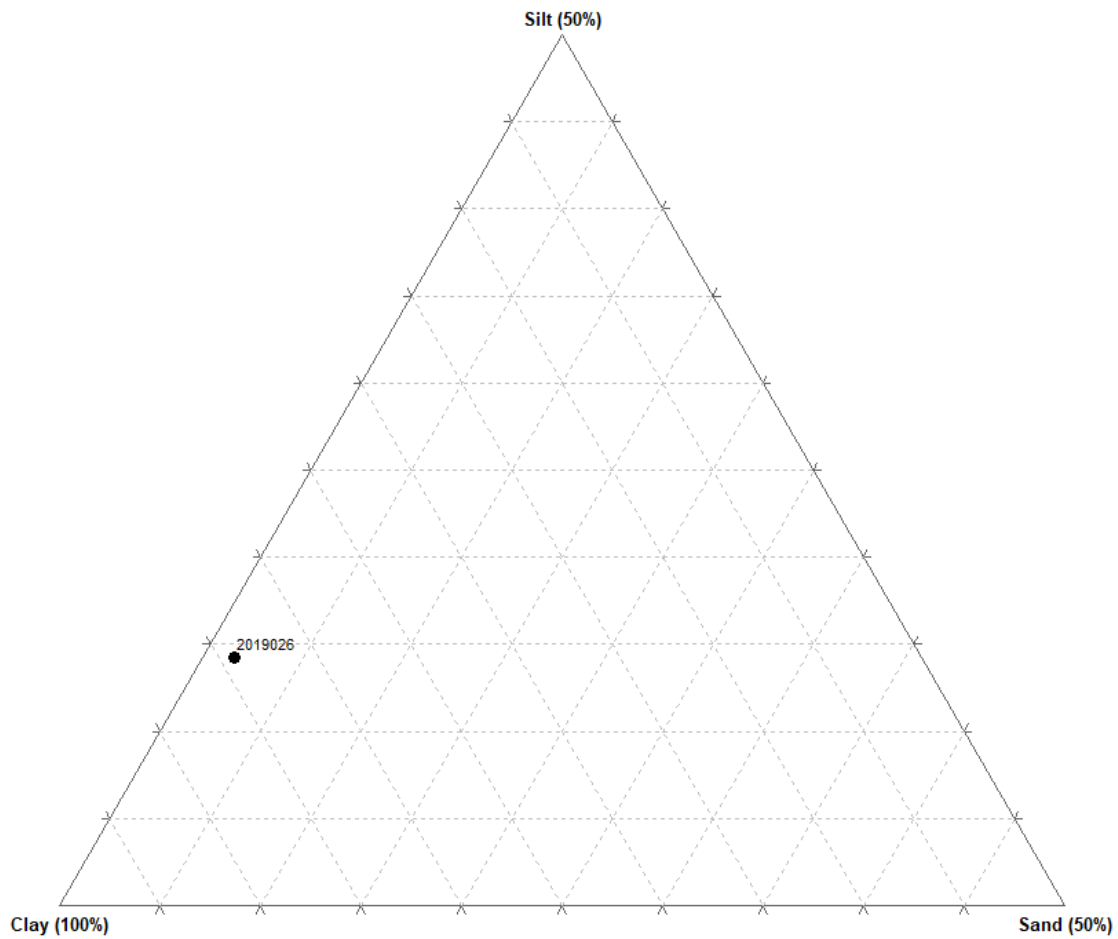


Figure 4.135 Ternary diagram of Sample 27 paste composition.

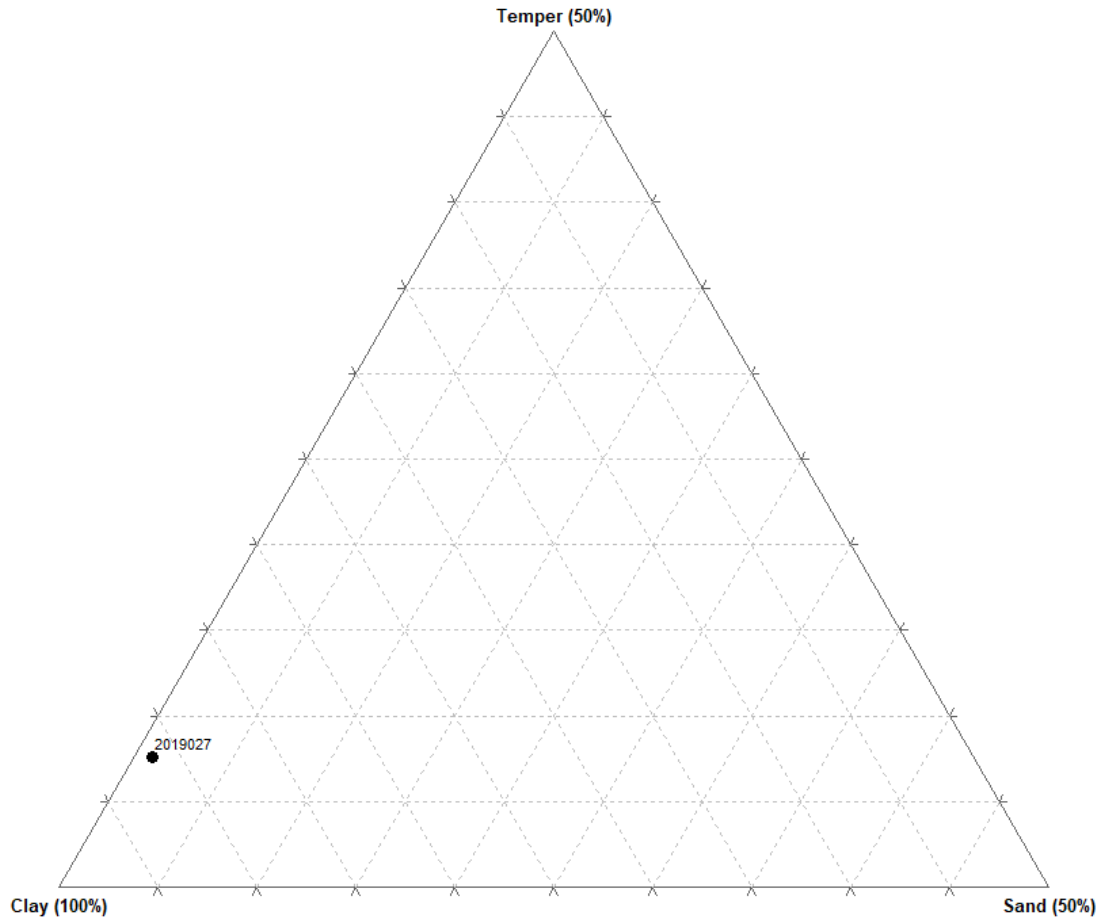


Figure 4.136 Ternary diagram of Sample 27 body composition.

## Regional Comparisons

### *Morphology*

The samples from southeastern Wisconsin can be classified as three categories of Middle Woodland pottery types. Rock Ware types, including Shorewood Cord Roughened and Kegonsa Stamped were defined by Baerreis (1952) but are considered diagnostic of the Waukesha phase (Haas 2019b; Haas and Picard 2019; Salzer n.d.). The Havana Ware types were defined by Griffin (1952), and include Havana Zoned, Naples Stamped, and Steuben Punctated. Hopewell Ware, which is usually identified by limestone tempering and relatively thinner vessel walls than

other Middle Woodland types was also defined by Griffin (1952). The two vessels that were classified in the Hopewell Ware category include a Hopewell-like incised vessel and an unclassified Hopewell Ware vessel.

Five samples represented two types of Rock Ware vessels in the southeastern Wisconsin collection of this analysis. These types include Kegonsa Stamped and Shorewood Cord Roughened. All these samples exhibited cordmarked surface treatment. These samples were also tempered with grit. All samples were identified as jars, with samples 2019010 and 2019012 from the Finch site being further identified as globular and conoidal shaped respectively.

The Kegonsa Stamped samples contained decorative treatments including tool impressions on the lip of the vessel. Bosses, which can be identified as bumps on the exterior of the vessel and punctates on the interior of the vessel, are also present on these vessels. The bosses are predominately located below the rim of the sherds. Sample 2019006 has rounded dowel tool impressions on the lip of the vessel. Sample 2019010 has bosses on the exterior and tooled notches along the interior of the lip.

The Shorewood Cord Roughened samples also exhibited some decorative treatments. Sample 2019005 is perforated by a hole that goes through the vessel wall below the rim. Sample 2019025 was decorated with a boss. Sample 2019012 was also classified as Shorewood Cord Roughened but did not contain any decorative treatment.

Eight samples representing three types of Havana ware were identified at the southeastern Wisconsin sites. These include Havana Zoned, Steuben Punctated, Naples Stamped, and Havana Cordmarked. All samples were tempered with grit. All samples represent jar shaped vessels, with 2019008 and 2019009 being further classified as conoidal jars.

The Havana Zoned sample (2019008) came from the Finch site. The surface treatment of this vessel is smoothed-over cordmarked. The decorative technique on the exterior of the sample includes incised lines, which section-off the zone of dentate-stamped decoration. The rim of the vessel also has dentate stamping directly below the exterior lip, separated from the plain, undecorated area by an incised line directly below the stamping.

Samples 2019002, 2019003, 2019004, and 2019007 all represent Steuben Punctated decorated vessels. All four Steuben Punctate vessels were recovered from the Peterson site (47WK199). Three have smoothed-over cordmarked surface treatment, and one (2019007) has smoothed surface treatment. According to Griffin (1952), Steuben Punctated vessels are most commonly located in the central and northern Illinois Valley. These vessels are decorated with rows of small hemi-conical punctates on the exterior of the vessels directly below the lip.

The Naples Stamped samples were both body sherds selected from the Finch site. They both have cordmarked surface treatment. Sample 2019009 has been decorated with cord-wrapped stick stamping, while sample 2019011 has been decorated with plain, linear tool stamping.

Sample 2019024 represents a Havana Cordmarked vessel from the Alberts site. The vessel has a beveled lip. Decorations include cord-wrapped stick stamping on the interior lip and bosses on the exterior below the rim.

Two samples of Hopewell-Related ware are included in the southeastern Wisconsin collection. These include a Hopewell-like incised bowl from the Peterson site, and a Hopewell-related subconoidal jar from the Finch site. The Hopewell-related wares have thinner rims and walls on average compared to the other ware types. However, the small sample size of each ware

type could influence these averages. Both samples are grit tempered and were decorated. The bowl is decorated with incised lines on the exterior rim oriented parallel to the lip of the vessel. The jar is decorated with thin trailed lines, where “the upper rim area features a triangle formed of four parallel lines” (Haas and Picard 2019:280). Haas and Picard (2019:280) also note that the paste is more compact than other Middle Woodland vessels in the Finch assemblage.

Of the twelve samples selected from the Illinois sites, ten are classified as Havana Ware. These types include Havana Cordmarked, Havana Plain, Havana Zoned, Hummel Stamped, Naples Stamped, and one unclassified Havana Ware sample. All samples have some form of decoration, which will be described in further detail below. All but two samples were identified as jars. Sample 2019019 was left indeterminate because it is an unclassified Havana vessel that shows some decorative styles similar to Hopewell ware. Sample 2019021 was left indeterminate because it is a body sherd, however it has Havana Zoned decorative techniques. It can be inferred that the Havana Zoned vessel is a jar form because Havana ware vessel forms are primarily jars with nearly vertical walls (Haas 2019b; Griffin 1952).

The Havana Cordmarked sample (2019026) was selected from the Blythe site. It has vertical cordmarking on the exterior surface and a smoothed interior surface. The sample is tempered with grit. It is decorated with bosses on the exterior located below the rim. The rim stance is everted with a pinched shape. The lip shape is rounded.

Two samples were identified as Havana Plain. Both samples were selected from the Sloan site. They both have smoothed surface treatment and are tempered with grit. The samples each have bosses on the exterior below the rim. The samples were too small to determine the rim



stance. Sample 2019014 has an unmodified rim with a rounded lip. This sample also has a black slip on the interior of the sherd. Sample 2019016 has a folded rim with a beveled lip.

The Havana Zoned samples both have smoothed surface treatments and grit temper. Sample 2019021 is a body sherd from the Sloan site. The sample is decorated with dentate stamps that are separated from the smooth, undecorated part of the surface by an incised line. Sample 2019023 is a rim sherd selected from the Kautz site. The sample has dentate stamps along the rim margin on the exterior surface, there is an undecorated section below these dentates, and an incised line separating additional dentate stamps on the body of the vessel below the undecorated area. Additionally, the cord-wrapped stick stamping is present on the interior rim of the sample. The rim of 2019023 is direct and unmodified, and the lip has been flattened.

Sample 2019027 is the only Hummel Stamped sample in the collection. The sample was selected from the DeWitte/Liphardt Habitation site. Hummel Stamped is similar to Naples Stamped, however the dentate stamps are pressed in at a curve, rather than straight rows (Griffin 1952). The sample has a slightly inverted rim stance, with an unmodified shape and flattened lip.

The Naples Stamped samples come from both Sloan and Albany Village site. Two samples have slightly inverted rims, and sample 2019015 is direct. all three samples have unmodified rim shapes with beveled lips. Grit is present in all three tempers and grog has been added to the temper of both Sloan samples. Sample 2019015 also has limestone added to the temper. This sample is cordmarked and has cord-wrapped stick stamps along the exterior rim of the vessel, as well as bosses below the rim. Additionally, a single cord impressed line is present on the exterior, nearly vertical down the rim. Sample 2019020 is cordmarked with diagonal cord-wrapped stick dentate stamping on the exterior rim. Sample 2019022 was recovered from Albany

Village. The sample has dentate stamps below the rim, a row of bosses below the stamps, and a row of dentate stamps below the bosses.

One sample was unable to be classified into a specific Havana type category. The sample has grit temper. The rim is slightly everted and unmodified, with a beveled lip. The sample has several decorative techniques including a perforation that goes through the vessel wall, a series of diagonal incised lines along the exterior rim, a row of punctates below the incised lines, and stamping similar to Naples Stamped vessels located below the punctates and surrounding the perforation. Benchley et al. suggested that the sample is “reminiscent of Hopewell ware that has a row of punctates setting off a band near the rim that is diagonally incised” (1976:103).

Two samples selected from the Sloan site represent Hopewell vessels. Sample 2019017 is a crosshatched rim sherd. The sample has smoothed-over cordmarked surface treatment and is grit tempered. The crosshatch decorative style is limited to the exterior rim of the vessel. The rim is slightly inverted and unmodified and has a flattened lip. Sample 2019018 is a body sherd that has rocker stamped decorative techniques. The rocker stamps are present along a single incised line on the exterior of the vessel. This sample has grit, limestone, and grog temper. Because this is a body sherd, the vessel form and rim morphology could not be determined.

### *Mineralogy*

The identification of minerals in thin sections is a qualitative aspect of ceramic petrography. Additionally, the counts of minerals were tracked to determine the quantity of each identified in the samples. Most minerals were present in the ceramic paste of both southeastern Wisconsin and northern Illinois samples, while some were only present in one region. Biotite, calcite, p-feldspar, and quartz were identified in all twenty-seven samples. Hornblende,

microcline, k-feldspar, quartzite, myrmekite, sericite, and opaque minerals were present in samples from both regions. Apatite was only present in one sample from the Peterson site in the southeastern Wisconsin region. Muscovite was only present in one sample from the Sloan site in the northwestern Illinois region.

Opaque minerals were present in all samples from southeastern Wisconsin. However, not all minerals were identified in all samples from each site. Apatite was present only in one sample of the Peterson site. Hornblende was present in all samples except the Crab Apple Point site and one sample from the Peterson site. Microcline was present in three samples from each the Finch and Peterson site. K-feldspar was present in four Finch site samples, the Crab Apple Point sample, and one sample from the Peterson site. Quartzite was present in the Alberts and Crab Apple Point samples, as well as one of the Finch and one of the Peterson samples. Myrmekite was present in all but three samples from the Finch site. And sericite was present in one Finch site sample, six Peterson site samples, and all other southeastern Wisconsin samples.

K-feldspar and opaque minerals were present in samples from all the sites Illinois. However, the Sloan site only had six samples with k-feldspar and five samples with opaque minerals. All other minerals were present to varying degrees in the Illinois sites. Hornblende was present in the Kautz site sample and one of the Sloan samples. Microcline was present in the Albany Village and DeWitte/Liphardt Habitation samples, as well as seven of the Sloan samples. Quartzite was present in the Blythe and DeWitte/Liphardt Habitation site as well as three of the Sloan site samples. Myrmekite was present in the Albany Village, DeWitte/Liphardt Habitation, and Kautz samples, as well as six of the Sloan samples. Sericite was present in all samples except the Blythe site sample.

In addition to the minerals, conglomerates, chert, and sandstone were also identified in some samples. Conglomerates were only present in southeastern Wisconsin site samples, one from the Finch site, and one from Peterson. Chert was present in sherds from both southeastern Wisconsin and northwestern Illinois sites. In Illinois, chert was present in the Blythe site sample, and two of the Sloan site samples. In southeastern Wisconsin, it was present in the Alberts and Crab Apple Point samples as well as three of the Finch samples and four of the Peterson samples. Sandstone was present in one Sloan site sample and one Peterson site sample.

### *Paste and Body Composition*

The paste is the natural clay used to construct ceramic vessels, excluding the human-added temper. The paste consists of silt, sand, and clay particles. In the petrographic analysis, the number of silt, sand, and clay particles were counted for each sample and the percentage of each was calculated for the sample paste.

The sherds from sites in Illinois had a higher average of sand (2.3%) and clay (86.3%) and a lower average of silt (11.4%) than the southeastern Wisconsin collection. The sand (1.7%) and clay (82.1%) are lower and the silt (16.2%) is higher in the samples from southeastern Wisconsin sites than in Illinois. A total of three samples did not have any natural inclusions that fell into the sand size-grade category. These samples include the only sample from the Kautz site in northeastern Illinois, as well as a single sample from both the Finch and Peterson sites in Wisconsin.

The paste composition data for the individual samples and sites were also plotted on ternary diagrams. The diagrams allowed different variables, including morphological and

attribute characteristics, to be displayed across the spatial location each sample represents based on individual paste characteristics (Figure 4.137).

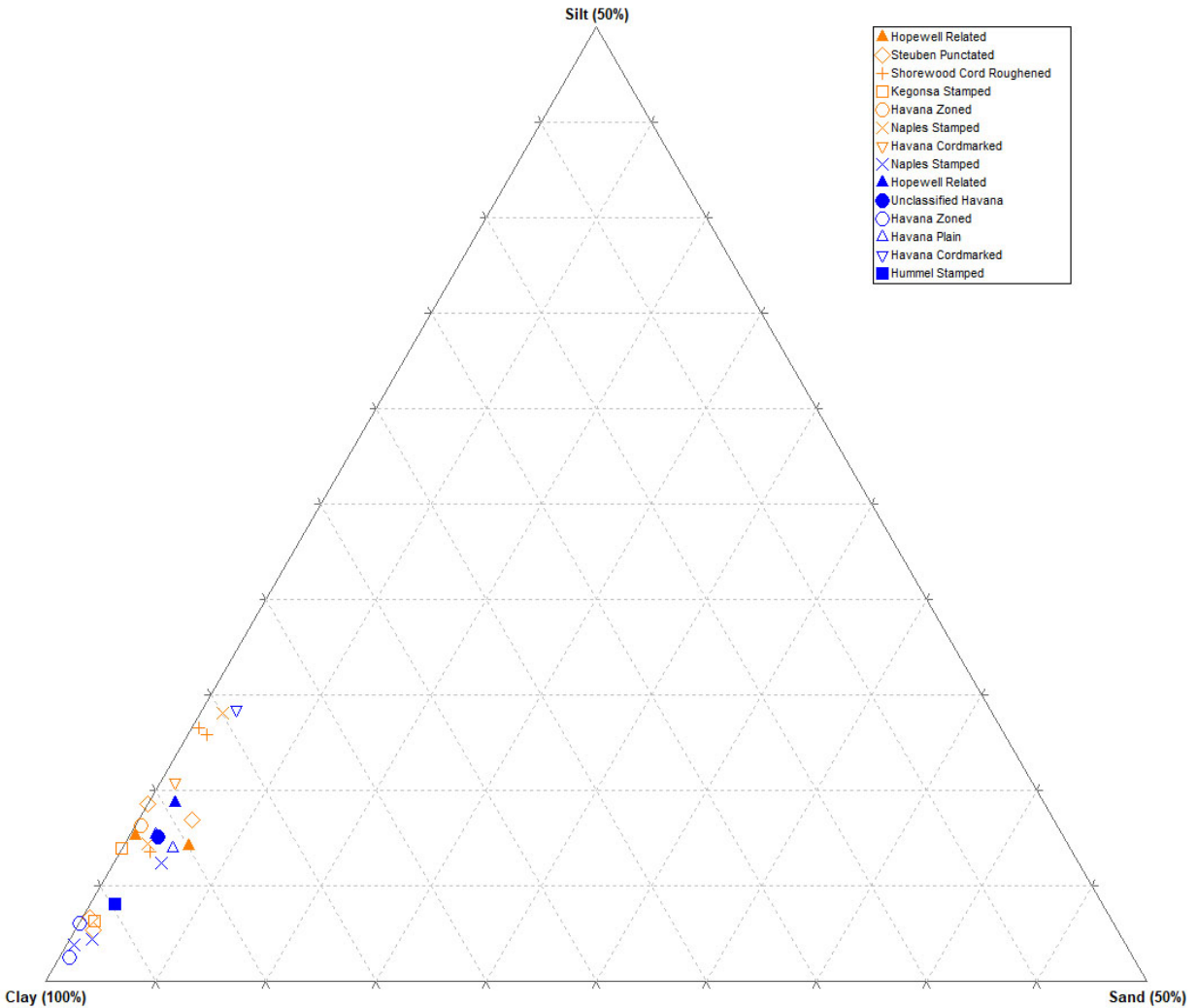


Figure 4.137 Ternary diagram of paste composition based on pottery type. The orange points represent samples from southeast Wisconsin sites, blue points represent samples from Illinois sites.

The following diagrams were created to identify the statistical significance of the paste variation between sites in this analysis (Figure 4.138). Each point represents an archaeological site. The isoproportion lines run from each corner of the ternary diagram to the center of the opposite side. Using the plotout function, this diagram plots the 90% and 99% confidence

interval for each point. The ellipses surrounding each site cross the isoproportion lines at the 90% and 99% confidence interval for each point. All ellipses are shown to overlap, which suggest that the relationship between the elements of silt, matrix, and sand, are the same for each site, and there is no change in the sub-composition.

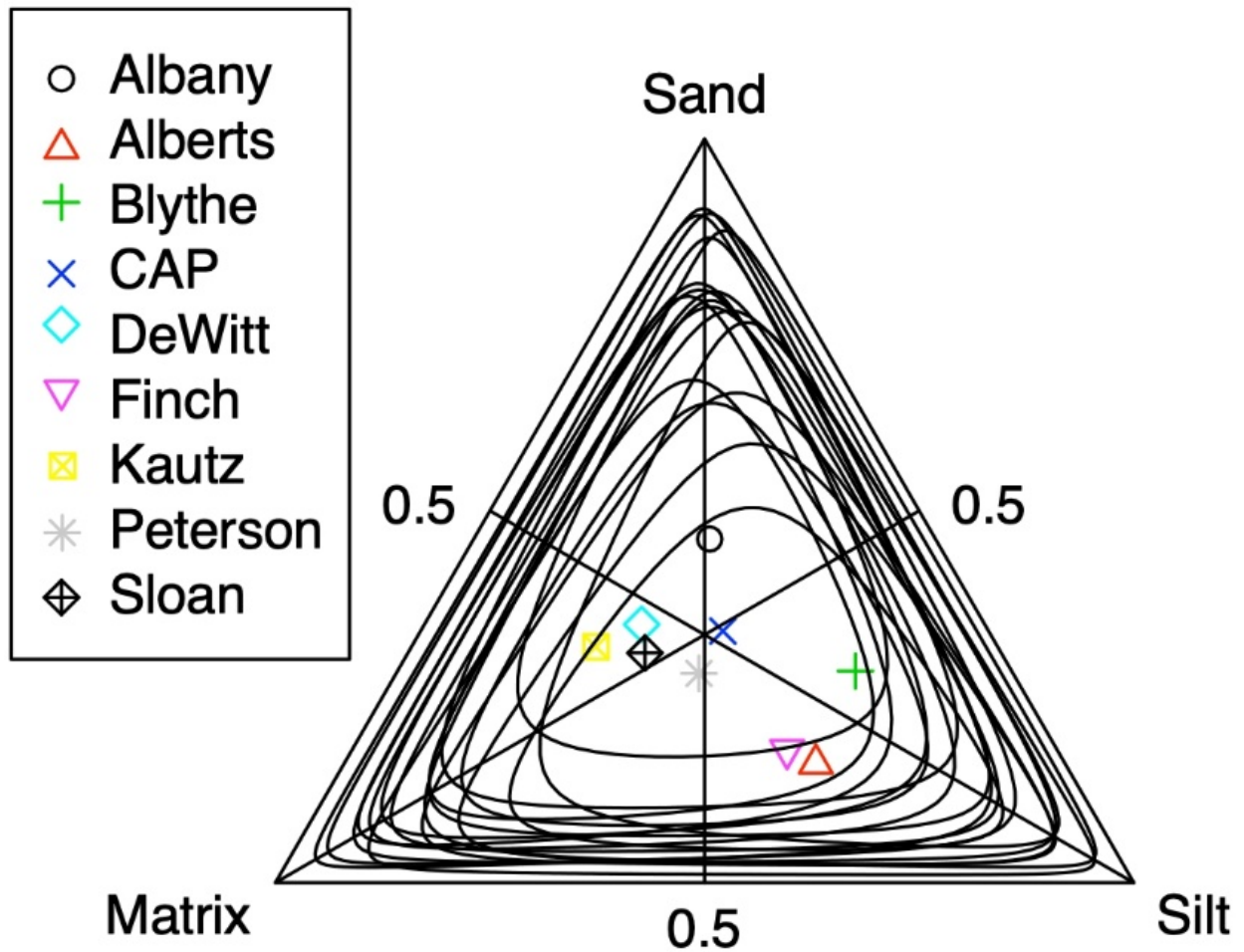


Figure 4.138 Ternary diagram plotting the estimation of variance of the full vector of the linear regression model of paste composition. The 90% and 99% confidence intervals are represented by ellipses around each site.

The body is the natural clay, sand, and added temper, which all constitute the recipe of paste used for ceramic construction. In the petrographic analysis, the sand and temper were

counted, and the silt and matrix particles were combined to calculate the clay. The mean count and percentage for each site and region were calculated using these data.

The sherds from northern Illinois sites have a higher mean percentage of sand (2.08%) but a lower mean percentage of temper (9.30%) and clay (87.64%) than the southeastern Wisconsin sites. In samples from southeastern Wisconsin, the mean percentage of sand (1.54%) is lower while temper (10.11%) and clay (88.35%) are both higher. The lack of natural inclusions that fell into the sand size-grade category in the sample at the Kautz site and the individual samples from both the Finch and Peterson sites also affected the mean sand percentages in the body composition.

The body composition data for the individual samples and sites were plotted on ternary diagrams. The diagrams allowed variables to be displayed across the chart based on the body composition characteristics (Figure 4.139).

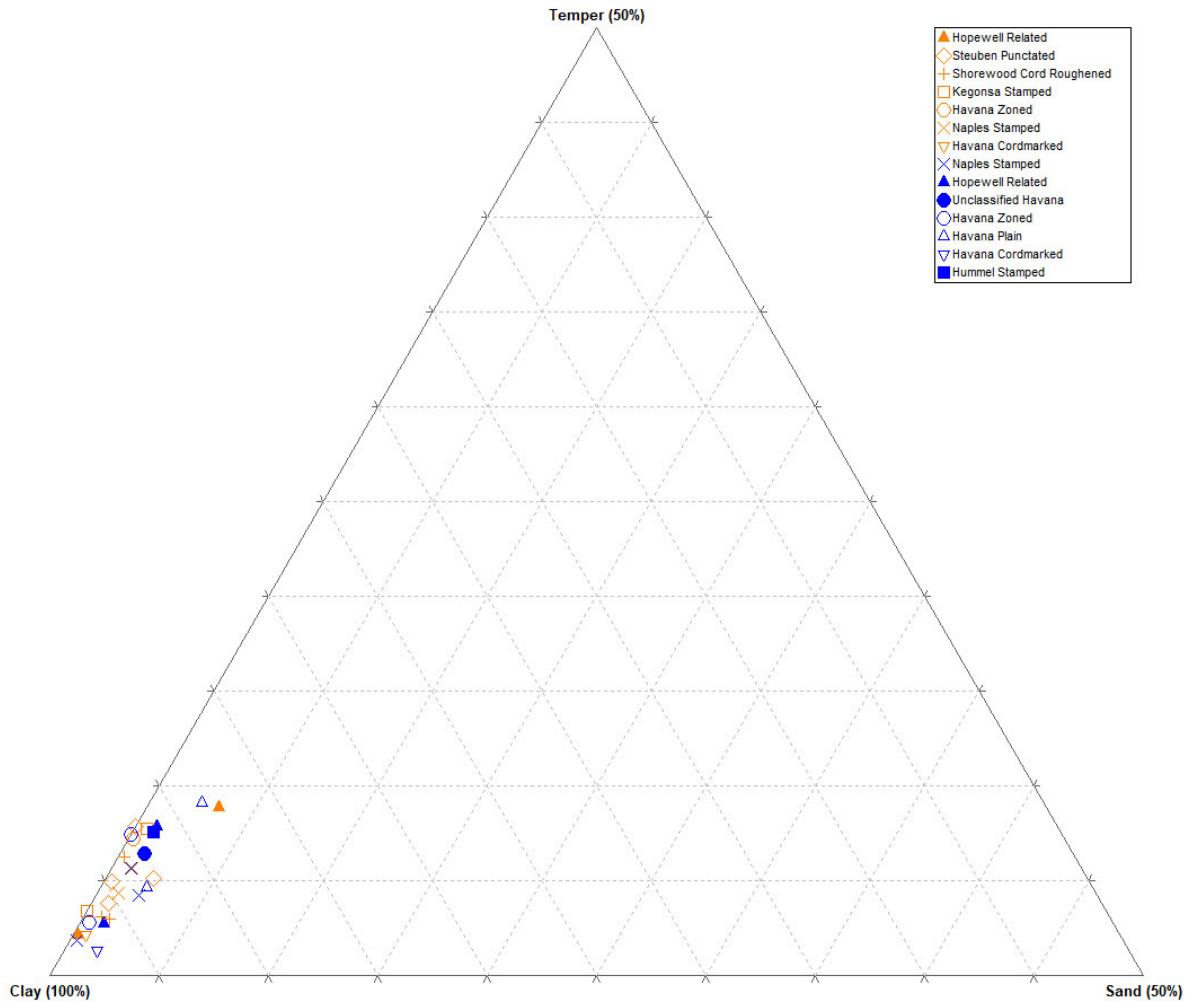


Figure 4.139 Ternary diagram of body composition based on pottery type. The orange points represent sherds from southeast Wisconsin sites, blue points represent sherds from northern Illinois sites.

The isoproportion ternary diagram in Figure 4.140 identifies the statistical significance of the body composition variation between the sites in the study. Each point represents one archaeological site. The isoproportion lines run from each corner of the ternary diagram to the center of the opposite side. Using the plotout function, this diagram plots the 90% and 99% confidence interval for each point. The ellipses surrounding each site cross the isoproportion lines at the 90% and 99% confidence interval for each point. All ellipses are shown to overlap,



which suggest that the relationship between the elements of temper, matrix, and sand, are the same for each site. Thus, there appears to be no change in the sub-composition of the samples.

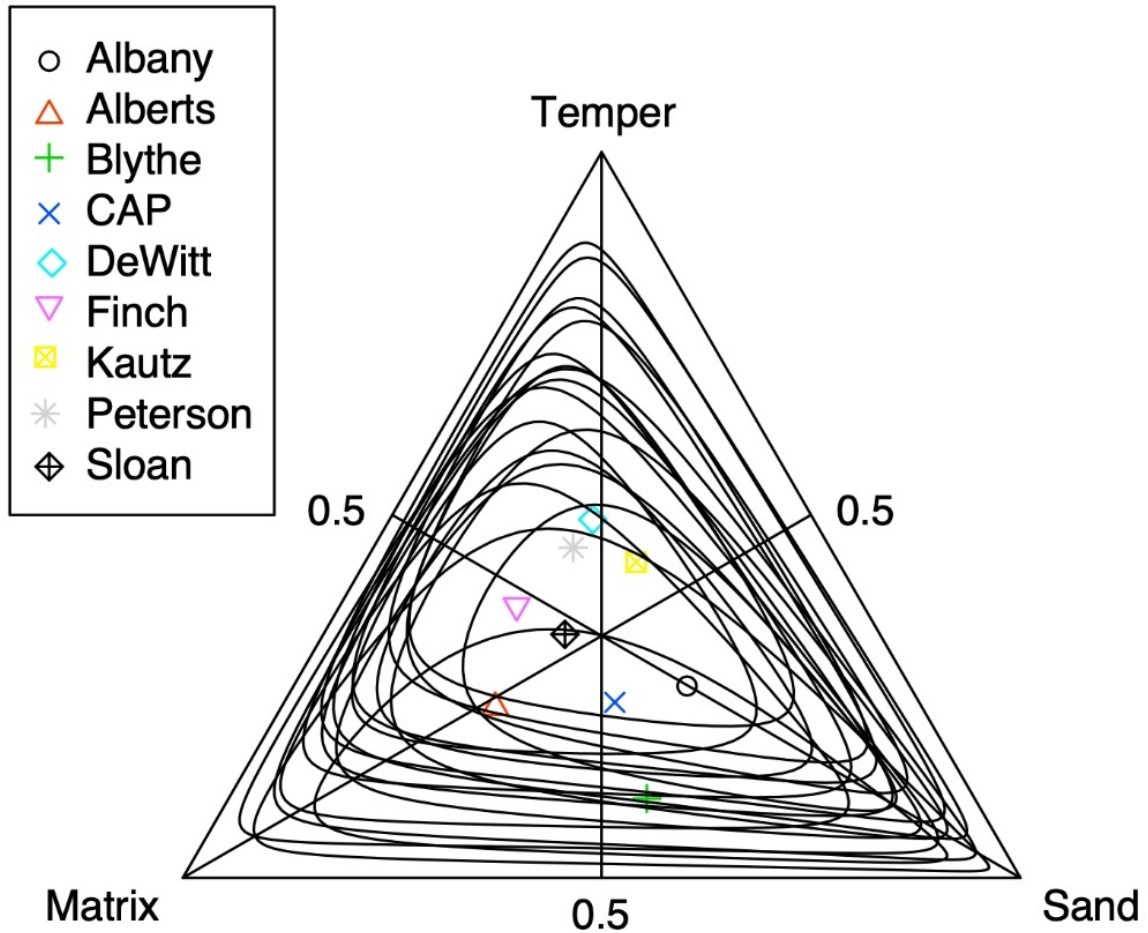


Figure 4.140 Ternary diagram plotting the estimation of variance of the full vector of the linear regression model of body composition. The 90% and 99% confidence intervals are represented by ellipses around each site.

## CHAPTER 5: SUMMARY AND CONCLUSION

### Summary

The results from the ceramic petrographic analysis indicate some variation, as well as some similarities, between the stylistic, morphological, and petrographic variables. The Waukesha phase Rock Ware pottery types, Kegonsa Stamped and Shorewood Cord Roughened, are considered local variants of cognate pottery styles found throughout southern Wisconsin and northern Illinois. However, in the present sample, sherds of Kegonsa Stamped and Shorewood Cord Roughened were restricted to southeastern Wisconsin recovery locations. Conversely, the Havana Ware pottery styles in the sample set were obtained from sites located in both northern Illinois and southern Wisconsin. Steuben Punctated ceramics have been suggested to compose a northeastern Illinois-southern Wisconsin microstyle (Wolforth 1995). However, the samples analyzed in the present study were all obtained from the Peterson site, located in southeastern Wisconsin. Havana Zoned, Naples Stamped, and Havana Cordmarked types were obtained from both regions. Havana Plain and Hummel Stamped were obtained only from sites in northern Illinois. Unclassified and Hopewell-Related pottery was obtained from sites in both regions. The vessels exhibiting Hopewell decorative styles were present within both regions. In the sample, these vessels are set apart from the other stylistic types by smaller average orifice diameters and thinner walls.

The sample used in this analysis is not representative of all Middle Woodland pottery in the research area. The samples selected were restricted to artifacts within the UWM ARL collections. In addition, sample size was limited by cost considerations. Therefore, the samples, and the analysis, cannot be accepted as fully indicative of the regional distribution of Middle

Woodland pottery types and ceramic pastes. Nonetheless, the data do suggest some interesting patterns.

Nearly all sherds in the sample set were tempered with grit. The only samples that included grog, or grog and limestone, in addition to grit temper, are from the Sloan site in northwestern Illinois. Notably absent are pastes composed primarily of limestone. Nearly all minerals were present in samples from both regions, with the exception of apatite and muscovite, which were only present in sherds from Wisconsin and Illinois, respectively.

There is some variation in the paste and body composition of sherds from the two regions. Sherds from northern Illinois sites exhibit a greater mean percentage of sand and clay, while southeastern Wisconsin sherds have a greater mean percentage of silt in the paste composition. The body composition of sherds from northern Illinois sites includes a higher mean percentage of sand, while sherds from the southeastern Wisconsin sites have higher percentages of temper and clay. However, based on the statistical analysis displaying the isoproportion lines at the 90% and 99% confidence interval, the data do not indicate any statistically significant difference in either the paste or body compositions between the sites. This suggests that the overall clay composition and ceramic paste recipes from the selected samples are similar in both regions. While this analysis focused on relatively few samples, that were not evenly distributed across sites and pottery types, the samples did exhibit a relatively homogenous paste composition. There was no evidence of a preferred paste or recipe that was specific to either region. Overall, the mean paste and body compositions for each site overlapped the other sites in this analysis.

## Conclusions

The first goal of this thesis was to determine the extent to which the samples are similar or different. The samples are all representative of Middle Woodland vessels in the region. All samples were tempered with grit, while some samples also include grog, or grog and limestone tempering. Overall, the paste and body compositions across all samples are relatively homogenous. The mineralogical analysis suggests standardization with minor variation in paste and recipes likely due to variation on locally available clay and temper sources. Four of the identified minerals were present in all samples and represented the highest mean percentage of minerals identified in all samples, biotite (19.42%), calcite (14.33%), p-feldspar (12.93%), and quartz (25.10%). Opaque minerals (8.28%) were identified in samples from every site, although they were not identified in all samples. All other minerals identified in this analysis were present in sherds from both regions, except for apatite, which was only identified in a sherd from the Peterson site in southeast Wisconsin, and muscovite, which was only identified in a sherd from the Sloan site in northwest Illinois. Sericite (7.59%) was identified in nineteen samples and was relatively abundant compared to the remaining minerals which ranged between 0.07% to 3.39%.

The petrographic analysis also identified some variation between the composition of samples. The paste composition analysis identified a greater percentage of silt in the southeastern Wisconsin samples. The Illinois sample paste composition is higher in sand. The percentage of silt in Wisconsin samples is highest at the Alberts site at 20.89%, but none of the average percentages fall below 13% silt. However, the sand percentages are highest at the Crab Apple Point site and Peterson site, which both have the lowest percentage of silt in the Wisconsin samples at 13.51% and 13.59%, respectively. The percentage of silt and sand in the Illinois samples vary more than the Wisconsin samples. The Blythe site has the highest average

percentage of silt of all sites at 28.42%, and a sand percentage of 3.16%, the clay at the Blythe site accounts for the smallest percentage of all samples at only 68.42%. No other site from the Illinois region exhibits an average percentage of silt greater than 12.35%, which is average for the Albany Village site. The Kautz site samples exhibit the lowest percentage of silt at 6.11%, and lack any sand-sized particles. As a result, at the Kautz site clay particles account for about 93.9% of the paste matrix (Table 5.1). Body composition also exhibits higher percentages of temper and lower percentages of sand in the Wisconsin sites in comparison to the Illinois sites. In the Wisconsin sample, the Alberts site exhibits the lowest percent of temper at 4.24%. Sherds from the Crab Apple Point are also low in temper but have the highest percent of sand in the Wisconsin sample. The Blythe site sample has the lowest percent of temper overall at 2.56% while the DeWitte/Liphardt Habitation site has the highest percentage of temper overall at 15.12% (Table 5.2). Consequently, these results suggest that both paste and body composition of sherds from the Illinois sites include a greater percentage of sand, while the sherds from the Wisconsin sites have a greater average percentage of both temper and silt.

TABLE 5.1 SUMMARY OF PASTE DATA BY SITE

Mean Percentage of Paste Composition			
Site	Silt (mean %)	Sand (mean %)	Clay (mean %)
<b>Northern Illinois</b>	<b>11.408</b>	<b>2.297</b>	<b>86.294</b>
Albany Village (11WT1)	12.346	4.321	83.333
Blythe (11HA40)	28.421	3.158	68.421
DeWitte/Liphardt Habitation (11RI57)	8.046	2.299	89.655
Kautz (11DU46)	6.107	0.000	93.893
Sloan (11MC86)	10.247	2.224	87.529
<b>Southeastern Wisconsin</b>	<b>16.169</b>	<b>1.737</b>	<b>82.094</b>
Alberts (47JE887)	20.886	1.266	77.848
CAP (47JE93)	13.514	2.703	83.784
Finch (47JE902)	18.955	1.165	79.880
Peterson (47WK199)	13.487	2.157	84.356
<b>Grand Total</b>	<b>14.053</b>	<b>1.986</b>	<b>83.961</b>

TABLE 5.2 SUMMARY OF BODY DATA BY SITE

Mean Percentage of Body Composition			
Site	Temper (mean %)	Sand (mean %)	Clay (mean %)
<b>Northern Illinois</b>	<b>9.300</b>	<b>2.081</b>	<b>87.635</b>
Albany Village (11WT1)	8.475	3.955	87.571
Blythe (11HA40)	2.564	3.077	94.359
DeWitte/Liphardt Habitation (11RI57)	15.122	1.951	82.927
Kautz (11DU46)	14.935	0.000	85.065
Sloan (11MC86)	8.813	1.999	87.713
<b>Southeastern Wisconsin</b>	<b>10.107</b>	<b>1.544</b>	<b>88.349</b>
Alberts (47JE887)	4.242	1.212	94.545
CAP (47JE93)	5.932	2.542	91.525
Finch (47JE902)	8.613	1.060	90.327
Peterson (47WK199)	12.822	1.864	85.314
<b>Grand Total</b>	<b>9.749</b>	<b>1.783</b>	<b>88.032</b>

Finally, the last goal of this research was to determine if the samples could be separated by region using statistical analysis. A statistical analysis was conducted using isoproportion lines to plot the 90% and 99% confidence interval for each site. Results suggest that the relative proportions of clay, silt, and sand cannot be statistically differentiated between sites. This suggests selection of broadly similar clay sources throughout the region. In southeast Wisconsin and northeast Illinois, it has proved difficult to identify specific clay sources due to the widespread similarity of extensive glacial clay deposits (see Clauter 2012; Hulit 2012; Naunapper 2007; Schneider 2015; Watson 1992). This is not the case in the Illinois River valley where studies have identified localized clay resources tied to particular site locations (Fie 2008; White and O'Brien 1964). Additionally, the statistical analysis using isoproportion lines to plot the 90% and 99% confidence interval for each site shows that the relative proportions of clay, sand, and temper cannot be differentiated between the sites. This suggests broadly similar temper preferences throughout the study region. While minor differences are apparent, likely due to variation in locally available temper, potters do not seem to have exhibited a preference for a specific raw mineral. The lack of individualized compositions between sites may indicate that

paste recipes were widely shared throughout the study area. This aligns with Haas's (2019b) suggestion that a persistent relationship was established during Early Woodland times between people in southern Wisconsin and northern Illinois and continued through the Middle Woodland period. Additionally, these results follow a similar pattern to Clauter's (2012) research on Late Woodland pottery. Clauter identified some patterns, including decorative motif and temper types, that follow a divide between sites in eastern Wisconsin and western Wisconsin, while the petrographic data did not show statistically significant variation between sites. Finally, Schneider's analysis of Oneota ceramic pastes from various Wisconsin localities led him to argue that while clay and temper sources varied locally, "the petrographic data indicate that the recipe used by Oneota potters is similar among all the sites and localities" in his study (Schneider 2015:330).

## **Future Research**

Future analysis of Middle Woodland sites in southeastern Wisconsin and northern Illinois could be designed to expand upon the preliminary research documented in this thesis. Ideally, this would include additional petrographic analysis of Middle Woodland sherds from a more representative set of sites in both southern Wisconsin and northern Illinois.

This additional research could be completed in two primary ways. First, more samples could be analyzed from the already selected sites to provide a more statistically representative sample of Middle Woodland pottery from these sites. This would be especially beneficial for those sites only represented by a single sherd in this study. Second, samples from additional sites in the region should be included in the analysis. A larger sample size may identify localized variation within the broader regional sample. Further research should include cognate varieties of

vessels from both regions, especially within sites that could be within the proposed expanded Waukesha phase boundaries. Data on a larger sample of vessels may support the provisional results that suggest overall homogeneity within and between sites, or it may identify compositional variation masked by sampling error in the present analysis.

Another opportunity for future research would be to expand the temporal boundaries of this research project. In this way, the compositional data of Early Woodland ceramics in the region could be added to this database. The addition of Early Woodland vessels could be used to further strengthen Haas's (2019b) argument that the Middle Woodland groups were adapting to Havana-Hopewell stylistic influences using existing technological practices. If the paste composition of Early Woodland vessels in the region exhibits the same homogeneity identified in this analysis, it could potentially indicate that ceramic recipes in southeast Wisconsin did not change dramatically between the Early and Middle Woodland periods, while decorative and stylistic changes were occurring. Likewise, variation in ceramic pastes could suggest that the recipes used to construct Early Woodland vessels were distinct from the Middle Woodland recipes.

Another opportunity for future research would be the addition of chemical compositional analyses. Techniques such as Energy Dispersive X-ray Fluorescence, Wave Dispersive X-ray Fluorescence, Inert Neutron Activation, radiography, and other methods have been shown to be complementary to ceramic petrography. However, like ceramic petrography, all are destructive techniques, and most are somewhat more expensive than the production of ceramic thin sections. Thus, large sample sizes would necessitate a major grant and access to a wide range of collections.



## REFERENCES CITED

Abrams, Elliot M

2009 Hopewell Archaeology: A View from the Northern Woodlands. In *Journal of Archaeological Research* 17:169-204.

Asch, David L.

1976 *The Middle Woodland Populations of the Lower Illinois River Valley*. Scientific Papers 1. Northwestern University Archaeological Program, Evanston.

Auten, Madison, Samantha Bomkamp, Megan Harding, Paul Moriarity, Kirby Pezley, Megan Thornton, Monea Warrington

2017 Overview of the James Bussey Collection from the Crab Apple Point Site (47JE93). Anthropology department, University of Wisconsin, Milwaukee.

Baerreis, David A.

1952 Pottery Type Descriptions. Paper presented at a conference of the Wisconsin Archaeological Survey. Madison, Wisconsin.

Benchley, Elizabeth, Blane Nansel, Clark A. Dobbs, Susan M. Thurston Myster, and Barbara H. O'Connell

1997 *Archaeology and Bioarchaeology of the Northern Woodlands*. The Central and Northern Plains Archaeological Overview vol. 52, Hester A. Davis, series editor. Arkansas Archaeological Survey, Fayetteville, Arkansas.

Benchley, Elizabeth, and Mark Dudzik

1976 *Final Report on an Archaeological Survey of the Albany Mound Group Whiteside County, Illinois*. Archaeological Research Laboratories, Department of Anthropology University of Wisconsin-Milwaukee. Report of Investigations No. 10.

Benchley, Elizabeth, and Michael L. Gregg

1975 *Final Report of an Intensive Archaeological Survey of the Meredosia Levee Project*. Archaeological Research Laboratories, Department of Anthropology University of Wisconsin Milwaukee. Report of Investigations No. 5.

Benchley, Elizabeth and William Billeck

1977 *Final Report on a Predictive Models Survey in the Rock River Drainage, Illinois*. University of Wisconsin-Milwaukee Archaeological Research Laboratory. Report of Investigations No. 17.

Benchley, Elizabeth, Harold Hassen, and William Billeck

1979 *Final Report of Archaeological Investigations at the Sloan Site (11-MC-86) FAS Project 1210, Mercer County, Illinois*. University of Wisconsin-Milwaukee Archaeological Research Laboratory. Report of Investigations No. 36.

- Bennett, John W.  
 1952 The Prehistory of the Northern Mississippi Valley. In *The Archaeology of the Eastern United States*, edited by James B. Griffin, pp. 108-123. University of Chicago Press, Chicago.
- Bishop, Ronald L., Robert L. Rands, and George R. Holley.  
 1982 Ceramic Compositional Analysis in Archaeological Perspective. In *Advances in Archaeological Method and Theory*, Vol. 5, pp. 275-330. Springer, New York.
- Brazeau, Linda A., Patricia A. Bruhy and David F. Overstreet  
 1980 *Archaeological Survey and Test Excavations in the Fox River Drainage--Waukesha, Racine, and Walworth Counties - Survey Results*. Great Lakes Archaeological Research Center, Inc. Copies available from 90.
- Brose, David S. and N'omi Greber  
 1979 *Hopewell Archaeology - the Chillicothe Conference*. The Kent State University Press, Kent, Ohio.
- Brown, Charles E.  
 1923b Waukesha County, Southern Townships2(2):69-119.
- Brown, James A.  
 1964 The Northeastern Extension of the Havana Tradition. In *Hopewellian Studies*, Vol. 12, edited by Joseph R. Caldwell and Robert L. Hall, pp. 107-122. Illinois State Museum Scientific Papers, Springfield.
- Buikstra, Jane E.  
 1976 *Hopewell in the Lower Illinois Valley: A Regional Study of Human Biological Variability and Prehistoric Mortuary Behavior*. Scientific Papers 2. Northwestern University Archaeological Program, Evanston.
- Caldwell, Joseph R.  
 1964 Interaction Spheres in Prehistory. In *Hopewellian Studies*, Vol. 12, edited by Joseph R. Caldwell and Robert L. Hall, pp. 133-143. Illinois State Museum Scientific Papers, Springfield.
- Charles, Douglas K.  
 1992 Woodland Demographic and Social Dynamics in the American Midwest: Analysis of a Burial Mound Survey. *World Archaeology* 24:175-197.  
 2012 Origins of the Hopewell Phenomenon. In *The Oxford Handbook of North American Archaeology*, pp. 471-482. Oxford University Press, New York.
- Charles, D. K. and J. E. Buikstra  
 2006 *Recreating Hopewell*. University Press of Florida, Gainesville.

Chayes, F.

1954 The Theory of Thin-Section Analysis. *The Journal of Geology* 62:92-101.

1956 *Petrographic Modal Analysis*. John Wiley & Sons, New York.

Chivis, Jeff

2016 The Introduction of Havana-Hopewell in West Michigan and Northwest Indiana: An Integrative Approach to the Identification of Communities, Interaction Networks, and Mobility Patterns. PhD dissertation, Department of Anthropology, Michigan State University, East Lansing.

Clauter, Jody

2012 *Effigy Mounds, Social Identity, and Ceramic Technology: Decorative Style, Clay Composition, and Petrography of Wisconsin Late Woodland Vessels*, Unpublished PhD dissertation, University of Wisconsin-Milwaukee, Milwaukee, Wisconsin.

Druc, Isabelle C.

2015 *Portable Digital Microscope. Atlas of ceramic pastes. Components, texture and technology* (with the technical collaboration of B. Velde and L. Chavez). Deep University Press, WI.

Esri

2020 ArcGIS and ArcMap software. Electronic document, accessed March 23, 2020.

Faithfull, John

1998 Identification Tables for Common Minerals in Thin Section. Electronic document, <http://funnel.sfsu.edu/courses/geol426/Handouts/mintable.pdf>, accessed March 19, 2020.

Fie, Shannon M.

2008 Middle Woodland Ceramic Exchange in the Lower Illinois Valley. *Midcontinental Journal of Archaeology* 33:1, 5-40.

Fowler, Melvin L.

1955 Ware Grouping and Decorations of Woodland Ceramics in Illinois, *American Antiquity* Vol. 20 No. 3 pp. 213-224.

Fowler, Melvin L. and Mark J. Dudzik

1973 An Archaeological Survey of the Illinois Side of the Mississippi River Valley from the Mouth of the Des Moines River to the Wisconsin Border. University of Wisconsin-Milwaukee Anthropology Department.

Gates, Sanford H.

1983 An Archaeological Survey of the Du Page River Drainage. *Chicago Area Archaeology* Illinois Archaeological Survey Bulletin No. 3.

Geraci, Peter J.

- 2016 The Prehistoric Economics of the Kautz Site: A Late Archaic and Woodland Site in Northeastern Illinois M.S. thesis, Department of Anthropology University of Wisconsin-Milwaukee, Milwaukee, Wisconsin.

Goldstein, Lynne

- 1984 The Southeastern Wisconsin Archaeology Program: 1983- 1984. University of Wisconsin-Milwaukee Archaeological Research Laboratory Report of Investigations No. 77. University of Wisconsin-Milwaukee, Milwaukee, Wisconsin.
- 1992 Middle Woodland Study Unit. In *The Southeastern Wisconsin Archaeology Program: 1991- 1992*. edited by L. Goldstein. University of Wisconsin-Milwaukee Archaeological Research Laboratory Report of Investigations No. 112. University of Wisconsin-Milwaukee, Milwaukee, Wisconsin.

Griffin, J.B.

- 1952 Some Early and Middle Woodland Pottery Types in Illinois. In *Hopewellian Communities in Illinois*, edited by T. Deuel, pp. 95-129. Scientific Papers No. 5. Illinois State Museum, Springfield, Illinois.

Haas, Jennifer

- 2017 Summary of Archaeological Investigations at the Peterson Site (47WK0199). Unpublished document, University of Wisconsin Milwaukee Cultural Resource Management. Milwaukee, Wisconsin.
- 2019a *Archaeological Data Recovery at the Finch Site (47JE0902), Jefferson County, Wisconsin*. University of Wisconsin-Milwaukee Archaeological Research Laboratory Report of Investigations No. 445. University of Wisconsin-Milwaukee, Milwaukee, Wisconsin.
- 2019b Community Identity, Culinary Traditions and Foodways in the Western Great Lakes. PhD dissertation, Department of Anthropology University of Wisconsin-Milwaukee, Milwaukee, Wisconsin.

Haas, Jennifer and Jennifer Picard

- 2019 Ceramic Analysis. In *Archaeological Data Recovery at the Finch Site (47JE0902), Jefferson County, Wisconsin*. University of Wisconsin-Milwaukee Archaeological Research Laboratory Report of Investigations No. 445:241-310. University of Wisconsin-Milwaukee, Milwaukee, Wisconsin.

Haas, Jennifer R., Katherine Shillinglaw, and Rhiannon Jones

- 2015 *Archaeological Investigations at the Finch Family Cemetery 47JE0902/BJE-0101), Jefferson County, Wisconsin*. University of Wisconsin-Milwaukee Archaeological Research Laboratory Report of Investigations No. 216. University of Wisconsin-Milwaukee, Milwaukee, Wisconsin.

Herold, Elaine Bluhm, ed.

1971 *The Indian Mounds at Albany, Illinois*. Davenport Museum Anthropological Papers No. 1. Davenport, Iowa.

Hulit, Elissa

2012 *The Promise and Potential in Generating Models of Prehistoric Clay Resources Using Energy Dispersive X-Ray Fluorescence*. M.S. thesis, Department of Anthropology, University of Wisconsin-Milwaukee, Milwaukee, Wisconsin.

IIAPS

2020 *Illinois Inventory of Archaeological and Paleontological Sites*. Illinois State Museum, Springfield.

Illinois State Geological Survey

2005 *Bedrock Geology of Illinois*. Illinois Department of Natural Resources, Champaign.

Jeske, Robert J.

2003 *Lake Koshkonong 2002/2003: Archaeological Investigations at Three Sites in Jefferson County, Wisconsin*. University of Wisconsin-Milwaukee Archaeological Research Laboratory Report of Investigations, No. 153. University of Wisconsin-Milwaukee, Milwaukee, Wisconsin.

2006 *Hopewell Regional Interactions in Southeastern Wisconsin and Northern Illinois*. In *Recreating Hopewell*, edited by D. K. Charles and J. E. Buikstra, pp. 286-309. University Press of Florida, Gainesville.

Jeske, Robert J. and Kira E. Kaufmann

2000 *The Alberts Site Complex (47Je887 and 47Je903): A Late Archaic through Mississippian Occupation in Jefferson County*. In *The Southeastern Wisconsin Archaeology Program: 1999-2000*. Archaeological Research Laboratory Report of Investigations 144. Edited by R.J. Jeske, 79-98. University of Wisconsin-Milwaukee, Milwaukee, Wisconsin.

Lapham, Increase A.

1855 *The Antiquities of Wisconsin as Surveyed and Described*. Smithsonian Contributions to Knowledge 4. Smithsonian Institution, Washington, D.C.

Mason, Ronald J.

2001[1981] *Great Lakes Archaeology*. Academic Press, New York. pp. 237-293.

McKern, W.C.

1942 *The First Settlers of Wisconsin*. *Wisconsin Magazine of History* 25:153-169.

National Petrographic Services Inc.

2018 Thin Section Preparation. Electronic document, <http://www.nationalpetrographic.com/petrographic-thin-sections.html>, accessed March 13, 2018.

Naunapper, Linda H.

2007 History, Archaeology and the Construction of Ethnicity: Bell Type II Ceramics and the Potawatomi. PhD dissertation, Department of Anthropology, University of Wisconsin-Milwaukee, Milwaukee, Wisconsin.

Nelson, Stephen A.

2019 Twinning, Polymorphism, Polytypism, Pseudomorphism. Electronic document, <https://www.tulane.edu/~sanelson/eens211/twinning.htm>, accessed March 19, 2020.

Peet, Stephen D.

1890 Prehistoric America--Vol. 2, Emblematic Mounds and Animal Effigies. American Antiquarian Office, Chicago.

Perkins, Dexter

1998 *Mineralogy*. Prentice Hall, Upper Saddle River, NJ.

Pozza, Jacqueline M.

2016 Investigating the Functions of Copper Material Culture from Four Oneota Sites in the Lake Koshkonong Locality of Wisconsin. M.S. thesis, Department of Anthropology, University of Wisconsin-Milwaukee, Milwaukee, Wisconsin.

Rice, Prudence M.

1987 *Pottery Analysis: A Sourcebook*. University of Chicago Press, Chicago.

Richards, John D.

1992 Ceramics and Culture at Aztalan: A Late Prehistoric Village in Southeast Wisconsin. PhD dissertation, Department of Anthropology, University of Wisconsin-Milwaukee, Milwaukee, Wisconsin.

Riederer, J.

2004 Thin Section Microscopy Applied to the Study of Archaeological Ceramics. In *Hyperfine Interactions* 154:143-158.

Rye, Owen S.

1981 *Pottery Technology: Principles and Reconstruction*. Taraxacum, Washington, D.C.

Salzer, Robert J.

nd *The Waukesha Focus: Hopewell In Southeastern Wisconsin*. Unpublished Manuscript, The Logan Museum, Beloit College, Beloit. [PART]

1986 The Middle Woodland Stage. *The Wisconsin Archeologist* 67(3-4):263-282.

Schenian, Pamela A.

- 1983 The Current Status of the Archaeological Materials from the Kautz Site (11-DU-46). Northwestern University. Manuscript on file, University of Wisconsin-Milwaukee Archaeological Research Laboratory Archives Object ID# 1960.2.7.

Schneider, Seth A.

- 2015 Oneota Ceramic Production and Exchange: Social, Economic, and Political Interactions in Eastern Wisconsin Between A.D. 1050-1400. PhD dissertation, Department of Anthropology, University of Wisconsin-Milwaukee, Milwaukee.

Schneider, Seth A., Jennifer R. Haas, Catherine R. Jones, and Brianne E. Charles

- 2017 *Archaeological Investigations and Monitoring at Crab Apple Point (47JE93), Rufus Bingham Mound Group (47JE96), and North Mound Group (47DA28), Dane and Jefferson Counties, Wisconsin*. University of Wisconsin-Milwaukee Archaeological Research Laboratory Report of Investigations No. 433. University of Wisconsin-Milwaukee, Milwaukee, Wisconsin

Seeman, Mark F.

- 1977 The Hopewell Interaction Sphere: The Evidence for Interregional Trade and Structural Complexity. PhD dissertation, Department of Anthropology, Indiana University, Bloomington.

Shepard, Anna O.

- 1956 *Ceramics for the Archaeologist*. Publication 609. Carnegie Institution of Washington, Publication 519, Washington D.C.

Sinopoli, Carla M.

- 1991 *Approaches to Archaeological Ceramics*. Plenum Press, New York.

Spector, Janet D.

- 1975 Crabapple Point (Je 93): An Historic Winnebago Indian Site in Jefferson County, Wisconsin. *The Wisconsin Archeologist* 56(4):270-345.

Stevenson, Katherine P., Robert F. Boszhardt, Charles R. Moffat, Philip H. Salkin, Thomas C. Pleger, James L. Theler, and Constance M. Arzigian

- 1997 The Woodland Tradition. *Wisconsin Archeologist* 78:140-201. [pp. 157-166]

Stoltman, James B.

- 1989 A Quantitative Approach to the Petrographic Analysis of Ceramic Thin Sections. *American Antiquity* 54:147-160.

- 1991 Ceramic Petrography as a Technique for Documenting Cultural Interaction: An Example from the Upper Mississippi Valley. *American Antiquity* 56(1):103-120.

- 1999 The Chaco-Chuska Connection: In Defense of Anna Shepard. In *Pottery and People*, edited by James M. Skibo and Gary M. Feinman, pp. 9-24. University of Utah Press, Salt Lake City.
- 2001 The Role of Petrography in the Study of Archaeological Ceramics. In *Earth Sciences in Archaeology*, edited by Paul Goldberg, Vance T. Holliday, and C. Reid Ferring, pp. 297-326. Kluwer Academic/Plenum Publishers, New York.
- 2011 New Petrographic Evidence Pertaining to Ceramic Production and Importation at the Olmec Site of San Lorenzo. In *Archaeometry* 53(3):510-527.
- 2015 *Ceramic Petrography and Hopewell Interaction*. University of Alabama Press.
- Stoltman, James B. and RC Mainfort
- 2002 Minerals and Elements: Using Petrography to Reconsider the Findings of Neutron Activation in the Compositional Analysis of Ceramics from Pinson Mounds, Tennessee. *MCJA. Midcontinental Journal of Archaeology* (27(1):1-33.
- Stout, A.B. and H.L. Skavlem
- 1906 The Archaeology of the Lake Koshkonong Region. *The Wisconsin Archeologist* 7(2).
- Strekeisen, Alex
- 2018a Alkali Feldspar. Electronic document, <http://www.alexstrekeisen.it/english/pluto/alkalifeldspar.php>, accessed March 19, 2020.
- 2018b Calcite. Electronic document, <http://www.alexstrekeisen.it/meta/calcite.php>, accessed March 19, 2020.
- Struever, Stuart
- 1964 The Hopewell Interaction Sphere in Riverine – Western Great Lakes Cultural History. In *Hopewellian Studies*, Vol. 12, edited by Joseph R. Caldwell and Robert L. Hall, pp. 85-106. Illinois State Museum Scientific Papers, Springfield.
- 1965 Middle Woodland Culture History in the Great Lakes-Riverine Area. *American Antiquity* 31:211-223.
- Thompson, Todd
- Todd Thompson Software website, TriPlot 4.1.2. Electronic document, <http://mypage.iu.edu/~tthomps/programs/html/tnttriplot.htm>, accessed February 29, 2020.
- Watson, Richard A.
- 1992 The Place of Archaeology in Science. In *Metaarchaeology*, edited by Lester Embree, pp. 255-268 Kluwer Academic Publishers, Dordrecht.



- Watson, Robert J., Jennifer R. Harvey, James L. McEachran, Machel R. Lee  
2003 *Phase I & II Archaeological Investigations of the Preferred Alternative Route for the STH 26 Reconstruction in Dodge, Jefferson and Rock Counties, Wisconsin*. Great Lakes Archaeological Research Center, Inc. Report of Investigations No. 518.
- Wenner, David  
1960 Original unpublished field notes from the Kautz Site 11-DU-46. Manuscript on file, University of Wisconsin-Milwaukee Archaeological Research Laboratory Archives.
- White, W.A. and N.R. O'Brien  
1964 *Illinois Clay Resources for Lightweight Ceramic Block*. Illinois State Geologic Survey Circular No. 371, Urbana.
- WHPD  
2018 Wisconsin Archaeological Site Inventory. Wisconsin Historical Society State Historic Preservation Office, Madison.
- Wisconsin Department of Natural Resources  
2011 Bedrock Geology. Ecological Landscapes of Wisconsin Handbook.
- Wood, E. F.  
1936 A Central Basin Manifestation in Eastern Wisconsin. *American Antiquity* 1(3):215-219.
- Wolforth, Thomas R.  
1995 An Analysis of the Distribution of Steuben Punctated Ceramics. *The Wisconsin Archeologist* 76:27-47.
- Yingst, James R.  
1990 Introduction: A Historical Perspective on the Archaeology of Short-Term Middle Woodland Sites in West-Central Illinois. In *Illinois Archaeology*, 2(1&2):5-16.

## APPENDIX A: CERAMIC ATTRIBUTE ANALYSIS DATABASE

Sample Number	Region	Site Name (Number)	ID Number	Artifact No
2019001	Southeastern Wisconsin	Peterson (47WK199)	1980.3_34C	8
2019002	Southeastern Wisconsin	Peterson (47WK199)	01.029-014.01	1
2019003	Southeastern Wisconsin	Peterson (47WK199)	01.029-014.01	2
2019004	Southeastern Wisconsin	Peterson (47WK199)	01.029-018	23
2019005	Southeastern Wisconsin	Peterson (47WK199)	01.029-027	2
2019006	Southeastern Wisconsin	Peterson (47WK199)	01.029-034	1
2019007	Southeastern Wisconsin	Peterson (47WK199)	1980.3-14	12
2019008	Southeastern Wisconsin	Finch (47JE902)	09.089-2370	2
2019009	Southeastern Wisconsin	Finch (47JE902)	09.089-1929	1
2019010	Southeastern Wisconsin	Finch (47JE902)	09.089-3426	2
2019011	Southeastern Wisconsin	Finch (47JE902)	09.089-1536	1
2019012	Southeastern Wisconsin	Finch (47JE902)	09.089-0516	2
2019013	Southeastern Wisconsin	Finch (47JE902)	09.089-3111	1
2019014	Northern Illinois	Sloan (11MC86)	78-X-806	0
2019015	Northern Illinois	Sloan (11MC86)	78-X-847	0
2019016	Northern Illinois	Sloan (11MC86)	78-X-804	0
2019017	Northern Illinois	Sloan (11MC86)	78-X-739	0
2019018	Northern Illinois	Sloan (11MC86)	78-X-805	0
2019019	Northern Illinois	Sloan (11MC86)	78-X-807	0
2019020	Northern Illinois	Sloan (11MC86)	78-X-237	0
2019021	Northern Illinois	Sloan (11MC86)	TP39 Lvl 4	0
2019022	Northern Illinois	Albany Village (11WT1)	E-75-342	0
2019023	Northern Illinois	Kautz (11DU46)		0
2019024	Southeastern Wisconsin	Alberts (47JE887)	JE887-415	0
2019025	Southeastern Wisconsin	CAP (47JE93)	JE93-353	0
2019026	Northern Illinois	Blythe (11HA40)	73F (proj. no.)	0
2019027	Northern Illinois	DeWitte/Liphardt Habitation (11RI57)	77B (proj. no.)	0

Vessel Number	RGI Number	Material Detail	Exterior Surface	Interior Surface
0	RGI Sample 15, 34C.8	Rim	smooth	smooth
0		Rim	smoothed-over cordmarked	smooth
0		Rim	smooth	smooth
0		Rim	smoothed-over cordmarked	smooth
0		Rim	cordmarked	smooth
0		Rim	cordmarked	smooth
0		Rim	smoothed-over cordmarked	smooth
2002		Body	smoothed-over cordmarked	smooth
2004		Body	cordmarked	smooth
2008		Rim	cordmarked	smooth
2020		Body	cordmarked	smooth
2038		Rim	cordmarked	smooth
3034		Rim	smoothed-over cordmarked	smooth
0	RGI 143 I	Rim	smooth	smooth
0		Rim	smooth	smooth
0	RGI 144 I	Rim	smooth	smooth
0	RGI 147 I	Rim	smoothed-over cordmarked	smooth
0	RGI 152 I	Body	smooth	smooth
0	RGI 154 I	Rim	smoothed-over cordmarked	smooth
0		Rim	cordmarked	smooth
0		Body	smooth	smooth
0	RGI 68	Rim	smooth	smooth
0	RGI 158	Rim	smooth	smooth
0		Rim	cordmarked	exfoliated
0		Rim	cordmarked	smooth
0		Rim	cordmarked	smooth
0		Rim	smooth	smooth

Temper	Core (Int/Ext)	Decorated	Decoration 1 Type	Decoration 1 Location
grit	reduced	TRUE	incised	exterior rim margin
grit	ro	TRUE	punctates	exterior rim margin
grit	uneven	TRUE	punctates	exterior rim margin
grit	or	TRUE	punctates	exterior rim margin
grit	uneven	TRUE	perforated	below rim
grit	uneven	TRUE	tool stamp - rounded dowel	lip
grit	reduced	TRUE	punctates	exterior rim margin
grit	uneven	TRUE	incised (zoning)	exterior body
grit	oxidized	TRUE	cord-wrapped stick	exterior body
grit	uneven	TRUE	boss	exterior rim margin
grit	oxidized	TRUE	linear stamped	exterior body
grit	reduced	FALSE		
grit	oxidized	TRUE	incised	exterior base of rim (horizontal)
grit	reduced	TRUE	boss	exterior rim margin
limestone/grit/grog	oro	TRUE	boss	exterior rim margin
grit	reduced	TRUE	boss	exterior rim margin
grit	reduced	TRUE	cross-hatched incise	exterior rim margin
limestone/grit/grog	reduced	TRUE	incised	exterior body
grit	uneven	TRUE	perforated	below rim
grit/grog	oro	TRUE	dentate stamp -CWS	exterior rim margin
grit	uneven/reduced	TRUE	incised	exterior body
grit	reduced	TRUE	boss	exterior rim margin
grit	reduced	TRUE	dentate stamp	exterior rim margin, within zone (below incised)
grit	oxidized	TRUE	boss	exterior rim margin
grit	uneven	TRUE	boss	exterior rim margin
grit	uneven	TRUE	boss	exterior rim margin
grit	reduced	TRUE	dentate stamp	exterior rim margin

Decoration 1 Length 1 (mm)	Decoration 1 Length 2 (mm)	Decoration 1 Length Avg	Decoration 1 Width 1
26.32	26.85	26.585	1.73
6.5	6.85	6.675	4.19
5.86	6.07	5.965	5.87
3.12	3.55	3.335	2.75
9.1	9.62	9.36	0
6.33	6.59	6.46	3.03
3.81	4.16	3.985	2.57
31.82	33.58	32.7	3.44
15.43	14.16	14.795	3.19
11.29	9.2	10.245	9.55
8.64	9.07	8.855	2.34
0	0	0	0
0	0	0	1.3
5.71	5.85	5.78	5.28
14.08	14.63	14.355	0
5.21	5.3	5.255	4.54
16.53	17.23	16.88	0.98
0	0	0	1.69
9.92	10.56	10.24	0
2.71	3.36	3.035	2.21
5.07	5.67	5.37	2.32
7.34	7.75	7.545	0
25.13	24.59	24.86	3.57
10.97	11.65	11.31	0
8.34	8.84	8.59	0
7.16	7.22	7.19	7.58
19.01	18.51	18.76	3.83

Decoration 1 Width 2	Decoration 1 Width Avg	Decoration 1 Depth 1	Decoration 1 Depth 2
0.86	1.295	0.4	0.5
4.29	4.24	1.2	1.34
5.83	5.85	0.97	0.93
2.88	2.815	0.82	0.97
0	0	5.74	6.18
3.36	3.195	1.3	1.21
2.83	2.7	1.37	1.92
4.17	3.805	1.26	0.84
3.76	3.475	0.7	0.97
8.46	9.005	3.5	2.97
2.01	2.175	1.85	2.03
0	0	0	0
1.52	1.41	0.01	0.01
5.34	5.31	1.3	1.58
0	0	4.62	3.94
4.63	4.585	1.5	1.25
1.17	1.075	0.77	0.64
1.45	1.57	0.25	0.37
0	0	6.95	7.42
2.06	2.135	0.53	0.69
2.84	2.58	0.87	0.9
0	0	1.92	2.02
3.01	3.29	0.83	0.75
0	0	2.39	2.67
0	0	2.39	2.65
7.93	7.755	2.05	1.54
4.28	4.055	1.52	0.85

Decoration 1 Depth Avg	Decoration 2 Type	Decoration 2 Location	Decoration 2 Length 1
0.45			0
1.27	punctates	exterior rim margin, directly below dec 1	5.46
0.95	punctates	exterior rim margin, directly below dec 1	5.74
0.895	punctates	exterior rim margin, directly below dec 1	3.12
5.96			0
1.255			0
1.645			0
1.05	dentate stamp	exterior body	4.15
0.835			0
3.235	tooled notches	interior lip margin	6.3
1.94			0
0			0
0.01	incised	exterior	0
1.44			0
4.28	CWS stamp	exterior rim margin	17.26
1.375			0
0.705			0
0.31	rocker stamp	exterior body, alongside incised line	10.47
7.185	incised/tool impression	exterior rim	10.46
0.61			0
0.885	dentate stamp	exterior body, alongside incised groove	0
1.97	dentate stamp	exterior rim margin, below bosses	2.34
0.79	CWS stamp	interior lip margin	4.15
2.53	CWS stamp	interior lip/rim	8.54
2.52			0
1.795			0
1.185			0

Decoration 2 Length 2	Decoration 2 Length Avg	Decoration 2 Width 1	Decoration 2 Width 2
0	0	0	0
6.34	5.9	4.75	5.38
5.98	5.86	5.42	5.64
3.55	3.335	2.75	2.88
0	0	0	0
0	0	0	0
0	0	0	0
4.07	4.11	3.56	3.88
0	0	0	0
6.7	6.5	4.91	5.86
0	0	0	0
0	0	0	0
0	0	1.3	1.57
0	0	0	0
17.15	17.205	7.91	8.02
0	0	0	0
0	0	0	0
9.69	10.08	3.86	4.64
11.54	11	1.73	2.32
0	0	0	0
0	0	3.85	4.03
2.63	2.485	1.52	1.65
4.62	4.385	3.63	4.23
8.34	8.44	6.62	6.39
0	0	0	0
0	0	0	0
0	0	0	0



Decoration 2 Width Avg	Decoration 2 Depth 1	Decoration 2 Depth 2	Decoration 2 Depth Avg
0	0	0	0
5.065	1.57	1.77	1.67
5.53	1.52	1.01	1.265
2.815	0.82	0.97	0.895
0	0	0	0
0	0	0	0
0	0	0	0
3.72	0.86	1.09	0.975
0	0	0	0
5.385	1.68	2.18	1.93
0	0	0	0
0	0	0	0
1.435	0.01	0.01	0.01
0	0	0	0
7.965	1.98	1.34	1.66
0	0	0	0
0	0	0	0
4.25	0.01	0.01	0.01
2.025	0.8	1.07	0.935
0	0	0	0
3.94	0.34	0.36	0.35
1.585	0.01	0.01	0.01
3.93	1.25	1.28	1.265
6.505	1.58	2.42	2
0	0	0	0
0	0	0	0
0	0	0	0

Overall Decorative Motif	Wall Thickness 1	Wall Thickness 2
incised	5.68	5.91
punctates	6.05	6.5
punctates	6.99	7.81
punctates	7.28	7.5
perforated	7.08	8.18
parallel plain tool stamps/impressions on lip	9.73	9.58
punctates	5.62	5.71
zoned	10.15	9.56
cord-wrapped-stick stamped	9.01	9.41
row of bosses/nodes along exterior below rim/lip, crenelaed interior lip	8.73	8.46
stamped	9.49	9.74
nodes (not on selected sherd)	9.11	9.51
curvilinear incised lines	6.72	7.08
	6.61	6.84
row of punctates below rim, cws impressions along rim/lip exterior - CWS variation	12.35	12.73
	6.61	6.72
cross-hatched	5.02	5.53
rocker stamping	6.49	5.43
Also punctates/impressions below lines and stamping below that	7.74	8.52
dentate stamping - CWS variation	8.88	9.74
dentate stamping/zoned - dentate variation	8.33	9.11
dentate stamping - dentate variation	7.2	7.27
stamping/zone - dentate variation	9.69	10.16
boss/cws	8.04	7.64
	8.72	8.93
punctate/nodes	7.85	8.41
dentate stamping - curved	6.86	6.93

Wall Thickness Avg	Rim Stance	Rim Shape	Rim Width 1	Rim Width 2	Rim Width Avg	Lip Shape	Orifice Diameter (cm)
5.795	slightly inverted	folded	7.22	6.87	7.045	flattened	20
6.275	slightly everted	folded	7.6	7.82	7.71	beveled	18
7.4	direct	folded	9.35	9.57	9.46	beveled	20
7.39	slightly everted	unmodified	7.4	7.46	7.43	rounded	30
7.63	direct	folded	7.13	7.35	7.24	flattened	20
9.655	slightly everted	folded	9.92	10.07	9.995	rounded	40
5.665	direct	pinched	5.62	5.93	5.775	beveled	27
9.855	direct	unmodified	0	0	0	flattened	30
9.21	slightly everted	unmodified	0	0	0	flattened	30
8.595	direct	unmodified	8.43	7.65	8.04	rounded	20
9.615	direct	folded	0	0	0	flattened	30
9.31	direct	folded	9.87	9.59	9.73	flattened	22
6.9	everted	folded	5.85	6.06	5.955	rounded	16
6.71	indeterminate	unmodified	6.4	6.83	6.615	rounded	11
12.54	direct	unmodified	10	10.13	10.065	beveled	30
6.665	indeterminate	folded	7.33	7.54	7.435	beveled	17
5.275	slightly inverted	unmodified	5.34	5.73	5.535	flattened	25
5.96	N/A	N/A	0	0	0	N/A	0
8.13	slightly everted	unmodified	7.23	7.61	7.42	beveled	35
9.31	slightly inverted	unmodified	9.63	10.34	9.985	beveled	20
8.72	N/A	N/A	0	0	0	N/A	0
7.235	slightly inverted	unmodified	7.71	7.56	7.635	beveled	12
9.925	direct	unmodified	10.06	10.14	10.1	flattened	21
7.84	slightly everted	unmodified	8.44	8.71	8.575	beveled	17
8.825	direct	unmodified	8.95	9.02	8.985	rounded	18
8.13	everted	pinched	5.09	5.62	5.355	rounded	25
6.895	slightly inverted	unmodified	6.67	7.25	6.96	flattened	20

Orifice %	Vessel Form	Ware Type	Pottery Type	Weight (g)	Count
5	bowl	Hopewell-Related	Hopewell-Like Incised	6.22	1
5	jar	Havana Ware	Steuben Punctated	12.68	1
2.5	jar	Havana Ware	Steuben Punctated	25.17	1
2.5	jar	Havana Ware	Steuben Punctated	13.04	1
5	jar	Rock Ware	Shorewood Cord Roughened	26.57	1
7	jar	Rock Ware	Kegonsa Stamped	39.9	1
3	jar	Havana Ware	Steuben Punctated	38.5	1
4	conoidal jar	Havana Ware	Havana Zoned	32.7	1
2.5	conoidal jar	Havana Ware	Naples Stamped	27.7	1
10	globular jar	Rock Ware	Kegonsa Stamped	40.58	1
10	conoidal jar	Havana Ware	Naples Stamped	21.29	1
5	conoidal jar	Rock Ware	Shorewood Cord Roughened	19.78	1
20	subconoidal jar	Hopewell-Related	Hopewell-Related	9.11	1
1	jar	Havana Ware	Havana Plain	5.7	1
5	jar	Havana Ware	Naples Stamped	37.1	1
3.5	jar	Havana Ware	Havana Plain	5.21	1
3.5	jar	Hopewell-Related	Hopewell - crosshatched rim	10.9	1
0	unidentified	Hopewell-Related	Hopewell - rocker stamped	18.91	1
6	unidentified	Havana Ware	Unclassified Havana	40.43	1
3	jar	Havana Ware	Naples Stamped	12.34	1
0	unidentified	Havana Ware	Havana Zoned	17.9	1
4	jar	Havana Ware	Naples Stamped	10.69	1
7	jar	Havana Ware	Havana Zoned	42.8	1
9	jar	Havana Ware	Havana Cordmarked	35.23	1
3	jar	Rock Ware	Shorewood Cord Roughened	11.3	1
8	jar	Havana Ware	Havana Cordmarked	54.86	1
8	unidentified	Havana Ware	Hummel Stamped	21.7	1

## APPENDIX B: CERAMIC MINERALOGY DATABASE

Sample Numb	Apat	Biot	Calc	Hornblen	Microcli	Muscovi	K-Feldsp	P-Feldsp	Qua	Quartz	Opaq	Myrmek
2019001		13	12	4				2	14	13	10	4
2019002	4	18	14	4	1				5	20	4	12
2019003		27	17	9					23	7		13
2019004		25	19		3				29	9		10
2019005		7	15	3	3				7	15	2	1
2019006		38	22	5					25	12	20	22
2019007		22	18	2					8	19	23	2
2019008		27	30	1	4		1	1	16	21	9	1
2019009		15	12		8		6	6	4	21	9	5
2019010		16	8	7			1	1	24	12	3	12
2019011		8	10	3					6	18		8
2019012		9	8	4	1		7	7	16	39		8
2019013		6	3	3					7	26		5
2019014		10	5		3		3	2	2	12	4	2
2019015		6	7	2	1		1	1	2	19		
2019016		9	6		2		1	1	5	12	1	2
2019017		9	6				3	3	6	14		2
2019018		6	1		1	1			11	30	1	2
2019019		27	23		4		1	1	18	44		8
2019020		18	17		3			13	13	29	7	1
2019021		14	6		2		3	3	4	12	3	3
2019022		21	9		1		6	6	12	24	2	4
2019023		19	13	10			2	2	15	8		10
2019024		9	9	2					6	8	2	6
2019025		9	6				2	2	3	6	1	6
2019026		6	3				2	2	2	11	3	1
2019027		26	15		2		2	2	6	20	3	3

Seric	Gr	Conglomera	Ch	Sandsto	dy-Temp	ody-Sanc	ody-Clay	ody-Temper	Body-Sand	Body-Clay
7		2			19	5	80	18.26923077	4.807692308	76.92307692
9			5		21	9	175	10.24390244	4.390243902	85.36585366
4					15	1	135	9.933774834	0.662251656	89.40397351
2			2		20	4	239	7.604562738	1.520912548	90.87452471
13				2	21	1	146	12.5	0.595238095	86.9047619
			4		29	2	156	15.50802139	1.069518717	83.42245989
21			1		35	0	188	15.69506726	0	84.30493274
11					31	1	183	14.41860465	0.465116279	85.11627907
			1		30	5	231	11.27819549	1.879699248	86.84210526
					13	0	180	6.735751295	0	93.2642487
		3			14	3	143	8.75	1.875	89.375
			4		15	4	221	6.25	1.666666667	92.08333333
			2		9	1	202	4.245283019	0.471698113	95.28301887
2			2	1	11	5	103	9.243697479	4.201680672	86.55462185
7			3		11	2	286	3.244837758	0.589970501	84.36578171
3					10	3	127	7.142857143	2.142857143	90.71428571
9					16	2	84	15.68627451	1.960784314	82.35294118
1	2				12	5	204	5.429864253	2.262443439	92.30769231
16					34	6	225	12.83018868	2.264150943	84.90566038
16	3				32	5	246	11.30742049	1.766784452	86.92579505
7					14	2	233	5.62248996	0.803212851	93.57429719
12					15	7	155	8.474576271	3.95480226	87.57062147
4					23	0	131	14.93506494	0	85.06493506
2			2		14	4	312	4.242424242	1.212121212	94.54545455
4			3		7	3	108	5.932203339	2.542372881	91.52542373
			1		5	6	184	2.564102564	3.076923077	94.35897436
14					31	4	170	15.12195122	1.951219512	82.92682927

Paste-Silt (	Paste-Sand	Paste-Clay (	Paste-Silt (	Paste-Sand	Paste-Clay (
12	5	68	14.11764706	5.882352941	80
31	9	144	16.84782609	4.891304348	78.26086957
9	1	126	6.617647059	0.735294118	92.64705882
13	4	226	5.349794239	1.646090535	93.00411523
39	1	107	26.53061224	0.680272109	72.78911565
10	2	146	6.329113924	1.265822785	92.40506329
35	0	153	18.61702128	0	81.38297872
30	1	153	16.30434783	0.543478261	83.15217391
34	5	197	14.40677966	2.118644068	83.47457627
25	0	155	13.88888889	0	86.11111111
41	3	102	28.08219178	2.054794521	69.8630137
58	4	163	25.77777778	1.777777778	72.44444444
31	1	171	15.27093596	0.492610837	84.2364532
15	5	88	13.88888889	4.62962963	81.48148148
11	2	275	3.819444444	0.694444444	95.48611111
20	3	107	15.38461538	2.307692308	82.30769231
7	2	77	8.139534884	2.325581395	89.53488372
39	5	165	18.66028708	2.392344498	78.94736842
35	6	190	15.15151515	2.597402597	82.25108225
11	5	235	4.38247012	1.992031873	93.62549801
6	2	227	2.553191489	0.85106383	96.59574468
20	7	135	12.34567901	4.320987654	83.33333333
8	0	123	6.106870229	0	93.89312977
66	4	246	20.88607595	1.265822785	77.84810127
15	3	93	13.51351351	2.702702703	83.78378378
54	6	130	28.42105263	3.157894737	68.42105263
14	4	156	8.045977011	2.298850575	89.65517241

## APPENDIX C: POINT COUNTING RAW DATA

Sample ID	Region	Site Name	Microscope	Power	Matrix	Silt	Sand:M	Sand:F	Sand:Total
2019001	Southeastern Wisconsin	Peterson (47WK199)	OMAX	10X	68	12		5	5
2019002	Southeastern Wisconsin	Peterson (47WK199)	OMAX	10X	144	31		9	9
2019003	Southeastern Wisconsin	Peterson (47WK199)	OMAX	10X	126	9		1	1
2019004	Southeastern Wisconsin	Peterson (47WK199)	OMAX	10X	226	13		4	4
2019005	Southeastern Wisconsin	Peterson (47WK199)	OMAX	10X	107	39		1	1
2019006	Southeastern Wisconsin	Peterson (47WK199)	OMAX	10X	146	10		2	2
2019007	Southeastern Wisconsin	Peterson (47WK199)	OMAX	10X	153	35			0
2019008	Southeastern Wisconsin	Finch (47JE902)	OMAX	10X	153	30		1	1
2019009	Southeastern Wisconsin	Finch (47JE902)	OMAX	10X	197	34		5	5
2019010	Southeastern Wisconsin	Finch (47JE902)	OMAX	10X	155	25			0
2019011	Southeastern Wisconsin	Finch (47JE902)	OMAX	10X	102	41		3	3
2019012	Southeastern Wisconsin	Finch (47JE902)	OMAX	10X	163	58		4	4
2019013	Southeastern Wisconsin	Finch (47JE902)	OMAX	10X	171	31		1	1
2019014	Northern Illinois	Sloan (11MC86)	OMAX	10X	88	15		5	5
2019015	Northern Illinois	Sloan (11MC86)	OMAX	10X	275	11		2	2
2019016	Northern Illinois	Sloan (11MC86)	OMAX	10X	107	20		3	3
2019017	Northern Illinois	Sloan (11MC86)	OMAX	10X	77	7		2	2
2019018	Northern Illinois	Sloan (11MC86)	OMAX	10X	165	39	2	3	5
2019019	Northern Illinois	Sloan (11MC86)	OMAX	10X	190	35		6	6
2019020	Northern Illinois	Sloan (11MC86)	OMAX	10X	235	11		5	5
2019021	Northern Illinois	Sloan (11MC86)	OMAX	10X	227	6		2	2
2019022	Northern Illinois	Albany Village (11WT1)	OMAX	10X	135	20		7	7
2019023	Northern Illinois	Kautz (11DU46)	OMAX	10X	123	8			0
2019024	Southeastern Wisconsin	Alberts (47JE887)	OMAX	10X	246	66		4	4
2019025	Southeastern Wisconsin	CAP (47JE93)	OMAX	10X	93	15	1	2	3
2019026	Northern Illinois	Blythe (11HA40)	OMAX	10X	130	54	1	5	6
2019027	Northern Illinois	DeWitte/Liphardt Habitation (11RI57)	OMAX	10X	156	14		4	4



Grog:F	Grog:Total	Grit:C	Grit:M	Grit:F	Grit:Total	Slip	Void	Total Points	Average:Matrix	Average:Silt	Average:Sand
	0			19	19		13	104	0.653846154	0.115384615	0.048076923
	0		3	18	21		17	205	0.702439024	0.151219512	0.043902439
	0		2	13	15		14	151	0.834437086	0.059602649	0.006622517
	0		1	19	20		33	263	0.859315589	0.049429658	0.015209125
	0		1	20	21		28	168	0.636904762	0.232142857	0.005952381
	0		6	23	29		35	187	0.780748663	0.053475936	0.010695187
	0		9	26	35		37	223	0.686098655	0.156950673	0
	0		4	27	31		12	215	0.711627907	0.139534884	0.004651163
	0		2	28	30		17	266	0.740601504	0.127819549	0.018796992
	0		3	10	13		16	193	0.803108808	0.129533679	0
	0	3	2	9	14		53	160	0.6375	0.25625	0.01875
	0	1	2	12	15		30	240	0.679166667	0.241666667	0.016666667
	0		1	8	9		27	212	0.806603774	0.146226415	0.004716981
	0		2	9	11		5	119	0.739495798	0.12605042	0.042016807
	0		1	10	11		90	299	0.919732441	0.036789298	0.006688963
	0			10	10		18	140	0.764285714	0.142857143	0.021428571
	0		2	14	16		6	102	0.754901961	0.068627451	0.019607843
2	2		1	9	10		12	221	0.746606335	0.176470588	0.022624434
	0			34	34		16	265	0.716981132	0.132075472	0.022641509
3	3		2	27	29		15	283	0.830388693	0.038869258	0.017667845
	0			14	14		25	249	0.911646586	0.024096386	0.008032129
	0		1	14	15		8	177	0.762711864	0.11299435	0.039548023
	0		6	17	23		26	154	0.798701299	0.051948052	0
	0		2	12	14		17	330	0.745454545	0.2	0.012121212
	0			7	7		10	118	0.788135593	0.127118644	0.025423729
	0			5	5		41	195	0.666666667	0.276923077	0.030769231
	0			31	31		15	205	0.76097561	0.068292683	0.019512195

Average:Grog	Average:Grit	Percentage Totals
0	0.182692308	1
0	0.102439024	1
0	0.099337748	1
0	0.076045627	1
0	0.125	1
0	0.155080214	1
0	0.156950673	1
0	0.144186047	1
0	0.112781955	1
0	0.067357513	1
0	0.0875	1
0	0.0625	1
0	0.04245283	1
0	0.092436975	1
0	0.036789298	1
0	0.071428571	1
0	0.156862745	1
0.009049774	0.045248869	1
0	0.128301887	1
0.010600707	0.102473498	1
0	0.0562249	1
0	0.084745763	1
0	0.149350649	1
0	0.042424242	1
0	0.059322034	1
0	0.025641026	1
0	0.151219512	1

## APPENDIX D: COMPOSITION STATISTICAL ANALYSIS DATA

### *Paste Data*

R version 3.6.3 (2020-02-29) -- "Holding the Windsock"  
Copyright (C) 2020 The R Foundation for Statistical Computing  
Platform: x86\_64-apple-darwin15.6.0 (64-bit)

R is free software and comes with ABSOLUTELY NO WARRANTY.  
You are welcome to redistribute it under certain conditions.  
Type 'license()' or 'licence()' for distribution details.

Natural language support but running in an English locale

R is a collaborative project with many contributors.  
Type 'contributors()' for more information and  
'citation()' on how to cite R or R packages in publications.

Type 'demo()' for some demos, 'help()' for on-line help, or  
'help.start()' for an HTML browser interface to help.  
Type 'q()' to quit R.

```
> foo<-read.table("Thornton_Paste.txt",header = TRUE)
Error in scan(file = file, what = what, sep = sep, quote = quote, dec = dec, :
  line 1 did not have 5 elements
> foo<-read.table("Thornton_Paste.txt",header = TRUE)
> library(boot)
> library(compositions)
Loading required package: tensorA
```

Attaching package: 'tensorA'

The following object is masked from 'package:base':

norm

Loading required package: robustbase

Attaching package: 'robustbase'

The following object is masked from 'package:boot':

salinity

Loading required package: bayesm  
Welcome to compositions, a package for compositional data analysis.  
Find an intro with "? compositions"

Attaching package: 'compositions'

The following objects are masked from 'package:stats':

cor, cov, dist, var

The following objects are masked from 'package:base':

%\*%, scale, scale.default

```
> library(energy)
> library(MASS)
> library(sp)
> elem<-[,2:4]
Error: unexpected '[' in "elem<-["
> elem<-foo[,2:4]
> sites<-foo[,1]
> elem.ac<-acomp(elem)
> plot(elem.ac, pch = c(1:9)[sites], col = c(1:9)[sites])
> legend(x = "topleft", levels(sites), pch = 20, col = c(1:9), xpd = NA,
+       yjust = 0)
> mean(elem.ac)
  Matrix  Silt  Sand
0.8538052 0.1209920 0.0252028
attr("class")
[1] acomp
> elem.cen<-elem.ac-mean(elem.ac)
> head(elem.cen)
[1] 0.2111359 0.2156804 0.5640417 0.4986246 0.2571565 0.5135026
> plot(elem.cen, pch = c(1:9)[sites], col = c(1:9)[sites])
> legend(x = "topleft", levels(sites), pch = 20, col = c(1:9), xpd = NA,
+       yjust = 0)
> res<-lm(ilr(elem.cen)~sites)
> anova(res)
Analysis of Variance Table

            Df Pillai approx F num Df den Df Pr(>F)
(Intercept) 1 0.21287 2.29872   2  17 0.1307
sites       8 0.61256 0.99339  16  36 0.4843
Residuals  18
> compcoef<-ilrInv(coef(res),orig=elem.cen)
> print(compcoef)
  Matrix  Silt  Sand
(Intercept) 0.2630165 0.2749674 0.4620161
sitesAlberts 0.3200446 0.5795930 0.1003624
sitesBlythe  0.2130399 0.5973311 0.1896289
```

```

sitesCAP 0.3688908 0.4016150 0.2294943
sitesDeWitte 0.4761282 0.2884238 0.2354480
sitesFinch 0.3491790 0.5380533 0.1127677
sitesKautz 0.5480361 0.2406012 0.2113627
sitesPeterson 0.4236762 0.3908985 0.1854253
sitesSloan 0.4854865 0.3089508 0.2055627
attr("class")
[1] acomp
> (Albany<-compcoef[1,])
  Matrix  Silt  Sand
0.2630165 0.2749674 0.4620161
> print(acomp(Albany+mean(elem.ac)))
  Matrix  Silt  Sand
0.83333333 0.12345679 0.04320988
attr("class")
[1] acomp
> cenmat<-matrix(rep(0,27),nrow = 9)
> orimat<-cenmat
> rownames(cenmat)<-levels(sites)
> `colnames<-`c("Matrix","Silt","Sand")
Error: unexpected symbol in "`colnames<-`c"
> colnames(cenmat)<-c("Matrix","Silt","Sand")
> rownames(orimat)<-rownames(cenmat)
> colnames(orimat)<-rownames(cenmat)
Error in dimnames(x) <- dn :
  length of 'dimnames' [2] not equal to array extent
> colnames(orimat)<-colnames(cenmat)
> cenmat[1,]<-Albany
> orimat[1,]<-acomp(Albany+mean(elem.ac))
Error: unexpected ',' in "orimat[1,]"
>
> orimat[1,]<-acomp(Albany+mean(elem.ac))
> (Alberts<-Albany+acomp(compcoef[2,]))
  Matrix  Silt  Sand
0.2903504 0.5497096 0.1599400
attr("class")
[1] acomp
> print(acomp(Alberts+mean(elem.ac)))
  Matrix  Silt  Sand
0.77848101 0.20886076 0.01265823
attr("class")
[1] acomp
> cenmat[2,]<-Alberts
> orimat[2,]<-Alberts
> (Blythe<-Albany+acomp(compcoef[3,]))
  Matrix  Silt  Sand
0.1819896 0.5334566 0.2845538
attr("class")

```

```

[1] acomp
> print(acomp(Blythe+mean(elem.ac)))
  Matrix  Silt  Sand
0.68421053 0.28421053 0.03157895
attr("class")
[1] acomp
> cenmat[3,]<-Blythe
> orimat[3,]<-Blythe
> (CAP<-Albany+acomp(compcoef[4,]))
  Matrix  Silt  Sand
0.3095019 0.3522685 0.3382296
attr("class")
[1] acomp
> print(acomp(CAP+mean(elem.ac)))
  Matrix  Silt  Sand
0.83783784 0.13513514 0.02702703
attr("class")
[1] acomp
> cenmat[3,]<-CAP
> cenmat[3,]<-Blythe
> cenmat[4,]<-CAP
> orimat[4,]<-CAP
> (DeWitte<-Albany+acomp(compcoef[5,]))
  Matrix  Silt  Sand
0.3996890 0.2531208 0.3471902
attr("class")
[1] acomp
> print(acomp(DeWitte+mean(elem.ac)))
  Matrix  Silt  Sand
0.89655172 0.08045977 0.02298851
attr("class")
[1] acomp
> cenmat[5,]<-DeWitte
> orimat[5,]<-DeWitte
> (Finch<-Albany+acomp(compcoef[6,]))
  Matrix  Silt  Sand
0.3146412 0.5068636 0.1784951
attr("class")
[1] acomp
> print(acomp(Finch+mean(elem.ac)))
  Matrix  Silt  Sand
0.80319445 0.18335557 0.01344998
attr("class")
[1] acomp
> cenmat[6,]<-Finch
> orimat[6,]<-Finch
> (Kautz<-Albany+acomp(compcoef[7,]))
  Matrix  Silt  Sand

```

```

0.4680666 0.2148298 0.3171036
attr(,"class")
[1] acomp
> print(acom(Kautz+mean(elem.ac)))
  Matrix  Silt  Sand
0.92162627 0.05994317 0.01843056
attr(,"class")
[1] acomp
> cenmat[7,]<-Kautz
> orimat[7,]<-Kautz
> (Peterson<-Albany+acom(compcoef[8,]))
  Matrix  Silt  Sand
0.3658514 0.3528848 0.2812638
attr(,"class")
[1] acomp
> print(acom(Peterson+mean(elem.ac)))
  Matrix  Silt  Sand
0.86252994 0.11789634 0.01957372
attr(,"class")
[1] acomp
> cenmat[8,]<-Peterson
> orimat[8,]<-Peterson
> (Sloan<-Albany+acom(compcoef[9,]))
  Matrix  Silt  Sand
0.4150990 0.2761609 0.3087401
attr(,"class")
[1] acomp
> print(acom(Sloan+mean(elem.ac)))
  Matrix  Silt  Sand
0.89587073 0.08446052 0.01966875
attr(,"class")
[1] acomp
> cenmat[9,]<-Sloan
> orimat[9,]<-Sloan
> print(cenmat)
  Matrix  Silt  Sand
Albany 0.2630165 0.2749674 0.4620161
Alberts 0.2903504 0.5497096 0.1599400
Blythe 0.1819896 0.5334566 0.2845538
CAP 0.3095019 0.3522685 0.3382296
DeWitte 0.3996890 0.2531208 0.3471902
Finch 0.3146412 0.5068636 0.1784951
Kautz 0.4680666 0.2148298 0.3171036
Peterson 0.3658514 0.3528848 0.2812638
Sloan 0.4150990 0.2761609 0.3087401
> print(orimat)
  Matrix  Silt  Sand
Albany 0.8333333 0.1234568 0.04320988

```

```
Alberts 0.2903504 0.5497096 0.15994003
Blythe 0.1819896 0.5334566 0.28455380
CAP 0.3095019 0.3522685 0.33822958
DeWitte 0.3996890 0.2531208 0.34719024
Finch 0.3146412 0.5068636 0.17849513
Kautz 0.4680666 0.2148298 0.31710357
Peterson 0.3658514 0.3528848 0.28126383
Sloan 0.4150990 0.2761609 0.30874009
```

```
> vaux<-vcov(res)
```

```
> source("vcovout.r")
```

```
> matout<-vcovout(vaux)
```

```
> print(matout)
```

```
[[1]]
```

```
      1      2      3
1 0.18968418 -0.07369774 -0.11598644
2 -0.07369774 0.15709802 -0.08340028
3 -0.11598644 -0.08340028 0.19938671
```

```
[[2]]
```

```
      1      2      3
1 0.3793684 -0.1473955 -0.2319729
2 -0.1473955 0.3141960 -0.1668006
3 -0.2319729 -0.1668006 0.3987734
```

```
[[3]]
```

```
      1      2      3
1 0.3793684 -0.1473955 -0.2319729
2 -0.1473955 0.3141960 -0.1668006
3 -0.2319729 -0.1668006 0.3987734
```

```
[[4]]
```

```
      1      2      3
1 0.3793684 -0.1473955 -0.2319729
2 -0.1473955 0.3141960 -0.1668006
3 -0.2319729 -0.1668006 0.3987734
```

```
[[5]]
```

```
      1      2      3
1 0.3793684 -0.1473955 -0.2319729
2 -0.1473955 0.3141960 -0.1668006
3 -0.2319729 -0.1668006 0.3987734
```

```
[[6]]
```

```
      1      2      3
1 0.2212982 -0.08598070 -0.13531751
2 -0.0859807 0.18328102 -0.09730033
3 -0.1353175 -0.09730033 0.23261783
```



```
[[7]]
      1      2      3
1 0.3793684 -0.1473955 -0.2319729
2 -0.1473955 0.3141960 -0.1668006
3 -0.2319729 -0.1668006 0.3987734
```

```
[[8]]
      1      2      3
1 0.21678192 -0.08422599 -0.1325559
2 -0.08422599 0.17954060 -0.0953146
3 -0.13255593 -0.09531460 0.2278705
```

```
[[9]]
      1      2      3
1 0.21339470 -0.08290996 -0.13048474
2 -0.08290996 0.17673527 -0.09382531
3 -0.13048474 -0.09382531 0.22431005
```

```
> source("plotout.r")
> plotout(cenmat,sites,matout)
> save.image("~/Library/Mobile
Documents/com~apple~CloudDocs/Seth/Archaeology/thornton/Working Directory/Thornton
Petro/Thornton_Paste.RData")
>
```

## *Body Data*

R version 3.6.3 (2020-02-29) -- "Holding the Windssock"  
Copyright (C) 2020 The R Foundation for Statistical Computing  
Platform: x86\_64-apple-darwin15.6.0 (64-bit)

R is free software and comes with ABSOLUTELY NO WARRANTY.  
You are welcome to redistribute it under certain conditions.  
Type 'license()' or 'licence()' for distribution details.

Natural language support but running in an English locale

R is a collaborative project with many contributors.  
Type 'contributors()' for more information and  
'citation()' on how to cite R or R packages in publications.

Type 'demo()' for some demos, 'help()' for on-line help, or  
'help.start()' for an HTML browser interface to help.  
Type 'q()' to quit R.

[Workspace loaded from ~/Library/Mobile Documents/com~apple~CloudDocs/Seth/Archaeology/thornton/Working Directory/Thornton Petro/Thornton\_Paste.RData]

```
> library(boot)
> library(compositions)
Loading required package: tensorA
```

Attaching package: 'tensorA'

The following object is masked from 'package:base':

norm

Loading required package: robustbase

Attaching package: 'robustbase'

The following object is masked from 'package:boot':

salinity

Loading required package: bayesm  
Welcome to compositions, a package for compositional data analysis.  
Find an intro with "? compositions"

Attaching package: 'compositions'

The following objects are masked from 'package:stats':

cor, cov, dist, var

The following objects are masked from 'package:base':

%\*%, scale, scale.default

```
> library(energy)
> library(MASS)
> library(sp)
> foo<-read.table("Thornton_Body.txt",header = TRUE)
> elem<-foo[,2:4]
> sites<-foo[,1]
> elem.ac<-acomp(elem)
> plot(elem.ac,pch=c(1:9)[sites],col=c(1:9)[sites])
> legend(x="topleft",levels(sites),pch=20,col=c(1:9),xpd = NA,yjust = 0)
> mean(elem.ac)
Matrix Sand Temper
```

```

0.89049851 0.02276608 0.08673540
attr(,"class")
[1] acomp
> elem.cen<-elem.ac-mean(elem.ac)
> head(elem.cen)
[1] 0.1699793 0.2356458 0.4114377 0.3978047 0.3643453 0.2932504
> plot(elem.cen,pch=c(1:9)[sites],col=c(1:9)[sites])
> legend(x="topleft",levels(sites),pch=20,col=c(1:9),xpd = NA,yjust = 0)
> res<-lm(ilr(elem.cen)~sites)
> anova(res)
Analysis of Variance Table

```

```

      Df Pillai approx F num Df den Df Pr(>F)
(Intercept) 1 0.19229  2.0235   2  17 0.1628
sites      8 0.75613  1.3677  16  36 0.2125
Residuals 18

```

```

> compcoef<-irlInv(coef(res),orig=elem.cen)
Error in irlInv(coef(res), orig = elem.cen) :
  could not find function "irlInv"
> compcoef<-ilrInv(coef(res),orig=elem.cen)
> print(compcoef)
      Matrix Sand Temper
(Intercept) 0.2659535 0.4698043 0.2642422
sitesAlberts 0.5722271 0.1624454 0.2653275
sitesBlythe 0.4992893 0.3605117 0.1401990
sitesCAP 0.4376689 0.2692011 0.2931301
sitesDeWitt 0.2936580 0.1529983 0.5533438
sitesFinch 0.4545850 0.1311601 0.4142549
sitesKautz 0.2797760 0.2126405 0.5075835
sitesPeterson 0.3407793 0.1501779 0.5090428
sitesSloan 0.4289518 0.1861562 0.3848921
attr(,"class")

```

```

[1] acomp
> (Albany<-compcoef[1,])
      Matrix Sand Temper
0.2659535 0.4698043 0.2642422
> print(acomp(Albany+mean(elem.ac)))

```

```

      Matrix Sand Temper
0.87570621 0.03954802 0.08474576
attr(,"class")

```

```

[1] acomp
> cenmat<-matrix(rep(0,27),nrow=9)
> orimat<-cenmat
> rownames(cenmat)<-levels(sites)
Error in rownames(cenmat) <- levels(sites) :
  could not find function "rownames<-"
> rownames(cenmat)<-levels(sites)

```

```

> colnames(cenmat)<-c("Matrix","Sand","Temper")
> rownames(orimat)<-rownames(cenmat)
> colnames(orimat)<-colnames(cenmat)
> cenmat[1,]<-Albany
> orimat[1,]<-acomp(Albany+mean(elem.ac))
> (Blythe<-Albany+acomp(compcoef[2,]))
  Matrix  Sand  Temper
0.5096404 0.2555725 0.2347870
attr("class")
[1] acomp
> (Alberts<-Albany+acomp(compcoef[2,]))
  Matrix  Sand  Temper
0.5096404 0.2555725 0.2347870
attr("class")
[1] acomp
> print(acomp(Alberts+mean(elem.ac)))
  Matrix  Sand  Temper
0.94545455 0.01212121 0.04242424
attr("class")
[1] acomp
> cenmat[2,]<-Alberts
> orimat[2,]<-acomp(Alberts+mean(elem.ac))
> (Blythe<-Albany+acomp(compcoef[3,]))
  Matrix  Sand  Temper
0.3914685 0.4993156 0.1092159
attr("class")
[1] acomp
> print(acomp(Blythe+mean(elem.ac)))
  Matrix  Sand  Temper
0.94358974 0.03076923 0.02564103
attr("class")
[1] acomp
> cenmat[3,]<-Blythe
> orimat[3,]<-acomp(Blythe+mean(elem.ac))
> (CAP<-Albany+acomp(compcoef[4,]))
  Matrix  Sand  Temper
0.3633754 0.3948189 0.2418057
attr("class")
[1] acomp
> print(acomp(CAP+mean(elem.ac)))
  Matrix  Sand  Temper
0.91525424 0.02542373 0.05932203
attr("class")
[1] acomp
> cenmat[4,]<-CAP
> orimat[4,]<-acomp(CAP+mean(elem.ac))
> (DeWitt<-Albany+acomp(compcoef[5,]))
  Matrix  Sand  Temper

```

```

0.2636752 0.2426751 0.4936497
attr(,"class")
[1] acomp
> print(acom(DeWitt+mean(elem.ac)))
  Matrix  Sand  Temper
0.8292683 0.0195122 0.1512195
attr(,"class")
[1] acomp
> cenmat[5,]<-DeWitt
> orimat[5,]<-acom(DeWitt+mean(elem.ac))
> (Finch<-Albany+acom(compcoef[6,]))
  Matrix  Sand  Temper
0.4140619 0.2110392 0.3748989
attr(,"class")
[1] acomp
> print(acom(Finch+mean(elem.ac)))
  Matrix  Sand  Temper
0.90808476 0.01183258 0.08008267
attr(,"class")
[1] acomp
> cenmat[6,]<-Finch
> orimat[6,]<-acom(Finch+mean(elem.ac))
> (Kautz<-Albany+acom(compcoef[7,]))
  Matrix  Sand  Temper
0.2412443 0.3238947 0.4348610
attr(,"class")
[1] acomp
> print(acom(Kautz+mean(elem.ac)))
  Matrix  Sand  Temper
0.82651675 0.02836962 0.14511363
attr(,"class")
[1] acomp
> cenmat[7,]<-Kautz
> orimat[7,]<-acom(Kautz+mean(elem.ac))
> (Peterson<-Albany+acom(compcoef[8,]))
  Matrix  Sand  Temper
0.3065019 0.2386037 0.4548944
attr(,"class")
[1] acomp
> print(acom(Peterson+mean(elem.ac)))
  Matrix  Sand  Temper
0.85876744 0.01709128 0.12414128
attr(,"class")
[1] acomp
> cenmat[8,]<-Peterson
> orimat[8,]<-acom(Peterson+mean(elem.ac))
> (Sloan<-Albany+acom(compcoef[9,]))
  Matrix  Sand  Temper

```

```

0.3762041 0.2884056 0.3353902
attr(,"class")
[1] acomp
> print(acomp(Sloan+mean(elem.ac)))
  Matrix  Sand  Temper
0.90380520 0.01771374 0.07848106
attr(,"class")
[1] acomp
> cenmat[9,]<-Sloan
> orimat[9,]<-acomp(Sloan+mean(elem.ac))
> print(cenmat)
  Matrix  Sand  Temper
Albany 0.2659535 0.4698043 0.2642422
Alberts 0.5096404 0.2555725 0.2347870
Blythe 0.3914685 0.4993156 0.1092159
CAP 0.3633754 0.3948189 0.2418057
DeWitt 0.2636752 0.2426751 0.4936497
Finch 0.4140619 0.2110392 0.3748989
Kautz 0.2412443 0.3238947 0.4348610
Peterson 0.3065019 0.2386037 0.4548944
Sloan 0.3762041 0.2884056 0.3353902
> print(orimat)
  Matrix  Sand  Temper
Albany 0.8757062 0.03954802 0.08474576
Alberts 0.9454545 0.01212121 0.04242424
Blythe 0.9435897 0.03076923 0.02564103
CAP 0.9152542 0.02542373 0.05932203
DeWitt 0.8292683 0.01951220 0.15121951
Finch 0.9080848 0.01183258 0.08008267
Kautz 0.8265168 0.02836962 0.14511363
Peterson 0.8587674 0.01709128 0.12414128
Sloan 0.9038052 0.01771374 0.07848106
> vaux<-vcov(res)
> source("vcovout.r")
> matout<-vcovout(vaux)
> print(matout)
[[1]]
  1 2 3
1 0.118923635 -0.1158467 -0.003076921
2 -0.115846714 0.2173321 -0.101485358
3 -0.003076921 -0.1014854 0.104562279

[[2]]
  1 2 3
1 0.237847271 -0.2316934 -0.006153842
2 -0.231693428 0.4346641 -0.202970715
3 -0.006153842 -0.2029707 0.209124558

```

```
[[3]]
      1      2      3
1 0.237847271 -0.2316934 -0.006153842
2 -0.231693428 0.4346641 -0.202970715
3 -0.006153842 -0.2029707 0.209124558
```

```
[[4]]
      1      2      3
1 0.237847271 -0.2316934 -0.006153842
2 -0.231693428 0.4346641 -0.202970715
3 -0.006153842 -0.2029707 0.209124558
```

```
[[5]]
      1      2      3
1 0.237847271 -0.2316934 -0.006153842
2 -0.231693428 0.4346641 -0.202970715
3 -0.006153842 -0.2029707 0.209124558
```

```
[[6]]
      1      2      3
1 0.138744241 -0.1351545 -0.003589741
2 -0.135154500 0.2535541 -0.118399584
3 -0.003589741 -0.1183996 0.121989325
```

```
[[7]]
      1      2      3
1 0.237847271 -0.2316934 -0.006153842
2 -0.231693428 0.4346641 -0.202970715
3 -0.006153842 -0.2029707 0.209124558
```

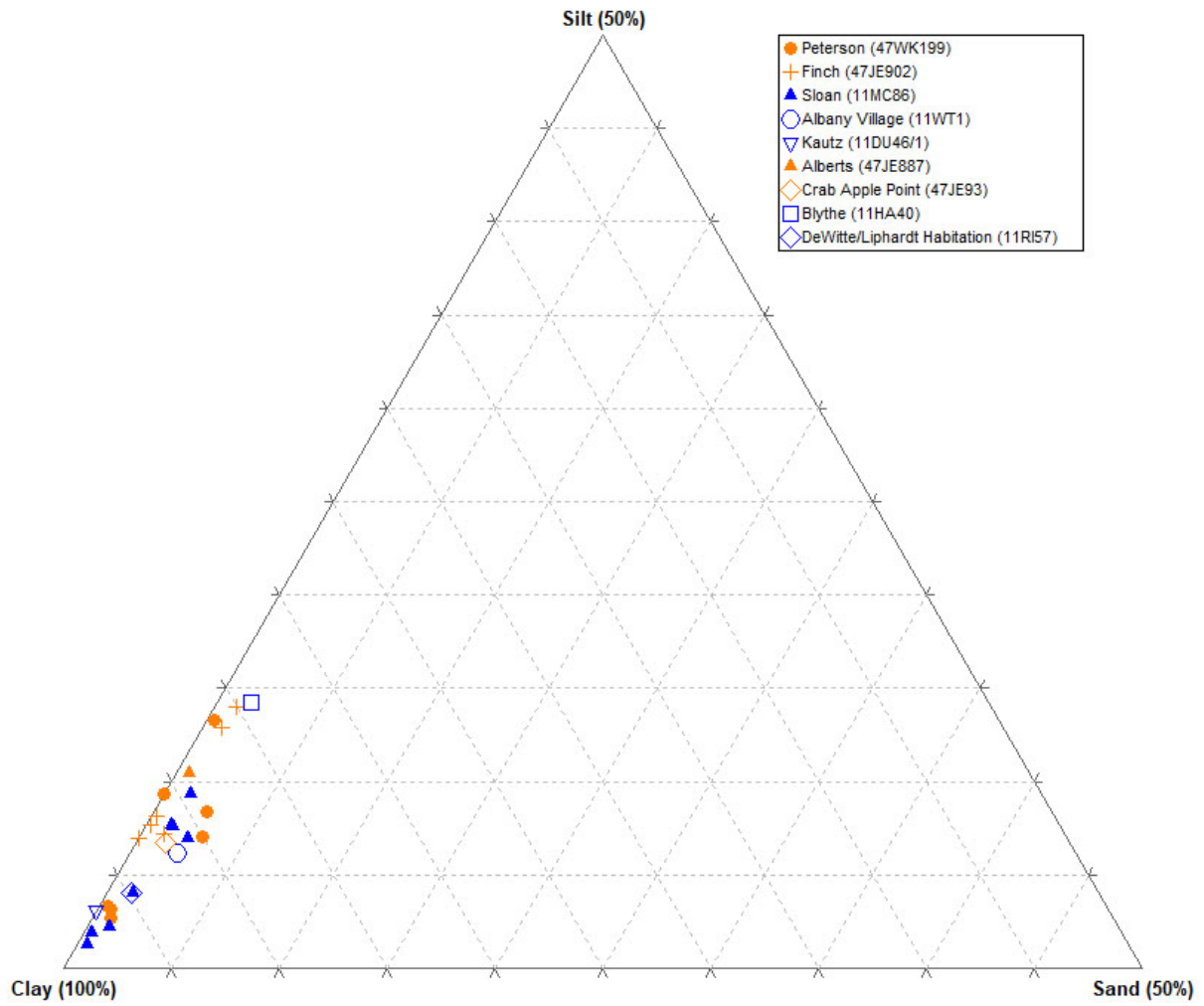
```
[[8]]
      1      2      3
1 0.135912726 -0.1323962 -0.003516481
2 -0.132396245 0.2483795 -0.115983266
3 -0.003516481 -0.1159833 0.119499747
```

```
[[9]]
      1      2      3
1 0.133789090 -0.1303276 -0.003461536
2 -0.130327553 0.2444986 -0.114171027
3 -0.003461536 -0.1141710 0.117632564
```

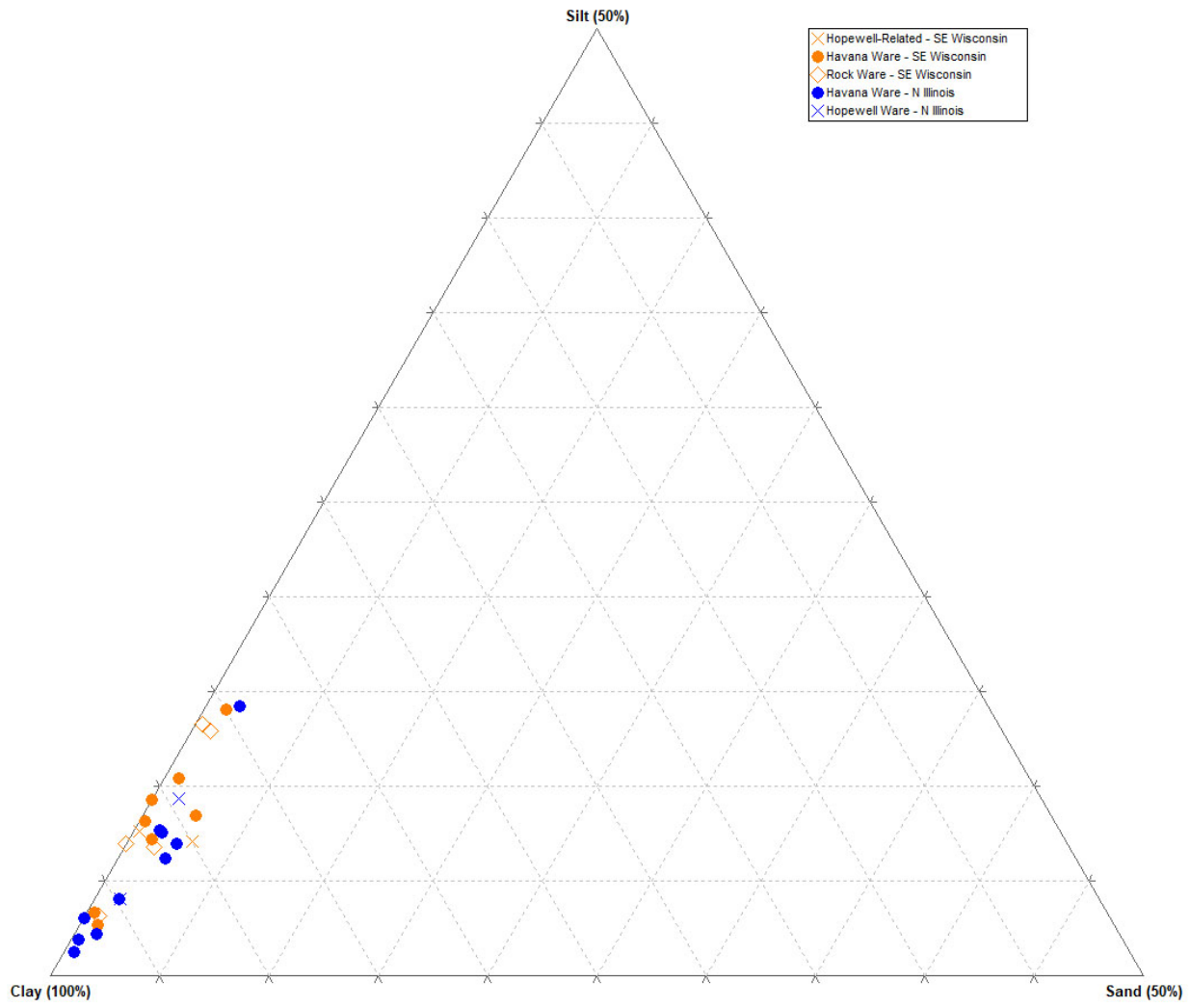
```
> source("plotout.r")
> plotout(cenmat,sites,matout)
```

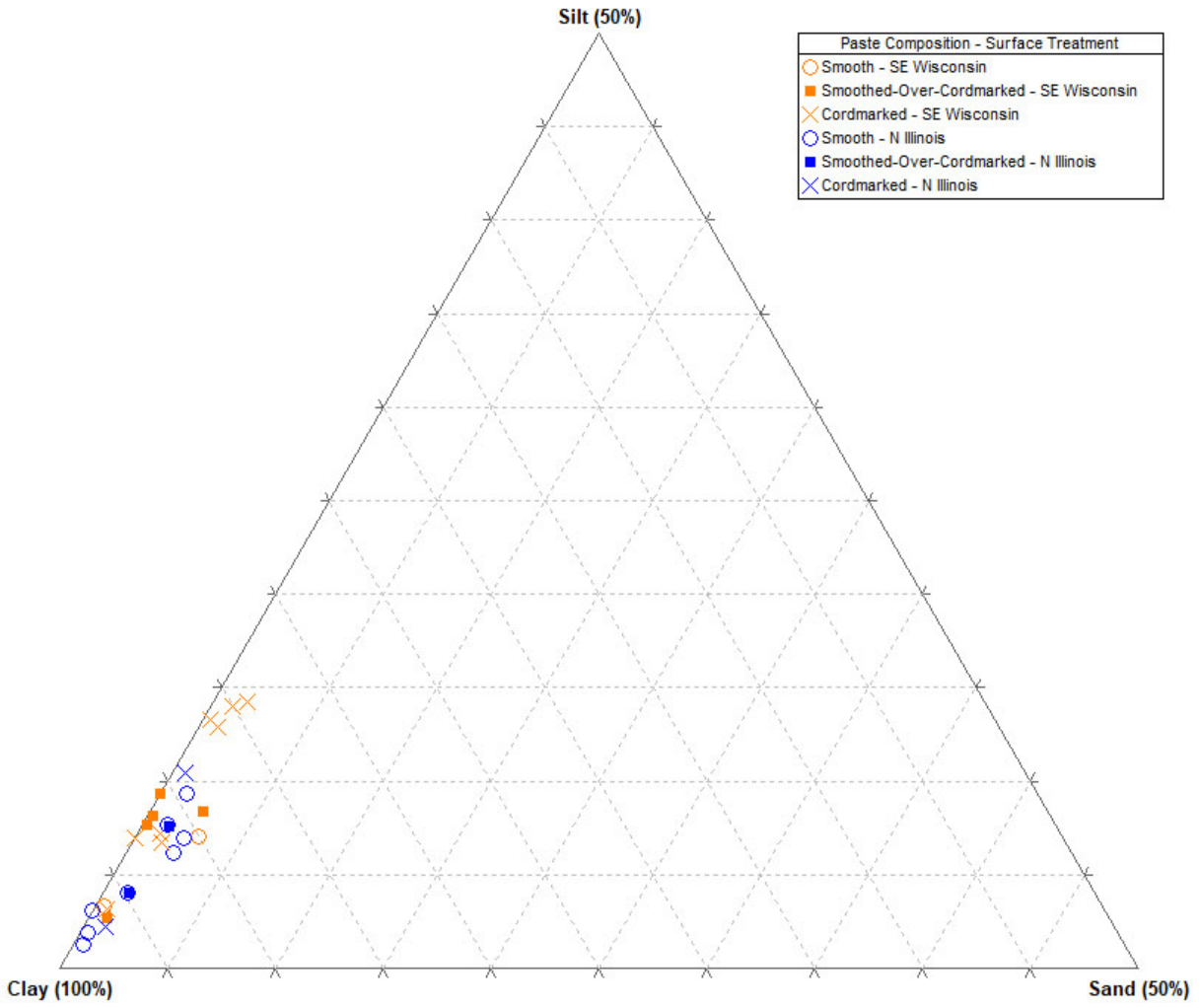
# APPENDIX E: TERNARY DIAGRAMS

## Paste Composition









# Body Composition

